# **Distribution Agreement**

In presenting this thesis or dissertation as a partial fulfillment of the requirements for an advanced degree from Emory University, I hereby grant to Emory University and its agents the non-exclusive license to archive, make accessible, and display my thesis or dissertation in whole or in part in all forms of media, now or hereafter known, including display on the world wide web. I understand that I may select some access restrictions as part of the online submission of this thesis or dissertation. I retain all ownership rights to the copyright of the thesis or dissertation. I also retain the right to use in future works (such as articles or books) all or part of this thesis or dissertation.

Signature: Brenda Stephanie Al	rtezana
Brenda Stephanie Antezana	6/23/2023   11:30 AM EDT
Name	Date

Title	Horizontal Transfer of Ant	ibiotic Resistance in Streptococcus pneumoniae
Author Degree Program	Brenda Stephanie Antezana Doctor of Philosophy Biological and Biomedical S Microbiology and Molecula	Sciences
Approved by the Docusigned by:  David Styr 7BFE4762C2F64C	he Committee	David Stephens  Advisor
DocuSigned by:  4 Jilu-Ling 1  540A03E90B03496	zeng, Ph.D.	Yih-Ling Tzeng, Ph.D.  Advisor
DocuSigned by: USLY MG 9C9548F3CF7142'	Eu, Ph.D.	Lesley McGee, Ph.D.  Committee Member
Philip Rather FA78B593895547	r, ph.D.	Philip Rather, Ph.D.  Committee Member
DocuSigned by: William M D41BC35C42164E	- •	William M Shafer  Committee Member
DocuSigned by:  JOYAL E. U  0D4FB851CF8542	ridal, Ph.D.	Jorge E. Vidal, Ph.D.  Committee Member
Accepted by the		y Jacob Arriola, Ph.D, MPH mes T. Laney Graduate School

Date

By

Brenda Stephanie Antezana
B.S., University of Florida, 2016

Advisor: David S. Stephens, M.D. Advisor: Yih-Ling Tzeng, Ph.D.

# An abstract of

A dissertation submitted to the Faculty of the

James T. Laney School of Graduate Studies of Emory University
in partial fulfillment of the requirements for the degree of

Doctor of Philosophy

in

Graduate Division of Biological and Biomedical Sciences
Microbiology and Molecular Genetics
2023

#### Abstract

# Horizontal Transfer of Antibiotic Resistance in Streptococcus pneumoniae

# By Brenda Stephanie Antezana

Streptococcus pneumoniae (pneumococcus) is a nasopharyngeal commensal that may spread to local or sterile sites, causing non-invasive or invasive pneumococcal disease. Antibiotic resistance was first observed in S. pneumoniae during the 1960s against penicillin and expanded to macrolides in the 1990s. One key contributor to macrolide resistance is Tn916-related integrative and conjugative elements (ICEs), such as Tn2009 (23.5 kb), Tn6002 (20.8 kb), and Tn2010 (26.3 kb). Unlike in vitro planktonic cell transformation, efficient Tn916-related ICE transfer was observed in dual-strain biofilms formed on human nasopharyngeal cells. Investigation of the transfer mechanism disproved the involvement of conjugation based on limited conjugative gene expression, absence of ICE circular intermediates, and no change in ICE transfer frequency with a conjugative mutant donor. However, competence and transformation mutant studies, extracellular DNA removal by DNase I treatment, and recombinant genome analyses supported transformation and homologous recombination as the major mechanism for pneumococcal Tn916related ICE dissemination. Contribution of Tn916-related ICEs to pneumococcal macrolide resistance and effects of pneumococcal conjugate vaccines (PCVs) to ICE circulation were explored in the United States using genomes of 4,560 PubMLST S. pneumoniae isolates collected during 1916-2021. In this collection, Tn916-related ICE frequency increased over time. This rise was associated with a decrease in ICE+ isolates of vaccine serotypes upon PCV introductions, but a marked increase in ICE+ isolates of non-vaccine serotypes, such as 15A and 23A, which are not included in the current PCV15 and PCV20. Tn916-related ICE macrolide resistance shifted from Tn2009 mefE/mel-mediated macrolide efflux to ermB-mediated ribosomal methylation of Tn6002 and Tn2010 by the 2010s. Transformation of DNA associated with naturally released pneumococcal extracellular vesicles (EVs) was evaluated under planktonic and biofilm conditions and was not more efficient compared to free DNA. While in vitro conditions enabled EV transformation of streptomycin (rpsL/K56T) and erythromycin (738-bp ermB) resistance, biofilms facilitated natural EV transformation of the 5.4-kb Mega element and Tn2009. SNP analyses of biofilm EV recombinants revealed homologous recombination of ~9-26 kb DNA fragments. This work contributes new mechanistic and population findings of antibiotic resistance dissemination in S. pneumoniae, highlighting the importance of transformation, biofilms, and continuing pneumococcal evolution.

By

Brenda Stephanie Antezana B.S., University of Florida, 2016

Advisor: David S. Stephens, M.D. Advisor: Yih-Ling Tzeng, Ph.D.

A dissertation submitted to the Faculty of the

James T. Laney School of Graduate Studies of Emory University
in partial fulfillment of the requirements for the degree of

Doctor of Philosophy

in

Graduate Division of Biological and Biomedical Sciences
Microbiology and Molecular Genetics
2023

#### ACKNOWLEDGEMENTS

I want to give a huge thank you to every single individual that has helped me develop into the independent scientist that I am today. With your guidance, I have become more adept in experimental design, troubleshooting, and critically analyzing scientific data. To Dr. David S. Stephens, my advisor, I want to thank you for the time you dedicated to mentoring me throughout these years. Under your tutelage, I have developed the skills necessary to experimentally address important scientific questions and to convey these findings to others. I am also grateful for my coadvisor, Dr. Yih-Ling Tzeng, particularly for all our discussions, whether it'd be in your office or on Zoom at random times of the day, I really appreciated every single one.

I also would like to acknowledge others that have directly contributed to my success during my PhD journey. To my committee members: Drs. Jorge Vidal, William Shafer, Philip Rather, and Lesley McGee, thank you for the constant encouragement and direction. Receiving your feedback and helping me track my progress ultimately helped me stay focused and finish this body of work. Specifically, to Dr. Jorge Vidal who took me in as a new student during 2018-2019, I want to thank you for initially teaching me about *Streptococcus pneumoniae* and demonstrating to me the public health importance of this pathogen. I also want to acknowledge Dr. Sarah Satola for providing me with advice and endless opportunities to grow in my career as well as for being a mentor and inspiration.

To all my friends, both old and new, thank you for all the fun adventures! I want to specifically give a shout out to everyone in HSRB's E-169, you know who you are. Many of you have become a huge part of my life and I hope to keep it that way. Tubing trips, inspiring conversations, fun dinners, game nights...I could go on and on, but every single adventure with all of you encompass some of my greatest memories. When I describe us as the "E-169 family," I truly mean it. To other

friends that I have met in Emory or that have been in my life since childhood, I am grateful for you all as well for always keeping me grounded and giving me an escape throughout this PhD journey.

I want to thank my brother and his family for keeping me company and providing advice when I needed it the most. I also can't forget the great meals we shared together! To my wonderful pets, Amber and RooRoo - thank you for all the snuggles, walks, and love. I simply can't imagine my life without the two of you.

To my family to whom I dedicate this dissertation: Jose Guillermo Antezana (dad), Juana Bertha Antezana (mom), and Hedwin Kitdorlang Dkhar (my partner). Words simply can't describe how grateful I am for you. Mom and dad, the sacrifices that you have made and the struggles that you had to endure, particularly when you first moved to the US, they have not gone unnoticed. I want to thank you both from the bottom of my heart for all that you have done for me and for teaching me the value of hard work. Although I am not sure if I can ever really repay these debts, I hope that this PhD and all the corresponding accomplishments can provide even a small sense of pride and fulfill the dreams you have had for me. I can't wait to give you both the lives that you deserve. Kit, it would be an understatement to say that meeting you was the best thing that ever happened to me, but there is truly no other way to say it. You have been there for me at my highest highs and even at my lowest lows, always providing words of encouragement, love, and support. Thank you for those moments. I don't think I could have ever completed this PhD journey without you by my side. I can't wait to see what the future has in store for us.

# TABLE OF CONTENTS

Chapter 1: Introduction to Streptococcus pneumoniae	1
Chapter 2: Dissemination of Tn916-related integrative and conjugative elements	in
Streptococcus pneumoniae occurs by transformation and homologous recombination	in
nasopharyngeal biofilms	30
Abstract	31
Importance	32
Introduction	33
Results	34
Discussion	46
Materials and Methods	50
Acknowledgements	60
Figures and Tables	61
Supplemental Figures and Tables	70
References	82
Chapter 3: Streptococcus pneumoniae Tn916-related integrative and conjugative elements	s in
the United States in the pre- and post-pneumococcal conjugate vaccine eras	
(1916-2021)	95
Abstract	96
Importance	97
Introduction	98
Results	100
Discussion	104

Materials and Methods	110
Acknowledgements	112
Figures	113
Supplemental Figures	118
References	119
Chapter 4: Extracellular vesicles and transformation of antimicrobial resis	tance genetic
determinants in Streptococcus pneumoniae	132
Abstract	133
Importance	134
Introduction	135
Results	137
Discussion	143
Materials and Methods	147
Acknowledgements	151
Figures and Tables	153
Supplemental Tables	158
References	159
Chapter 5: Conclusions and future directions	168
Appendix A: Interaction between Streptococcus pneumoniae and Staphylod	coccus aureus
Generates *OH Radicals That Rapidly Kill Staphylococcus aureus Strains	191
Appendix B: Lactoferrin Disaggregates Pneumococcal Biofilms and Inhibits	Acquisition of
Resistance Through Its DNase Activity	210

# LIST OF FIGURES AND TABLES

Chapter 2: Dissemination of Tn916-related integrative and conjugative elements in
Streptococcus pneumoniae occurs by transformation and homologous recombination in
nasopharyngeal biofilms 30
Figure 1. Efficient transfer of pneumococcal Tn916-related ICEs occurs in dual-strain
nasopharyngeal biofilms. 61
Figure 2. Sequence alignments of prototype Tn916 with pneumococcal Tn916-related
ICEs. 62
Figure 3. Pneumococcal Tn2009 does not form circular intermediates (CIs) nor transfer by
conjugation. 63
<b>Figure 4.</b> Pneumococcal Tn2009 transfer in human nasopharyngeal biofilms requires competence
and transformation machinery in the recipient. 64
Figure 5. Partial pneumococcal Tn6002 lacking conjugative regulatory mechanism transfers via
transformation and homologous recombination in a strain-dependent manner. 66
Figure 6. Whole-genome sequencing reveals homologous recombination of large Tn2009-
containing fragments (~33 to ~55 kb) from GA16833 into D39 bioreactor recombinants. 67
Figure 7. Efficient transfer of Tn916-related ICEs via transformation and homologous
recombination in nasopharyngeal biofilms occurs in other <i>S. pneumoniae</i> strains. 68
<b>Table 1.</b> Tetracycline-induced fold change in <i>tetM</i> and conjugative gene expression of Tn916 and
Tn2009.
Table 2. Homologous recombination of donor DNA fragments of various sizes with intact
Tn2009 into D39 bioreactor recombinant genomes. 69

<b>Table 3.</b> Early <i>com</i> gene expression in recipient D39 <sup>Ery/Str</sup> from dual-strain bioreactor biofi	lm with
BASP8 compared to in vitro transformation without CSP addition.	69
Figure S1. Similar extracellular DNA concentrations are secreted from competence-d	eficient
mutant recipient strain BASP2 and Tn2009 ICE donor GA16833 in nasopharyngeal dua	ıl-strain
biofilms.	70
Figure S2. Single recipient strain biofilm transforms point mutation-mediated resistance	but not
Tn916-related ICE resistance.	71
<b>Figure S3.</b> <i>In vitro</i> transformation at 35°C and 37°C facilitates recipient uptake of point me	utation-
mediated resistance but not Tn916-related ICE resistance.	72
<b>Table S1.</b> Strains used in this study.	73
<b>Table S2.</b> Primers and probes used in this study.	75
Table S3. Genetic identity and rF data for D39 <sup>Str/Tmp</sup> and GA16833 <sup>Tet/Ery</sup> or GA47281 <sup>Tet/Ery</sup>	y
bioreactor co-inoculation strains and recombinants.	79
Table S4. Homologous recombination of variably sized donor DNA fragments with intact	ICE
into bioreactor recombinant genomes.	80
Chapter 3: Streptococcus pneumoniae Tn916-related integrative and conjugative elements	nents
in the United States in the pre- and post-pneumococcal conjugate vaccine eras	
(1916-2021)	95
Figure 1. Tn916-related ICE frequency has increased in US S. pneumoniae isolates.	113
Figure 2. Shift in the distribution of Tn916-related ICEs in the US during pre-PCV7, PC	V7, and
PCV13 eras.	114
<b>Figure 3.</b> Tn916-related ICE-containing <i>S. pneumoniae</i> isolates from 1916 to 2021 in the	
US.	115

Figure 4. Tn916-related ICEs emerged in non-vaccine serotypes after PCV7 and PCV13	
introductions in the US.	I
Figure 5. Serotype-specific analysis for Tn916-related ICE-containing isolates in the US, 1995-	
2021.	,
Figure S1. S. pneumoniae isolates carrying Tn916-related ICEs in US, Thailand, and South Africa	L
during pre-PCV7 and post-PCV7/13 eras.	1
Chapter 4: Extracellular vesicles and transformation of antimicrobial resistance genetic	
determinants in Streptococcus pneumoniae 132	1
Figure 1. Transmission electron microscopy (TEM) images of S. pneumoniae extracellular	•
vesicles. 153	i
Figure 2. S. pneumoniae extracellular vesicles transform externally associated DNA into	
planktonic cells or pneumococcal biofilms at reduced frequencies compared to genomic DNA	
transformation. 154	-
Figure 3. EV-mediated transformation of larger antimicrobial resistance determinant occurs in	
pneumococcal biofilms as opposed to planktonic cells though at reduced frequencies compared to	
genomic DNA transformation. 155	
Figure 4. EV-mediated transformation of pneumococcal biofilms occurs in presence or absence	;
of synthetic competence stimulating peptide.	<b>,</b>
Table 1. Quantification of S. pneumoniae extracellular vesicle (EV) protein and DNA	
content. 157	,
Table 2. Integration of donor DNA fragments delivered by S. pneumoniae extracellular vesicles	1
occurs via homologous recombination.	,
<b>Table S1.</b> Strains used in this study.	,

## Chapter 1: Introduction to Streptococcus pneumoniae

### I. The pneumococcus

Streptococcus pneumoniae (or pneumococcus) is a facultative anaerobic commensal of the human nasopharynx as well as an opportunistic pathogen that can cause non-invasive and invasive disease in humans<sup>(1, 2)</sup>. In addition to causing localized infections like otitis media and non-bacteremic pneumonia, *S. pneumoniae* can invade the bloodstream, resulting in more severe disease, such as bacteremia or meningitis<sup>(3)</sup>. Children less than two years of age, the elderly over 65 years of age, the immunocompromised, and individuals with chronic conditions are those at greater risk for pneumococcal disease<sup>(4)</sup>. Though effective pneumococcal conjugate vaccines are available, *S. pneumoniae* remains as a global public health concern, primarily due to dissemination of antibiotic resistance in this pathogen. Thus, the World Health Organization listed *S. pneumoniae* as a priority pathogen for research and development of novel treatments in 2017<sup>(5)</sup>.

# A. Discovery of Streptococcus pneumoniae

The discovery of *S. pneumoniae* occurred due to malaria and rabies research simultaneously conducted by George Miller Sternberg and Louis Pasteur, respectively<sup>(6)</sup>. In September 1880 in the United States (US), Sternberg inoculated two rabbits as well as other animals with his own saliva resulting in their deaths, which were distinct compared to that of malaria and subsequently isolated the organism responsible for these deaths using rabbit broth<sup>(7, 8)</sup>. In December 1880 in France, Pasteur obtained a saliva sample from a rabies-infected child, inoculated rabbits with it, and observed their deaths that were also different from rabies<sup>(9)</sup>. Utilizing microscopy, Pasteur detected an "8"-shaped organism with a halo around its perimeter and he successfully isolated the organism in veal broth<sup>(7, 9)</sup>. Referred to as *Microbe septicemique du salive* by Pasteur<sup>(9)</sup> and *Micrococcus pasteuri* by Sternberg<sup>(10)</sup>, both microbiologists described the same lancet-shaped,

diplococcal bacteria. In subsequent years, the bacterium went through multiple name changes until reaching its final designation as *Streptococcus pneumoniae* in 1974<sup>(11)</sup>.

### B. Disease and economic burden

Globally, *S. pneumoniae* remains as the leading cause of pneumonia mortality in children<sup>(12)</sup>. In 2000, O'Brien et al. reported that there were ~14.5 million cases of pneumococcal disease worldwide with 826,000 deaths in children aged 1-59 months<sup>(13)</sup>. In 2015, total global deaths in children aged 1-59 months were reduced to 318,000 and an estimated total case number of ~9.2 million individuals with pneumococcal disease was calculated<sup>(14)</sup>. Due to the continued spread of disease, the economic tolls remain problematic. A study found that PCV20 serotypes, or distinct variants of *S. pneumoniae* characterized by their capsular polysaccharide, resulted in \$213.5 million in annual direct medical costs across 13 different countries between 2017-2019<sup>(15)</sup>. During 2012-2014, there was an average cost of \$6,534 in at-risk adults and \$9,168 in high-risk adults compared to \$4,725 in healthy adults per pneumococcal disease episode<sup>(16)</sup>.

# II. Colonization and pathogenesis

# A. Nasopharyngeal colonization

Nasopharyngeal colonization by *S. pneumoniae* is a perquisite for transmission to new human hosts. Upon colonization, *S. pneumoniae* first encounters nasal mucus composed of mucin glycoproteins, antimicrobial peptides, and immunoglobulins<sup>(17)</sup>. To avoid mucus entrapment and mucociliary clearance, *S. pneumoniae* employs mucus degradation via pneumococcal proteins neurominidase A (NanA), beta-galactosidase (BgaA), and beta-N-acetylglucosaminidase (StrH), providing *S. pneumoniae* an opportunity to access and adhere to the host epithelial cell surface<sup>(3)</sup>.

Several pneumococcal adhesins have been implicated for bacterial attachment. Pneumococcal adherence and virulence protein A (PavA), PavB, and enolase (Eno) bind host cell fibronectin and

plasminogen<sup>(18-20)</sup> while phosphorylcholine (ChoP) on the *S. pneumoniae* cell wall interacts with the epithelial cell platelet-activating factor receptor (PAFR)<sup>(21)</sup>. Choline-binding protein A (CbpA) interacts with the polymeric immunoglobulin receptor (PIGR), facilitating the translocation of *S. pneumoniae* across nasopharyngeal cells<sup>(22)</sup>. Surface-exposed lipoproteins, streptococcal lipoprotein rotamase A (SlrA) and putative proteinase maturation protein A (PpmA), can also contribute to pneumococcal adherence of the epithelial cells in the nasopharynx<sup>(23, 24)</sup>.

# **B.** Biofilm formation

Following pneumococcal colonization, persistence in the nasopharynx is enabled by biofilm formation. Planktonic bacteria adhere to a surface, develop a monolayer-to-multilayer bacterial community, and mature into a complex three-dimensional structure<sup>(25)</sup>. The ability for *S. pneumoniae* to form biofilms *in vivo* on nasopharyngeal cells has been established. Scanning electron microscopy of excised murine nasopharyngeal tissue demonstrated an increased density of pneumococcal biofilm in posterior sections<sup>(26)</sup> while biopsy samples from human colonization studies have revealed *S. pneumoniae* biofilm structures and microcolonies<sup>(27)</sup>.

The pneumococcal biofilm begins as a honeycomb-like structure, speculated to provide stability<sup>(28)</sup>, and eventually matures into towers with water channels and to a thickness of ~25-30 μm. The biofilm contains fibrous connections between bacteria and an extracellular matrix<sup>(26, 29)</sup> composed of exopolysaccharides, proteins, nucleic acids, and lipids, and which protects from host immune responses, antibiotics, and other environmental stressors<sup>(30, 31)</sup>. Optimal biofilms form with a pH of 7.0-8.0<sup>(29)</sup>, a CO<sub>2</sub>-enriched environment<sup>(32)</sup>, and temperatures of ~34-35°C<sup>(26, 33)</sup>.

# C. Non-invasive pneumococcal diseases

S. pneumoniae can spread to other local infection sites from the nasopharynx, leading to non-invasive diseases. Otitis media is an acute inflammatory middle ear infection that can manifest in

ear pain, a red and swollen ear drum, and low-grade fever<sup>(34)</sup>. To cause otitis media, *S. pneumoniae* can travel from the nasopharynx to the middle ear via Eustachian tubes <sup>(35)</sup>.

Inflammation of air sacs, or alveoli, in the lungs and build-up of fluid or pus can result in pneumonia<sup>(36)</sup>, leading to fever, chills, a wet or dry cough, and abnormal breathing patterns<sup>(36)</sup>. Pneumonia can be bacteremic or non-bacteremic. The latter is non-invasive when *S. pneumoniae* spreads to the lower respiratory tract and infects the lungs without invading the bloodstream.

## D. Invasive pneumococcal diseases

Pneumococcal invasion of sterile host sites via breaching of the host cell barrier is termed as invasive pneumococcal disease (IPD). Invasion occurs via pneumococcal interactions with host cells, such as CbpA-PIGR<sup>(3, 22, 37)</sup> or ChoP-PAFR<sup>(21)</sup> as previously discussed. Once *S. pneumoniae* has gained access to the bloodstream, this can result in bacteremia<sup>(3)</sup>, which manifests as fever, shaking chills, hypotension, gastrointestinal distress, and altered sensory perception<sup>(38)</sup>. Invasion of the blood-brain barrier leads to meningitis. Pneumococcal access to the cerebral spinal fluid occurs in the choroid plexus or *S. pneumoniae* may pass through the blood-brain barrier utilizing the cerebral capillaries that cover the subarachnoid space<sup>(35)</sup>. Interactions, such as pneumococcal CbpA and the host cell laminin receptor<sup>(39)</sup> or ChoP-PAFR<sup>(40)</sup>, have been implicated in blood-brain barrier passage as well. Pneumococcal meningitis is life-threatening and manifests as inflammation of the meninges, or the outer membranes that protect the brain and spinal cord, cerebral edema, and blood vessel infection that can lead to brain parenchyma damage<sup>(41)</sup>. It has been demonstrated that meningitis survivors experience permanent neurological sequelae<sup>(42)</sup>.

# III. Treatment and prevention

### A. Vaccines

Pneumococcal vaccination studies commenced in 1911 in Johannesburg, South Africa when Sir Almroth Wright utilized heat-killed pneumococcal lysates at various dosage concentrations and observed a reduction of pneumococcal pneumonia cases and deaths in gold miners<sup>(43, 44)</sup>. However, the notion of distinguishing between various *S. pneumoniae* serotypes was becoming more apparent as serotyping methods, such as Quellung reaction, were being developed<sup>(43)</sup>. In 1914, Sir F. Spencer Lister developed serotype-specific whole-cell pneumococcal vaccines and demonstrated with 10,866 newly arrived miners that this type-specific vaccine was 100% effective in averting infection caused by pneumococcal types 1 and 2<sup>(45)</sup>.

As research into pneumococcal vaccination increased with the knowledge of serotype specificity, several companies developed pneumococcal polysaccharide vaccines (PPSVs) with varying valency between 1947 to 1983, such as PPSV6, PPSV14, and PPSV23<sup>(43, 46)</sup>. However, PPSVs were poorly immunogenic in children less than 2 years of age<sup>(47)</sup>. Thus, pneumococcal conjugate vaccines (PCVs) were developed with capsular polysaccharides conjugated to the CRM197 diphtheria protein, which helped activate T-cell dependent antibody production, enhancing their immunogenicity<sup>(47)</sup>. In 2000, PCV7 was introduced in the US and contained serotypes 4, 6B, 9V, 14, 18C, 19F, and 23F<sup>(48, 49)</sup> while PCV13 was introduced in 2010 with PCV7 serotypes plus 1, 3, 5, 6A, 7F, and 19A<sup>(49)</sup>. PCV15 (PCV13 serotypes plus 22F and 33F) and PCV20 (PCV15 plus serotypes 8, 10A, 11A, 12F, and 15B) were approved for use in adults in 2021 while in children, PCV15 and PCV20 were approved in 2022<sup>(50)</sup> and 2023<sup>(51)</sup>, respectively.

### **B.** Antibiotics

In 1939, a soluble sulfonamide, sulfapyridine, was being widely used for treatment of pneumococcal disease<sup>(52)</sup>. Although penicillin replaced sulfonamides by the mid-1940s<sup>(52)</sup>, resistance to this drug<sup>(53)</sup> led to the transition to using macrolides in the 1990s, which became the

first line of treatment for upper respiratory infections and community-acquired pneumonia (CAP)<sup>(54)</sup>. The widespread use of macrolides resulted in the emergence of resistant pneumococci as well<sup>(55, 56)</sup>. Currently, low-risk CAP is treated with macrolide monotherapy while higher-risk CAP patients are administered respiratory fluoroquinolones<sup>(57)</sup>. For otitis media, amoxicillin is used sometimes in conjunction with clavulanic acid<sup>(58)</sup>. For invasive disease, combination therapy of cefotaxime or ceftriaxone with vancomycin has been shown to be effective<sup>(59)</sup>.

### IV. Antibiotic resistance

### A. Macrolide resistance

Macrolide resistance in S. pneumoniae is predominantly accredited to expression of resistance genes ermB and mefE/mel on the macrolide efflux genetic assembly (Mega)<sup>(54)</sup>. ErmB is a ribosomal methylase that will dimethylate the 23s rRNA on the bacterial 50s ribosomal subunit to prevent the antibiotic from binding to its target site (60), conferring constitutive, high-level resistance to 14-, 15-, and 16-membered macrolides and resulting in lincosamide and streptogramin B resistance (MLS<sub>B</sub> phenotype)<sup>(54, 61)</sup>. Macrolide efflux is mediated by MefE/Mel from either Mega-1 (5.5 kb) or Mega-2 (5.4 kb), leading to lower-level resistance to 14- and 15membered macrolides while remaining susceptible to lincosamides and streptogramin B (M phenotype)<sup>(62-64)</sup>. This low-level resistance provided by Mega can be induced by the same 14- and 15-membered macrolide antibiotics to higher levels of resistance<sup>(65)</sup>. Specifically, MefE utilizes a proton-motive force for the efflux of macrolide antibiotics while Mel is a ribosomal protection protein that prevents the binding of the antibiotic (54, 64, 66). Mega has been identified in at least five distinct genomic loci of the pneumococcal genome, including insertion into larger mobile genetic elements<sup>(67)</sup>. Although rare, point mutations in rplD and rplV encoding for ribosomal proteins L4 and L22, respectively, can serve as a third mechanism for macrolide resistance (68, 69).

## B. Multidrug resistance via Tn916-related integrative and conjugative elements

Pneumococcal multidrug resistance to macrolides and tetracycline had also emerged as early as the 1990s due to the dissemination of Tn916-related integrative and conjugative elements (ICEs). Typically, ICEs are mobile genetic elements integrated in a bacterial chromosome that horizontally disseminate via conjugative machinery encoded by ICE genes<sup>(67, 70)</sup>. The 18.0 kb Tn916 ICE serves as a prototype for conjugative transfer whereby the element excises from the chromosome, circularizes, and transfers to a recipient cell using a type IV secretion system that is encoded by conjugative genes located on the 5' end of the element that are expressed only when Tn916 is in its circular form<sup>(71-73)</sup>. Tn916 conjugative gene induction can occur with tetracycline presence initiating at the *tetM* promoter, and is regulated at the transcriptional attenuation level (74). In S. pneumoniae, ICEs of the Tn916 family have been identified: Tn2009 (23.5 kb), Tn6002 (20.8 kb), and Tn2010 (26.3 kb). Integration of Mega into orf6 of Tn916 resulted in Tn2009<sup>(75)</sup>. A 2.8 kb fragment with ermB inserted into orf20 was named Tn6002<sup>(76)</sup>. Lastly, Tn2010 carries both orf6::Mega and orf20::ermB<sup>(77)</sup>. Tn916-related ICEs also contain a tetM gene encoding for a ribosomal protection protein, thus conferring tetracycline resistance<sup>(78)</sup>. Though pneumococcal Tn916-related ICEs contain the necessary machinery to conjugate as the prototype Tn916, the molecular mechanism for horizontal transfer in S. pneumoniae remained unknown.

# V. Horizontal exchange of genetic determinants

# A. Griffith 1928 experiment

Utilizing *S. pneumoniae* as a model, in 1928, Frederick Griffith published his findings from pioneering experiments that led to the discovery of DNA as the hereditary material in cells that can genetically modify microorganisms<sup>(79-81)</sup>. For his experiments, Griffith inoculated mice with either rough, unencapsulated (R) or smooth, encapsulated (S) strains and observed that only the S

strain-inoculated mice died while the R strain-inoculated mice survived. At the completion of these experiments, Griffith was able to recover only non-virulent R strain from surviving mice while recovering virulent S strain from dead mice. Griffith also inoculated mice with heat-killed S strain, leading to the survival of the mice and no recovery of S strain bacteria from the live mice<sup>(79, 81)</sup>. Finally, inoculating mice with a mixture of live R strain and heat-killed S strain, Griffith found that the mice died, isolating bacteria of only the S strain morphology. It was determined that an unknown feature from the heat-killed S strain was being donated to the live R strain, thus "transforming" the R strain into the smooth, virulent phenotype and leading to the deaths of the mice<sup>(79)</sup>. This unknown feature was aptly titled as the "transforming principle." More evidence supporting DNA as the transforming material was provided by Oswald Avery, Colin MacLeod, and Maclyn McCarty in 1944 where they excluded the role of RNA and protein in transformable<sup>(80,81)</sup>.

# **B.** Induction of competence

*S. pneumoniae* is naturally competent becoming capable of taking up genetic material from its surroundings<sup>(82, 83)</sup>. To induce competence, an immature competence stimulating peptide (CSP), encoded by *comC*, gets processed and secreted out via the ABC transporter ComAB<sup>(84, 85)</sup>. Mature CSP accumulates until a particular concentration threshold is reached and then the peptide will bind to sensor kinase ComD<sup>(86)</sup>. This kinase will autophosphorylate and transfer the phosphate group to the response regulator, ComE, which will then be activated<sup>(87)</sup> to further stimulate expression of *comAB* and *comCDE*, and promote competence development<sup>(88)</sup>. Other early *com* genes include *comX*, which encodes for an alternative sigma factor that enables specific binding of the RNA polymerase to promoters of late *com* genes involved in fratricide, DNA uptake, and homologous recombination, as well as *comM*, encoding for a fratricide immunity protein<sup>(89-91)</sup>.

# C. Transformation and homologous recombination

Competence induction results in uptake of exogenous double-stranded DNA (dsDNA) via a 2-3 µm type IV pilus that forms on the pneumococcal cell surface<sup>(92)</sup>. Powered by the ATPase ComGA, pilus formation initiates with assembly of major pilin ComGC subunits and minor pilin subunits (ComGD, E, F, G)<sup>(93)</sup>. DNA binds to the pilus, which retracts<sup>(94)</sup> allowing this dsDNA to bind to the membrane protein, ComEA. Endonuclease EndA is recruited and degrades one of the strands of the dsDNA, resulting in single-stranded DNA (ssDNA)<sup>(95, 96)</sup>. This ssDNA is then transported through the protein channel ComEC into the recipient pneumococcal cell<sup>(97)</sup> and is coated with single-stranded binding proteins (SsbB) to protect it from nucleic acid degradation – this complex is known as an eclipse complex<sup>(98, 99)</sup>. The DNA processing chain A protein (DprA) displaces SsbB, and aids in recombinase RecA loading onto the eclipse complex<sup>(100)</sup>. RecA, with help from RadA and CoiA, promotes strand exchange via homologous recombination<sup>(101-103)</sup>.

# D. Role of fratricide on gene transfer

Pneumococcal fratricide involves the production of fratricins, or bacteriolytic cell wall hydrolases, such as CbpD<sup>(104, 105)</sup>. To protect themselves against their own fratricins, S. pneumoniae will produce the ComM immunity protein during competence development<sup>(89)</sup>. In a mixed bacterial community, such as a biofilm, a subpopulation of noncompetent cells will be lysed by fratricins, leading to DNA release that can then be taken up by competent bacteria <sup>(91)</sup>. Thus, fratricide can contribute to genetic exchange with the acquisition of homologous DNA. This was primarily demonstrated by Johnsborg et al. where, in mixed planktonic cultures of competent and non-competent S. pneumoniae, there is a 1,000-fold more efficient transfer of resistance markers when the competent, fratricin-producing cells have an intact  $cbpD^{(106)}$ . It has also been shown that CbpD damage stimulates murein hydrolases LytA and LytC to be involved in fratricide<sup>(107)</sup>.

# E. Extracellular vesicles for genetic transformation

Extracellular vesicles (EVs), or lipid-membrane bound particles, are secreted by both Gramnegative as well as Gram-positive microorganisms and have been demonstrated to contain nucleic acids as cargo<sup>(108-110)</sup>. Vesicle-mediated plasmid DNA transformation containing antimicrobial resistance determinants has been extensively studied among Gram-negative species<sup>(111-113)</sup>. However, investigations into the role of EV-mediated DNA transformation by Gram-positive species are limited. One such example of Gram-positive EV transformation is that of ruminococci EVs rescuing a phenotype in deletion mutants for crystalline cellulose degradation<sup>(114)</sup>. Specifically, *S. pneumoniae* secretes significant amounts of EVs during late-log phase that range from 20-80 nm in diameter on average and can stimulate protective host immunogenicity<sup>(115)</sup>. In addition to surface protein and short-chain fatty acid content, pneumococcal EVs have been shown to harbor transforming DNA<sup>(116)</sup>. However, the extent to which pneumococcal EVs can serve as a vehicle for DNA delivery and contribute to horizontal exchange of antimicrobial resistance determinants among *S. pneumoniae* strains remains unclear.

## VI. Summary of dissertation

Increasing pneumococcal antimicrobial resistance has prompted research into mechanisms of resistance as well as for development of novel therapeutics for treatment of pneumococcal infections. In this dissertation, we explored the molecular mechanism for efficient transfer of Tn916-related ICEs, conferring macrolide and tetracycline resistance, between *S. pneumoniae* strains forming human nasopharyngeal biofilms as well as Tn916-related ICE distribution pre- and post- PCV introductions among *S. pneumoniae* isolates collected in the US between 1916-2021. Moreover, the role of pneumococcal extracellular vesicles harboring DNA with variably sized antimicrobial resistance determinants was investigated for genetic transformation.

### REFERENCES

- 1. Henriques-Normark B, Tuomanen EI. The pneumococcus: epidemiology, microbiology, and pathogenesis. Cold Spring Harb Perspect Med. 2013;3(7). Epub 2013/07/03. doi: 10.1101/cshperspect.a010215. PubMed PMID: 23818515; PMCID: PMC3685878.
- 2. Shak JR, Vidal JE, Klugman KP. Influence of bacterial interactions on pneumococcal colonization of the nasopharynx. Trends Microbiol. 2013;21(3):129-35. Epub 2013/01/01. doi: 10.1016/j.tim.2012.11.005. PubMed PMID: 23273566; PMCID: PMC3729046.
- 3. Weiser JN, Ferreira DM, Paton JC. Streptococcus pneumoniae: transmission, colonization and invasion. Nat Rev Microbiol. 2018;16(6):355-67. Epub 2018/03/31. doi: 10.1038/s41579-018-0001-8. PubMed PMID: 29599457; PMCID: PMC5949087.
- 4. Fletcher MA, Laufer DS, McIntosh ED, Cimino C, Malinoski FJ. Controlling invasive pneumococcal disease: is vaccination of at-risk groups sufficient? Int J Clin Pract. 2006;60(4):450-6. Epub 2006/04/20. doi: 10.1111/j.1368-5031.2006.00858.x. PubMed PMID: 16620359; PMCID: PMC1448695.
- 5. Nadimpalli M, Delarocque-Astagneau E, Love DC, Price LB, Huynh BT, Collard JM, Lay KS, Borand L, Ndir A, Walsh TR, Guillemot D, Bacterial I, antibiotic-Resistant Diseases among Young children in low-income countries Study G. Combating Global Antibiotic Resistance: Emerging One Health Concerns in Lower- and Middle-Income Countries. Clin Infect Dis. 2018;66(6):963-9. Epub 2018/01/19. doi: 10.1093/cid/cix879. PubMed PMID: 29346620.
- 6. Watson DA, Musher DM, Jacobson JW, Verhoef J. A brief history of the pneumococcus in biomedical research: a panoply of scientific discovery. Clin Infect Dis. 1993;17(5):913-24. Epub 1993/11/01. doi: 10.1093/clinids/17.5.913. PubMed PMID: 8286641.

- 7. Sanchez-Rosario Y, Johnson MDL. Media Matters, Examining Historical and Modern Streptococcus pneumoniae Growth Media and the Experiments They Affect. Front Cell Infect Microbiol. 2021;11:613623. Epub 2021/04/10. doi: 10.3389/fcimb.2021.613623. PubMed PMID: 33834003; PMCID: PMC8021847.
- 8. Sternberg GM. A Fatal Form of Septicaemia in the Rabbit Produced by the Subcutaneous Injection of Human Saliva
- . Annual Reports of the National Board of Health1881. p. 87-108.
- 9. Pasteur L, Chamberland, M.M., Roux, E. Sur une maladie nouvelle, provoquée par la salive d'un enfant mort de la rage. Comptes rendus de l'Académie des sciences. 1881:159-65.
- 10. The Pneumonia-Coccus of Friedlander. Buffalo Med Surg J. 1885;25(3):112-3. Epub 1885/10/01. PubMed PMID: 36665774; PMCID: PMC9439405.
- 11. Deibel RH, Seeley, H.W. Jr. Family II. Streptococcaceae fam. nov. In: Buchanan RE, Gibbons, NE, editor. Bergey's manual of determinative bacteriology (8th edition). Baltimore: The Williams & Wilkins Co.; 1974. p. 490-517.
- 12. Pneumonia in children. World Health Organization2022 [December 29, 2022]. Available from: https://www.who.int/news-room/fact-sheets/detail/pneumonia.
- 13. O'Brien KL, Wolfson LJ, Watt JP, Henkle E, Deloria-Knoll M, McCall N, Lee E, Mulholland K, Levine OS, Cherian T, Hib, Pneumococcal Global Burden of Disease Study T. Burden of disease caused by Streptococcus pneumoniae in children younger than 5 years: global estimates. Lancet. 2009;374(9693):893-902. Epub 2009/09/15. doi: 10.1016/S0140-6736(09)61204-6. PubMed PMID: 19748398.
- 14. Wahl B, O'Brien KL, Greenbaum A, Majumder A, Liu L, Chu Y, Luksic I, Nair H, McAllister DA, Campbell H, Rudan I, Black R, Knoll MD. Burden of Streptococcus pneumoniae

and Haemophilus influenzae type b disease in children in the era of conjugate vaccines: global, regional, and national estimates for 2000-15. Lancet Glob Health. 2018;6(7):e744-e57. Epub 2018/06/16. doi: 10.1016/S2214-109X(18)30247-X. PubMed PMID: 29903376; PMCID: PMC6005122.

- 15. Wasserman MD, Perdrizet J, Grant L, Hayford K, Singh S, Saharia P, Horn EK, Farkouh RA. Clinical and Economic Burden of Pneumococcal Disease Due to Serotypes Contained in Current and Investigational Pneumococcal Conjugate Vaccines in Children Under Five Years of Age. Infect Dis Ther. 2021;10(4):2701-20. Epub 2021/10/12. doi: 10.1007/s40121-021-00544-1. PubMed PMID: 34633639; PMCID: PMC8503717.
- 16. Zhang D, Petigara T, Yang X. Clinical and economic burden of pneumococcal disease in US adults aged 19-64 years with chronic or immunocompromising diseases: an observational database study. BMC Infect Dis. 2018;18(1):436. Epub 2018/08/31. doi: 10.1186/s12879-018-3326-z. PubMed PMID: 30157781; PMCID: PMC6116536.
- 17. Rose MC, Voynow JA. Respiratory tract mucin genes and mucin glycoproteins in health and disease. Physiol Rev. 2006;86(1):245-78. Epub 2005/12/24. doi: 10.1152/physrev.00010.2005. PubMed PMID: 16371599.
- 18. Bergmann S, Rohde M, Chhatwal GS, Hammerschmidt S. alpha-Enolase of Streptococcus pneumoniae is a plasmin(ogen)-binding protein displayed on the bacterial cell surface. Mol Microbiol. 2001;40(6):1273-87. Epub 2001/07/10. doi: 10.1046/j.1365-2958.2001.02448.x. PubMed PMID: 11442827.
- 19. Holmes AR, McNab R, Millsap KW, Rohde M, Hammerschmidt S, Mawdsley JL, Jenkinson HF. The pavA gene of Streptococcus pneumoniae encodes a fibronectin-binding protein

- that is essential for virulence. Mol Microbiol. 2001;41(6):1395-408. Epub 2001/10/03. doi: 10.1046/j.1365-2958.2001.02610.x. PubMed PMID: 11580843.
- 20. Jensch I, Gamez G, Rothe M, Ebert S, Fulde M, Somplatzki D, Bergmann S, Petruschka L, Rohde M, Nau R, Hammerschmidt S. PavB is a surface-exposed adhesin of Streptococcus pneumoniae contributing to nasopharyngeal colonization and airways infections. Mol Microbiol. 2010;77(1):22-43. Epub 2010/05/07. doi: 10.1111/j.1365-2958.2010.07189.x. PubMed PMID: 20444103.
- 21. Cundell DR, Gerard NP, Gerard C, Idanpaan-Heikkila I, Tuomanen EI. Streptococcus pneumoniae anchor to activated human cells by the receptor for platelet-activating factor. Nature. 1995;377(6548):435-8. Epub 1995/10/05. doi: 10.1038/377435a0. PubMed PMID: 7566121.
- 22. Zhang JR, Mostov KE, Lamm ME, Nanno M, Shimida S, Ohwaki M, Tuomanen E. The polymeric immunoglobulin receptor translocates pneumococci across human nasopharyngeal epithelial cells. Cell. 2000;102(6):827-37. Epub 2000/10/13. doi: 10.1016/s0092-8674(00)00071-4. PubMed PMID: 11030626.
- 23. Cron LE, Bootsma HJ, Noske N, Burghout P, Hammerschmidt S, Hermans PWM. Surface-associated lipoprotein PpmA of Streptococcus pneumoniae is involved in colonization in a strain-specific manner. Microbiology (Reading). 2009;155(Pt 7):2401-10. Epub 2009/04/25. doi: 10.1099/mic.0.026765-0. PubMed PMID: 19389773.
- 24. Hermans PW, Adrian PV, Albert C, Estevao S, Hoogenboezem T, Luijendijk IH, Kamphausen T, Hammerschmidt S. The streptococcal lipoprotein rotamase A (SlrA) is a functional peptidyl-prolyl isomerase involved in pneumococcal colonization. J Biol Chem. 2006;281(2):968-76. Epub 2005/11/02. doi: 10.1074/jbc.M510014200. PubMed PMID: 16260779.

- 25. Costerton JW, Lewandowski Z, Caldwell DE, Korber DR, Lappin-Scott HM. Microbial biofilms. Annu Rev Microbiol. 1995;49:711-45. Epub 1995/01/01. doi: 10.1146/annurev.mi.49.100195.003431. PubMed PMID: 8561477.
- 26. Marks LR, Parameswaran GI, Hakansson AP. Pneumococcal interactions with epithelial cells are crucial for optimal biofilm formation and colonization in vitro and in vivo. Infect Immun. 2012;80(8):2744-60. Epub 2012/05/31. doi: 10.1128/IAI.00488-12. PubMed PMID: 22645283; PMCID: PMC3434590.
- 27. Hall-Stoodley L, Hu FZ, Gieseke A, Nistico L, Nguyen D, Hayes J, Forbes M, Greenberg DP, Dice B, Burrows A, Wackym PA, Stoodley P, Post JC, Ehrlich GD, Kerschner JE. Direct detection of bacterial biofilms on the middle-ear mucosa of children with chronic otitis media. JAMA. 2006;296(2):202-11. Epub 2006/07/13. doi: 10.1001/jama.296.2.202. PubMed PMID: 16835426; PMCID: PMC1885379.
- 28. Domenech M, Garcia E, Moscoso M. Biofilm formation in Streptococcus pneumoniae. Microb Biotechnol. 2012;5(4):455-65. Epub 2011/09/13. doi: 10.1111/j.1751-7915.2011.00294.x. PubMed PMID: 21906265; PMCID: PMC3815323.
- 29. Moscoso M, Garcia E, Lopez R. Biofilm formation by Streptococcus pneumoniae: role of choline, extracellular DNA, and capsular polysaccharide in microbial accretion. J Bacteriol. 2006;188(22):7785-95. Epub 2006/08/29. doi: 10.1128/JB.00673-06. PubMed PMID: 16936041; PMCID: PMC1636320.
- 30. Chao Y, Marks LR, Pettigrew MM, Hakansson AP. Streptococcus pneumoniae biofilm formation and dispersion during colonization and disease. Front Cell Infect Microbiol. 2014;4:194. Epub 2015/01/30. doi: 10.3389/fcimb.2014.00194. PubMed PMID: 25629011; PMCID: PMC4292784.

- 31. Domenech M, Garcia E, Prieto A, Moscoso M. Insight into the composition of the intercellular matrix of Streptococcus pneumoniae biofilms. Environ Microbiol. 2013;15(2):502-16. Epub 2012/08/24. doi: 10.1111/j.1462-2920.2012.02853.x. PubMed PMID: 22913814.
- 32. Camilli R, Pantosti A, Baldassarri L. Contribution of serotype and genetic background to biofilm formation by Streptococcus pneumoniae. Eur J Clin Microbiol Infect Dis. 2011;30(1):97-102. Epub 2010/09/17. doi: 10.1007/s10096-010-1060-6. PubMed PMID: 20844912.
- 33. Lattar SM, Wu X, Brophy J, Sakai F, Klugman KP, Vidal JE. A Mechanism of Unidirectional Transformation, Leading to Antibiotic Resistance, Occurs within Nasopharyngeal Pneumococcal Biofilm Consortia. mBio. 2018;9(3). Epub 2018/05/17. doi: 10.1128/mBio.00561-18. PubMed PMID: 29764945; PMCID: PMC5954218.
- 34. Pneumococcal Disease: Symptoms and Complications Centers for Disease Control and Prevention2022 [March 21, 2023]. Available from: <a href="https://www.cdc.gov/pneumococcal/about/symptoms-complications.html">https://www.cdc.gov/pneumococcal/about/symptoms-complications.html</a>.
- 35. Loughran AJ, Orihuela CJ, Tuomanen EI. Streptococcus pneumoniae: Invasion and Inflammation. Microbiol Spectr. 2019;7(2). Epub 2019/03/16. doi: 10.1128/microbiolspec.GPP3-0004-2018. PubMed PMID: 30873934; PMCID: PMC6422050.
- 36. What Is Pneumonia?. National Institutes of Health: National Heart, Lung, and Blood Institute2022 [January 3, 2023]. Available from: <a href="https://www.nhlbi.nih.gov/health/pneumonia">https://www.nhlbi.nih.gov/health/pneumonia</a>.
- 37. Lu L, Lamm ME, Li H, Corthesy B, Zhang JR. The human polymeric immunoglobulin receptor binds to Streptococcus pneumoniae via domains 3 and 4. J Biol Chem. 2003;278(48):48178-87. Epub 2003/09/19. doi: 10.1074/jbc.M306906200. PubMed PMID: 13679368.
- 38. Smith DA, Nehring SM. Bacteremia. StatPearls. Treasure Island (FL)2023.

- 39. Orihuela CJ, Mahdavi J, Thornton J, Mann B, Wooldridge KG, Abouseada N, Oldfield NJ, Self T, Ala'Aldeen DA, Tuomanen EI. Laminin receptor initiates bacterial contact with the blood brain barrier in experimental meningitis models. J Clin Invest. 2009;119(6):1638-46. Epub 2009/05/14. doi: 10.1172/JCI36759. PubMed PMID: 19436113; PMCID: PMC2689107.
- 40. Ring A, Weiser JN, Tuomanen EI. Pneumococcal trafficking across the blood-brain barrier. Molecular analysis of a novel bidirectional pathway. J Clin Invest. 1998;102(2):347-60. Epub 1998/07/17. doi: 10.1172/JCI2406. PubMed PMID: 9664076; PMCID: PMC508893.
- 41. Panackal AA, Williamson KC, van de Beek D, Boulware DR, Williamson PR. Fighting the Monster: Applying the Host Damage Framework to Human Central Nervous System Infections. mBio. 2016;7(1):e01906-15. Epub 2016/01/28. doi: 10.1128/mBio.01906-15. PubMed PMID: 26814182; PMCID: PMC4742705.
- 42. Chandran A, Herbert H, Misurski D, Santosham M. Long-term sequelae of childhood bacterial meningitis: an underappreciated problem. Pediatr Infect Dis J. 2011;30(1):3-6. Epub 2010/08/05. doi: 10.1097/INF.0b013e3181ef25f7. PubMed PMID: 20683377.
- 43. Grabenstein JD, Klugman KP. A century of pneumococcal vaccination research in humans. Clin Microbiol Infect. 2012;18 Suppl 5:15-24. Epub 2012/08/14. doi: 10.1111/j.1469-0691.2012.03943.x. PubMed PMID: 22882735.
- 44. Wright AE, et al. Observations on prophylactic inoculation against pneumococcus infections, and on the results which have been achieved by it. Lancet. 1914;183(4715). doi: https://doi.org/10.1016/S0140-6736(01)56449-1.
- 45. Lister S. The use of pneumococcal vaccine. South African Medical Record. 1924.

- 46. Grabenstein JD. Effectiveness and serotype coverage: key criteria for pneumococcal vaccines for adults. Clin Infect Dis. 2012;55(2):255-8. Epub 2012/04/13. doi: 10.1093/cid/cis354. PubMed PMID: 22495543.
- 47. Daniels CC, Rogers PD, Shelton CM. A Review of Pneumococcal Vaccines: Current Polysaccharide Vaccine Recommendations and Future Protein Antigens. J Pediatr Pharmacol Ther. 2016;21(1):27-35. Epub 2016/03/22. doi: 10.5863/1551-6776-21.1.27. PubMed PMID: 26997927; PMCID: PMC4778694.
- 48. Black S, Shinefield H, Fireman B, Lewis E, Ray P, Hansen JR, Elvin L, Ensor KM, Hackell J, Siber G, Malinoski F, Madore D, Chang I, Kohberger R, Watson W, Austrian R, Edwards K. Efficacy, safety and immunogenicity of heptavalent pneumococcal conjugate vaccine in children. Northern California Kaiser Permanente Vaccine Study Center Group. Pediatr Infect Dis J. 2000;19(3):187-95. Epub 2000/04/05. doi: 10.1097/00006454-200003000-00003. PubMed PMID: 10749457.
- 49. Gierke R, Wodi, A.P., Kobayashi, M. Pneumococcal Disease. Centers for Disease Control and Prevention2021 [December 29, 2022]. Available from: <a href="https://www.cdc.gov/vaccines/pubs/pinkbook/pneumo.html#streptococcus-pneumoniae">https://www.cdc.gov/vaccines/pubs/pinkbook/pneumo.html#streptococcus-pneumoniae</a>.
- 51. Prevnar 20. Food and Drug Administration. 2023. [April 30, 2023]. Available from: <a href="https://www.fda.gov/vaccines-blood-biologics/vaccines/prevnar-20">https://www.fda.gov/vaccines-blood-biologics/vaccines/prevnar-20</a>.

- 52. Singer M, Nambiar S, Valappil T, Higgins K, Gitterman S. Historical and regulatory perspectives on the treatment effect of antibacterial drugs for community-acquired pneumonia. Clin Infect Dis. 2008;47 Suppl 3:S216-24. Epub 2008/11/18. doi: 10.1086/591407. PubMed PMID: 18986293.
- 53. Hansman D, Bullen, M.M. A RESISTANT PNEUMOCOCCUS. The Lancet. 1967;290(7509):264-5. doi: https://doi.org/10.1016/S0140-6736(67)92346-X.
- 54. Schroeder MR, Stephens DS. Macrolide Resistance in Streptococcus pneumoniae. Front Cell Infect Microbiol. 2016;6:98. Epub 2016/10/07. doi: 10.3389/fcimb.2016.00098. PubMed PMID: 27709102; PMCID: PMC5030221.
- 55. Bergman M, Huikko S, Huovinen P, Paakkari P, Seppala H, Finnish Study Group for Antimicrobial R. Macrolide and azithromycin use are linked to increased macrolide resistance in Streptococcus pneumoniae. Antimicrob Agents Chemother. 2006;50(11):3646-50. Epub 2006/08/31. doi: 10.1128/AAC.00234-06. PubMed PMID: 16940064; PMCID: PMC1635217.
- 56. Malhotra-Kumar S, Lammens C, Coenen S, Van Herck K, Goossens H. Effect of azithromycin and clarithromycin therapy on pharyngeal carriage of macrolide-resistant streptococci in healthy volunteers: a randomised, double-blind, placebo-controlled study. Lancet. 2007;369(9560):482-90. Epub 2007/02/13. doi: 10.1016/S0140-6736(07)60235-9. PubMed PMID: 17292768.
- 57. Dion CF, Ashurst JV. Streptococcus Pneumoniae. StatPearls. Treasure Island (FL)2022.
- 58. Easton J, Noble S, Perry CM. Amoxicillin/clavulanic acid: a review of its use in the management of paediatric patients with acute otitis media. Drugs. 2003;63(3):311-40. Epub 2003/01/22. doi: 10.2165/00003495-200363030-00005. PubMed PMID: 12534334.

- 59. Kaplan SL. Management of pneumococcal meningitis. Pediatr Infect Dis J. 2002;21(6):589-91; discussion 613-4. Epub 2002/08/17. doi: 10.1097/00006454-200206000-00034. PubMed PMID: 12182395.
- 60. Skinner R, Cundliffe E, Schmidt FJ. Site of action of a ribosomal RNA methylase responsible for resistance to erythromycin and other antibiotics. J Biol Chem. 1983;258(20):12702-6. Epub 1983/10/25. PubMed PMID: 6195156.
- 61. Johnston NJ, De Azavedo JC, Kellner JD, Low DE. Prevalence and characterization of the mechanisms of macrolide, lincosamide, and streptogramin resistance in isolates of Streptococcus pneumoniae. Antimicrob Agents Chemother. 1998;42(9):2425-6. Epub 1998/09/16. doi: 10.1128/AAC.42.9.2425. PubMed PMID: 9736575; PMCID: PMC105845.
- 62. Ambrose KD, Nisbet R, Stephens DS. Macrolide efflux in Streptococcus pneumoniae is mediated by a dual efflux pump (mel and mef) and is erythromycin inducible. Antimicrob Agents Chemother. 2005;49(10):4203-9. Epub 2005/09/29. doi: 10.1128/AAC.49.10.4203-4209.2005. PubMed PMID: 16189099; PMCID: PMC1251515.
- 63. Chancey ST, Zahner D, Stephens DS. Acquired inducible antimicrobial resistance in Gram-positive bacteria. Future Microbiol. 2012;7(8):959-78. Epub 2012/08/24. doi: 10.2217/fmb.12.63. PubMed PMID: 22913355; PMCID: PMC3464494.
- 64. Gay K, Stephens DS. Structure and dissemination of a chromosomal insertion element encoding macrolide efflux in Streptococcus pneumoniae. J Infect Dis. 2001;184(1):56-65. Epub 2001/06/09. doi: 10.1086/321001. PubMed PMID: 11398110.
- 65. Chancey ST, Zhou X, Zahner D, Stephens DS. Induction of efflux-mediated macrolide resistance in Streptococcus pneumoniae. Antimicrob Agents Chemother. 2011;55(7):3413-22.

- Epub 2011/05/04. doi: 10.1128/AAC.00060-11. PubMed PMID: 21537010; PMCID: PMC3122420.
- 66. Tait-Kamradt A, Clancy J, Cronan M, Dib-Hajj F, Wondrack L, Yuan W, Sutcliffe J. mefE is necessary for the erythromycin-resistant M phenotype in Streptococcus pneumoniae. Antimicrob Agents Chemother. 1997;41(10):2251-5. Epub 1997/10/23. doi: 10.1128/AAC.41.10.2251. PubMed PMID: 9333056; PMCID: PMC164101.
- 67. Chancey ST, Agrawal S, Schroeder MR, Farley MM, Tettelin H, Stephens DS. Composite mobile genetic elements disseminating macrolide resistance in Streptococcus pneumoniae. Front Microbiol. 2015;6:26. Epub 2015/02/25. doi: 10.3389/fmicb.2015.00026. PubMed PMID: 25709602; PMCID: PMC4321634.
- 68. Chittum HS, Champney WS. Ribosomal protein gene sequence changes in erythromycin-resistant mutants of Escherichia coli. J Bacteriol. 1994;176(20):6192-8. Epub 1994/10/01. doi: 10.1128/jb.176.20.6192-6198.1994. PubMed PMID: 7928988; PMCID: PMC196958.
- 69. Wittmann HG, Stoffler G, Apirion D, Rosen L, Tanaka K, Tamaki M, Takata R, Dekio S, Otaka E. Biochemical and genetic studies on two different types of erythromycin resistant mutants of Escherichia coli with altered ribosomal proteins. Mol Gen Genet. 1973;127(2):175-89. Epub 1973/12/20. doi: 10.1007/BF00333665. PubMed PMID: 4589347.
- 70. Johnson CM, Grossman AD. Integrative and Conjugative Elements (ICEs): What They Do and How They Work. Annu Rev Genet. 2015;49:577-601. Epub 2015/10/17. doi: 10.1146/annurev-genet-112414-055018. PubMed PMID: 26473380; PMCID: PMC5180612.
- 71. Celli J, Trieu-Cuot P. Circularization of Tn916 is required for expression of the transposonencoded transfer functions: characterization of long tetracycline-inducible transcripts reading

- through the attachment site. Mol Microbiol. 1998;28(1):103-17. Epub 1998/05/21. doi: 10.1046/j.1365-2958.1998.00778.x. PubMed PMID: 9593300.
- 72. Delavat F, Miyazaki R, Carraro N, Pradervand N, van der Meer JR. The hidden life of integrative and conjugative elements. FEMS Microbiol Rev. 2017;41(4):512-37. Epub 2017/04/04. doi: 10.1093/femsre/fux008. PubMed PMID: 28369623; PMCID: PMC5812530.
- 73. Marra D, Scott JR. Regulation of excision of the conjugative transposon Tn916. Mol Microbiol. 1999;31(2):609-21. Epub 1999/02/23. doi: 10.1046/j.1365-2958.1999.01201.x. PubMed PMID: 10027977.
- 74. Su YA, He P, Clewell DB. Characterization of the tet(M) determinant of Tn916: evidence for regulation by transcription attenuation. Antimicrob Agents Chemother. 1992;36(4):769-78. Epub 1992/04/01. doi: 10.1128/AAC.36.4.769. PubMed PMID: 1323953; PMCID: PMC189400.
- 75. Del Grosso M, Scotto d'Abusco A, Iannelli F, Pozzi G, Pantosti A. Tn2009, a Tn916-like element containing mef(E) in Streptococcus pneumoniae. Antimicrob Agents Chemother. 2004;48(6):2037-42. Epub 2004/05/25. doi: 10.1128/AAC.48.6.2037-2042.2004. PubMed PMID: 15155196; PMCID: PMC415626.
- 76. Cochetti I, Tili E, Vecchi M, Manzin A, Mingoia M, Varaldo PE, Montanari MP. New Tn916-related elements causing erm(B)-mediated erythromycin resistance in tetracycline-susceptible pneumococci. J Antimicrob Chemother. 2007;60(1):127-31. Epub 2007/05/08. doi: 10.1093/jac/dkm120. PubMed PMID: 17483548.
- 77. Del Grosso M, Northwood JG, Farrell DJ, Pantosti A. The macrolide resistance genes erm(B) and mef(E) are carried by Tn2010 in dual-gene Streptococcus pneumoniae isolates belonging to clonal complex CC271. Antimicrob Agents Chemother. 2007;51(11):4184-6. Epub 2007/08/22. doi: 10.1128/AAC.00598-07. PubMed PMID: 17709465; PMCID: PMC2151421.

- 78. Doherty N, Trzcinski K, Pickerill P, Zawadzki P, Dowson CG. Genetic diversity of the tet(M) gene in tetracycline-resistant clonal lineages of Streptococcus pneumoniae. Antimicrob Agents Chemother. 2000;44(11):2979-84. Epub 2000/10/19. doi: 10.1128/AAC.44.11.2979-2984.2000. PubMed PMID: 11036009; PMCID: PMC101589.
- 79. Griffith F. The Significance of Pneumococcal Types. J Hyg (Lond). 1928;27(2):113-59. Epub 1928/01/01. doi: 10.1017/s0022172400031879. PubMed PMID: 20474956; PMCID: PMC2167760.
- 80. McCarty M. Discovering genes are made of DNA. Nature2003 [March 21, 2023]. Available from: <a href="https://www.nature.com/scitable/content/Discovering-genes-are-made-of-DNA-14028/">https://www.nature.com/scitable/content/Discovering-genes-are-made-of-DNA-14028/</a>.
- 81. O'Connor C. Isolating Hereditary Material: Frederick Griffith, Oswald Avery, Alfred Hershey, and Martha Chase. Nature Education2008 [January 17, 2023]. Available from: <a href="https://www.nature.com/scitable/topicpage/isolating-hereditary-material-frederick-griffith-oswald-avery-336/">https://www.nature.com/scitable/topicpage/isolating-hereditary-material-frederick-griffith-oswald-avery-336/</a>.
- 82. Johnsborg O, Havarstein LS. Regulation of natural genetic transformation and acquisition of transforming DNA in Streptococcus pneumoniae. FEMS Microbiol Rev. 2009;33(3):627-42. Epub 2009/04/28. doi: 10.1111/j.1574-6976.2009.00167.x. PubMed PMID: 19396959.
- 83. Morrison DA, Lee MS. Regulation of competence for genetic transformation in Streptococcus pneumoniae: a link between quorum sensing and DNA processing genes. Res Microbiol. 2000;151(6):445-51. Epub 2000/08/29. doi: 10.1016/s0923-2508(00)00171-6. PubMed PMID: 10961457.
- 84. Havarstein LS, Coomaraswamy G, Morrison DA. An unmodified heptadecapeptide pheromone induces competence for genetic transformation in Streptococcus pneumoniae. Proc

- Natl Acad Sci U S A. 1995;92(24):11140-4. Epub 1995/11/21. doi: 10.1073/pnas.92.24.11140. PubMed PMID: 7479953; PMCID: PMC40587.
- 85. Pestova EV, Havarstein LS, Morrison DA. Regulation of competence for genetic transformation in Streptococcus pneumoniae by an auto-induced peptide pheromone and a two-component regulatory system. Mol Microbiol. 1996;21(4):853-62. Epub 1996/08/01. doi: 10.1046/j.1365-2958.1996.501417.x. PubMed PMID: 8878046.
- 86. Straume D, Stamsas GA, Havarstein LS. Natural transformation and genome evolution in Streptococcus pneumoniae. Infect Genet Evol. 2015;33:371-80. Epub 2014/12/03. doi: 10.1016/j.meegid.2014.10.020. PubMed PMID: 25445643.
- 87. Salvadori G, Junges R, Morrison DA, Petersen FC. Competence in Streptococcus pneumoniae and Close Commensal Relatives: Mechanisms and Implications. Front Cell Infect Microbiol. 2019;9:94. Epub 2019/04/20. doi: 10.3389/fcimb.2019.00094. PubMed PMID: 31001492; PMCID: PMC6456647.
- 88. Weyder M, Prudhomme M, Berge M, Polard P, Fichant G. Dynamic Modeling of Streptococcus pneumoniae Competence Provides Regulatory Mechanistic Insights Into Its Tight Temporal Regulation. Front Microbiol. 2018;9:1637. Epub 2018/08/09. doi: 10.3389/fmicb.2018.01637. PubMed PMID: 30087661; PMCID: PMC6066662.
- 89. Havarstein LS, Martin B, Johnsborg O, Granadel C, Claverys JP. New insights into the pneumococcal fratricide: relationship to clumping and identification of a novel immunity factor. Mol Microbiol. 2006;59(4):1297-307. Epub 2006/01/25. doi: 10.1111/j.1365-2958.2005.05021.x. PubMed PMID: 16430701.
- 90. Luo P, Morrison DA. Transient association of an alternative sigma factor, ComX, with RNA polymerase during the period of competence for genetic transformation in Streptococcus

- pneumoniae. J Bacteriol. 2003;185(1):349-58. Epub 2002/12/18. doi: 10.1128/JB.185.1.349-358.2003. PubMed PMID: 12486073; PMCID: PMC141820.
- 91. Steinmoen H, Knutsen E, Havarstein LS. Induction of natural competence in Streptococcus pneumoniae triggers lysis and DNA release from a subfraction of the cell population. Proc Natl Acad Sci U S A. 2002;99(11):7681-6. Epub 2002/05/29. doi: 10.1073/pnas.112464599. PubMed PMID: 12032343; PMCID: PMC124321.
- 92. Laurenceau R, Pehau-Arnaudet G, Baconnais S, Gault J, Malosse C, Dujeancourt A, Campo N, Chamot-Rooke J, Le Cam E, Claverys JP, Fronzes R. A type IV pilus mediates DNA binding during natural transformation in Streptococcus pneumoniae. PLoS Pathog. 2013;9(6):e1003473. Epub 2013/07/05. doi: 10.1371/journal.ppat.1003473. PubMed PMID: 23825953; PMCID: PMC3694846.
- 93. Oliveira V, Aschtgen MS, van Erp A, Henriques-Normark B, Muschiol S. The Role of Minor Pilins in Assembly and Function of the Competence Pilus of Streptococcus pneumoniae. Front Cell Infect Microbiol. 2021;11:808601. Epub 2022/01/11. doi: 10.3389/fcimb.2021.808601. PubMed PMID: 35004361; PMCID: PMC8727766.
- 94. Lam T, Ellison CK, Eddington DT, Brun YV, Dalia AB, Morrison DA. Competence pili in Streptococcus pneumoniae are highly dynamic structures that retract to promote DNA uptake. Mol Microbiol. 2021;116(2):381-96. Epub 2021/03/24. doi: 10.1111/mmi.14718. PubMed PMID: 33754381.
- 95. Berge M, Moscoso M, Prudhomme M, Martin B, Claverys JP. Uptake of transforming DNA in Gram-positive bacteria: a view from Streptococcus pneumoniae. Mol Microbiol. 2002;45(2):411-21. Epub 2002/07/19. doi: 10.1046/j.1365-2958.2002.03013.x. PubMed PMID: 12123453.

- 96. Berge MJ, Kamgoue A, Martin B, Polard P, Campo N, Claverys JP. Midcell recruitment of the DNA uptake and virulence nuclease, EndA, for pneumococcal transformation. PLoS Pathog. 2013;9(9):e1003596. Epub 2013/09/17. doi: 10.1371/journal.ppat.1003596. PubMed PMID: 24039578; PMCID: PMC3764208.
- 97. Draskovic I, Dubnau D. Biogenesis of a putative channel protein, ComEC, required for DNA uptake: membrane topology, oligomerization and formation of disulphide bonds. Mol Microbiol. 2005;55(3):881-96. Epub 2005/01/22. doi: 10.1111/j.1365-2958.2004.04430.x. PubMed PMID: 15661011; PMCID: PMC3835657.
- 98. Morrison DA. Transformation in pneumococcus: existence and properties of a complex involving donor deoxyribonucleate single strands in eclipse. J Bacteriol. 1977;132(2):576-83. Epub 1977/11/01. doi: 10.1128/jb.132.2.576-583.1977. PubMed PMID: 21166; PMCID: PMC221898.
- 99. Morrison DA, Mortier-Barriere I, Attaiech L, Claverys JP. Identification of the major protein component of the pneumococcal eclipse complex. J Bacteriol. 2007;189(17):6497-500. Epub 2007/07/03. doi: 10.1128/JB.00687-07. PubMed PMID: 17601792; PMCID: PMC1951911. 100. Mortier-Barriere I, Velten M, Dupaigne P, Mirouze N, Pietrement O, McGovern S, Fichant G, Martin B, Noirot P, Le Cam E, Polard P, Claverys JP. A key presynaptic role in transformation for a widespread bacterial protein: DprA conveys incoming ssDNA to RecA. Cell. 2007;130(5):824-36. Epub 2007/09/07. doi: 10.1016/j.cell.2007.07.038. PubMed PMID: 17803906.
- 101. Marie L, Rapisarda C, Morales V, Berge M, Perry T, Soulet AL, Gruget C, Remaut H, Fronzes R, Polard P. Bacterial RadA is a DnaB-type helicase interacting with RecA to promote

- bidirectional D-loop extension. Nat Commun. 2017;8:15638. Epub 2017/06/01. doi: 10.1038/ncomms15638. PubMed PMID: 28561029; PMCID: PMC5512693.
- 102. Desai BV, Morrison DA. An unstable competence-induced protein, CoiA, promotes processing of donor DNA after uptake during genetic transformation in Streptococcus pneumoniae. J Bacteriol. 2006;188(14):5177-86. Epub 2006/07/04. doi: 10.1128/JB.00103-06. PubMed PMID: 16816189; PMCID: PMC1539964.
- 103. Desai BV, Morrison DA. Transformation in Streptococcus pneumoniae: formation of eclipse complex in a coiA mutant implicates CoiA in genetic recombination. Mol Microbiol. 2007;63(4):1107-17. Epub 2007/01/20. doi: 10.1111/j.1365-2958.2006.05558.x. PubMed PMID: 17233830.
- 104. Berg KH, Ohnstad HS, Havarstein LS. LytF, a novel competence-regulated murein hydrolase in the genus Streptococcus. J Bacteriol. 2012;194(3):627-35. Epub 2011/11/30. doi: 10.1128/JB.06273-11. PubMed PMID: 22123253; PMCID: PMC3264080.
- 105. Claverys JP, Martin B, Havarstein LS. Competence-induced fratricide in streptococci. Mol Microbiol. 2007;64(6):1423-33. Epub 2007/06/09. doi: 10.1111/j.1365-2958.2007.05757.x. PubMed PMID: 17555432.
- 106. Johnsborg O, Eldholm V, Bjornstad ML, Havarstein LS. A predatory mechanism dramatically increases the efficiency of lateral gene transfer in Streptococcus pneumoniae and related commensal species. Mol Microbiol. 2008;69(1):245-53. Epub 2008/05/20. doi: 10.1111/j.1365-2958.2008.06288.x. PubMed PMID: 18485065.
- 107. Eldholm V, Johnsborg O, Haugen K, Ohnstad HS, Havarstein LS. Fratricide in Streptococcus pneumoniae: contributions and role of the cell wall hydrolases CbpD, LytA and

- LytC. Microbiology (Reading). 2009;155(Pt 7):2223-34. Epub 2009/04/25. doi: 10.1099/mic.0.026328-0. PubMed PMID: 19389766.
- 108. Briaud P, Carroll RK. Extracellular Vesicle Biogenesis and Functions in Gram-Positive Bacteria. Infect Immun. 2020;88(12). Epub 2020/09/30. doi: 10.1128/IAI.00433-20. PubMed PMID: 32989035; PMCID: PMC7671900.
- 109. Dell'Annunziata F, Folliero V, Giugliano R, De Filippis A, Santarcangelo C, Izzo V, Daglia M, Galdiero M, Arciola CR, Franci G. Gene Transfer Potential of Outer Membrane Vesicles of Gram-Negative Bacteria. Int J Mol Sci. 2021;22(11). Epub 2021/07/03. doi: 10.3390/ijms22115985. PubMed PMID: 34205995; PMCID: PMC8198371.
- 110. Domingues S, Nielsen KM. Membrane vesicles and horizontal gene transfer in prokaryotes. Curr Opin Microbiol. 2017;38:16-21. Epub 2017/04/26. doi: 10.1016/j.mib.2017.03.012. PubMed PMID: 28441577.
- 111. Johnston EL, Zavan L, Bitto NJ, Petrovski S, Hill AF, Kaparakis-Liaskos M. Planktonic and Biofilm-Derived Pseudomonas aeruginosa Outer Membrane Vesicles Facilitate Horizontal Gene Transfer of Plasmid DNA. Microbiol Spectr. 2023;11(2):e0517922. Epub 2023/03/23. doi: 10.1128/spectrum.05179-22. PubMed PMID: 36946779; PMCID: PMC10100964.
- 112. Rumbo C, Fernandez-Moreira E, Merino M, Poza M, Mendez JA, Soares NC, Mosquera A, Chaves F, Bou G. Horizontal transfer of the OXA-24 carbapenemase gene via outer membrane vesicles: a new mechanism of dissemination of carbapenem resistance genes in Acinetobacter baumannii. Antimicrob Agents Chemother. 2011;55(7):3084-90. Epub 2011/04/27. doi: 10.1128/AAC.00929-10. PubMed PMID: 21518847; PMCID: PMC3122458.
- 113. Yaron S, Kolling GL, Simon L, Matthews KR. Vesicle-mediated transfer of virulence genes from Escherichia coli O157:H7 to other enteric bacteria. Appl Environ Microbiol.

- 2000;66(10):4414-20. Epub 2000/09/30. doi: 10.1128/AEM.66.10.4414-4420.2000. PubMed PMID: 11010892; PMCID: PMC92318.
- 114. Klieve AV, Yokoyama MT, Forster RJ, Ouwerkerk D, Bain PA, Mawhinney EL. Naturally occurring DNA transfer system associated with membrane vesicles in cellulolytic Ruminococcus spp. of ruminal origin. Appl Environ Microbiol. 2005;71(8):4248-53. Epub 2005/08/09. doi: 10.1128/AEM.71.8.4248-4253.2005. PubMed PMID: 16085810; PMCID: PMC1183309.
- 115. Olaya-Abril A, Prados-Rosales R, McConnell MJ, Martin-Pena R, Gonzalez-Reyes JA, Jimenez-Munguia I, Gomez-Gascon L, Fernandez J, Luque-Garcia JL, Garcia-Lidon C, Estevez H, Pachon J, Obando I, Casadevall A, Pirofski LA, Rodriguez-Ortega MJ. Characterization of protective extracellular membrane-derived vesicles produced by Streptococcus pneumoniae. J Proteomics. 2014;106:46-60. Epub 2014/04/29. doi: 10.1016/j.jprot.2014.04.023. PubMed PMID: 24769240.
- 116. Domenech M, Garcia, E. Autolysin-Independent DNA Release in Streptococcus pneumoniae Invitro Biofilms. Clinical Infectious Diseases: Open Access. 2018;2(3):114.

**Chapter 2:** Dissemination of Tn916-related integrative and conjugative elements in *Streptococcus* pneumoniae occurs by transformation and homologous recombination in nasopharyngeal biofilms

Brenda S. Antezana<sup>a</sup>, Sarah Lohsen<sup>b</sup>, Xueqing Wu<sup>c</sup>, Jorge E. Vidal<sup>d</sup>, Yih-Ling Tzeng<sup>b</sup>, David S. Stephens<sup>b</sup>

<sup>a</sup> Microbiology and Molecular Genetics Program, Graduate Division of Biological and Biomedical Sciences, Emory University Laney Graduate School, Atlanta, Georgia, USA

<sup>b</sup> Department of Medicine, Division of Infectious Diseases, Emory University School of Medicine, Atlanta, Georgia, USA

<sup>c</sup> Department of Infectious Diseases, Sir Run Run Shaw Hospital, Zhejiang University College of Medicine, Hangzhou, China

<sup>d</sup> Department of Cell and Molecular Biology, University of Mississippi Medical Center, Jackson, Mississippi, USA

#Address correspondence to David S. Stephens, dstep01@emory.edu.

The work of this chapter was published on March 13, 2023 in the American Society for Microbiology's *Microbiology Spectrum* journal.

#### **Citation:**

Antezana BS, Lohsen S, Wu X, Vidal JE, Tzeng YL, Stephens DS. Dissemination of Tn916-Related Integrative and Conjugative Elements in *Streptococcus pneumoniae* Occurs by Transformation and Homologous Recombination in Nasopharyngeal Biofilms. Microbiol Spectr. 2023:e0375922. Epub 2023/03/14. doi: 10.1128/spectrum.03759-22. PubMed PMID: 36912669.

### B. Antezana performed laboratory experiments, analyzed data, wrote and edited the paper.

#### **ABSTRACT**

Multidrug resistance in *Streptococcus pneumoniae* (or pneumococcus) continues to be a global challenge. An important class of antibiotic resistance determinants disseminating in S. pneumoniae are >20-kb Tn916-related integrative and conjugative elements (ICEs), such as Tn2009, Tn6002, and Tn2010. Although conjugation has been implicated as the transfer mechanism for ICEs in several bacteria, including S. pneumoniae, the molecular basis for widespread dissemination of pneumococcal Tn916-related ICEs remains to be fully elucidated. We found that Tn2009 acquisition was not detectable via in vitro transformation nor conjugative mating with donor GA16833, yielding a transfer frequency of <10<sup>-7</sup>. GA16833 Tn2009 conjugative gene expression was not significantly induced, and ICE circular intermediate formation was not detected in biofilms. Consistently, Tn2009 transfer efficiency in biofilms was not affected by deletion of the ICE conjugative gene ftsK. However, GA16833 Tn2009 transfer occurred efficiently at a recombination frequency (rF) of 10<sup>-4</sup> in dual-strain biofilms formed in a human nasopharyngeal cell bioreactor. DNase I addition and deletions of the early competence gene comE or transformation apparatus genes comEA and comEC in the D39 recipient strain prevented Tn2009 acquisition (rF of <10<sup>-7</sup>). Genome sequencing and single nucleotide polymorphism analyses of independent recombinants of recipient genotype identified ~33- to ~55-kb donor DNAs containing intact Tn2009, supporting homologous recombination. Additional pneumococcal donor and recipient combinations were demonstrated to efficiently transfer Tn916-related ICEs at a rF of 10<sup>-1</sup> <sup>4</sup> in the biofilms. Tn916-related ICEs horizontally disseminate at high frequency in human nasopharyngeal S. pneumoniae biofilms by transformation and homologous recombination of >30kb DNA fragments into the pneumococcal genome.

#### **IMPORTANCE**

The World Health Organization has designated *Streptococcus pneumoniae* as a priority pathogen for research and development of new drug treatments due to extensive multidrug resistance. Multiple strains of *S. pneumoniae* colonize and form mixed biofilms in the human nasopharynx, which could enable exchange of antibiotic resistance determinants. Tn916-related integrative and conjugative elements (ICEs) are largely responsible for the widespread presence of macrolide and tetracycline resistance in *S. pneumoniae*. Utilizing a system that simulates colonization of donor and recipient *S. pneumoniae* strains in the human nasopharynx, efficient transfer of Tn916-related ICEs occurred in human nasopharyngeal biofilms, in contrast to *in vitro* conditions of planktonic cells with exogenous DNA. This high-frequency Tn916-related ICE transfer between *S. pneumoniae* strains in biofilms was due to transformation and homologous recombination, not conjugation. Understanding the molecular mechanism for dissemination of Tn916-related ICEs can facilitate the design of new strategies to combat antibiotic resistance.

#### INTRODUCTION

Streptococcus pneumoniae (or pneumococcus) is a Gram-positive bacterial human pathogen and inhabitant of the human nasopharynx. Colonization with pneumococci occurs during early childhood, with carriage rates ranging from 20 to 93.4% and persisting into adulthood at lower levels<sup>(1-3)</sup>. S. pneumoniae may remain as a commensal in the nasopharynx, spread to other mucosal sites and cause otitis media or pneumonia, or it may invade the bloodstream, resulting in bacteremia or meningitis<sup>(4)</sup>. Individuals at risk for invasive pneumococcal disease are children less than 2 years of age, those over 65 years of age, and immunocompromised individuals with other underlying chronic conditions<sup>(5)</sup>. Although new, effective pneumococcal conjugate vaccines are available, invasive pneumococcal disease still poses as a global public health concern. In 2017, the World Health Organization (WHO) recognized S. pneumoniae as a priority pathogen due to extensive multidrug resistance<sup>(6)</sup>. The widespread use of antibiotics, such as macrolides for treatment of community-acquired pneumonia and other upper respiratory infections, has led to marked increases in S. pneumoniae antibiotic resistance<sup>(7, 8)</sup>. The horizontal transfer of resistance determinants followed by the selection of resistant strains is the major driver for the development of antibiotic resistance in S. pneumoniae, yet the molecular mechanisms of resistance determinant dissemination have not been clearly defined.

Large, mobile genetic elements known as integrative and conjugative elements (ICEs) of the Tn916 family are responsible for tetracycline and macrolide resistance in *S. pneumoniae*. Tn916-related ICEs that have been widely identified in *S. pneumoniae* include Tn2009 (23.5 kb), Tn6002 (20.8 kb), and Tn2010 (26.3 kb)<sup>(9-13)</sup>. Although prototype Tn916 (18.0 kb) and other classes of ICEs are disseminated via conjugation in several Gram-positive species, such as *Bacillus subtilis*, *Enterococcus faecalis*, *Clostridium difficile*, and many streptococcal species<sup>(14-16)</sup>, the role of

conjugation as an efficient horizontal exchange process for Tn916-related ICEs in *S. pneumoniae* is unclear. While conjugation of *S. pneumoniae* Tn6002 into *Streptococcus pyogenes* has been demonstrated by mating experiments at the low frequency of 10<sup>-8</sup>, Tn2009 and Tn2010 did not conjugate into *S. pneumoniae*<sup>(10, 11)</sup>. Another common horizontal genetic exchange strategy is transformation as *S. pneumoniae* naturally becomes competent for extracellular DNA uptake during growth<sup>(17)</sup>. Transformation has long been associated with *S. pneumoniae* genome evolution<sup>(18, 19)</sup>, particularly for acquiring point mutations and small ~1- to ~5-kb determinants conferring antibiotic resistance.

To investigate the molecular mechanism for horizontal dissemination of Tn916-related ICEs among *S. pneumoniae* strains, we utilized a bioreactor system consisting of a dual-strain pneumococcal biofilm on human nasopharyngeal cells<sup>(20)</sup> with Tn2009 as a model. Gene expression, mutation studies in key conjugative and transformation genes, ICE circular intermediate quantification, genome sequencing, and single nucleotide polymorphism (SNP) analyses revealed that transformation and homologous recombination are responsible for efficient horizontal transfer of *S. pneumoniae* Tn2009. These mechanistic observations were applicable to additional Tn916-related ICEs and *S. pneumoniae* strains.

#### **RESULTS**

Classic *in vitro* transformation failed to demonstrate acquisition of Tn916-related ICEs by S. pneumoniae.

*S. pneumoniae* is naturally competent for extracellular DNA (eDNA) uptake. Classic *in vitro* transformation assays were used to examine uptake of genomic DNA carrying ICEs. Planktonic cells of D39<sup>Str</sup> or TIGR4, treated with the cognate synthetic competence stimulating peptide (CSP) to initiate competence development, were incubated with various amounts of genomic DNA.

Control reactions for competency demonstrated that D39<sup>Str</sup> acquired trimethoprim (Tmp) resistance (*fola/*1100L)<sup>(21)</sup> at a recombination frequency (rF) of 4.08x10<sup>-5</sup>±4.33x10<sup>-5</sup> per μg DNA, whereas TIGR4 obtained streptomycin (Str) resistance (*rpsL/*K56T)<sup>(22)</sup> at a rF of 1.03x10<sup>-5</sup>±7.88x10<sup>-6</sup> per μg DNA. However, *in vitro* transformation of D39<sup>Str</sup> under analogous conditions with genomic DNA harboring Tn2009 (23.5 kb) or Tn2010 (26.3 kb) yielded no recombinants with tetracycline (Tet) resistance and the rFs were <1.13x10<sup>-7</sup>±1.04x10<sup>-7</sup> and <2.68x10<sup>-8</sup> for Tn2009 and Tn2010, respectively. Similarly, no Tet-resistant TIGR4 recombinants were recovered with genomic DNA carrying Tn2009 (rF of <3.75x10<sup>-8</sup>±3.63x10<sup>-9</sup>). Agarose gel electrophoresis confirmed that purified genomic DNA preparations contained fragments significantly larger than the ICEs (data not shown) and increasing CSP concentrations from 100 ng/mL to 5000 ng/mL in *in vitro* transformations did not enhance recombination frequencies for uptake of Str resistance. Thus, classic *in vitro* transformation aided by exogenous CSP did not result in uptake of Tn916-related ICEs by D39 nor TIGR4.

## Efficient transfer of pneumococcal Tn916-related ICEs occurred in dual-strain biofilms formed on human nasopharyngeal cells.

A continuous flow bioreactor system, characterized by formation of dual-strain biofilms on a confluent monolayer of human pharyngeal Detroit 562 cells at 35°C has previously been shown to yield high rF for transfer of Str, Tmp, and Tet (*tetM*-mediated) resistance between D39 and TIGR4<sup>(20)</sup>. Thus, we investigated pneumococcal Tn916-related ICE dissemination using the bioreactor system with a 6-hr incubation, which was previously found to be sufficient for efficient recombination. The ICE donor clinical isolates GA16833<sup>Tet/Ery</sup> (serotype 19F with Tn2009) or GA47281<sup>Tet/Ery</sup> (serotype 19F with Tn2010), were coinoculated in the bioreactor with designated

recipient D39 (serotype 2) derivatives containing either Str (D39<sup>Str</sup>) or dual Str and Tmp (D39<sup>Str/Tmp</sup>) resistance.

When GA16833<sup>Tet/Ery</sup> served as the Tn2009 donor, the rFs of Tet+Str resistance was 2.60x10<sup>-4</sup>±2.08x10<sup>-4</sup> for recipient D39<sup>Str/Tmp</sup> (Fig 1) and 1.34x10<sup>-4</sup>±7.02x10<sup>-5</sup> for recipient D39<sup>Str</sup>. The rF of 10<sup>-4</sup> obtained in the bioreactor system represented an ~1,000-fold enhancement over the *in vitro* rF of <10<sup>-7</sup> where no recombinants were recovered. Similarly, with coinoculation of the recipient D39<sup>Str/Tmp</sup> and the Tn2010 donor GA47281<sup>Tet/Ery</sup>, we obtained a rF of 1.34x10<sup>-4</sup>±1.62x10<sup>-4</sup> for Tetresistant recombinants of D39<sup>Str/Tmp</sup>, once again demonstrating an ~1,000-fold enhancement over the *in vitro* transformation (Fig 1). Additional selection combinations, Ery+Str, Tet+Ery+Str, and Ery+Str+Tmp, were also tested and yielded similar rFs (Table S3). When Tet was used for recombinant selection, Tn2009 and Tn2010 yielded comparable rFs (10<sup>-4</sup>). However, when Ery was included in the selection, higher rF values were observed for Tn2010 relative to those obtained with Tn2009 (Table S3). This difference could be due to the constitutively expressed *ermB* on Tn2010, whereas Tn2009 carries inducible Ery resistance on the macrolide efflux genetic assembly (Mega) element.

# Conjugation was not involved in the highly efficient transfer of Tn916-related ICEs (>20 kb) between pneumococci in bioreactor biofilms.

Transcriptional regulation of conjugation genes and the molecular mechanism resulting in Tn916 conjugative transfer has been well characterized<sup>(23)</sup>. Conjugation of Tn916 is stimulated by tetracycline at the *tetM* promoter, which mediates antisense mRNA derepression of downstream regulatory genes<sup>(23, 24)</sup> and subsequently results in expression of the *xis* and *int* genes encoding essential enzymes for the excision of Tn916<sup>(23, 24)</sup> as well as the formation of the Tn916 circular intermediate (CI). CI formation occurs via binding of coupling sequences on the 5' and 3' ends of

the ICE<sup>(23, 25, 26)</sup>. This physical association of the 5' and 3' ends of the circularized Tn916 allows for upregulated transcription at the 3' end of Tn916 to extend through to the conjugative genes at the 5' end, encoding the necessary conjugative machinery, such as the type IV secretion system. Subsequent passage of a single-stranded Tn916 DNA from a donor to the recipient cell occurs<sup>(25)</sup>, resulting in the integration of Tn916 into the recipient genome via precise site-specific recombination<sup>(27)</sup>. While conjugation of Tn916 and other ICEs has been demonstrated in Grampositive bacteria, we obtained several lines of evidence to exclude conjugation as the mechanism responsible for Tn2009 dissemination among *S. pneumoniae* as described below.

#### Conjugative gene expression in Tn2009 was limited.

We performed BLASTN analysis and demonstrated that all three pneumococcal Tn916-related ICEs contained genes encoding the excisionase, Xis, and the integrase, Int, which are required for Tn916 excision and site-specific recombination<sup>(26, 28, 29)</sup>. Tn916-related ICEs also contained open reading frames (ORFs) that had >99% sequence identity to the corresponding ORFs in Tn916 involved in conjugative transfer (Fig 2).

Expression of *xis* and *int* is coupled with tetracycline-inducible *tetM* transcription and subinhibitory concentrations of tetracycline result in enhanced conjugative transfer of Tn916 in *E. faecalis* and *B. subtilis*<sup>(23, 30)</sup>. We first compared the basal expression of conjugative genes in pneumococcal Tn2009 with the prototype Tn916 in a *B. subtilis* donor strain CMJ253<sup>(31)</sup>. Expression of *tetM*, *int*, *orf20* (relaxase), and *ftsK* in Tn2009 was significantly lower: *tetM* and *int* were expressed 19.7- and 32.4-fold lower, respectively, while *orf20* and *ftsK* were expressed about 300-fold lower than the corresponding genes in Tn916.

Tetracycline induces transcriptional upregulation of conjugative genes at the 5' end of  $Tn916^{(23)}$ . To investigate if such a regulatory coupling was present in pneumococcal Tn2009, we

grew the Tn2009-containing GA16833 strain (Tet MIC of 24 µg/mL) and the Tn916-containing CMJ253 strain in the presence or absence of 2.5 µg/mL tetracycline for 2.5 hours<sup>(27)</sup>. As expected for Tn916, there was a 4-fold induction of *tetM*, and similar levels of induction were detected for *orf20* and *ftsK* (Table 1). There was no induction of *int* expression in Tn916 (Table 1), consistent with the observation by Celli et al. using Northern blotting<sup>(25)</sup>. In contrast, while *tetM* expression in Tn2009 was induced nearly 28-fold by a sublethal concentration of tetracycline, no concerted upregulation of conjugative genes was detected and only ~2.3- to ~3.7-fold changes were seen in *int*, *orf20*, and *ftsK* (Table 1) relative to no-tetracycline controls. Thus, unlike Tn916, conjugative gene expression was not coupled to *tetM* induction in Tn2009.

We also investigated if conjugative gene expression in the Tn2009 donor was induced in the dual-strain biofilm of recipient D39<sup>Str</sup> and donor GA16833Δ*comCDE::cat*<sup>Cm/Tet/Ery</sup> (BASP1), where Tn2009 transfer was detected at high frequency. When normalized to broth cultures of the single donor strain BASP1 or a 1:1 mixture of donor and recipient strains, there was no induction of conjugative genes in biofilms, with a fold change of 1.13 or 1.04 for *int* and 0.28 or 0.94 for *orf20*, respectively. These data suggested that conjugative gene expression from pneumococcal Tn2009 was minimal and not induced under the bioreactor biofilm conditions, and thus was unlikely to support efficient Tn2009 transfer.

#### There was no detectable circular intermediate formation of Tn2009.

Circular intermediate (CI) formation resulting from excision from the donor chromosome and circularization of Tn916, mediated by Xis and Int proteins, is a prerequisite for Tn916 conjugative transfer and is induced by tetracycline<sup>(25, 26)</sup>. The circular junction is the same between the prototype Tn916 and Tn2009. Thus using quantitative PCR (qPCR), we quantified CIs derived from Tn2009 in GA16833 and Tn916 in CMJ253 with tetracycline induction. The CI copy number

was normalized to the chromosomal copy number of ftsK. The positive control, B. subtilis donor CMJ253, produced a Tn916 CI/chromosome ratio of  $2.50x10^{-2}\pm1.42x10^{-2}$ , while the S. pneumoniae donor GA16833 yielded no detectable Tn2009 CIs, with a ratio of  $<2.48x10^{-7}\pm1.47x10^{-7}$ .

We further examined CI production under two additional conditions<sup>(15, 32)</sup>: mating assays used for conjugation and bioreactor biofilm reactions that yielded efficient Tn2009 transfer. A positive control of donor CMJ253 broth culture in the absence of tetracycline produced a Tn916 CI ratio of 9.66x10<sup>-3</sup>±1.06x10<sup>-3</sup>, while the bioreactor samples did not yield detectable Tn2009 CIs, with a ratio of <3.09x10<sup>-7</sup>±1.56x10<sup>-7</sup> (Fig 3A). Mating assays of *B. subtilis* donor CMJ253 and recipient CAL419 resulted in a Tn916 CI ratio of 1.17x10<sup>-2</sup>±3.14x10<sup>-3</sup>, while mating reactions of *S. pneumoniae* donor GA16833 and recipient D39Δ*comE::cat*<sup>Str</sup> (BASP2) did not yield detectable CIs (ratio of <5.87x10<sup>-9</sup>±7.11x10<sup>-9</sup>) (Fig 3A). These data confirmed the lack of pneumococcal Tn2009 CI formation, either by tetracycline induction or under dual-strain conditions, such as mating reactions and bioreactor biofilms.

#### Mating reactions did not support conjugative transfer of Tn2009.

Transfer of large mobile genetic elements via conjugation has been observed in mating experiments<sup>(15, 32)</sup>. We reproduced this observation with mating experiments of *B. subtilis* Tn916 donor CMJ253 and two *B. subtilis* recipients, LDW737<sup>(27)</sup> and CAL419<sup>(31)</sup>. We obtained conjugation frequencies (cFs) of 1.27x10<sup>-5</sup>±8.76x10<sup>-6</sup> and 1.82x10<sup>-5</sup>±2.14x10<sup>-5</sup>, respectively (Fig 3B). However, mating between the *S. pneumoniae* Tn2009 donor GA16833 and BASP2, an incompetent *S. pneumoniae* recipient used to eliminate the contribution of transformation, yielded no transconjugants, with an estimated cF of <1.02x10<sup>-8</sup>±8.80x10<sup>-9</sup> (Fig 3B). Santoro et al.<sup>(15)</sup> had shown that conjugative transfer of Tn5251 occurred in a strain-dependent manner in *S.* 

*pneumoniae*. Thus, three additional recipients were investigated: TIGR4 $\Delta comE$ :: $cat^{Tmp}$  (BASP5), GA40410 $\Delta comE$ :: $cat^{Tmp}$  (BASP6), and GA43265 $\Delta comE$ :: $cat^{Tmp}$  (BASP7). Mating experiments with the donor GA16833 did not yield Tn2009 Tet-resistant transconjugants, and the cFs were <3.71x10<sup>-9</sup>±3.53x10<sup>-9</sup>, <1.35x10<sup>-9</sup>±6.82x10<sup>-10</sup>, and <5.07x10<sup>-9</sup>±4.57x10<sup>-9</sup>, respectively (Fig 3B).

#### Mutation of ftsK had no effect on the transfer of Tn2009 in mixed nasopharyngeal biofilms.

During conjugation, Orf21 (FtsK) of Tn916 serves as a coupling protein for translocating the DNA through the secretion system from the donor to recipient cell<sup>(33-35)</sup>. Given the critical role of a coupling protein in the conjugative machinery, an *ftsK* mutant was created in the donor strain (GA16833Δ*ftsK::cat*<sup>Tet/Ery</sup> [BASP3]). Coinoculation of donor BASP3 with recipient D39<sup>Str</sup> in the bioreactor yielded a rF of ~10<sup>-4</sup>, similar to that obtained when wildtype GA16833 served as the Tn2009 donor. Thus, disruption of conjugation via the *ftsK* mutation had no impact on the transfer of Tn2009 (Fig 3C), supporting that conjugation played no significant role in the highly efficient dissemination of Tn2009 under the bioreactor biofilm conditions.

### Competence development and transformation machinery in the pneumococcal recipient were required for efficient ICE uptake in human nasopharyngeal biofilms.

Natural competence for DNA uptake via transformation is an important mechanism for horizontal gene transfer in *S. pneumoniae*. Early competence development depends on expression of the *comCDE* operon, encoding a competence-stimulating peptide (CSP), ComC, a histidine kinase, ComD, and a response regulator, ComE<sup>(19, 36)</sup>. Recipient BASP2 (D39 $\Delta$ *comE*), confirmed by *in vitro* transformation to be incompetent in acquiring point mutations, was examined in the bioreactor with donor GA16833. As shown in Figure 4A, no Tet-resistant recombinants were observed (rF of <1.21x10<sup>-7</sup>±6.35x10<sup>-8</sup>), suggesting that recipient competence initiation was critical for Tn2009 uptake.

The involvement of two late competence proteins, ComEA and ComEC, was also examined. ComEA is a DNA receptor that binds double-stranded DNA captured by the type IV pilus as it retracts, and the ComEC protein channel subsequently imports single-stranded DNA fragments<sup>(37)</sup>. The *comEA* and *comEC* genes, which are transcribed in tandem, were deleted and replaced with the *cat* cassette in strain D39<sup>Str</sup>. The recipient D39Δ*comEA/EC::cat*<sup>Str</sup> double mutant (BASP4), when coinoculated with donor GA16833 in the bioreactor, yielded no detectable Tet-resistant recombinants and a rF of <8.34x10<sup>-8</sup>±4.16x10<sup>-8</sup> (Fig 4A). When recovered from bioreactor experiments, BASP2 and BASP4 recipients were at similar cell counts to that of donor GA16833, indicating that rF reductions were not caused by growth defects or lower mutant densities relative to the donor strain (Fig 4B).

As extracellular DNA (eDNA) levels influence transformation efficiency, we recovered eDNA in spent medium from the bioreactor experiments<sup>(20)</sup> and quantified eDNA concentrations of each strain using qPCR with serogroup-specific primers. Comparable eDNA concentrations were recovered from both wildtype donor GA16833 and wildtype recipient D39<sup>Str</sup> (Fig 4C) as well as for wildtype donor GA16833 and recipient BASP2 (Fig S1). Additionally, the consequence of eDNA degradation was investigated by treating the biofilm with exogenous DNase I during a 6-hour incubation. Compared to the parallel positive control of no treatment (rF of 2.60x10<sup>-4</sup>±2.08x10<sup>-4</sup>), DNase I treatment resulted in no recombinant recovery, with an estimated rF of <5.34x10<sup>-7</sup>±4.34x10<sup>-7</sup> (Fig 4D). Thus, eDNA degradation eliminated Tn2009 transfer.

The increase in rF of Tn2009 transfer in the bioreactor relative to that observed by *in vitro* transformation implied differential competence development under these two conditions, and we hypothesized that competence gene expression would be higher in the bioreactor environment. As no synthetic CSP was added in the bioreactor, the comparison was made with *in vitro* 

transformation reactions without CSP added. Coinoculating in the bioreactor a D39<sup>Ery/Str</sup> recipient and the BASP1 donor with a  $\Delta comCDE$  deletion to avoid detecting donor com gene expression, comD and comE expression in the D39 recipient was about 120-fold greater in the bioreactor biofilm than under the  $in\ vitro$  transformation condition (Fig 4E). Interestingly, this recipient upregulation of early com genes in the bioreactor biofilm was also much greater than that of classic  $in\ vitro$  transformation reactions, where 100 ng/mL synthetic CSP induced 83- and 57-fold increases in comD and comE expression, respectively, compared to reactions without CSP addition. The higher recipient competence gene expression in the donor GA16833 and recipient D39 mixed biofilm formed in the absence of exogenously added CSP supported a more robust competent state of D39 recipient cells relative to  $in\ vitro$  transformation conditions, which corroborated the efficient biofilm-mediated transfer of Tn2009.

# Integration of intact Tn916-related ICEs into the recipient pneumococcal genome occurred by homologous recombination.

The assumption that the Tet-resistant recombinants with the recipient genotype had integrated the entire Tn2009 was confirmed by whole-genome sequencing (WGS). To analyze the extent of Tn2009 integration in the recipient genome, four Tn2009 recombinants independently recovered from selections on Tet+Str, Ery+Str, Tet+Ery+Str, and Ery+Str+Tmp were first characterized in detail. Quellung reactions and serotype-specific conventional PCRs confirmed that the recombinants were serotype 2 of the D39 recipient. Multilocus sequence typing (MLST) analysis of seven housekeeping genetic loci<sup>(38)</sup> showed all recombinants were sequence type 595 (ST595) of recipient D39 and not ST236 of donor GA16833 (Table 2), confirming that the recombinants were of the D39 genetic lineage and not a result of GA16833 undergoing capsule switching.

WGS of D39 recombinants was performed to probe the extent of recombination. WGS data confirmed that all four recombinants indeed harbored the entire 23.5-kb Tn2009 integrated at the same genomic locus as the GA16833 donor. There was an ~9.5-kb genome sequence of D39 replaced by Tn2009 in the GA16833 genome, and this expected deletion was also confirmed in the recombinants. Based on donor-specific SNP distributions, donor DNA fragments of various sizes flanking Tn2009 were detected in the recombinant genomes. As shown in Table 2, there was an ~33.2-kb donor DNA fragment incorporated in the Tet+Str recombinant, while the Ery+Str recombinant had an insertion of an ~55.2-kb donor DNA fragment. The Tet+Ery+Str-selected recombinant carried Tn2009 on an ~35.6-kb donor DNA fragment, whereas the recombinant from the Ery+Str+Tmp selection had incorporated an ~40.6-kb donor DNA fragment (Table 2). Thus, these Tn2009-containing D39 recombinants incorporated donor DNA fragments that ranged from ~33 kb to ~55 kb. Genomes of two Tn2010-containing D39 recombinants, independently selected on Tet+Str and Ery+Str after the coinoculation with donor GA47281, were also examined. Donor DNA fragments of ~38.4 and ~34.5 kb containing the intact Tn2010 were identified, respectively (Table S4). Conjugative transfer of prototype Tn916 is expected to result in site-specific recombination with a precise excision and integration of Tn916 flanked by coupling sequences, thus incapable of transferring additional flanking SNPs from the donor genome<sup>(39)</sup>. The variable donor DNA lengths indicated that integration of Tn2009 and Tn2010 into pneumococcal genomes occurred by homologous recombination.

Additionally, we identified two clinical isolates, GA47179 (serotype 15A) and GA44194 (serotype 19A), each containing an incomplete copy of Tn6002 (~17.0 kb), that retained both *ermB* and *tetM*. Tn6002 in these isolates was truncated ~100 bp downstream of *tetM*, thus missing critical conjugative *xis* and *int* genes. Bioreactor experiments with donor GA44194 only recovered

serotype 19A recombinants, indicating that GA44194 acquired Str resistance more efficiently from D39<sup>Str</sup> leading to a rF of  $<4.09x10^{-8}\pm3.40x10^{-8}$  for uptake of Tet resistance by the designated D39 recipient (Fig 5). Utilizing recipient D39<sup>Ery/Str</sup> and donor GA44194Δ*comCDE*::*cat*<sup>Str</sup> (BASP8), we detected that comD expression in the D39 recipient was about 10.8-fold greater, while comE expression showed no changes (0.7-fold) in the biofilm when compared to the in vitro transformation condition without synthetic CSP (Table 3). Thus, when coinoculated with donor BASP8, the induction of *com* gene expression in the D39<sup>Ery/Str</sup> recipient was significantly lower than that obtained with donor BASP1 (Fig 4E). These data suggested a less competent D39 recipient with the GA44194 donor strain, potentially contributing to the lower rF. When examined with the bioreactor system, Tet resistance of another partial Tn6002 donor, GA47179, was transferred to recipient D39Str at a rF of 3.44x10<sup>-5</sup>±1.69x10<sup>-5</sup> (Fig 5). WGS and SNP analysis of a Tet+Str-selected D39 recombinant found that Tn6002 was incorporated within an estimated donor length of ~101.0 kb (Table S4). The strain-dependent, efficient transfer of an incomplete Tn6002 lacking critical conjugation genes again supported the horizontal transfer of large ICE-containing DNA fragments between pneumococcal strains via transformation and homologous recombination.

Congression, the cotransformation of distinct unlinked fragments of DNA into the same cell, can occur during transformation. Although rare, congression has been previously demonstrated in *S. pneumoniae*<sup>(40)</sup>. To detect additional independent recombination events distant from integration of the ICE-containing fragments, we conducted whole-genome variant analyses. SNPs transferred from the donor GA16833 genome into the recombinants were identified, and the presence of multiple consecutive GA16833 SNPs flanked by extensive recipient D39 sequence was considered as incorporation of a donor DNA fragment and, thus, a possible transformation event. The

outermost 5' and 3' donor SNPs were then used to estimate the minimal donor DNA length recombined into the recipient genome. Multiple possible cotransformation events at various genomic locations in each of the four Tn2009 recombinant genomes were detected (Fig 6).

# Efficient transfer of Tn916-related ICEs occurred between other S. pneumoniae donors and recipients in human nasopharyngeal biofilms.

To assess whether Tn916-related ICE dissemination via transformation was widely applicable in S. pneumoniae, additional Tn2009- and Tn2010-containing S. pneumoniae clinical isolates were studied in the bioreactor using the Tet+Str selection. Tn2009 was integrated in SP 1638 (TIGR4 annotation) in GA49542 (serotype 9V), distinct from GA16833 with Tn2009 integrated in SP\_1947 (TIGR4 annotation). When donor GA49542 was coinoculated with recipient D39Str in the bioreactor, we observed a rF of 4.71x10<sup>-4</sup>±1.77x10<sup>-4</sup> (Fig 7A) for Tn2009 transfer, similar to the rF obtained with donor GA16833. We also investigated another strain, GA44288 (serotype 19A), with Tn2010 incorporated into the same genomic locus as in GA47281 (serotype 19F). The rF for recipient D39<sup>Str</sup> uptake of Tn2010 from donor GA44288 was 1.02x10<sup>-4</sup>±5.96x10<sup>-5</sup>, comparable to that obtained from donor GA47281 (Fig 7B). WGS analysis of three independent Tet+Str recombinants indicated that the donor fragments encompassing Tn2010 were 43.4, 35.2, and 44.5 kb in size (Table S4). Thus, Tn2009 and Tn2010 were transferred from multiple donor strains to recipient D39 efficiently (rF of  $\sim 10^{-4}$ ), indicating that the dissemination of Tn916-related pneumococcal ICEs in biofilms was independent of donor genomic lineages and the genomic location of ICEs.

We also sought to determine if the two serotype 19A Tmp-resistant clinical isolates, GA40410 and GA43265, examined as recipients in mating experiments, could acquire ICEs as efficiently as D39. To prevent the trimethoprim resistance marker uptake by the donor, we used the competence-

deficient donor BASP1. Tn2009 was efficiently taken up by recipient GA40410 at a recombination frequency of 9.87x10<sup>-4</sup>± 2.80x10<sup>-4</sup>, while recipient GA43265 incorporated Tn2009 at a rF of 6.92x10<sup>-4</sup>±2.41x10<sup>-5</sup> (Fig 7C). WGS analysis indicated that GA40410 recombinants incorporated Tn2009 on donor fragments of 40.5, 73.7, and 92.3 kb, while GA43265 recombinants incorporated Tn2009 on fragments of 89.6 and 50.6 kb in size (Table S4). Together, these data demonstrated efficient Tn916-related ICE transfer between multiple *S. pneumoniae* strains in a dual-strain, nasopharyngeal biofilm via transformation and homologous recombination.

#### **DISCUSSION**

The continued emergence of multidrug resistance in *S. pneumoniae* limits treatment options for invasive pneumococcal disease. Thus, a WHO initiative, launched in 2017, emphasizes research into pneumococcal antibiotic resistance mechanisms and development of new antipneumococcal agents<sup>(6)</sup>. The mechanism of high-frequency horizontal transfer of >20-kb ICEs of the Tn916 family, such as Tn2009, Tn6002, and Tn2010, which carry the important resistance genes *tetM*, *mefE/mel*, and/or *ermB* in *S. pneumoniae*, was addressed in the present study.

During colonization, which can last for months, the pneumococcus forms highly organized biofilms on the epithelial surface of the human nasopharynx<sup>(41)</sup>. Approximately 50% of children carrying *S. pneumoniae* can be colonized by two different pneumococcal serotypes, and up to five cocolonizing pneumococcal serotypes can be detected at any one time<sup>(42-44)</sup>. We found that >20-kb Tn916-related ICEs horizontally disseminate at high frequencies between *S. pneumoniae* in dual-strain biofilms (rF of 10<sup>-4</sup>) established on a human nasopharyngeal cell monolayer and in a continuous flow bioreactor system, which mimics the microenvironment of the human respiratory epithelium. Previous work using the bioreactor has shown high rFs for the exchange of smaller antibiotic resistance determinants between *S. pneumoniae* strains<sup>(20, 45)</sup>.

Conjugation is a transfer mechanism for ICEs in several bacterial species, including S. pneumoniae. Examples of interspecies conjugation include those of pneumococcal ICEs Tn6002 (20.8 kb) into Streptococcus pyogenes (cF ~10<sup>-8</sup>)<sup>(10)</sup>, Tn6003 (25.1 kb) into Enterococcus faecalis  $(cF \sim 10^{-7})^{(10)}$ , and Tn1207.3 (52.5 kb) into S. pyogenes (cF  $\sim 10^{-3}$ ) or Streptococcus gordonii (cF ~10<sup>-4</sup>)<sup>(46)</sup>. Additionally, the large composite Tn5253 (64.5 kb) conjugates to pneumococcal recipients at cFs ranging from ~10<sup>-7</sup> to ~10<sup>-4(47)</sup>, and Tn5251, usually found within Tn5253, has been shown to conjugate independently from a pneumococcal Tn5253 donor to S. pneumoniae TIGR4 (cF  $\sim 10^{-5}$ )<sup>(15)</sup>. While we demonstrated Tn916 conjugation between B. subtilis strains at frequencies of 10<sup>-5</sup>, conjugative transfer of pneumococcal Tn916-related ICE, Tn2009, was not detected between S. pneumoniae under similar mating conditions (cF  $< 10^{-8}$ ). Tetracycline induces expression of conjugative genes on Tn916, resulting in formation of circular intermediates and subsequent transfer of Tn916 to recipient cells<sup>(24, 25)</sup>. However, conjugative gene expression in Tn2009 was not induced by tetracycline, likely due to insertion of the Mega element downstream of tetM, disrupting the regulatory coupling between tetM and conjugative genes. In addition, we did not detect Tn2009 CI formation and Tn2009 transfer in nasopharyngeal biofilms was not affected by a deletion of the critical conjugative gene ftsK. Collectively, these data demonstrated that conjugation is not the underlying mechanism for the high-frequency transfer of pneumococcal ICEs in biofilms on human nasopharyngeal cells.

Another potential horizontal gene transfer method is transduction mediated by bacteriophages. Prophages are abundantly present in pneumococcal genomes and contribute to virulence and pneumococcal physiology<sup>(48, 49)</sup>. However, the importance of phage transduction in the spread of antibiotic resistance in *S. pneumoniae* is much less clear. Wyres et al. identified a pneumococcal 1968 isolate, 18C/3, carrying a Tn916-related ICE that is associated with a streptococcal phage

similar to *Streptococcus* phage 040922<sup>(50)</sup>. We found no evidence that Tn2009, Tn6002, and Tn2010 carried by the donor strains examined in this study were part of or were associated with phage elements. Furthermore, the variable sizes of donor DNA fragments containing ICEs identified in the recombinant genomes did not support phage-mediated transfer of Tn916-related ICEs.

Transformation is the major mechanism of horizontal genetic exchange in naturally competent *S. pneumoniae. In vitro* transformation experiments using mixtures of planktonic pneumococci, exogenous synthetic CSP, and purified DNA generally yield frequencies of  $10^{-4}$  to  $10^{-6}$  with the uptake of ~2- to ~6-kb DNA fragments<sup>(51-54)</sup>. Our data reproduced these observations, in which recipients D39 and TIGR4 were transformed with point mutation-mediated Tmp or Str resistance at frequencies of  $10^{-5}$  per  $\mu g$  of DNA. However, analogous experiments using purified ICE-containing genomic DNA did not yield Tet-resistant transformants (rF < $10^{-7}$ ), and this was not caused by a DNA fragment size limitation.

Previously, Cowley et al. noted that an environment of close cell-to-cell contact, which consisted of pneumococcal coincubation on filters or mixed cultures forming mature biofilms, led to transformation of 8- to 30-kb DNA fragments<sup>(40)</sup>. Additionally, serotype switching events were a result of transformation of 22- to 39-kb DNA fragments<sup>(55)</sup>. We found that within biofilms on human nasopharyngeal cells, Tn916-related ICEs transferred efficiently to pneumococcal recipients, resulting in acquisition of these large antibiotic resistance elements at a rF of ~10<sup>-4</sup>. Similar results were shown with multiple *S. pneumoniae* donors, including two donors of Tn2009, two of Tn2010, and one of Tn6002, as well as with four recipient strains, D39<sup>Str/Tmp</sup>, D39<sup>Str</sup>, GA40410<sup>Tmp</sup>, and GA43265<sup>Tmp</sup>.

Efficient transfer of Tn916-related ICEs likely require close contact between donor and recipient S. pneumoniae strains in mixed biofilms<sup>(40)</sup>, an environment likely found during nasopharyngeal colonization<sup>(56)</sup>. The temperature maintained for the bioreactor (35°C) is lower than the *in vitro* transformation experiments (37°C). *In vitro* transformation conducted at 35°C resulted in a lower rF for streptomycin resistance uptake than that at 37°C, while no uptake of Tn2009-encoded tetracycline resistance was detected at either temperature (Fig S3). Thus, the difference in temperatures is unlikely to account for the efficient ICE transfer within dual-strain nasopharyngeal biofilms. Preliminary data from single-strain recipient D39<sup>Tmp</sup> or D39<sup>Str</sup> biofilms formed on nasopharyngeal cells and exposed to extracellular genomic DNA supplied in the flow medium resulted in the uptake of streptomycin resistance at a rF of 1.66x10<sup>-6</sup> per µg DNA, but not of Tn2009-mediated tetracycline resistance (rF of <7.68x10<sup>-8</sup> per µg DNA) (Fig S2). These data further support that close interaction between different donor and recipient strains within the dualstrain biofilms is needed for efficient transformation of Tn916-related ICEs. Induction of the competent state in S. pneumoniae initiates DNA release from a subfraction of different S. pneumoniae populations, potentially via cell lysis (57), and fratricide is critical for efficient gene transfer between donor and recipient pneumococci in biofilms<sup>(58)</sup>. Overall, this close contact, donor-recipient interactive environment is absent in the classic transformation of planktonic cells.

Whole-genome sequencing and minimum recombination junctions defined by SNP analysis confirmed the integration of very large donor DNA fragments containing intact ICE elements. For Tn2009, donor fragments were estimated to range from ~33 to ~55 kb in size, while Tn2010 was transferred on ~34- to ~45-kb DNA from two donor strains. Finally, we observed that the partial Tn6002 ICE missing critical conjugation genes recombined on a donor fragment size of ~101 kb.

Evidence of multiple homologous recombination events, or congression, was also detected in several Tn2009-containing recombinants.

S. pneumoniae develops a naturally competent state through a positive feedback mechanism involving the ComCDE signaling cascade<sup>(19, 36)</sup>. Upon pneumococcal colonization of the upper respiratory tract, biofilms are formed with upregulation of competence genes<sup>(59-61)</sup>. We detected 120-fold increases of comD and comE expression in the D39 recipient recovered from the mixed nasopharyngeal biofilm when compared to planktonic D39 cultures. Deletions of comE or comEA and comEC in the D39 recipient eliminated recovery of Tn2009-containing D39 recombinants. The elimination of recombinants after DNase I treatment further supported transformation as the mechanism responsible for efficient ICE transfer in the biofilms.

In conclusion, efficient Tn916-related ICE dissemination in *S. pneumoniae* was demonstrated in human nasopharyngeal cell biofilms via transformation and homologous recombination of large DNA fragments. High-frequency transfer of Tn916-related ICEs in biofilms occurred in multiple combinations of pneumococcal donors and recipients. A biofilm environment with close contact of pneumococcal cells and consequent upregulation of the competence pathway were critical for supporting horizontal dissemination of >20-kb Tn916-related ICEs and the antibiotic resistance determinants of these elements. Efficient transformation in mixed biofilms that mimic a natural nasopharyngeal colonization environment supports the epidemiological observations of widespread dissemination of *S. pneumoniae* ICEs in the pneumococcal population.

#### MATERIALS AND METHODS

**Bacterial strains, culture media, and antibiotics.** The strains of *S. pneumoniae* used in this study are listed in Table S1. Clinical isolates were provided by the Georgia Emerging Infections Program. All *S. pneumoniae* strains were cultured on blood agar plates or with Todd-Hewitt broth

with yeast extract (THY broth) and grown at 37°C with 5% CO<sub>2</sub>. *B. subtilis* strains were cultured on LB plates or LB broth at 37°C. Where indicated, the following antibiotics were utilized for preparation of antibiotic agar plates: tetracycline (1 or 2 μg/mL), streptomycin (100, 200, 220 μg/mL), trimethoprim (14 μg/mL), chloramphenicol (4.5 μg/mL) erythromycin (0.5 μg/mL), and spectinomycin (100 μg/mL). All antibiotics were purchased from Millipore-Sigma (Saint Louis, MO).

Mutant construction. Mutation constructs were created by sequential overlapping PCR or splicing by overlap extension (SOE) PCR. GA16833<sup>Tet/Ery</sup> served as the parental strain for the conjugation mutant ( $\Delta ftsK$ ), while D39<sup>Str</sup> and D39<sup>Str/Tmp</sup> were the parental strains for competence  $(\Delta comE \text{ or } \Delta comCDE)$  and transformation  $(\Delta comEA/EC)$  mutants. The primers utilized are listed in Table S2. The chloramphenicol resistance gene, cat, was amplified from pEVP3<sup>(62)</sup>. Purified genomic DNA was utilized as the template to amplify upstream (5'-end) and downstream (3'-end) regions of the target gene using the corresponding primers carrying the necessary overlapping sequences. These individual DNA fragments were amplified using Q5 high-fidelity polymerase (New England Biolabs, Ipswich, MA). Mixtures of two fragments (5'end plus cat or cat plus 3' end) were used as the template for the first round of overlapping PCRs. The third fragment was then linked by a second PCR using either One Taq (New England Biolabs) or Taq (Roche Diagnostics, Indianapolis, IN) DNA polymerase plus Taq Extender PCR additive (Agilent, Santa Clara, CA) to generate the final construct. PCR products purified with the Zymo DNA Clean and Concentrator kit (Irvine, CA) were sequenced to confirm the desired mutation. Purified PCR constructs (0.5-1 µg) were used to transform precompetent cells by in vitro transformation. Transformants selected on 4.5 µg/mL chloramphenicol were sequenced to confirm the presence of the intended mutation.

To generate the  $\Delta ftsK$  mutant, an upstream region was amplified with BSA17 and BSA18 and a downstream region was amplified with BSA19.1 and BSA20. The chloramphenicol resistance marker cat was amplified with primers EVP3\_CmF and EVP3\_CmR. SOE PCR was performed using three individual PCR products and with the outermost primers BSA17.1 and BSA20.1 to create the  $\Delta ftsK::cat$  cassette. The  $\Delta comE$  mutant was generated by amplifying a comEupstream region with MS93 and MS99, a comE downstream region with MS100 and MS96, and the cat gene with MS101 and MS102. The final  $\triangle comE$ ::cat cassette was obtained by SOE PCR with primers SL107 and SL108. The  $\Delta comEA/EC$  mutant was created by amplifying a comEA upstream region with BSA1a and comEA\_5RA3, a comEC downstream region with comEC\_3FA3 and BSA6a, and the cat gene with EVP3\_CmF and EVP3\_CmR. Primers BSA11a and BSA6a were utilized in SOE PCR to obtain the final  $\triangle comEA/EC$ ::cat cassette. Finally, the  $\triangle comCDE$ mutant was created by amplifying an upstream region of comC with MS96 and SL115, a downstream region of *comE* with SL118 and SL119, and the *cat* gene with SL116 and SL117. Primers MS96 and SL119 were utilized to generate the final ΔcomCDE::cat construct by SOE PCR.

*In vitro* transformation assay. D39 and TIGR4 pneumococcal strains were made precompetent using standard methods<sup>(63)</sup>. Briefly, an overnight plate culture was used to inoculate complete transformation medium (CTM) and grown to an optical density at 600 nm (OD<sub>600</sub>) of 0.6 to 0.7. This primary culture was used to make a 1:20-diluted secondary culture, which was grown to OD<sub>600</sub> of 0.35 to 0.45 (mid-log phase). Glycerol was then added to the competent cell aliquots at a final concentration of 10% (vol/vol) and stored at -80°C. These precompetent pneumococcal cells were transformed in CTM using 500 ng of purified genomic DNA and 100 ng/mL of synthetic CSP1 or CSP2 in 200- or 300-μL total reaction volumes. The CSPs were synthesized by Millipore-

Sigma (Saint Louis, MO), the Emory University Microchemical Facility<sup>(64)</sup> or GenScript (Piscataway, NJ). Recombination frequencies for *in vitro* transformation reactions were calculated as number of transformants on antibiotic selection plate divided by the total population of *S. pneumoniae* recovered on nonselective blood agar plate and normalized to micrograms of transforming DNA.

Cell culture. Human pharyngeal cells (Detroit 562; ATCC CCL-138) were maintained using 1X minimum essential medium (1X MEM) supplemented with 10% fetal bovine serum (FBS), 1% nonessential amino acids (100X), 1% L-glutamine (200 mM), 1% HEPES buffer (1M), and 1% penicillin-streptomycin (10,000 U/mL). All cell culture media and supplements were from Life Technologies, Gibco (Gaithersburg, MD). For routine passaging of cells, 0.25% trypsin-EDTA (1mM) was used to lift the cells. Cells were incubated in a sterile incubator at 37°C with 5% CO<sub>2</sub>. Human nasopharyngeal biofilm bioreactor coinoculations. A confluent monolayer of Detroit 562 cells (ATCC CCL-138) was grown on a Corning Snapwell with a 0.4-µm-pore polyester membrane (Corning, NY). These Snapwells were placed inside a sterile vertical diffusion chamber from the bioreactor, allowing the Detroit 562 cells to rest on the apical side (inner chamber) and to be perfused with flowing bioreactor medium composed of 1X MEM supplemented with 5% FBS, 1% nonessential amino acids (100X), 1% L-glutamine (200 mM), and 1% HEPES buffer (1M). The flow of bioreactor medium at a rate of ~0.2 mL/min was generated by a Cole Parmer Master Flex L/S peristaltic pump (Vernon Hills, IL). Where indicated, 20 U/mL of DNase I was added to the bioreactor medium. Spent medium (collected for eDNA quantification as described below) and planktonic cells exited the bioreactor chamber through a parallel outlet located at the top of the chamber<sup>(20)</sup>.

For the coinoculation, overnight plate cultures of each pneumococcal strain were washed three times with 1X Dulbecco's phosphate-buffered saline (DPBS) and resuspended in 500 µL of 1X DPBS, and the OD<sub>600</sub> was measured. Appropriate volumes of bacteria were mixed to make a suspension of equal densities at OD<sub>600</sub> of 0.1 (10<sup>6</sup> CFU/mL each) and inoculated through the apical perfusion path of the bioreactor chamber. After a static 1-hour incubation at 35°C to allow for S. pneumoniae adherence to Detroit 562 cells, the flow of medium was initiated and continued for another 5 hours. At the conclusion of the incubation period, the Snapwells were removed and the dual-strain biofilms formed on the Detroit 562 cells were gently washed and sonicated for 20 seconds in a Branson ultrasonic water bath (Danbury, CT). The bacteria were suspended by extensive pipetting and vortexing, and serial dilutions in 1X DPBS were performed. To obtain the total population for each strain in the coinoculations, serial dilutions were plated on antibiotic plates unique to each individual strain. The cells of the total recombinant population were plated on dual- or triple-antibiotic selection plates. The recombination frequencies (rFs) for bioreactor experiments were calculated as follows: (total number of recombinants\*serotype proportion of recombinants) / total population for specific serotype<sup>(20)</sup>.

**DNA extraction and serotype-specific qPCR.** Recombinants recovered from bioreactor experiments were pooled in 200 μL of sterile 1X DPBS. A lysis buffer containing 100 μL of TE Buffer (10 mM Tris, 1 mM EDTA [pH 8.0]), 40 mg/mL of lysozyme, and 75 U/mL of mutanolysin was added to each of the samples and incubated at 37°C for one hour. Two hundred microliters of Qiagen Buffer AL and 20 μL of Qiagen Proteinase K were added, and followed by incubation at 56°C for 30 minutes. DNA was extracted using the Qiagen QIAamp DNA Mini Kit (Valencia, CA) per the manufacturer's instructions. DNA was eluted in 100 μL of elution buffer and used for serotype-specific qPCR with the primers and probes listed in Table S2 as well as the Bio-Rad

SsoAdvanced Universal Probes supermix (Hercules, CA). These reactions targeted the capsule (*cps*) locus of specific pneumococcal serotypes. The cycling conditions were as follows: 1 cycle at 95°C for 2 minutes, 39 cycles of 95°C for 15 seconds and 60°C for 30 seconds. A standard curve for final genome equivalents per milliliter of each serotype was performed alongside the samples and consisted of serially diluted DNA standards corresponding to the following genome equivalents: 8.58x10<sup>6</sup>, 4.29x10<sup>6</sup>, 2.14x10<sup>6</sup>, 4.29x10<sup>5</sup>, 4.29x10<sup>4</sup>, 4.29x10<sup>3</sup>, 4.29x10<sup>2</sup>, 4.29x10<sup>1</sup>, 2.14x10<sup>1</sup>, and 2.14<sup>(42, 65)</sup>. The proportion of recombinants that belong to each serotype was calculated by dividing the number of genome equivalents for a specific serotype by the total sum of genome equivalents for both strains in the bioreactor coinoculations, and this value was utilized to calculate recombination frequencies (rFs).

Alignments of pneumococcal Tn916-related ICEs with prototype Tn916. BLASTN and outfmt 6 were utilized for generating comparison files between ICEs. Along with GenBank (.gbk) files, the comparison files were inputted into EasyFig 2.2.2<sup>(66)</sup> to produce sequence alignments as well as to determine percentages of identity.

Gene expression studies with qRT-PCR. For *tetM* and conjugative gene expression studies, single-strain broth cultures of *S. pneumoniae* strains and *B. subtilis* CMJ253 were grown in a primary culture to an OD<sub>600</sub> of 0.50 to 0.65. The primary cultures were then diluted 1:20 to inoculate a secondary culture. The secondary cultures were incubated in the presence or absence of 2.5 μg/mL tetracycline for 2.5 hours at 37°C. One milliliter of cultures (~10<sup>8</sup> CFU) was pelleted at 16,400 rcf for 8 minutes at room temperature. Five hundred microliters of supernatant was discarded, and the remaining 500 μL supernatant was used to resuspend the bacterial pellets. One milliliter of Qiagen's RNAProtect reagent was added, and the mixture was incubated at room temperature for 5 minutes. For single-donor strain or mixed donor-recipient broth cultures, *S.* 

pneumoniae strains were first grown separately in broth to OD<sub>600</sub> of about 0.4. A mixture of 10<sup>8</sup> CFU of both strains or a single-strain culture were incubated for another 2.5 hours and then treated with two volumes of RNAProtect reagent. For bioreactor experiments that underwent a 1-hour static incubation and 5-hour continuous flow incubation at 35 °C, total biofilm bacteria suspended in 1X DPBS were collected at the end of the 6-hour incubation period and treated with two volumes of RNAProtect reagent, while *in vitro* transformation reactions with or without synthetic CSP were incubated at 37°C for two hours and then treated with two volumes of RNAProtect reagent. Following incubation, the samples were centrifuged at 12,000 rcf for 10 minutes, the supernatant was discarded, and the pellets were stored at -80°C.

Qiagen RNeasy Mini Kit's protocol was followed, with the exception that 40 mg/mL of lysozyme and 75 U/mL of mutanolysin were used in TE buffer for bacterial cell lysis. RNA samples were treated with the TURBO DNA-free Kit (Gaithersburg, MD) and subsequently purified and concentrated with the Zymo RNA Clean and Concentrator kit (Irvine, CA). All RNA samples were verified to be free of DNA contamination via conventional PCR using primers targeting *S. pneumoniae recA* or *B. subtilis orf20* (relaxase) (BSA25 and BSA26). cDNA was prepared using the Bio-Rad iScript reverse transcription supermix (Hercules, CA) and 350 ng, 500 ng, 800 ng, or 1 μg of purified RNA. Quantitative reverse-transcription-PCR (RT-PCR) was conducted with the Bio-Rad iQ SYBR green supermix (Hercules, CA). All primers for the target and internal control genes were validated by the threshold cycle (2<sup>-ΔACt</sup>) method<sup>(67)</sup>. The following cycle conditions were utilized on a Bio-Rad CFX96 Touch real-time PCR machine (Hercules, CA): 1 cycle at 95°C for 3 minutes, 40 cycles of 95°C for 15 seconds, 57 °C or 60°C for 15 seconds, and 72°C for 30 seconds.

Fold change in expression was calculated using the  $2^{-\Delta\Delta Ct}$  method<sup>(67)</sup>. For the tetracycline-induced and uninduced broth cultures of *S. pneumoniae* strains and *B. subtilis* CMJ253, 16s rRNA was utilized as the internal control and fold change was normalized to the uninduced condition. Due to 16s rRNA being present in both wildtype donor and recipient *S. pneumoniae* strains in the bioreactor, the internal control for conjugative gene expression was the donor-specific *cat* gene from BASP1. When analyzing expression of *com* genes specifically from the recipient strain, expression of *ermB* inserted in the nonessential *bgaA* locus of the D39<sup>Ery/Str</sup> recipient served as the internal control for expression analysis of bioreactor biofilms.

Quantification of ICE circular intermediates. The formation of circular intermediates was examined under the following conditions: 1) broth cultures treated with or without 2.5  $\mu$ g/mL tetracycline for 2.5 hours at 37°C, 2) 4-hour mating reaction mixtures consisting of GA16833:BASP2 or CMJ253:CAL419 on a blood agar plate, and 3) the bioreactor experiment including D39<sup>Str</sup> and GA16833. One milliliter of each broth culture was pelleted down at 16,400 rcf for 10 minutes at room temperature, and the supernatants were discarded. The bacterial pellets were then resuspended in 200  $\mu$ L of 1X DPBS for DNA extraction. For the mating experiment, bacteria on the blood agar plate were collected in 400  $\mu$ L of 1X DPBS and aliquots of 200  $\mu$ L were utilized for DNA extraction. Finally, dual-strain biofilms were collected from the bioreactor and underwent DNA extraction. DNA was extracted with the Qiagen QIAamp DNA Mini Kit (Valencia, CA).

qPCR of the circular junctions was performed with the Bio-rad iQ SYBR green supermix (Hercules, CA). A standard curve using genomic DNA from *B. subtilis* strain LDW737<sup>(27)</sup>, containing a cloned copy of the circular junction sequence that is shared between the Tn916 prototype and the pneumococcal Tn916-related ICEs, was performed with the following genome

equivalents: 8.58x10<sup>6</sup>, 8.58x10<sup>5</sup>, 8.58x10<sup>4</sup>, 8.58x10<sup>3</sup>, 8.58x10<sup>2</sup>, 8.58x10<sup>1</sup>, 4.29x10<sup>1</sup>, 4.29x10<sup>1</sup>, 4.29. For the broth samples, 1 μL of 30 ng/μL DNA was added to the reaction mixtures. For the mating and bioreactor biofilm samples, 1 μL of 20 ng/μL DNA was utilized as the template for the qPCRs with the following cycling conditions: 1 cycle at 95°C for 3 minutes and 40 cycles of 95°C for 15 seconds, 53°C for 15 seconds, and 72°C for 30 seconds. The genome copy numbers were based on *ftsK* (1 chromosomal copy) quantification, and the data were calculated as copy number of circular junction per genome, or CI/chromosome.

Mating experiments. Strains were inoculated in LB broth or THY broth from overnight plate cultures and grown to the late-log phase. Donor and recipient strains were mixed at a 1:10 ratio of  $10^8/10^9$  CFU and centrifuged for 15 minutes at 3,000 rcf to pellet bacteria. The pellet was resuspended in 100 μL of LB or THY broth, and DNase I was added to the mating mixture at 10 μg/mL. The mixture was plated on blood agar plates and incubated at 37°C for four hours. The mating mixture was collected and resuspended in 1 mL LB or THY broth with 10% glycerol final concentration. Serial dilutions were performed, and multi-layer plating was carried out as described previously<sup>(32)</sup>. *S. pneumoniae* was selected with 2 μg/mL Tet and/or 220 μg/mL Str or  $14 \mu g/mL$  Tmp, while *B. subtilis* was selected with  $10 \mu g/mL$  Tet and/or  $100 \mu g/mL$  spectinomycin or  $100 \mu g/mL$  Str.

Quantification of extracellular DNA. Spent medium was collected from the outlets of the bioreactor chambers at hours 1, 2, 4, and 6 of incubation for one hour. The samples were centrifuged for 10 minutes at 15,000 rpm at 4°C (Eppendorf, Hauppauge, NY) and subsequently sterilized with a 0.45-μm-pore filter. Extracellular DNA was extracted from 400 μL of the sterile supernatant samples using the Qiagen QIAamp DNA Mini Kit following the instructions starting from addition of ethanol to the samples. The eDNA was eluted in 100 μL of elution buffer and

stored at -80°C for further use. The purified eDNA was utilized as templates for serotype-specific qPCR as described above, and the standard curve was built using  $1x10^3$ ,  $1x10^2$ ,  $1x10^1$ ,  $1x10^0$ ,  $1x10^1$ ,  $1x10^2$ , and  $1x10^2$ , are also as a substantial expectation of the appropriate serotype-specific qPCR as described above, and the standard curve was built using  $1x10^3$ ,  $1x10^2$ 

Whole-genome sequencing and variant analysis. Genomic DNA from bioreactor recombinants was purified using the Qiagen QIAamp DNA Mini Kit as instructed. Libraries were prepared utilizing the Illumina Nextera XT DNA library preparation kit (San Diego, CA) and sequenced by SeqCenter (Pittsburgh, PA) using the NextSeq 2000 platform. The paired-end read data were assembled and annotated using tools available on PATRIC's Bacterial and Viral Bioinformatics Resource Center. For variant analysis, the Illumina reads of the D39<sup>Str/Tmp</sup> or D39<sup>Str</sup> recipient strains were first mapped onto the closed genome sequence of reference strain D39 (NC 008533.2) using the DNAStar NGen program, and single nucleotide polymorphisms already present in the D39Str/Tmp or D39Str recipients were identified relative to the reference D39. These SNPs of D39Str/Tmp or D39Str were then discounted from the reference-guided assemblies of the recombinants to identify the remaining SNPs introduced by the donor strain. For the GA40410 and GA43265 recipient strains, the recombinants were assembled using individual WGS data as references to identify donor SNPs. Recombination blocks were estimated as clustering of consecutive donor SNPs flanked by recipient sequence. The outermost 5' and 3' donor SNPs were used to calculate the minimal length of the recombined donor DNA fragment.

**Statistical analysis.** All frequency, ratio, bacterial density, and eDNA concentration data were analyzed using two-tailed unpaired t-tests on GraphPad Prism8.

**Data availability.** All data supporting the research findings of this study are included within the article and in the supplemental material. Annotated whole-genome sequences have been deposited in NCBI GenBank under BioProject no. PRJNA933161.

## **ACKNOWLEDGEMENTS**

This study was supported by National Institute of Allergy and Infectious Diseases of the National Institutes of Health under award numbers F31 AI154792 and R21 AI144571. We thank the Georgia Emerging Infections Program for providing clinical *Streptococcus pneumoniae* strains and Alan Grossman at MIT for supplying *Bacillus subtilis* strains.

## FIGURES AND TABLES

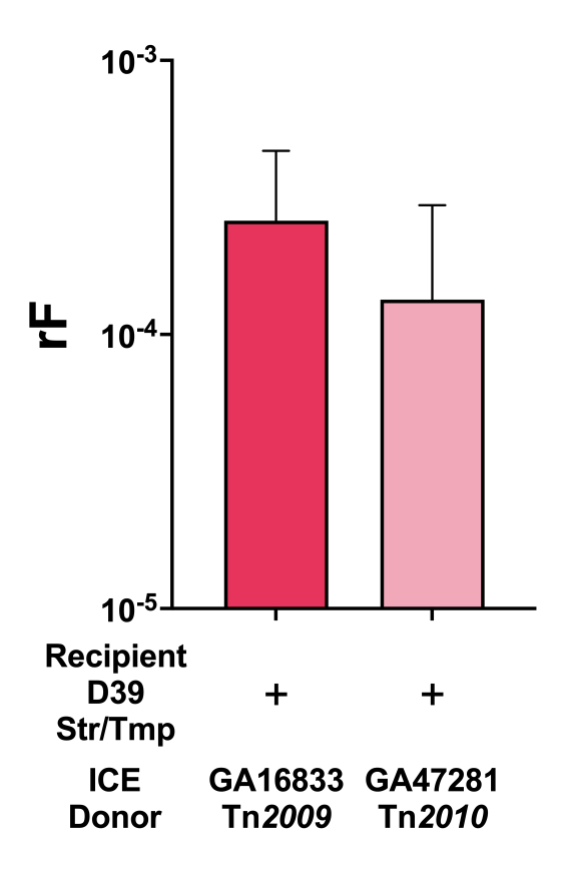


**Figure 1. Efficient transfer of pneumococcal Tn***916*-related ICEs occurs in dual-strain nasopharyngeal biofilms. The wild-type recipient D39<sup>Str/Tmp</sup> (serotype 2) and GA16833<sup>Tet/Ery</sup> (with Tn2009, serotype 19F) or GA47281<sup>Tet/Ery</sup> (with Tn2010, serotype 19F) were coinoculated in a bioreactor at 35°C on a confluent monolayer of human nasopharyngeal Detroit cells such that dual-strain biofilms formed. After a 6-h total incubation, recombination frequencies for D39 uptake of the tetracycline (Tet) resistance marker were calculated.

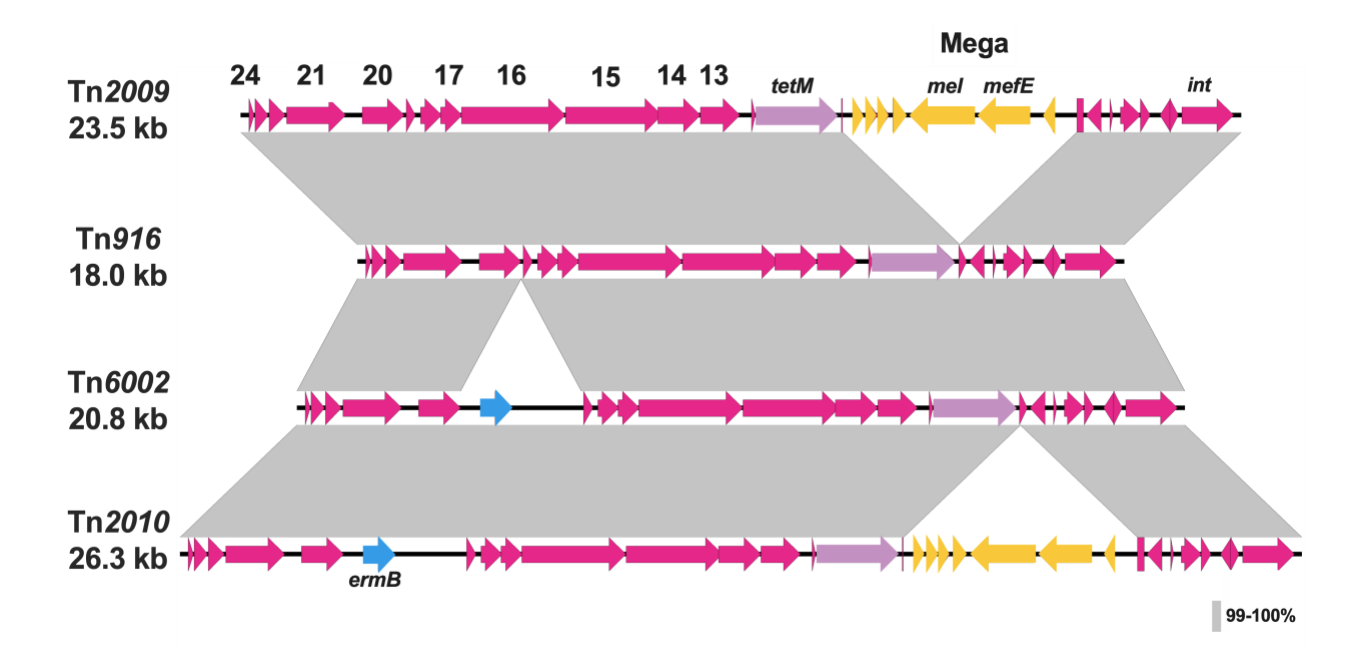


Figure 2. Sequence alignments of prototype Tn916 with pneumococcal Tn916-related ICEs.

EasyFig 2.2.2 was utilized to produce alignments of ICE elements using comparison files generated by BLASTN. Tetracycline resistance is conferred by the *tetM* gene (purple arrow) found in prototype Tn916 as well as pneumococcal ICEs. Pneumococcal Tn916-related ICEs harbor macrolide resistance via the *ermB* element (blue arrows) found on Tn6002 or Tn2010 as well as the macrolide efflux genetic assembly (Mega) element (yellow arrows) on Tn2009 or Tn2010. Conjugative genes shared by prototype Tn916 and pneumococcal Tn916-related ICEs are denoted by magenta arrows.

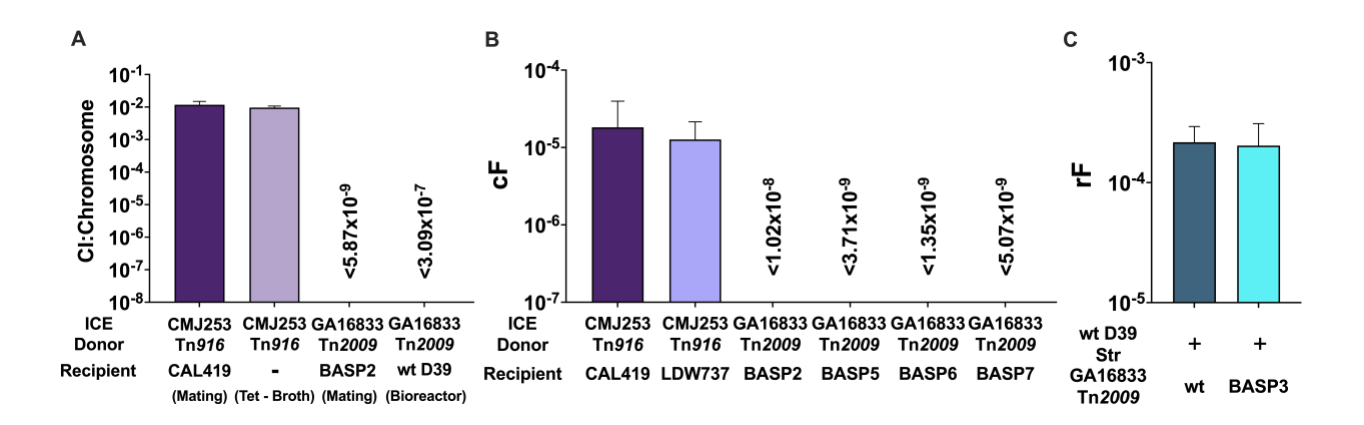
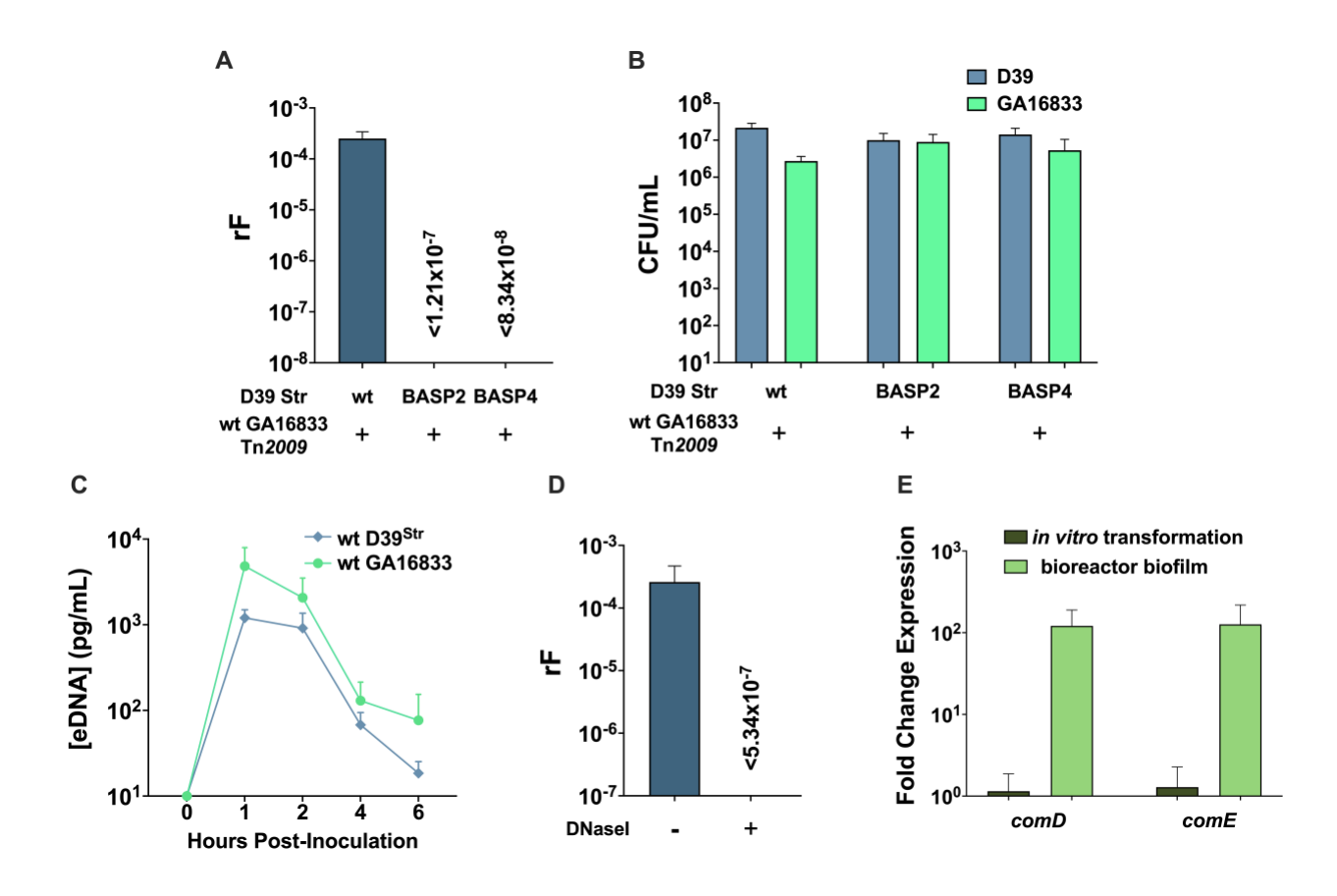
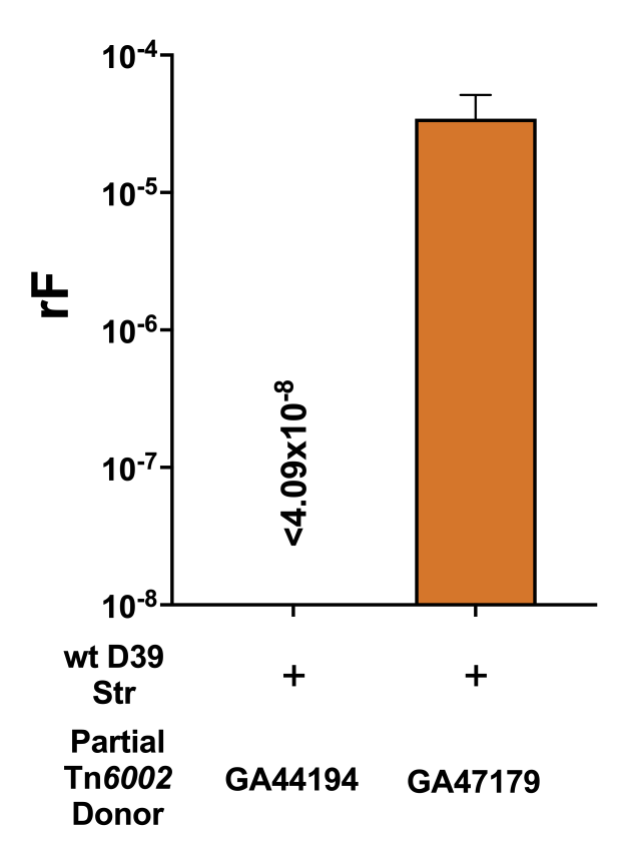


Figure 3. Pneumococcal Tn2009 does not form circular intermediates (CIs) nor transfer by conjugation. (A) Circular intermediate quantification of 4-h mating reactions performed utilizing  $10^8$  CFU of both the donor and recipient as well as bioreactor biofilms consisting of wild-type recipient D39<sup>Str</sup> and wild-type donor GA16833<sup>Tet/Ery</sup>. The data represent the frequency of CI copy number normalized to copy number of *ftsK* that is present on Tn2009 and Tn916. (B) Conjugation frequencies from mating reactions of  $10^8$ : $10^9$  CFU of donor-recipient mixtures. (C) Wild-type recipient D39<sup>Str</sup> was coinoculated with wild-type donor GA16833<sup>Tet/Ery</sup> or BASP3 (GA16833  $\Delta ftsK$ ) in the bioreactor. After a 6-h incubation, recombination frequencies for D39 uptake of Tet resistance were calculated.



**Figure 4. Pneumococcal Tn2009 transfer in human nasopharyngeal biofilms requires competence and transformation machinery in the recipient.** (**A**) Wild-type recipient D39<sup>Str</sup>, BASP2 (D39 Δ*comE*), or BASP4 (D39 Δ*comEA/EC*) were coinoculated with wild-type donor GA16833<sup>Tet/Ery</sup> in the bioreactor. The data represent recombination frequencies for D39 uptake of Tet resistance. (**B**) Total density (CFU per milliliter) of each strain in the bioreactor coinoculations was calculated by dilution plating. (**C**) Extracellular DNA from spent medium of the D39<sup>Str</sup> and GA16833<sup>Tet/Ery</sup> bioreactor coinoculation was quantified by serotype-specific qPCR for serotypes 2 and 19F. (**D**) Wild-type D39<sup>Str</sup> and GA16833<sup>Tet/Ery</sup> bioreactor coinoculations were incubated in the presence or absence of 20 U/mL DNase I, and recombination frequencies were calculated for D39 uptake of Tet resistance. (**E**) Fold change in early competence gene expression

of *comD* and *comE* in recipient strain D39<sup>Ery/Str</sup> was calculated from bioreactor coinoculation of D39<sup>Ery/Str</sup> and BASP1 normalized to an *in vitro* transformation without CSP addition.



**Figure 5. Partial pneumococcal Tn6002 lacking conjugative regulatory mechanism transfers via transformation and homologous recombination in a strain-dependent manner.** Wild-type recipient D39<sup>Str</sup> and GA44194<sup>Tet/Ery</sup> (with partial Tn6002, serotype 19A) or GA47179<sup>Tet/Ery</sup> (with partial Tn6002, serotype 15A) were coinoculated in the bioreactor at 35°C. After a 6-h total incubation, recombination frequencies for D39 uptake of the tetracycline (Tet) resistance marker were calculated.

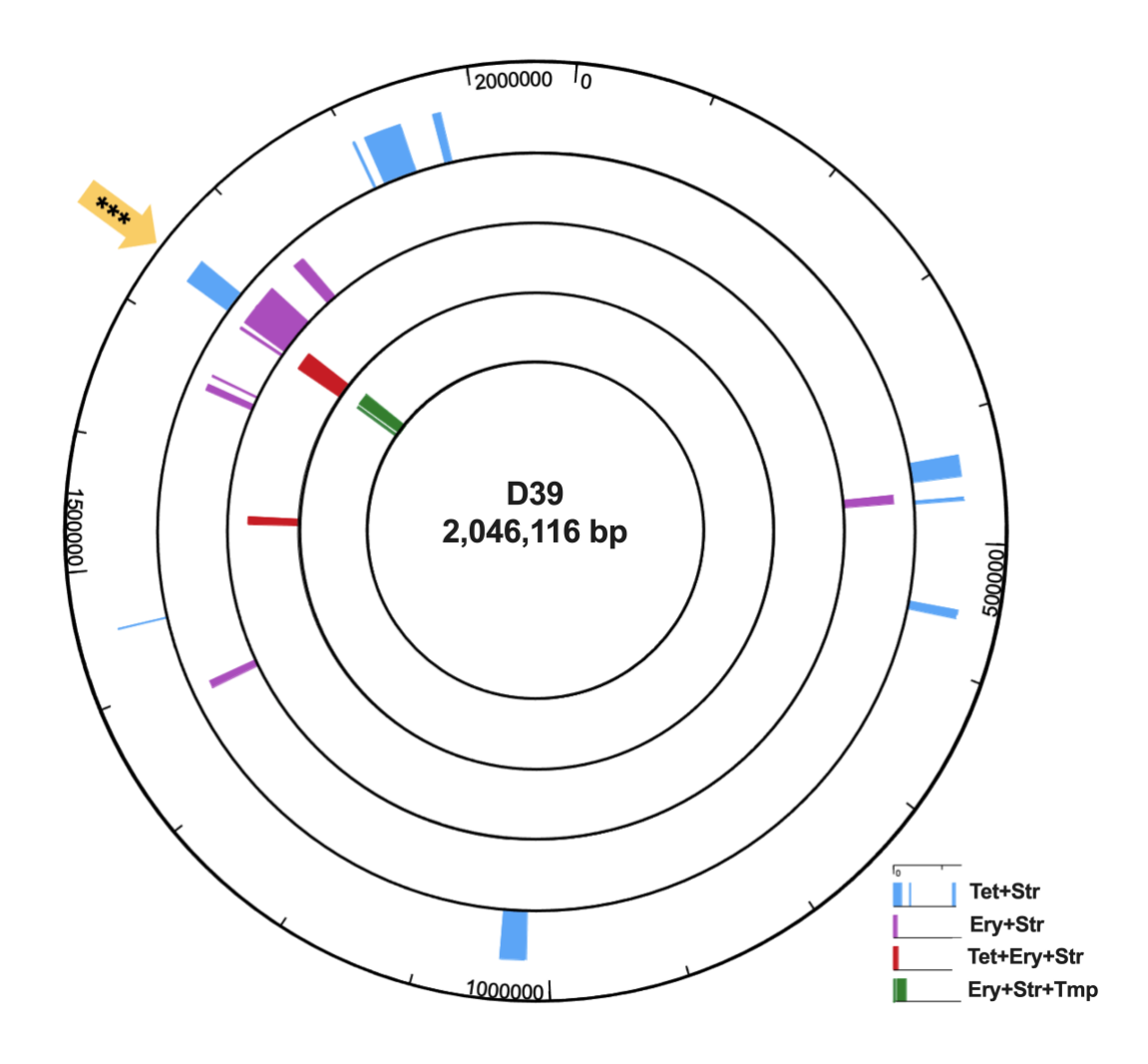


Figure 6. Whole-genome sequencing reveals homologous recombination of large Tn2009-containing fragments (~33 to ~55 kb) from GA16833 into D39 bioreactor recombinants. Bioreactor recombinants from the GA16833 and D39<sup>Str/Tmp</sup> coinoculation were mapped against the recipient strain D39<sup>Str/Tmp</sup>. Donor GA16833 DNA recombination regions, denoted by the different colored blocks, were determined by locating donor SNP clusters flanked by recipient sequence using variant SNP analyses. A yellow block arrow with asterisks denotes the blocks representing the recombined donor fragments containing Tn2009.

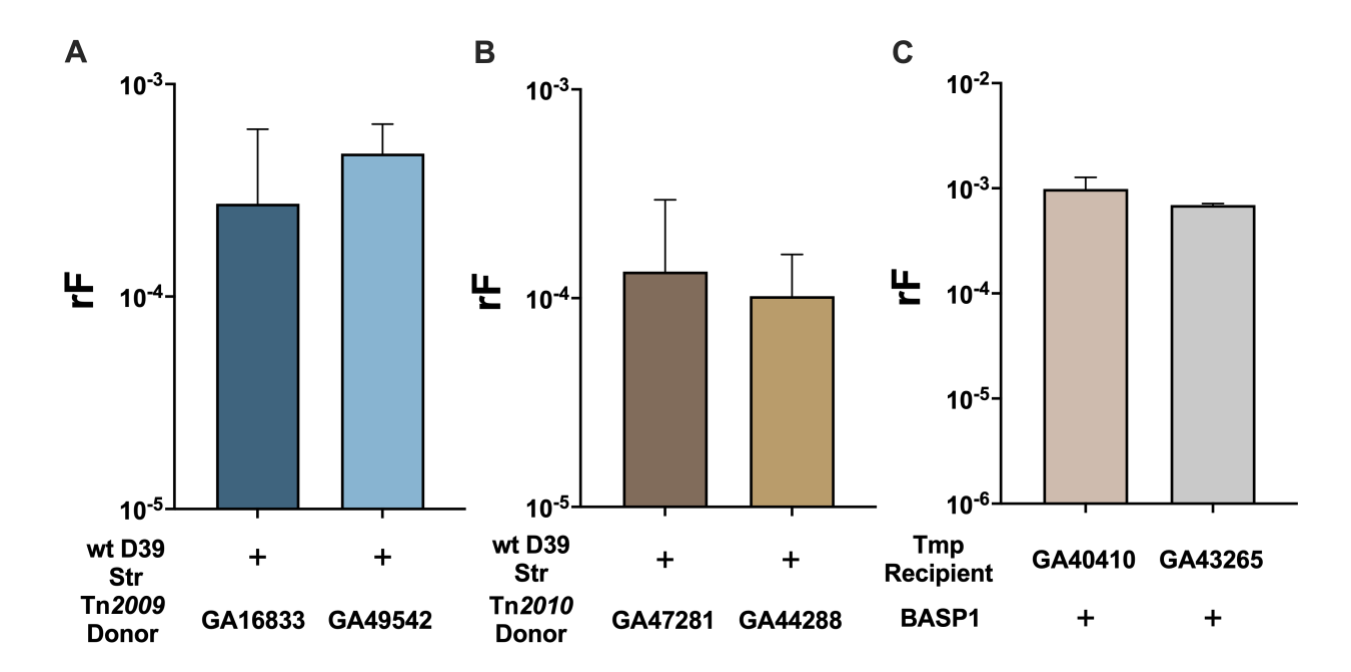


Figure 7. Efficient transfer of Tn916-related ICEs via transformation and homologous recombination in nasopharyngeal biofilms occurs in other *S. pneumoniae* strains. Pneumococcal recipients and Tn916-related ICE-containing donor isolates were coinoculated at 35°C in the bioreactor. After a 6-h total incubation, recombination frequencies were then calculated for recipient uptake of Tet resistance conferred by Tn916-related ICEs via selection of recombinants on Tet+Str or Tet+Tmp. (A) Wild-type D39<sup>Str</sup> and wild-type GA16833<sup>Tet/Ery</sup> or GA49542<sup>Tet/Ery</sup> (Tn2009); (B) wild-type D39<sup>Str</sup> and wild-type GA47281<sup>Tet/Ery</sup> or GA44288<sup>Tet/Ery</sup> (Tn2010); (C) wild-type GA40410<sup>Tmp</sup> or GA43265<sup>Tmp</sup> and BASP1 (Tn2009).

**Table 1.** Tetracycline-induced fold change in *tetM* and conjugative gene expression of Tn916 and Tn2009.

Strain	tetM (SD*)	int (SD*)	orf20 (SD*)	ftsK (SD*)
CMJ253 (Tn916)	4.00 (0.071)	1.10 (0.053)	4.02 (0.62)	3.34 (0.095)
GA16833 (Tn2009)	28.18 (15.24)	2.25 (1.08)	2.79 (0.99)	3.72 (0.38)

<sup>\*</sup>SD represents the standard deviation from two independent biological replicates.

**Table 2.** Homologous recombination of donor DNA fragments of various sizes with intact Tn2009 into D39 bioreactor recombinant genomes.

Donor (ICE, MLST)	Recipient	Recombinant	Size of Recombined Donor
Donor (ICE, WILST)	(MLST)	(MLST)	Fragment with ICE (bp)
GA16833	D39 <sup>Str/Tmp</sup>	Tet + Str	22 176
(Tn2009 <sup>Tet/Ery</sup> , ST 236)	(ST 595)	(ST 595)	33,176
GA16833	D39 <sup>Str/Tmp</sup>	Tet + Ery + Str	35,566
(Tn2009 <sup>Tet/Ery</sup> , ST 236)	(ST 595)	(ST 595)	33,300
GA16833	D39 <sup>Str/Tmp</sup>	Ery + Str	55,152
(Tn2009 <sup>Tet/Ery</sup> , ST 236)	(ST 595)	(ST 595)	33,132
GA16833	D39 <sup>Str/Tmp</sup>	Ery + Str + Tmp	40,575
(Tn2009 <sup>Tet/Ery</sup> , ST 236)	(ST 595)	(ST 595)	70,373

**Table 3.** Early *com* gene expression in recipient D39<sup>Ery/Str</sup> from dual-strain bioreactor biofilm with BASP8 compared to *in vitro* transformation without CSP addition.

Strain	comD (SD*)	comE (SD*)
D39 <sup>Ery/Str</sup>	10.81 (14.83)	0.70 (0.14)

<sup>\*</sup>SD represents the standard deviation from two independent biological replicates.

# SUPPLEMENTAL FIGURES AND TABLES

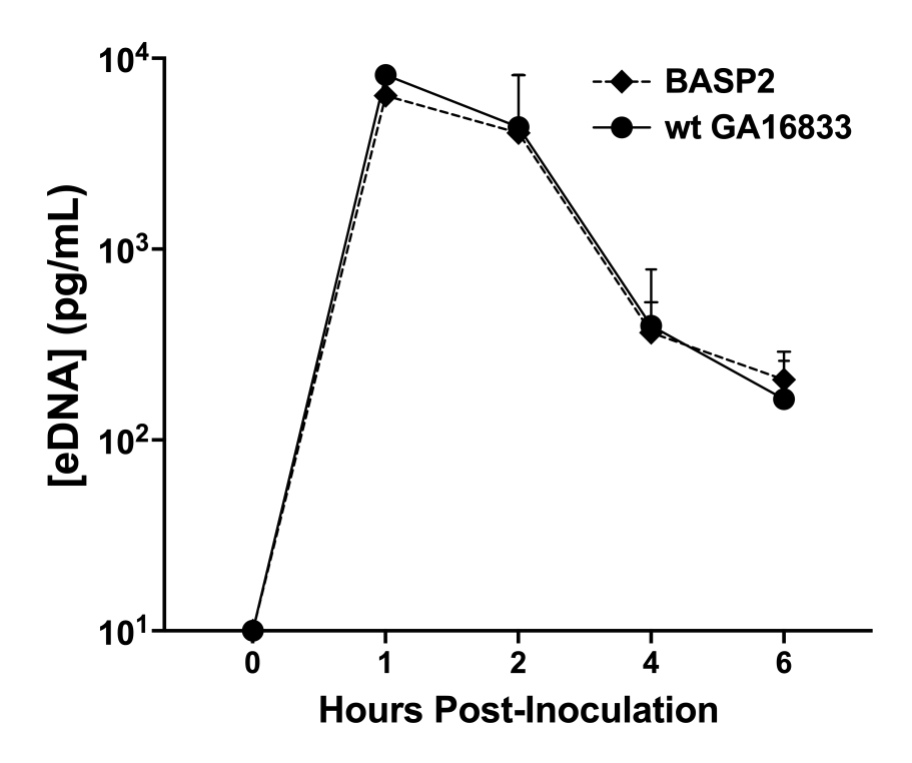
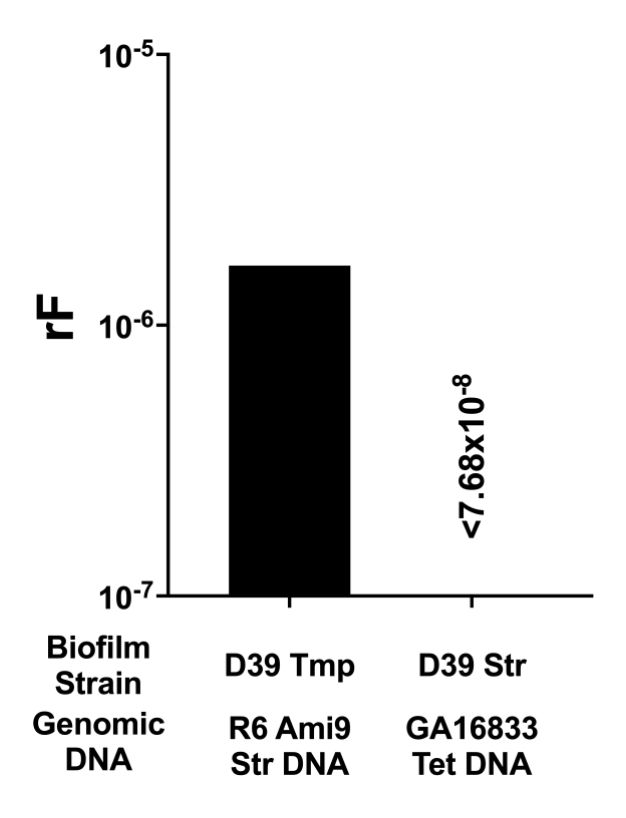
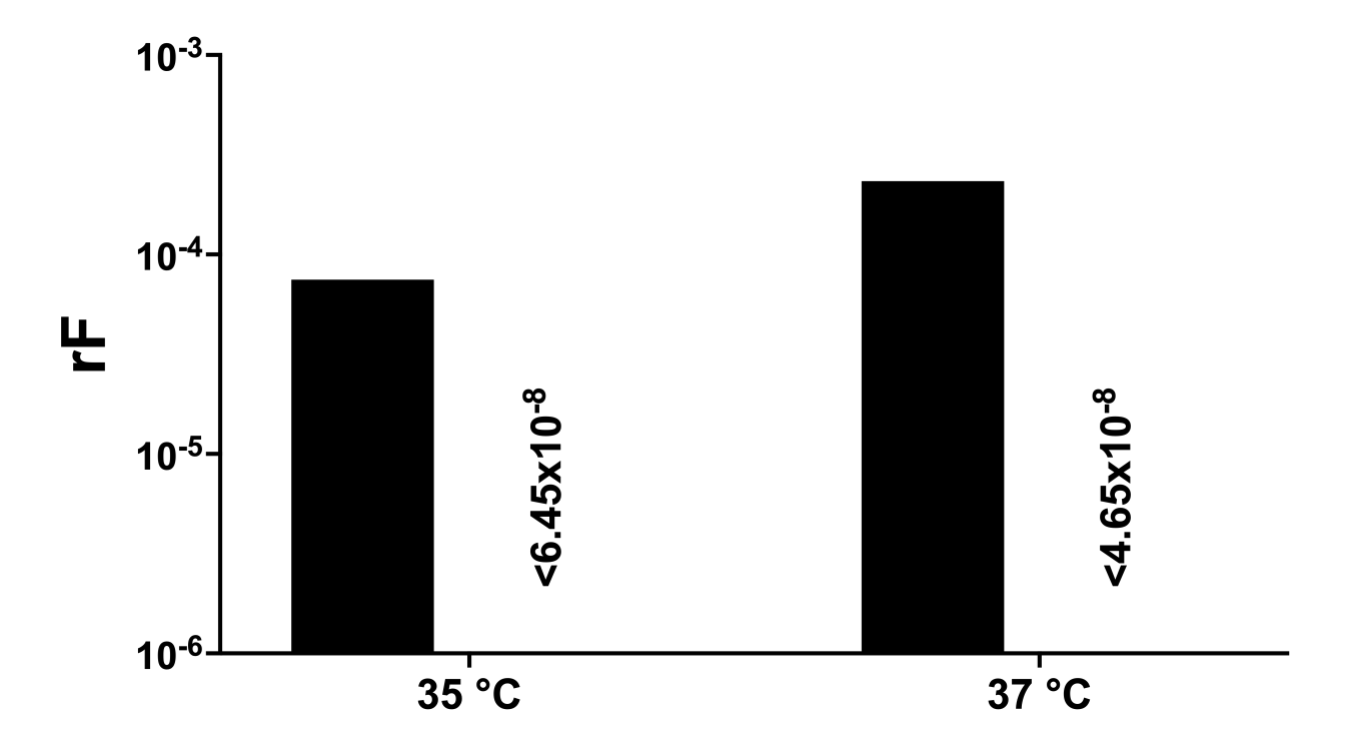


Figure S1. Similar extracellular DNA concentrations are secreted from competence-deficient mutant recipient strain BASP2 and Tn2009 ICE donor GA16833 in nasopharyngeal dual-strain biofilms. Extracellular DNA from spent media of BASP2 (D39Δ*comE*) and GA16833<sup>Tet/Ery</sup> bioreactor co-inoculation was quantified with serotype-specific qPCR for serotypes 2 and 19F.



**Figure S2. Single recipient strain biofilm transforms point mutation-mediated resistance but not Tn916-related ICE resistance.** Recipient pneumococcal strains D39<sup>Tmp</sup> or D39<sup>Str</sup> were inoculated in a bioreactor at 35°C on a confluent monolayer of human nasopharyngeal Detroit cells such that single strain biofilms formed. Flowing bioreactor media was supplemented with a final concentration of 700 ng/mL of genomic DNA from streptomycin (Str)-resistant R6 Ami9 or tetracycline (Tet)-resistant GA16833<sup>Tn2009</sup>. After a 6-hr total incubation, recombination frequencies per μg DNA for D39 uptake of Str or Tet resistance were calculated.



**Figure S3.** *In vitro* transformation at 35°C and 37°C facilitates recipient uptake of point mutation-mediated resistance but not Tn916-related ICE resistance. Pre-competent wildtype D39 cells were incubated in complete transformation medium with 100 ng/mL CSP1 and 500 ng of genomic DNA from R6 Ami9<sup>Str</sup> or GA16833 Tn2009<sup>Tet/Ery</sup> at 35°C or 37°C. After a 2-hr total incubation time, recombination frequencies per μg DNA were calculated for D39 uptake of Str (black bars) or Tet resistance (< numerical values).

Table S1. Strains used in this study.

Bacterial Strain	Description, Relevant Genotype and Phenotype	Reference or Source
	Streptococcus pneumoniae	
WT D39	Avery strain, serotype 2	(68)
WT TIGR4	Invasive isolate, serotype 4	(69)
WT D39 <sup>Str</sup>	D39 derivative transformed with genomic DNA containing K56T point mutation in <i>rpsL</i> , Str resistant	This study
GA16833	Clinical isolate from Georgia Emerging Infections Program, serotype 19F, ICE Tn2009 conferring Tet resistance ( <i>tetM</i> ), Ery resistance ( <i>mefE/mel</i> on Mega)	(9)
GA47281	Clinical isolate from Georgia Emerging Infections Program, serotype 19F, ICE Tn2010 conferring Tet resistance (tetM), Ery resistance (ermB and mefE/mel on Mega)	(9)
WT D39 <sup>Str/Tmp</sup>	D39 derivative transformed with genomic DNA containing K56T point mutation in <i>rpsL</i> (Str resistant) and I100L point mutation in <i>folA</i> (Tmp resistant)	(20)
BASP1	GA16833Δ <i>comCDE</i> – GA16833 derivative with <i>comCDE</i> coding sequence deleted and harboring <i>cat</i> gene, conferring chloramphenicol (Cm) resistance from pEVP3	This study
BASP2	D39Δ <i>comE</i> – D39 derivative with <i>comE</i> coding sequence deleted and harboring <i>cat</i> gene from pEVP3 (Cm resistant) as well as K56T point mutation in <i>rpsL</i> (Str resistant)	This study
BASP3	GA16833Δ <i>ftsK</i> – GA16833 derivative with <i>ftsK</i> coding sequence deleted in Tn2009 and harboring <i>cat</i> gene from pEVP3, conferring chloramphenicol (Cm) resistance	This study
BASP4	D39Δ <i>comEA/EC</i> – D39 derivative with <i>comEA</i> and <i>comEC</i> coding sequences deleted and harboring <i>cat</i> gene from pEVP3 (Cm resistant) as well as K56T point mutation in <i>rpsL</i> (Str resistant)	This study
BASP5	TIGR4Δ <i>comE</i> – TIGR4 derivative with <i>comE</i> coding sequence deleted and harboring <i>cat</i> gene from pEVP3 (Cm resistant) as well as I100L point mutation in <i>folA</i> (Tmp resistant)	This study
BASP6	GA40410Δ <i>comE</i> – GA40410 derivative with <i>comE</i> coding sequence deleted and harboring <i>cat</i> gene from pEVP3 (Cm resistant) as well as I100L point mutation in <i>folA</i> (Tmp resistant)	This study

BASP7	$GA43265\Delta comE - GA43265$ derivative with $comE$ coding sequence	This study
Briot /	deleted and harboring <i>cat</i> gene from pEVP3 (Cm resistant) as well as I100L point mutation in <i>folA</i> (Tmp resistant)	This study
BASP8	GA44194 $\Delta comCDE$ – GA44194 derivative with $comCDE$ coding sequence deleted and harboring $cat$ gene, conferring chloramphenicol (Cm) resistance from pEVP3	This study
WT D39 <sub>Ery/Str</sub>	D39 derivative transformed with genomic DNA containing <i>ermB</i> (Ery resistant) and K56T point mutation in <i>rpsL</i> (Str resistant)	This study
GA47179	Clinical isolate from Georgia Emerging Infections Program, serotype 15A, truncated Tn6002 (17.2 kb) conferring Tet resistance ( <i>tetM</i> ), Ery resistance ( <i>ermB</i> )	(9)
GA44194	Clinical isolate from Georgia Emerging Infections Program, serotype 19A, truncated Tn6002 (17.0 kb) conferring Tet resistance ( <i>tetM</i> ), Ery resistance ( <i>ermB</i> )	(9)
GA49542	Clinical isolate from Georgia Emerging Infections Program, serotype 9V, ICE Tn2009 conferring Tet resistance ( <i>tetM</i> ), Ery resistance ( <i>mefE/mel</i> on Mega)	(9)
GA44288	Clinical isolate from Georgia Emerging Infections Program, serotype 19A, ICE Tn2010 conferring Tet resistance ( <i>tetM</i> ), Ery resistance ( <i>ermB</i> and <i>mefE/mel</i> on Mega)	(9)
GA40410	Clinical isolate from Georgia Emerging Infections Program, serotype 19A and conferring Tmp resistance	This study
GA43265	Clinical isolate from Georgia Emerging Infections Program, serotype 19A and conferring Tmp resistance	This study
	Bacillus subtilis	
CMJ253	Tn916-containing strain, Tet resistant	(31)
LDW737	Strain with Tn916 and Tn916-related ICE circular junction cloned into $amyE$ gene and spectinomycin resistant	(27)
CAL419	Strain with <i>comK</i> coding sequence deleted and harboring <i>cat</i> gene (Cm resistant) as well as well streptomycin resistance	(31)

Table S2. Primers and probes used in this study.

Primer Name	Primer Name Primer Sequence 5' → 3'				
Conventional PCR					
D39_recA_5F	TGAGCAGGCACGAAGCAAGAC	This study			
D39_recA_3R	AGGAGCGACAAGAAACAGCAAACT	This study			
BSA25	TTGCGGACTTAGGTTCTGTG	This study			
BSA26	ACAAACCATGTCATTTGCGTAAAG	This study			
EVP3_CmF	GGTATCGATAAGCTTGATGAAAA	This study			
EVP3_CmR	TTAGTGACATTAGAAAACCGACTG	This study			
BSA17	AATCAAGAATCAAAAGGTCGTTCCC	This study			
BSA18	TTTTCATCAAGCTTATCGATACCGAA	This study			
	AAAGTCTCCTTTCTACCTAGCG				
BSA19.1	GTACTTTTACAGTCGGTTTTCTAATG	This study			
	TCACTAAGTACAAATCGACAGGAAA				
	CAGTCAA				
BSA20	TCCCATACATTCCTTTTCCTCTTTG	This study			
BSA17.1	GACCATCAAACATTCATTCAGCCA	This study			
BSA20.1	CGATAGCTTTTAAAACTGCGGAAGA	This study			
MS93	TAGTCAAAGCAAATCATAAATTGCG	This study			
MS99	GCTTATCGATACCGTCGAATATTCTC	This study			
	TCTAGTCTCACTTGATGTTC				
MS100	CGGTTTTCTAATGTCACTAACTCTCA	This study			
	AAAGTGATTGACAATTAGC				
MS96	CATGCTCATCACAAAAGAGACGC	This study			
MS101	GAACATCAAGTGAGACTAGAGAGAA	This study			
	TATTCGACGGTATCGATAAGC				
MS102	GCTAATTGTCAATCACTTTTGAGAGT	This study			
	TAGTGACATTAGAAAACCG				
SL107	CAACATAGAAGACTCAGC	This study			
SL108	GAATATCTAGAGTCAGAACC	This study			
BSA1a	TCAGCTCCTTGCTTTTGATAGTCAG	This study			

comEA_5RA3	TTTTCATCAAGCTTATCGATACCTCG	This study
	TAAGAGGAAGAAAAACAGTCG	
comEC_3FA3	CAGTCGGTTTTCTAATGTCACTAAGT	This study
	GTTCGATAGGAAGGATAAATGTT	
BSA6a	ACACCGAGTACAGATGCAAATAAAA	This study
BSA11a	GCATTTGTTTCGATAAGGACACG	This study
SL115	CGGTTTTCTAATGTCACTAACTCTCA	This study
	AAAGTGATTGACAATTAGC	
SL118	GCTTATCGATACCGTCGAGGAAAATT	This study
	CCCAGCTTTGC	
SL119	CGCTATTTTGTCTGTTTGCCG	This study
SL116	GCTAATTGTCAATCACTTTTGAGAGT	This study
	TAGTGACATTAGAAAACCG	
SL117	GCAAAGCTGGGAATTTTCCTCGACGG	This study
	TATCGATAAGC	
SL199	CGCTATTTTGTCTGTTTGCCG	This study
	Quantitative PCR	1
Serotype 2_F	TGTTATCCCATATAAGAACCGAGTGT	(70)
Serotype 2_R	AAAATTACCCCAAAAGCTATCCAA	(70)
Serotype 2_probe	<u>HEX</u> – TTGCAATTTCAATTTTTTTGCCCCAAT CTC – <u>BHQ1</u>	(70)
Serotype 19F_F	TGAGGTTAAGATTGCTGATCG	(70)
Serotype 19F_R	CACGAATGAGAACTCGAATAAAAG	(70)

Serotype 19F_probe	<u>CY5</u> – CGCACTGTCAATTCACCTTC – <u>BHQ3</u>	(70)
tetM_qF1	AGGAAGCGTGGACAAAGGTA	This study
tetM_qR1	GAGTTTGTGCTTGTACGCCA	This study
int_qF1	ATTGCCACACATCACTCCAC	This study
int_qR1	CAAGACGCTCCTGTTGCTTC	This study
orf 20_qF1 (relaxase)	CAGCAGGTGGTCGAAAACAT	This study
orf 20_qR1 (relaxase)	ACCAGCTTCTTTGTTGTCC	This study
ftsK_qF1	TCTCCCGGCACACTTCTTAA	This study
ftsK_qR1	TGGACGTTGACAAGCCAGTA	This study
cat_qF1	TCTCTGGTATTTGGACTCCTGT	This study
cat_qR1	TGCTGTAATAATGGGTAGAAGGT	This study
oLW526	AAACGTGAAGTATCTTCCTACAG	(27)
oLW527	TCGTCGTATCAAAGCTCATTC	(27)
ermB_qF1	TTTTGAAAGCCGTGCGTCTG	This study
ermB_qR1	CATCTGTGGTATGGCGGGTA	This study
comD_qF1	TCCGTGGTTTTCGACATGAT	This study

comD_qR1	ACTGAGCAACCAAACTTCGT	This study
comE_qF1	CCAGGTATCAGCCCTAGATTTTG	This study
comE_qR1	CGCAATTTATGAGATACCCCTGT	This study
Serotype 15A_F	AATTGCCTATAAACTCATTGAGAT	(70)
Serotype 15A_R	AG CCATAGGAAGGAAATAGTATTTG TTC	(70)
Serotype 15A_probe	<u>FAM</u> – CCCGCAAACTCTGTCCT – <u>BHQ1</u>	(70)
Serotype 19A_F	CGCCTAGTCTAAATACCA	(70)
Serotype 19A_R	GAGGTCAACTATAATAGTAAGAG	(70)
Serotype 19A_probe	FAM -TATCAATGAGCCGATCCGTCACTT - BHQ1	(70)
Serotype 9V_F	AGGTATCCTATATACTGCTTTAGG	(70)
Serotype 9V_R	CGAATCTGCCAATATCTGAAAG	(70)
Serotype 9V_probe	<u>HEX</u> – ACACATTGACAACCGCT – <u>BHQ1</u>	(70)
q16s_F2	CCAGATGGACCTGCGTTGTAT	(64)
q16s_R2	TCCGTCCATTGCCGAAGATT	(64)

**Table S3.** Genetic identity and rF data for D39<sup>Str/Tmp</sup> and GA16833<sup>Tet/Ery</sup> or GA47281<sup>Tet/Ery</sup> bioreactor co-inoculation strains and recombinants.

Bioreactor Co-Inoculation Strains					
Strain	MLST Sequence Type/Serotype				
wt D39str/Tmp	ST 595/serotype 2				
wt GA16833 <sup>Tet/Ery</sup> (Tn2009)	ST 236 <sub>slv</sub> /serotype 19F				
]	Recombinants				
Recombinant Antibiotic Selection	MLST Sequence rF				
	Type/Serotype				
Tet+Str	ST 595/serotype 2	2.60x10 <sup>-4</sup> ±2.08x10 <sup>-4</sup>			
Ery+Str	ST 595/serotype 2	1.37x10 <sup>-5</sup> ±7.34x10 <sup>-6</sup>			
Tet+Ery+Str	ST 595/serotype 2	2.00x10 <sup>-5</sup> ±2.09x10 <sup>-5</sup>			
Ery+Str+Tmp	ST 595/serotype 2	6.42x10 <sup>-6</sup> ±4.89x10 <sup>-6</sup>			
Bioreactor	Co-Inoculation Strains	1			
Strain	MLST Sequence	Type/Serotype			
wt D39Str/Tmp	ST 595/se	erotype 2			
wt GA47281 <sup>Tet/Ery</sup> (Tn2010)	ST 3039/sea	rotype 19F			
]	Recombinants				
<b>Recombinant Antibiotic Selection</b>	MLST Sequence	rF			
	Type/Serotype				
Tet+Str	ST 595/serotype 2	1.34x10 <sup>-4</sup> ±1.62x10 <sup>-4</sup>			
Ery+Str	ST 595/serotype 2	1.63x10 <sup>-4</sup> ±2.06x10 <sup>-4</sup>			
Tet+Ery+Str	ST 595/serotype 2	1.39x10 <sup>-4</sup> ±1.82x10 <sup>-4</sup>			
Ery+Str+Tmp	ST 595/serotype 2	1.65x10 <sup>-4</sup> ±1.93x10 <sup>-4</sup>			

**Table S4.** Homologous recombination of variably sized donor DNA fragments with intact ICE into bioreactor recombinant genomes.

Donor (ICE, MLST)	Recipient (MLST)	Recombinant (MLST)	Left (5') of ICE (bp)	Right (3') of ICE (bp)	Size of Recombined Donor Fragment with ICE (bp)
GA47281 (Tn2010 <sup>Tet/Ery</sup> , ST 3039)	D39Str/Tmp (ST 595)	Tet + Str (ST 595)	4890	7158	38,438
GA47281 (Tn2010 <sup>Tet/Ery</sup> , ST 3039)	D39str/Tmp (ST 595)	Ery + Str (ST 595)	918	7158	34,466
GA47179  (partial Tn6002 <sup>Tet/Ery</sup> , ST 63)	D39 <sup>Str</sup> (ST 595)	Tet + Str (ST 595)	82345	1480	101,025
GA44288 (Tn2010 <sup>Tet/Ery</sup> , ST 320)	D39 <sup>Str</sup> (ST 595)	Tet + Str (ST 595)	4717	12274	43,381
GA44288 (Tn2010 <sup>Tet/Ery</sup> , ST 320)	D39 <sup>Str</sup> (ST 595)	Tet + Str (ST 595)	4718	4132	35,240
GA44288 (Tn2010 <sup>Tet/Ery</sup> , ST 320)	D39 <sup>Str</sup> (ST 595)	Tet + Str (ST 595)	539	17536	44,465
BASP1 (Tn2009 <sup>Tet/Ery</sup> , ST 236)	GA40410 <sup>Tmp</sup> (ST 1936)	Tet + Tmp (ST 1936)	14916	2042	40,499
BASP1 (Tn2009 <sup>Tet/Ery</sup> , ST 236)	GA40410 <sup>Tmp</sup> (ST 1936)	Tet + Tmp (ST 1936)	1088	49071	73,700

BASP1 (Tn2009 <sup>Tet/Ery</sup> , ST 236)	GA40410 <sup>Tmp</sup> (ST 1936)	Tet + Tmp (ST 1936)	29167	39616	92,324
BASP1 (Tn2009 <sup>Tet/Ery</sup> , ST 236)	GA43265 <sup>Tmp</sup> (ST 2584)	Tet + Tmp (ST 2584)	44458	21649	89,648
BASP1 (Tn2009 <sup>Tet/Ery</sup> , ST 236)	GA43265 <sup>Tmp</sup> (ST 2584)	Tet + Tmp (ST 2584)	14577	12520	50,638

#### REFERENCES

- 1. Roca A, Hill PC, Townend J, Egere U, Antonio M, Bojang A, Akisanya A, Litchfield T, Nsekpong DE, Oluwalana C, Howie SR, Greenwood B, Adegbola RA. Effects of community-wide vaccination with PCV-7 on pneumococcal nasopharyngeal carriage in the Gambia: a cluster-randomized trial. PLoS Med. 2011;8(10):e1001107. Epub 2011/10/27. doi: 10.1371/journal.pmed.1001107. PubMed PMID: 22028630; PMCID: PMC3196470.
- 2. Regev-Yochay G, Raz M, Dagan R, Porat N, Shainberg B, Pinco E, Keller N, Rubinstein E. Nasopharyngeal carriage of Streptococcus pneumoniae by adults and children in community and family settings. Clin Infect Dis. 2004;38(5):632-9. Epub 2004/02/27. doi: 10.1086/381547. PubMed PMID: 14986245.
- 3. Shak JR, Vidal JE, Klugman KP. Influence of bacterial interactions on pneumococcal colonization of the nasopharynx. Trends Microbiol. 2013;21(3):129-35. Epub 2013/01/01. doi: 10.1016/j.tim.2012.11.005. PubMed PMID: 23273566; PMCID: PMC3729046.
- 4. Weiser JN, Ferreira DM, Paton JC. Streptococcus pneumoniae: transmission, colonization and invasion. Nat Rev Microbiol. 2018;16(6):355-67. Epub 2018/03/31. doi: 10.1038/s41579-018-0001-8. PubMed PMID: 29599457; PMCID: PMC5949087.
- 5. Fletcher MA, Laufer DS, McIntosh ED, Cimino C, Malinoski FJ. Controlling invasive pneumococcal disease: is vaccination of at-risk groups sufficient? Int J Clin Pract. 2006;60(4):450-6. Epub 2006/04/20. doi: 10.1111/j.1368-5031.2006.00858.x. PubMed PMID: 16620359; PMCID: PMC1448695.
- 6. Nadimpalli M, Delarocque-Astagneau E, Love DC, Price LB, Huynh BT, Collard JM, Lay KS, Borand L, Ndir A, Walsh TR, Guillemot D, Bacterial I, antibiotic-Resistant Diseases among Young children in low-income countries Study G. Combating Global Antibiotic Resistance:

- Emerging One Health Concerns in Lower- and Middle-Income Countries. Clin Infect Dis. 2018;66(6):963-9. Epub 2018/01/19. doi: 10.1093/cid/cix879. PubMed PMID: 29346620.
- 7. Bergman M, Huikko S, Huovinen P, Paakkari P, Seppala H, Finnish Study Group for Antimicrobial R. Macrolide and azithromycin use are linked to increased macrolide resistance in Streptococcus pneumoniae. Antimicrob Agents Chemother. 2006;50(11):3646-50. Epub 2006/08/31. doi: 10.1128/AAC.00234-06. PubMed PMID: 16940064; PMCID: PMC1635217.
- 8. Malhotra-Kumar S, Lammens C, Coenen S, Van Herck K, Goossens H. Effect of azithromycin and clarithromycin therapy on pharyngeal carriage of macrolide-resistant streptococci in healthy volunteers: a randomised, double-blind, placebo-controlled study. Lancet. 2007;369(9560):482-90. Epub 2007/02/13. doi: 10.1016/S0140-6736(07)60235-9. PubMed PMID: 17292768.
- 9. Chancey ST, Agrawal S, Schroeder MR, Farley MM, Tettelin H, Stephens DS. Composite mobile genetic elements disseminating macrolide resistance in Streptococcus pneumoniae. Front Microbiol. 2015;6:26. Epub 2015/02/25. doi: 10.3389/fmicb.2015.00026. PubMed PMID: 25709602; PMCID: PMC4321634.
- 10. Cochetti I, Tili E, Vecchi M, Manzin A, Mingoia M, Varaldo PE, Montanari MP. New Tn916-related elements causing erm(B)-mediated erythromycin resistance in tetracycline-susceptible pneumococci. J Antimicrob Chemother. 2007;60(1):127-31. Epub 2007/05/08. doi: 10.1093/jac/dkm120. PubMed PMID: 17483548.
- 11. Del Grosso M, Camilli R, Iannelli F, Pozzi G, Pantosti A. The mef(E)-carrying genetic element (mega) of Streptococcus pneumoniae: insertion sites and association with other genetic elements. Antimicrob Agents Chemother. 2006;50(10):3361-6. Epub 2006/09/29. doi: 10.1128/AAC.00277-06. PubMed PMID: 17005818; PMCID: PMC1610078.

- 12. Del Grosso M, Scotto d'Abusco A, Iannelli F, Pozzi G, Pantosti A. Tn2009, a Tn916-like element containing mef(E) in Streptococcus pneumoniae. Antimicrob Agents Chemother. 2004;48(6):2037-42. Epub 2004/05/25. doi: 10.1128/AAC.48.6.2037-2042.2004. PubMed PMID: 15155196; PMCID: PMC415626.
- 13. Li Y, Tomita H, Lv Y, Liu J, Xue F, Zheng B, Ike Y. Molecular characterization of erm(B)-and mef(E)-mediated erythromycin-resistant Streptococcus pneumoniae in China and complete DNA sequence of Tn2010. J Appl Microbiol. 2011;110(1):254-65. Epub 2010/10/22. doi: 10.1111/j.1365-2672.2010.04875.x. PubMed PMID: 20961364.
- 14. Johnson CM, Grossman AD. Integrative and Conjugative Elements (ICEs): What They Do and How They Work. Annu Rev Genet. 2015;49:577-601. Epub 2015/10/17. doi: 10.1146/annurev-genet-112414-055018. PubMed PMID: 26473380; PMCID: PMC5180612.
- 15. Santoro F, Oggioni MR, Pozzi G, Iannelli F. Nucleotide sequence and functional analysis of the tet (M)-carrying conjugative transposon Tn5251 of Streptococcus pneumoniae. FEMS Microbiol Lett. 2010;308(2):150-8. Epub 2010/05/22. doi: 10.1111/j.1574-6968.2010.02002.x. PubMed PMID: 20487027.
- 16. Santoro F, Romeo A, Pozzi G, Iannelli F. Excision and Circularization of Integrative Conjugative Element Tn5253 of Streptococcus pneumoniae. Front Microbiol. 2018;9:1779. Epub 2018/08/16. doi: 10.3389/fmicb.2018.01779. PubMed PMID: 30108581; PMCID: PMC6079316.
- 17. Laurenceau R, Pehau-Arnaudet G, Baconnais S, Gault J, Malosse C, Dujeancourt A, Campo N, Chamot-Rooke J, Le Cam E, Claverys JP, Fronzes R. A type IV pilus mediates DNA binding during natural transformation in Streptococcus pneumoniae. PLoS Pathog. 2013;9(6):e1003473. Epub 2013/07/05. doi: 10.1371/journal.ppat.1003473. PubMed PMID: 23825953; PMCID: PMC3694846.

- 18. Andam CP, Hanage WP. Mechanisms of genome evolution of Streptococcus. Infect Genet Evol. 2015;33:334-42. Epub 2014/12/03. doi: 10.1016/j.meegid.2014.11.007. PubMed PMID: 25461843; PMCID: PMC4430445.
- 19. Straume D, Stamsas GA, Havarstein LS. Natural transformation and genome evolution in Streptococcus pneumoniae. Infect Genet Evol. 2015;33:371-80. Epub 2014/12/03. doi: 10.1016/j.meegid.2014.10.020. PubMed PMID: 25445643.
- 20. Lattar SM, Wu X, Brophy J, Sakai F, Klugman KP, Vidal JE. A Mechanism of Unidirectional Transformation, Leading to Antibiotic Resistance, Occurs within Nasopharyngeal Pneumococcal Biofilm Consortia. MBio. 2018;9(3). Epub 2018/05/17. doi: 10.1128/mBio.00561-18. PubMed PMID: 29764945; PMCID: PMC5954218.
- 21. Pikis A, Donkersloot JA, Rodriguez WJ, Keith JM. A conservative amino acid mutation in the chromosome-encoded dihydrofolate reductase confers trimethoprim resistance in Streptococcus pneumoniae. J Infect Dis. 1998;178(3):700-6. Epub 1998/09/05. doi: 10.1086/515371. PubMed PMID: 9728538.
- 22. Salles C, Creancier L, Claverys JP, Mejean V. The high level streptomycin resistance gene from Streptococcus pneumoniae is a homologue of the ribosomal protein S12 gene from Escherichia coli. Nucleic Acids Res. 1992;20(22):6103. Epub 1992/11/25. doi: 10.1093/nar/20.22.6103. PubMed PMID: 1461744; PMCID: PMC334482.
- 23. Su YA, He P, Clewell DB. Characterization of the tet(M) determinant of Tn916: evidence for regulation by transcription attenuation. Antimicrob Agents Chemother. 1992;36(4):769-78. Epub 1992/04/01. doi: 10.1128/aac.36.4.769. PubMed PMID: 1323953; PMCID: PMC189400.

- 24. Delavat F, Miyazaki R, Carraro N, Pradervand N, van der Meer JR. The hidden life of integrative and conjugative elements. FEMS Microbiol Rev. 2017;41(4):512-37. Epub 2017/04/04. doi: 10.1093/femsre/fux008. PubMed PMID: 28369623; PMCID: PMC5812530.
- 25. Celli J, Trieu-Cuot P. Circularization of Tn916 is required for expression of the transposon-encoded transfer functions: characterization of long tetracycline-inducible transcripts reading through the attachment site. Mol Microbiol. 1998;28(1):103-17. Epub 1998/05/21. doi: 10.1046/j.1365-2958.1998.00778.x. PubMed PMID: 9593300.
- 26. Marra D, Scott JR. Regulation of excision of the conjugative transposon Tn916. Mol Microbiol. 1999;31(2):609-21. Epub 1999/02/23. doi: 10.1046/j.1365-2958.1999.01201.x. PubMed PMID: 10027977.
- 27. Wright LD, Grossman AD. Autonomous Replication of the Conjugative Transposon Tn916. J Bacteriol. 2016;198(24):3355-66. Epub 2016/10/05. doi: 10.1128/JB.00639-16. PubMed PMID: 27698087; PMCID: PMC5116939.
- 28. Poyart-Salmeron C, Trieu-Cuot P, Carlier C, Courvalin P. Molecular characterization of two proteins involved in the excision of the conjugative transposon Tn1545: homologies with other site-specific recombinases. EMBO J. 1989;8(8):2425-33. Epub 1989/08/01. PubMed PMID: 2551683; PMCID: PMC401188.
- 29. Storrs MJ, Poyart-Salmeron C, Trieu-Cuot P, Courvalin P. Conjugative transposition of Tn916 requires the excisive and integrative activities of the transposon-encoded integrase. J Bacteriol. 1991;173(14):4347-52. Epub 1991/07/01. doi: 10.1128/jb.173.14.4347-4352.1991. PubMed PMID: 1648556; PMCID: PMC208095.

- 30. Showsh SA, Andrews RE, Jr. Tetracycline enhances Tn916-mediated conjugal transfer. Plasmid. 1992;28(3):213-24. Epub 1992/11/11. doi: 10.1016/0147-619x(92)90053-d. PubMed PMID: 1334267.
- 31. Johnson CM, Grossman AD. Identification of host genes that affect acquisition of an integrative and conjugative element in Bacillus subtilis. Mol Microbiol. 2014;93(6):1284-301. Epub 2014/07/30. doi: 10.1111/mmi.12736. PubMed PMID: 25069588; PMCID: PMC4160349.
- 32. Iannelli F, Santoro F, Fox V, Pozzi G. A Mating Procedure for Genetic Transfer of Integrative and Conjugative Elements (ICEs) of Streptococci and Enterococci. Methods Protoc. 2021;4(3). Epub 2021/09/27. doi: 10.3390/mps4030059. PubMed PMID: 34564305; PMCID: PMC8482134.
- 33. Yamamoto M, Jones JM, Senghas E, Gawron-Burke C, Clewell DB. Generation of Tn5 insertions in streptococcal conjugative transposon Tn916. Appl Environ Microbiol. 1987;53(5):1069-72. Epub 1987/05/01. doi: 10.1128/aem.53.5.1069-1072.1987. PubMed PMID: 3038014; PMCID: PMC203811.
- 34. Llosa M, Gomis-Ruth FX, Coll M, de la Cruz Fd F. Bacterial conjugation: a two-step mechanism for DNA transport. Mol Microbiol. 2002;45(1):1-8. Epub 2002/07/09. doi: 10.1046/j.1365-2958.2002.03014.x. PubMed PMID: 12100543.
- 35. Parsons JA, Bannam TL, Devenish RJ, Rood JI. TcpA, an FtsK/SpoIIIE homolog, is essential for transfer of the conjugative plasmid pCW3 in Clostridium perfringens. J Bacteriol. 2007;189(21):7782-90. Epub 2007/08/28. doi: 10.1128/JB.00783-07. PubMed PMID: 17720795; PMCID: PMC2168741.
- 36. Pestova EV, Havarstein LS, Morrison DA. Regulation of competence for genetic transformation in Streptococcus pneumoniae by an auto-induced peptide pheromone and a two-

- component regulatory system. Mol Microbiol. 1996;21(4):853-62. Epub 1996/08/01. doi: 10.1046/j.1365-2958.1996.501417.x. PubMed PMID: 8878046.
- 37. Berge M, Moscoso M, Prudhomme M, Martin B, Claverys JP. Uptake of transforming DNA in Gram-positive bacteria: a view from Streptococcus pneumoniae. Mol Microbiol. 2002;45(2):411-21. Epub 2002/07/19. doi: 10.1046/j.1365-2958.2002.03013.x. PubMed PMID: 12123453.
- 38. Jolley KA, Bray JE, Maiden MCJ. Open-access bacterial population genomics: BIGSdb software, the PubMLST.org website and their applications. Wellcome Open Res. 2018;3:124. Epub 2018/10/23. doi: 10.12688/wellcomeopenres.14826.1. PubMed PMID: 30345391; PMCID: PMC6192448.
- 39. Scott JR, Kirchman PA, Caparon MG. An intermediate in transposition of the conjugative transposon Tn916. Proc Natl Acad Sci U S A. 1988;85(13):4809-13. Epub 1988/07/01. doi: 10.1073/pnas.85.13.4809. PubMed PMID: 2838847; PMCID: PMC280525.
- 40. Cowley LA, Petersen FC, Junges R, Jimson DJM, Morrison DA, Hanage WP. Evolution via recombination: Cell-to-cell contact facilitates larger recombination events in Streptococcus pneumoniae. PLoS Genet. 2018;14(6):e1007410. Epub 2018/06/14. doi: 10.1371/journal.pgen.1007410. PubMed PMID: 29897968; PMCID: PMC6016952.
- 41. Marks LR, Parameswaran GI, Hakansson AP. Pneumococcal interactions with epithelial cells are crucial for optimal biofilm formation and colonization in vitro and in vivo. Infect Immun. 2012;80(8):2744-60. Epub 2012/05/31. doi: 10.1128/IAI.00488-12. PubMed PMID: 22645283; PMCID: PMC3434590.
- 42. Sakai F, Chochua S, Satzke C, Dunne EM, Mulholland K, Klugman KP, Vidal JE. Single-plex quantitative assays for the detection and quantification of most pneumococcal serotypes.

- PLoS One. 2015;10(3):e0121064. Epub 2015/03/24. doi: 10.1371/journal.pone.0121064. PubMed PMID: 25798884; PMCID: PMC4370668.
- 43. Turner P, Hinds J, Turner C, Jankhot A, Gould K, Bentley SD, Nosten F, Goldblatt D. Improved detection of nasopharyngeal cocolonization by multiple pneumococcal serotypes by use of latex agglutination or molecular serotyping by microarray. J Clin Microbiol. 2011;49(5):1784-9. Epub 2011/03/18. doi: 10.1128/JCM.00157-11. PubMed PMID: 21411589; PMCID: PMC3122683.
- 44. Wyllie AL, Chu ML, Schellens MH, van Engelsdorp Gastelaars J, Jansen MD, van der Ende A, Bogaert D, Sanders EA, Trzcinski K. Streptococcus pneumoniae in saliva of Dutch primary school children. PLoS One. 2014;9(7):e102045. Epub 2014/07/12. doi: 10.1371/journal.pone.0102045. PubMed PMID: 25013895; PMCID: PMC4094488.
- 45. Vidal AGJ, Alibayov B, Frame IJ, Murin L, Creel A, Hu D, Wu X, Vidal JE. Induction of the macrolide-resistance efflux pump Mega inhibits intoxication of Staphylococcus aureus strains by Streptococcus pneumoniae. Microbiol Res. 2022;263:127134. Epub 2022/07/30. doi: 10.1016/j.micres.2022.127134. PubMed PMID: 35905580.
- 46. Santagati M, Iannelli F, Cascone C, Campanile F, Oggioni MR, Stefani S, Pozzi G. The novel conjugative transposon tn1207.3 carries the macrolide efflux gene mef(A) in Streptococcus pyogenes. Microb Drug Resist. 2003;9(3):243-7. Epub 2003/09/10. doi: 10.1089/107662903322286445. PubMed PMID: 12959402.
- 47. Iannelli F, Santoro F, Oggioni MR, Pozzi G. Nucleotide sequence analysis of integrative conjugative element Tn5253 of Streptococcus pneumoniae. Antimicrob Agents Chemother. 2014;58(2):1235-9. Epub 2013/12/04. doi: 10.1128/AAC.01764-13. PubMed PMID: 24295984; PMCID: PMC3910829.

- 48. Hsieh YC, Lin TL, Lin CM, Wang JT. Identification of PblB mediating galactose-specific adhesion in a successful Streptococcus pneumoniae clone. Sci Rep. 2015;5:12265. Epub 2015/07/22. doi: 10.1038/srep12265. PubMed PMID: 26193794; PMCID: PMC4508584.
- 49. Loeffler JM, Fischetti VA. Lysogeny of Streptococcus pneumoniae with MM1 phage: improved adherence and other phenotypic changes. Infect Immun. 2006;74(8):4486-95. Epub 2006/07/25. doi: 10.1128/IAI.00020-06. PubMed PMID: 16861634; PMCID: PMC1539626.
- 50. Wyres KL, van Tonder A, Lambertsen LM, Hakenbeck R, Parkhill J, Bentley SD, Brueggemann AB. Evidence of antimicrobial resistance-conferring genetic elements among pneumococci isolated prior to 1974. BMC Genomics. 2013;14:500. Epub 2013/07/25. doi: 10.1186/1471-2164-14-500. PubMed PMID: 23879707; PMCID: PMC3726389.
- 51. Evans BA, Rozen DE. Significant variation in transformation frequency in Streptococcus pneumoniae. ISME J. 2013;7(4):791-9. Epub 2013/01/11. doi: 10.1038/ismej.2012.170. PubMed PMID: 23303370; PMCID: PMC3603394.
- 52. Gurney T, Jr., Fox MS. Physical and genetic hybrids formed in bacterial transformation. J Mol Biol. 1968;32(1):83-100. Epub 1968/02/28. doi: 10.1016/0022-2836(68)90147-2. PubMed PMID: 4384454.
- 53. Joloba ML, Kidenya BR, Kateete DP, Katabazi FA, Muwanguzi JK, Asiimwe BB, Alarakol SP, Nakavuma JL, Bajaksouzian S, Windau A, Jacobs MR. Comparison of transformation frequencies among selected Streptococcus pneumoniae serotypes. Int J Antimicrob Agents. 2010;36(2):124-8. Epub 2010/05/18. doi: 10.1016/j.ijantimicag.2010.03.024. PubMed PMID: 20472405; PMCID: PMC2902549.

- 54. Lacks S. Integration efficiency and genetic recombination in pneumococcal transformation. Genetics. 1966;53(1):207-35. Epub 1966/01/01. PubMed PMID: 4379022; PMCID: PMC1211003.
- Croucher NJ, Harris SR, Fraser C, Quail MA, Burton J, van der Linden M, McGee L, von Gottberg A, Song JH, Ko KS, Pichon B, Baker S, Parry CM, Lambertsen LM, Shahinas D, Pillai DR, Mitchell TJ, Dougan G, Tomasz A, Klugman KP, Parkhill J, Hanage WP, Bentley SD. Rapid pneumococcal evolution in response to clinical interventions. Science. 2011;331(6016):430-4. Epub 2011/01/29. doi: 10.1126/science.1198545. PubMed PMID: 21273480; PMCID: PMC3648787.
- 56. Valente C, Cruz AR, Henriques AO, Sa-Leao R. Intra-Species Interactions in Streptococcus pneumoniae Biofilms. Front Cell Infect Microbiol. 2021;11:803286. Epub 2022/01/25. doi: 10.3389/fcimb.2021.803286. PubMed PMID: 35071049; PMCID: PMC8767070.
- 57. Steinmoen H, Knutsen E, Havarstein LS. Induction of natural competence in Streptococcus pneumoniae triggers lysis and DNA release from a subfraction of the cell population. Proc Natl Acad Sci U S A. 2002;99(11):7681-6. Epub 2002/05/29. doi: 10.1073/pnas.112464599. PubMed PMID: 12032343; PMCID: PMC124321.
- 58. Wei H, Havarstein LS. Fratricide is essential for efficient gene transfer between pneumococci in biofilms. Appl Environ Microbiol. 2012;78(16):5897-905. Epub 2012/06/19. doi: 10.1128/AEM.01343-12. PubMed PMID: 22706053; PMCID: PMC3406168.
- 59. Marks LR, Reddinger RM, Hakansson AP. High levels of genetic recombination during nasopharyngeal carriage and biofilm formation in Streptococcus pneumoniae. MBio. 2012;3(5).

- Epub 2012/09/28. doi: 10.1128/mBio.00200-12. PubMed PMID: 23015736; PMCID: PMC3448161.
- 60. Oggioni MR, Trappetti C, Kadioglu A, Cassone M, Iannelli F, Ricci S, Andrew PW, Pozzi G. Switch from planktonic to sessile life: a major event in pneumococcal pathogenesis. Mol Microbiol. 2006;61(5):1196-210. Epub 2006/08/24. doi: 10.1111/j.1365-2958.2006.05310.x. PubMed PMID: 16925554; PMCID: PMC1618759.
- 61. Trappetti C, Gualdi L, Di Meola L, Jain P, Korir CC, Edmonds P, Iannelli F, Ricci S, Pozzi G, Oggioni MR. The impact of the competence quorum sensing system on Streptococcus pneumoniae biofilms varies depending on the experimental model. BMC Microbiol. 2011;11:75. Epub 2011/04/16. doi: 10.1186/1471-2180-11-75. PubMed PMID: 21492426; PMCID: PMC3098770.
- 62. Claverys JP, Dintilhac A, Pestova EV, Martin B, Morrison DA. Construction and evaluation of new drug-resistance cassettes for gene disruption mutagenesis in Streptococcus pneumoniae, using an ami test platform. Gene. 1995;164(1):123-8. Epub 1995/10/16. doi: 10.1016/0378-1119(95)00485-o. PubMed PMID: 7590300.
- 63. Havarstein LS, Coomaraswamy G, Morrison DA. An unmodified heptadecapeptide pheromone induces competence for genetic transformation in Streptococcus pneumoniae. Proc Natl Acad Sci U S A. 1995;92(24):11140-4. Epub 1995/11/21. PubMed PMID: 7479953; PMCID: PMC40587.
- 64. Schroeder MR, Lohsen S, Chancey ST, Stephens DS. High-Level Macrolide Resistance Due to the Mega Element [mef(E)/mel] in Streptococcus pneumoniae. Front Microbiol. 2019;10:868. Epub 2019/05/21. doi: 10.3389/fmicb.2019.00868. PubMed PMID: 31105666; PMCID: PMC6491947.

- 65. Sakai F, Talekar SJ, Lanata CF, Grijalva CG, Klugman KP, Vidal JE, Group RP, Investigators G. Expression of Streptococcus pneumoniae Virulence-Related Genes in the Nasopharynx of Healthy Children. PLoS One. 2013;8(6):e67147. Epub 2013/07/05. doi: 10.1371/journal.pone.0067147. PubMed PMID: 23825636; PMCID: PMC3688971.
- 66. Sullivan MJ, Petty NK, Beatson SA. Easyfig: a genome comparison visualizer. Bioinformatics. 2011;27(7):1009-10. Epub 2011/02/01. doi: 10.1093/bioinformatics/btr039. PubMed PMID: 21278367; PMCID: PMC3065679.
- 67. Livak KJ, Schmittgen TD. Analysis of relative gene expression data using real-time quantitative PCR and the 2(-Delta Delta C(T)) Method. Methods. 2001;25(4):402-8. Epub 2002/02/16. doi: 10.1006/meth.2001.1262. PubMed PMID: 11846609.
- 68. Avery OT, Macleod CM, McCarty M. Studies on the Chemical Nature of the Substance Inducing Transformation of Pneumococcal Types: Induction of Transformation by a Desoxyribonucleic Acid Fraction Isolated from Pneumococcus Type Iii. J Exp Med. 1944;79(2):137-58. Epub 1944/02/01. doi: 10.1084/jem.79.2.137. PubMed PMID: 19871359; PMCID: PMC2135445.
- 69. Tettelin H, Nelson KE, Paulsen IT, Eisen JA, Read TD, Peterson S, Heidelberg J, DeBoy RT, Haft DH, Dodson RJ, Durkin AS, Gwinn M, Kolonay JF, Nelson WC, Peterson JD, Umayam LA, White O, Salzberg SL, Lewis MR, Radune D, Holtzapple E, Khouri H, Wolf AM, Utterback TR, Hansen CL, McDonald LA, Feldblyum TV, Angiuoli S, Dickinson T, Hickey EK, Holt IE, Loftus BJ, Yang F, Smith HO, Venter JC, Dougherty BA, Morrison DA, Hollingshead SK, Fraser CM. Complete genome sequence of a virulent isolate of Streptococcus pneumoniae. Science. 2001;293(5529):498-506. Epub 2001/07/21. doi: 10.1126/science.1061217. PubMed PMID: 11463916.

70. Pimenta FC, Roundtree A, Soysal A, Bakir M, du Plessis M, Wolter N, von Gottberg A, McGee L, Carvalho Mda G, Beall B. Sequential triplex real-time PCR assay for detecting 21 pneumococcal capsular serotypes that account for a high global disease burden. J Clin Microbiol. 2013;51(2):647-52. Epub 2012/12/12. doi: 10.1128/JCM.02927-12. PubMed PMID: 23224094; PMCID: PMC3553924.

93
Chapter 3: Streptococcus pneumoniae Tn916-related integrative and conjugative elements in the
United States in the pre- and post-pneumococcal conjugate vaccine eras (1916-2021)
Brenda S. Antezana <sup>a</sup> , Yih-Ling Tzeng <sup>b</sup> , David S. Stephens <sup>b</sup>
<sup>a</sup> Microbiology and Molecular Genetics Program, Graduate Division of Biological and Biomedical
Sciences, Emory University Laney Graduate School, Atlanta, Georgia, USA
<sup>b</sup> Department of Medicine, Division of Infectious Diseases, Emory University School of Medicine,
Atlanta, Georgia, USA
#Address correspondence to David S. Stephens, <a href="mailto:dstep01@emory.edu">dstep01@emory.edu</a> .

# Paper in preparation

B. Antezana conducted all analyses on genomic data as well as wrote and edited the chapter.

#### **ABSTRACT**

The dissemination of Tn916-related integrative and conjugative elements (ICEs), such as Tn2009 (23.5 kb), Tn6002 (20.8 kb), and Tn2010 (26.3 kb), which harbor tetM, mefE/mel, and/or ermB, are partly responsible for increasing antibiotic resistance in Streptococcus pneumoniae (S. pneumoniae). Utilizing the genomic sequences of 4,560 PubMLST-deposited S. pneumoniae isolates from the United States (US) from 1916-2021, trends in macrolide and tetracycline resistance conferred solely by Tn916-related ICEs were explored. Four distinct time periods, defined as historic (1916-1994), pre-PCV7 (1995-2000), PCV7 (2001-2010), and PCV13 (2011-2021), were examined. Although PCV introductions have reduced the overall incidence of invasive S. pneumoniae in the US, the frequency of Tn916-related ICEs increased steadily- 1.5%, 10%, 17%, and 22%, respectively, in S. pneumoniae isolates from these four periods. Tn2009-encoded macrolide efflux (mefE/mel) emerged during the 1990s-2000 in PCV7 serotypes (6B, 14, 19F and 23F) and in non-vaccine serotypes (3, 6A, 6E, 12F and 21). However, Tn6002-encoded ribosomal methylation (ermB) and Tn2010 with both ermB and mefE/mel dominated during the late PCV7 and in the PCV13 eras. In contrast to the decline in vaccine serotypes, including those carrying Tn916-related ICEs, a dramatic increase in the frequency of non-vaccine serotypes containing Tn916-related ICEs was observed during the PCV13 era, especially 15A and 23A, which are not included in the current introductions of PCV15 and PCV20 vaccines. These data highlight the importance for continued monitoring of Tn916-related ICE-containing S. pneumoniae to aid in the design of future PCV formulations and in treatment recommendations.

#### **IMPORTANCE**

Macrolide antibiotics are the primary choice for treatment of upper respiratory tract Streptococcus pneumoniae (S. pneumoniae) infections and extensive prescription of these drugs has facilitated the rise in macrolide-resistant S. pneumoniae in the United States (US). A major contributor to the dissemination of macrolide and tetracycline resistance is the horizontal transfer of large Tn916-related integrative and conjugative elements (ICEs), such as Tn2009, Tn6002, and Tn2010, which harbor tetM conferring tetracycline resistance as well as mefE/mel and/or ermB conferring macrolide resistance. We assessed the frequency of Tn916-related ICEs in the US in circulating S. pneumoniae serotypes based on whole genome sequences of 4,560 isolates in the PubMLST database, as well as the impact of pneumococcal conjugate vaccine (PCV) introductions on the spread of ICEs. The frequency of Tn916-related ICEs in S. pneumoniae in the US increased to 22% during 2011-2021. Macrolide resistance during the 1990s-2000 was mainly attributed to Tn2009 encoding the efflux pump MefE/Mel but had shifted to Tn6002 encoding ErmB-mediated ribosomal methylation as well as Tn2010 harboring both during the late 2000s-2010s. The increase in Tn916-related ICE frequency was observed predominantly in non-vaccine serotypes such as 15A and 23A, which are not included in the new PCV15 and PCV20 vaccines. Continued global monitoring of Tn916-related ICEs will better inform decisions on future pneumococcal vaccine design and treatment recommendations.

#### INTRODUCTION

Streptococcus pneumoniae (or pneumococcus) colonizes the human nasopharynx as a commensal or can spread to other local sites, causing otitis media or bacterial pneumonia<sup>(1-3)</sup>. When *S. pneumoniae* crosses the respiratory epithelium, enters the bloodstream, and spreads to other sterile sites, invasive pneumococcal disease (IPD), such as bacteremia and meningitis<sup>(2, 4)</sup>, can be the result. Introduced in the 1940s, penicillin was initially an effective treatment for pneumococcal infections. The subsequent increased resistance to beta-lactams motivated the transition to macrolides as a principal outpatient therapy <sup>(5, 6)</sup>. However, widespread macrolide usage again resulted in increased prevalence of macrolide-resistant *S. pneumoniae* strains in the 1990s<sup>(7-9)</sup>. This general increased prevalence of antibiotic resistance in *S. pneumoniae* motivated the World Health Organization to add this bacterium to the list of priority pathogens in need of research and development of novel therapeutics<sup>(10)</sup>.

One class of macrolide resistance in *S. pneumoniae* includes the chromosomally encoded integrative and conjugative elements (ICEs) of the Tn916 family, such as Tn2009 (23.5 kb), Tn6002 (20.8 kb), and Tn2010 (26.3 kb), all of which also confer tetracycline resistance via the *tetM* gene <sup>(11)</sup>. The macrolide resistance determinants present on Tn916-related ICEs include *ermB*, which encodes for a ribosomal methylase that dimethylates the bacterial ribosome to prevent antibiotic binding, as well as the *mefE/mel* genes on the macrolide efflux genetic assembly (Mega), which together mediate efflux of macrolides <sup>(5, 11)</sup>. Specifically, Tn2009 contains the Mega element integrated into *orf6* of the prototype Tn916<sup>(12)</sup>, Tn6002 has *ermB* inserted into *orf20* of Tn916<sup>(13)</sup>, and Tn2010 is comprised of Mega and *ermB* in *orf6* and *orf20* of Tn916<sup>(14)</sup>, respectively. We had previously shown that, although these Tn916-related ICEs in *S. pneumoniae* contain conjugative

genes like the prototype Tn916, the mechanism by which they disseminate is transformation followed by homologous recombination <sup>(15)</sup>.

Vaccination efforts for S. pneumoniae were initiated as early as 1911 in South Africa with the use of capsular polysaccharides for vaccine development (16, 17). However, a lack of immunogenicity in children less than two years of age, an age cohort most at risk for IPD, led to the development of pneumococcal conjugate vaccines with capsular polysaccharides conjugated to the diphtheria protein, CRM197<sup>(18)</sup>. In the US, PCV7 containing seven S. pneumoniae serotypes (4, 6B, 9V, 14, 18C, 19F, and 23F) was licensed and introduced in 2000 for use in children under five years of age<sup>(19)</sup>. Though there was a marked reduction in carriage and IPD caused by serotypes included in PCV7, non-vaccine serotypes began to emerge, such as serotype 19A, likely due to clonal expansion<sup>(20-22)</sup>. Thus, PCV13 (PCV7 serotypes plus 1, 3, 5, 6A, 7F, and 19A) was introduced in 2010, resulting in a similar decrease in carriage and IPD incidence of serotypes included in PCV13 (20, 23, 24). Further, both PCV7 and PCV13 introductions also reduced the macrolide-resistant S. pneumoniae strains (25-27). The development of broader pneumococcal conjugate vaccine serotype coverage has continued. PCV15 (PCV13 serotypes plus 22F and 33F) and PCV20 (PCV15 plus serotypes 8, 10A, 11A, 12F, and 15B) formulations have been licensed in the US in 2021 for use in adults, (28, 29) while PCV15 and PCV20 were approved for use in children in 2022<sup>(28)</sup> and 2023<sup>(30)</sup>, respectively. Population-based surveillance of carriage and IPD incidence following PCV15 and PCV20 introductions are currently underway.

In this study, we investigated the dissemination of Tn2009, Tn6002, and Tn2010 among *S. pneumoniae* isolated in the US. Utilizing 4,560 US isolates that were deposited in the PubMLST *Streptococcus pneumoniae* database<sup>(31)</sup> that spanned 1916 to 2021, isolates carrying specific Tn916-related ICEs were identified, and their frequency across distinct PCV coverage periods was

determined. Serotypes of these US ICE-containing isolates were categorized into vaccine and non-vaccine serotypes to determine if PCV7 and PCV13 introductions were associated with the distributions of Tn2009, Tn6002, and Tn2010. Trends of ICE distribution in Thailand and South Africa with different vaccine introduction schedules over similar time periods were also included for comparison.

# **RESULTS**

# Increasing frequency of Tn916-related ICEs in S. pneumoniae in the US, 1916-2021.

Previous studies have noted the rise of macrolide resistance in the US since the 1990s <sup>(8,9)</sup>. We utilized the genome data of 4,560 US isolates deposited in the PubMLST *Streptococcus pneumoniae* database to estimate the contribution of Tn916-related ICEs to macrolide resistance. Out of 4,560 isolates from 1916 to 2021, 751 isolates were found to contain Tn916-related ICEs (Tn2009, Tn6002 or Tn2010), resulting in an overall frequency of 16.5% of isolates. To assess changes in the frequency over time and the effects of vaccine introductions, we separated the Tn916-related ICE-containing isolates into four distinct periods: historic (1916-1994), pre-PCV7 (1995-2000), PCV7 (2001-2010), and PCV13 (2011-2021). During the historic period, out of 66 isolates, only one 1983 isolate contained a Tn916-related ICE, resulting in a 1.52% frequency (Fig 1). In the subsequent time periods, the percent of ICE+ isolates were as follows: 10.3% for pre-PCV7 (106 of 1,026 isolates), 17.0% for PCV7 (400 of 2,354 isolates), and 21.9% in PCV13 (244 of 1,114 isolates) (Fig 1). Thus, the increase in macrolide resistance in the US *S. pneumoniae* isolates beginning in the 1990s<sup>(8, 9)</sup> in part correlated with the increasing frequency of Tn916-related ICEs.

Distribution of Tn916-related ICEs in S. pneumoniae in the US, 1916-2021.

The distribution of Tn916-related ICE-containing isolates in the PubMLST database was examined. As noted, in the 1916-1994 historic period with 66 isolates from the US, only one ICE+ isolate from 1983 contained Tn6002 (ermB). During the 1995-2000 pre-PCV7 period, of the 106 S. pneumoniae isolates containing Tn916-related ICEs, the majority (58.5%) carried the Megacontaining Tn2009 (Fig 2A). This confirms previous reports in the 1990s and early 2000s demonstrating that the major mechanism of macrolide resistance in North America was due to efflux mediated by the *mefE/mel* genes on the Mega element including Mega found on Tn2009 <sup>(8)</sup>. <sup>32,33)</sup>. For the PCV7 period (2001-2010), 400 isolates contained Tn916-related ICEs where Tn2009 decreased to 14.7% of ICE-containing isolates (Fig 2B). Over 85% now harbored the ermBcontaining Tn6002 (47.5%) or Tn2010 (37.8%) with dual-macrolide resistance determinants (ermB and mefE/mel) (Fig 2B). Consequently, ermB was responsible for >85% of Tn916-related ICE macrolide resistance during 2001-2010. In the PCV13 period, most of 244 Tn916-related ICEcontaining isolates, mainly collected from 2012 and 2013, had the ermB-containing Tn6002 (67.2%) (Fig 2C). There was a modest increase of Tn2009 to 23.8% and a decrease of Tn2010 to 9.0%. Over 75% of Tn916-related ICE-containing isolates carried ermB-mediated macrolide resistance during the PCV13 era. While the number of US isolates deposited each year into the PubMLST database spanning 1916 to 2021 was quite variable (Fig 3), key shifts in the frequency of Tn916-related ICEs in the US isolates over time were noted.

In summary, prior to vaccine introduction in 2000, Tn916-related ICE macrolide resistance in the US was due to *mefE/mel*-encoded efflux. However, ribosomal methylation conferred by *ermB* was observed as the dominant mechanism of Tn916-related ICE macrolide resistance in the US after PCV vaccine introductions.

Shift in Tn916-related ICE distribution from vaccine to non-vaccine serotypes in the US, 1995-2021.

The emergence of serotypes not included in the pneumococcal polysaccharide conjugate vaccines, a phenomenon known as serotype replacement, poses a challenge for pneumococcal disease prevention<sup>(34, 35)</sup> as well as for treatment if multidrug resistance becomes prevalent in these non-vaccine serotypes. Therefore, we assessed vaccine or non-vaccine serotype distribution over time of Tn916-related ICE-containing US isolates (Fig 4). We separated the serotypes into three groups: the seven serotypes included in PCV7 (PCV7, teal bars), six additional serotypes added into PCV13 (non-PCV7, dark purple), and those not included in PCV13 (non-PCV13, light purple). During the pre-PCV7 era (1995-2000), 83.0% of the 106 US ICE+ isolates were PCV7 serotypes, 4.7% were non-PCV7 serotypes, and 12.3% were non-PCV13 serotypes (Fig 4). During the PCV7 era (2001-2010), a major shift in serotype distribution of the US ICE+ isolates was detected. Of 400 US ICE+ isolates in the PCV7 period, only 12.2% were of PCV7 serotypes, while non-PCV7 serotypes increased to 41.3% and non-PCV13 to 46.5% (Fig 4). Of 244 US ICE+ isolates in the PCV13 era, there was a further disappearance in PCV7 serotypes (1.6%), non-PCV7 serotypes decreased to 9.0%, and non-PCV13 serotypes now comprised 89.4% of ICE+ isolates (Fig 4). Thus, with the declines in PCV7 and PCV13 vaccine serotypes, Tn916-related ICEs were increasingly found in non-PCV13 serotypes in the US.

Analysis of Tn916-related ICE-containing US isolates by vaccine and non-vaccine serotypes, 1995-2021.

A detailed analysis of the circulating serotypes and the specific ICE elements found before and after the introductions of PVC7 and PCV13 was performed (Fig 5). For these analyses, vaccine types were defined as serotypes included in the designated vaccine for the corresponding period

(i.e., PCV7 serotypes in pre-PCV7 or PCV7 eras and PCV13 serotypes in PCV13 era). Non-vaccine serotypes encompassed all other serotypes not included in the designated vaccine for the corresponding era, such as non-PCV7 serotypes in the pre-PCV7 and PCV7 eras as well as non-PCV13 serotypes in the PCV13 era.

In the pre-PCV7 era, 88 ICE+ isolates of 596 PCV7 serotype isolates (14.8%) and 18 ICE+ isolates of 161 non-vaccine serotype isolates (11.2%), were noted. Tn916-related ICEs were found in 6B, 14, 19F, and 23F of the PCV7 serotypes where Tn2009 was the major ICE element. Tn2010 was found only in serotype 19F isolates (Fig 5A). Conversely, only Tn6002 and Tn2009 were present in the non-vaccine isolates in the pre-PCV7 era, which included serotypes 3, 6A, 6E (6Bii), 12F, and 21 (Fig 5D). In the PCV7 era, 49 ICE+ of 187 isolates (26.2%) belonging to the PCV7 serotypes and 351 ICE+ isolates of 1,535 (22.9%) non-vaccine serotypes were analyzed. Most of the ICE+ vaccine type isolates were serotypes 19F (34 out of 73, or 46.6%) and 23F (10 out of 28, or 35.7%) (Fig 5B). Both Tn2009 and Tn2010 were found in 19F isolates while 23F isolates predominantly harbored Tn2009 (Fig 5B). While a more diverse population of Tn916-related ICEcontaining non-vaccine serotypes was detected during the PCV7 era, serotypes 15A (120 out of 154, 77.9%) and 19A (160 out of 412, 38.8%) were the most prevalent (Fig 5E). Serotype 15A carried Tn6002 except for one Tn2010-containing isolate while 19A predominantly harbored Tn2010 followed by Tn6002 as the second-most prevalent ICE (Fig 5E). During the PCV13 era, the number of ICE+ PCV13 serotypes was low with 26 out of 127 PCV13 isolates (20.5%), while non-vaccine ICE+ serotypes encompassed 218 out of 803 non-vaccine isolates (27.1%). For the 26 ICE+ PCV13 serotypes, 20 out of a total of 43 were serotype 19A (46.5%), mostly carrying Tn2010 (Fig 5C). The ICE+ non-vaccine serotypes in the PCV13 era were mainly represented by serotypes 15A (123 out of 131, 93.9%), 15BC (50 out of 99, 50.5%), and 23A (28 out of 173,

16.2%) (Fig 5F). All serotype 15A and serotype 23A ICE+ isolates had Tn6002, but serotype 15BC had predominantly Tn2009. Taken together, we observed an increase in non-vaccine serotypes 15A and 19A that harbor Tn916-related ICEs in the PCV7 era, persistence of ICE+ 19A isolates into the PCV13 era, and an increase in ICE+ non-vaccine serotypes 15A, 15BC, and 23A in the PCV13 era. Serotypes 15A and 23A are not covered by the current PCV15 and PCV20 formulations.

# Analysis of *S. pneumoniae* Tn916-related ICEs in Thailand and South Africa during pre-PCV7 and post-PCV7/13 eras.

To compare the trends observed in US isolates with other geographical regions, preliminary analyses were conducted for Thailand and South Africa *S. pneumoniae* isolates deposited in the PubMLST database (Fig S1). The gaps between PCV7 and PCV13 introductions were relatively short in these two countries [4 years for Thailand (2007-2011) and 2 years for South Africa (2009-2011)] and the differential effects of PCV7 and PCV13 are likely to be less evident. Thus, we categorized the ICE+ isolates from these countries into two time periods: pre-PCV7 and post-PCV7/13. Tn916-related ICE frequency increased in the US (9.8% to 18.6%) from pre-PCV7 to post-PCV7/13 eras while, in comparison, the percent frequency in Thailand remained stable at 27% in both time periods and in South Africa changed from 18.7% to 12.1% during pre-PCV7 to post-PCV7/13 eras (Fig S1). The different profiles based on percent frequency were influenced by the total number of isolates deposited in the PubMLST *Streptococcus pneumoniae* database for a given country.

# **DISCUSSION**

S. pneumoniae continues as a global public health concern partly because of the spread of antibiotic resistance in the pathogen. In the US, the widespread use of macrolides, particularly the

semi-synthetic azithromycin and clarithromycin, has contributed to the emergence of macrolide-resistant *S. pneumoniae*<sup>(8, 36)</sup>. Prescription for macrolide antibiotics dramatically rose during the 1990s and has continued into the 2000s in the US<sup>(8, 36, 37)</sup>. Macrolide resistance is partly associated with the dissemination of Tn916-related ICEs (Tn2009, Tn6002, and Tn2010), which contain *tetM* (tetracycline resistance) as well as the two distinct macrolide resistance determinants, *ermB* and/or *mefE/mel* <sup>(11)</sup>. The distribution of Tn916-related ICEs in *S. pneumoniae* collected in the US (1916-2021) as well as changes associated with sequential vaccine (PCV7 and PCV13) introductions to ICE-conferred macrolide resistance were assessed.

Utilizing 4,560 *S. pneumoniae* genomes of US isolates deposited in the PubMLST database <sup>(31)</sup> that span 1916 to 2021 and cover two pneumococcal vaccine introductions, PCV7 in 2000 and PCV13 in 2010, the trends of Tn916-related ICE-containing isolate frequency divided into four distinct eras: historic (1916-1994), pre-PCV7 (1995-2000), PCV7 (2001-2010), and PCV13 (2011-2021), were examined. The percent frequency for each respective era was 1.52%, 10.3%, 17.0%, and 21.9%, which correlated with the overall development of increasing macrolide resistance in *S. pneumoniae*. There was a steady increase in frequency of Tn916-related ICEs in *S. pneumoniae* isolates during the vaccine eras compared to the pre-PCV7 era.

While the collection of over 4,500 pneumococcal isolates from the PubMLST database is robust, there are limitations in the analyses based on isolate records examined in the database<sup>(31)</sup>. First, PubMLST is not a surveillance-based collection of isolates, thus the incidence of ICE+ isolates in the US pneumococcal population cannot be determined. Future investigations using a population-based database, such as the CDC's Active Bacterial Core surveillance database, that collects and characterizes invasive isolates from ten states dispersed around the US, would address this limitation. Second, certain years of isolation had significantly more isolates due to major

studies that were conducted and might not appropriately reflect the circulating pneumococcal population in the US. Some of these studies sequenced isolates collected from isolate banks, such as the Global Pneumococcal Sequencing (GPS) Project, or came from observational cohort investigations of pneumococcal carriage or invasive pneumococcal disease. Other studies used genomic data that was already published or accessible from publicly available databases (GenBank, GPS Project). During the pre-PCV7 era, there were a total of 358 US isolates collected in 1998, the majority of which came from two studies investigating the evolutionary impact on the pneumococcal pangenome by PCV introduction<sup>(38)</sup> as well as pneumococcal strain serotype, sequence type, antibiotic sensitivity, and invasiveness using genomes grouped into Global Pneumococcal Sequence Clusters<sup>(39)</sup>. The majority of the total 549 1999 US isolates were from four studies including the two previously cited<sup>(38, 39)</sup>, one study that explored *cps* loci in genomes from the GPS project to identify novel cps loci<sup>(40)</sup>, and the last that explored S. pneumoniae genomes for blp bacteriocin cassettes to characterize their genetic composition and sequence diversity<sup>(41)</sup>. In the PCV7 era, the 630 US isolates collected in 2007 were associated with three reports: 1) the pangenome study<sup>(38)</sup>, 2) the genome analyses of Global Pneumococcal Sequence Clusters<sup>(39)</sup>, and 3) an investigation of PCV7 impact on genomic evolution of S. pneumoniae carriage isolates<sup>(42)</sup>. In 2009, the 811 US isolates were from three studies, including the Global Pneumococcal Sequence Clusters genomic analyses<sup>(39)</sup> and novel cps loci identification study<sup>(40)</sup> as well as a third study focusing on analyzing genomic data from non-vaccine serotype pneumococci not susceptible to penicillin<sup>(43)</sup>. Lastly, in the PCV13 era, in 2012, 708 US isolates originated from three aforementioned reports<sup>(38, 39, 43)</sup> while the 252 total US isolates of 2013 came from the genomic analyses by Andam et al. (43) of pneumococci not susceptible to penicillin. Thus, the percent frequency calculations of Figure 1 are influenced by the year of isolation. Despite these

limitations, the data demonstrate an increase in PubMLST US isolates carrying Tn916-related ICEs, which likely contribute to the overall increase in pneumococcal macrolide resistance observed in the US.

Macrolide resistance determinants associated with Tn916-related ICEs include ermB and mefE/mel, which encode ribosomal methylation or macrolide efflux, respectively<sup>(5, 11)</sup>. Overall, during the 1990s and 2000, the data supported the emergence of macrolide resistance in the US mediated by the Mega mefE and mel genes as found in the high frequency of Tn2009 during this time. However, the predominant mechanism for macrolide resistance transitioned to ermB during the late 2000s and 2010s as seen with the large increases in Tn6002 and Tn2010. In previous work using in vitro competition assays in the presence of macrolides, high-level macrolide resistance conferred by ermB provided a fitness advantage for pneumococcal growth over the low-level macrolide resistance conferred by mefE/mel (44). The clonal expansion of serotype 19A during the PCV7 era also contributed to this shift. These serotype 19A ICE-containing US isolates mostly carried Tn2010, which has both ermB and Mega(45, 46). Schroeder et al. demonstrated with a Tn2010-containing strain (GA44288, serotype 19A) that the pneumococcal growth advantage was attributed to ermB-mediated high-level resistance and not the mefE/mel-mediated low-level resistance<sup>(44)</sup>. Therefore, this switch from mefE/mel-mediated to ermB-mediated macrolide resistance in the late 2000s and 2010s could be partly due to the advantage that high-level macrolide resistance provides to S. pneumoniae and the subsequent expansion of these strains in the US population.

The US introductions of PCV7 and PCV13 in 2000 and 2010, respectively, were very effective in reducing the carriage and infections caused by *S. pneumoniae* vaccine serotypes<sup>(20, 23)</sup>. This impact was also evident in the ICE+ pneumococcal isolates examined in this study. During the

pre-PCV7 era, Tn916-related ICE-containing isolates of PCV7 serotypes represented 83.0% of isolates (Fig 4), but with PCV introductions, this percentage decreased to 12.2 % and 1.6% in the PCV7 and PCV13 eras, respectively. With the introduction of PCV7 into the US vaccination programs, serotype replacement was documented with serotype 19A that emerged rapidly during the 2000s up to 2010<sup>(21)</sup>. We detected an ~9-fold increase from 4.7% to 41.3% of non-PCV7 serotypes during the transition from the pre-PCV7 to PCV7 era. Many of the emerging serotype 19A isolates were products of capsule switching from serotype 19F<sup>(47)</sup>. Therefore, the capsule switching from 19F to 19A followed by expansion of these 19A isolates during the 2000s to 2010 contributed to the large increase in non-PCV7 serotypes that we witnessed during the PCV7 era (Fig 4). Additionally, non-PCV13 ICE-containing isolates drastically increased from 12.3%, 46.5%, to 89.4% in the pre-PCV7, PCV7, and PCV13 eras, respectively. Therefore, PCV introductions resulted in selective pressure for the emergence of non-vaccine serotypes.

Within the non-vaccine serotype pool in the PCV13 era, we saw an emergence of serotypes 15A (123 isolates), 15BC (50 isolates), and 23A (28 isolates). The newer PCV20 vaccine includes serotype 15B, but neither PCV15 nor PCV20 contains serotype 15A. The PubMLST database groups serotypes 15B and 15C together as serotype 15BC, presumably due to the identical capsular polysaccharides except for an O-acetyl group present in 15B and the reported reversible switching between the two serotypes (48, 49). The addition of serotype 15B to PCV20 would likely provide cross-protection against serotype 15C, but not 15A. Hao et al. demonstrated robust opsonophagocytic antibody titers against both 15B and 15C, but not 15A in PCV20-vaccinated adults (50). Serotype 15A has been on the rise globally, such as in the United Kingdom (51), Germany (52), Taiwan (53), Japan (54), and in the US (55, 56). Additionally, our data indicated a rise in isolates of serotype 23A from the PCV7 to PCV13 eras. The rise in serotype 23A has been reported

worldwide, including in several Asian countries (Korea, Malaysia, Singapore, Thailand, Taiwan)<sup>(57, 58)</sup>, the United Kingdom<sup>(59)</sup>, and the US<sup>(56, 60)</sup>. Pai et al. reported that there was a clonal association between US serotype 23A isolates and the international Pneumococcal Molecular Epidemiology Network (PMEN) Colombia<sup>23F</sup>-26 clone<sup>(61)</sup>. They hypothesized that the 23A isolates present in the US originated from serotype 23F, possibly due to an intra-strain genetic alteration or by capsular switching of 23F to 23A <sup>(61)</sup>. Although the close relatedness of non-vaccine serotype 23A and vaccine serotype 23F implies a potential cross-protection by the existing PCV vaccines, our data suggests that non-vaccine serotype 23A is still increasing in frequency and has not been reduced by the existing PCVs.

Given the geographical variability in macrolide resistance that has been previously reported<sup>(62)</sup>, Tn916-related ICE distribution trends in Thailand and South Africa were investigated and compared to the US in preliminary studies. Thailand and South Africa represent two continents with different PCV introduction schedules. Approximately 12% to 27% of Tn916-related ICE-mediated macrolide resistance was observed in *S. pneumoniae* isolates in all three countries in the post-PCV7/13 time period. Additional analyses would shed light on the distribution of the three Tn916-related ICEs among the *S. pneumoniae* population in Thailand and South Africa as well as if there are changes in non-PCV13 serotypes.

In conclusion, investigating *S. pneumoniae* isolates deposited in the PubMLST *Streptococcus pneumoniae* database demonstrated that the frequency of Tn2009, Tn6002, and Tn2010 increased over time in the US pneumococcal population. The mechanism for macrolide resistance associated with Tn916-related ICEs transitioned from *mefE/mel*-induced efflux to high-level macrolide resistance conferred by the ribosomal modifications of *ermB*. Moreover, the increase in Tn916-related ICEs in US pneumococcal isolates has occurred in non-vaccine serotypes. The emergence

of non-vaccine serotypes 15A and 23A not included in the current PCV15 nor PCV20 vaccines is of particular concern. Surveillance of multidrug resistance conferred by Tn916-related ICEs in *S. pneumoniae* should continue to help determine future PCV formulations and antibiotic treatment options for suspected pneumococcal disease.

#### MATERIALS AND METHODS

S. pneumoniae isolates. For this study, meta-data from United States (US) S. pneumoniae isolates database<sup>(31)</sup> the exported from **PubMLST Streptococcus** pneumoniae were (https://pubmlst.org/organisms/streptococcus-pneumoniae) on January 23, 2023. In the database, there was a total of 4,617 US isolates deposited with a sequence bin for total genome length of  $\geq 1$ Mbp. However, for data analysis purposes, 4,560 isolates were utilized in this study as these had year of isolation (spanning from 1916-2021) and serotype data available. Similarly, data for Thailand and South Africa were also pulled from the PubMLST Streptococcus pneumoniae database on January 23, 2023. Thailand had 3,457 isolates (spanning 2000-2014) while South Africa had 5,336 isolates (spanning 1977-2020) with year of isolation and serotype data available. **Tn916-related ICE designation.** To identify the specific Tn916-related ICE in the total isolates for a given country, the Genome Comparator tool on the PubMLST Streptococcus pneumoniae database was utilized. Briefly, an annotated reference sequence composed of Tn2010 (containing ermB, mefE, mel, tetM, and conjugative genes) was used for comparison to all other isolates' genomes. For the comparison parameters, 70% minimum percent identity, 50% minimum percent alignment, 90% core genome threshold, and a 20 BLASTN word size was used while default options were utilized for the distance matrix calculation. The exported data files with isolate ID number and isolate name contained the comparisons with the following designations: the presence of a gene was denoted by blue and an allele number label, the absence of a gene was denoted by

black and an "X" mark, and an incomplete gene was denoted by green and an "I" mark. To identify the isolates that contained Tn916-related ICEs, the presence of conjugative genes, ftsK, xis, and int, as well as resistance genes tetM, mefE, mel, and ermB was probed. To designate an isolate as ICE-containing, resistance genes had to be present as complete or incomplete alleles while presence or absence of conjugative genes were considered alike. Specifically, isolates with Tn2009 contained tetM and mefE and/or mel, isolates with Tn6002 contained tetM and ermB, and isolates with Tn2010 contained tetM, ermB, and mefE and/or mel. After ICE designation, there were 751, 945, and 779 ICE-containing isolates in the US, Thailand, and South Africa, respectively. Metadata for all Tn916-related ICE-containing isolates was exported from the PubMLST Streptococcus pneumoniae database, including isolate ID number, isolate name, country of isolation, year of isolation, date\_sampled, serotype, diagnosis, source, erythromycin MICs, tetracycline MICs, BioProject accession, BioSample accession, and ENA\_run\_accession. Although not all isolates had all identifier data available, year of isolation and serotype was ensured.

Categorization of Tn916-related ICE-containing isolates. *S. pneumoniae* isolates that were identified as positive for Tn2009, Tn6002, or Tn2010 were subsequently categorized into distinct eras based on pneumococcal conjugate vaccine (PCV) introduction in children. In the US, PCV7 was introduced in 2000 while PCV13 was introduced in 2010<sup>(63)</sup>, so the 751 ICE-containing isolates were divided into: historic (1916-1994), pre-PCV7 (1995-2000), PCV7 (2001-2010), and PCV13 (2011-2021) eras. In Thailand, PCV7 was introduced in 2007 while PCV13 was introduced in 2011<sup>(64)</sup>, so the 945 ICE-containing isolates were separated into: pre-PCV7 (2000-2007) and post-PCV7/13 (2008-2014) eras. In South Africa, PCV7 was introduced in 2009 while PCV13 was introduced in 2011<sup>(65)</sup>, so the 779 ICE-containing isolates were categorized into: pre-PCV7 (1977-2009) and post-PCV7/13 (2010-2020) eras. Additionally, the ICE-containing isolates in the US

were further categorized into vaccine versus non-vaccine serotypes, i.e. serotypes in PCV7 (4, 6B, 9V, 14, 18C, 19F, 23F) or PCV13 (PCV7 serotypes plus 1, 3, 5, 6A, 7F, 19A) vaccines versus serotypes that are not in either vaccine. For non-vaccine serotypes, "inconclusive" in our analyses encompassed serotypes that were labeled as genetic variants, nontypeable, or inconclusive in the PubMLST *Streptococcus pneumoniae* database.

# **ACKNOWLEDGEMENTS**

We thank the National Institute of Allergy and Infectious Diseases of the National Institutes of Health for supporting this study under the award number F31 AI154792.

# **FIGURES**

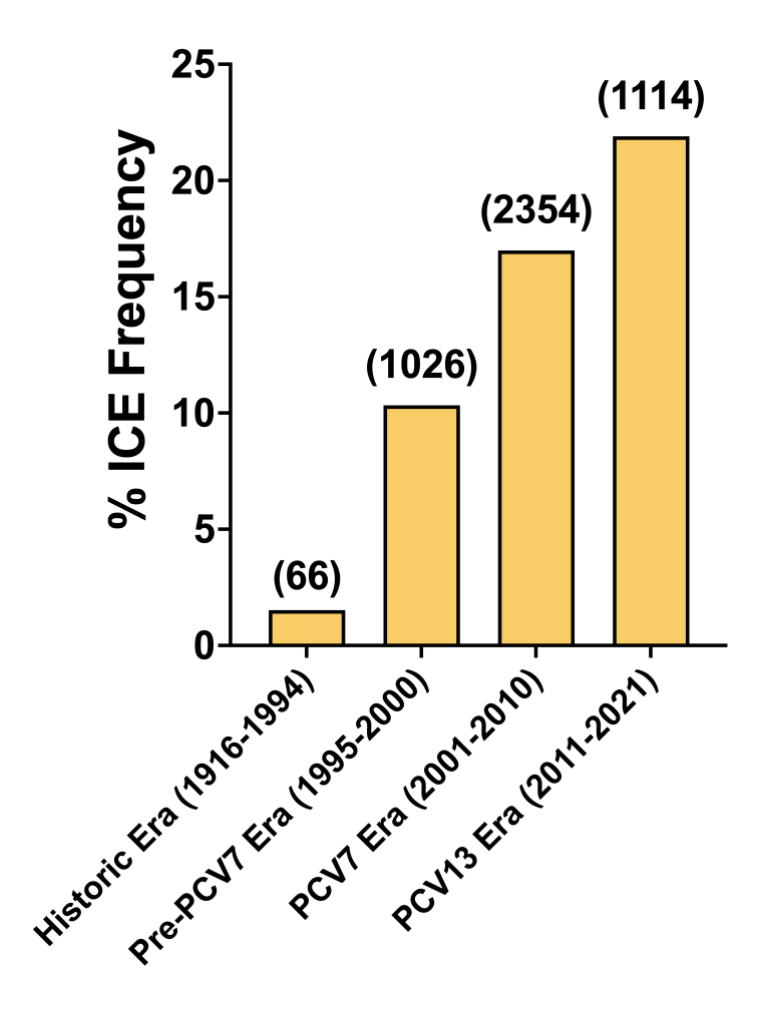


**Figure 1.** Tn916-related ICE frequency has increased in US *S. pneumoniae* isolates. Graph represents the frequency of Tn916-related ICEs (Tn2009, Tn6002, and Tn2010) in US *S. pneumoniae* isolates during the historic (1916-1994), pre-PCV7 (1995-2000), PCV7 (2001-2010), and PCV13 (2011-2021) eras. The numbers above the bars indicate the total number of US isolates deposited in the PubMLST database during those time periods.

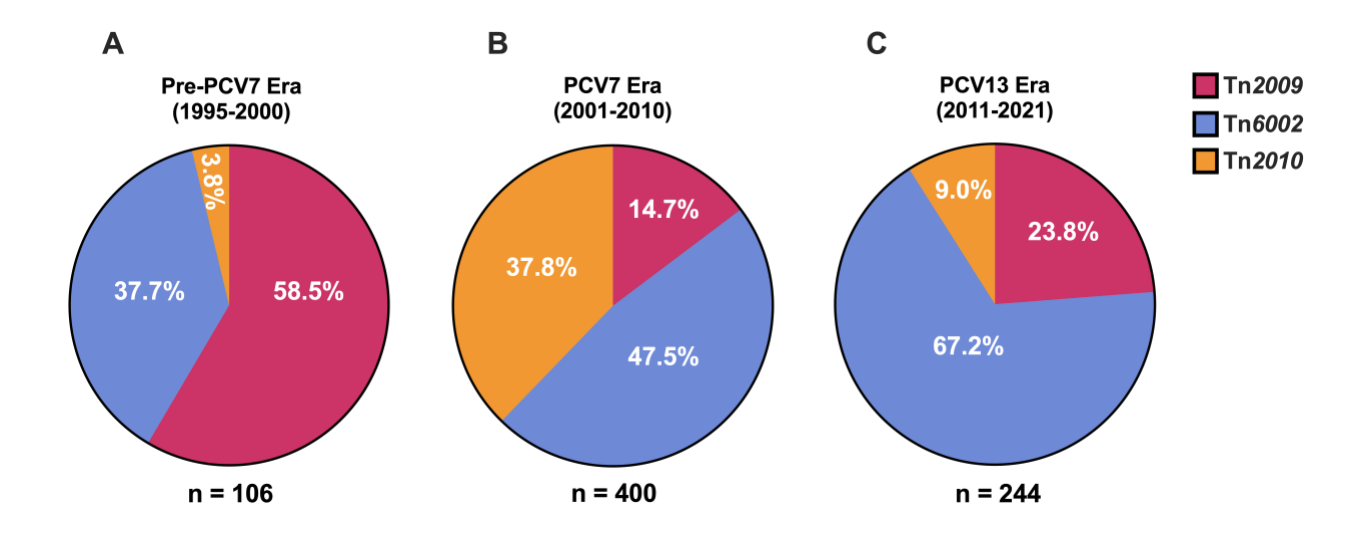


**Figure 2. Shift in the distribution of Tn916-related ICEs in the US during pre-PCV7, PCV7,** and PCV13 eras. Frequency of Tn2009 (magenta), Tn6002 (blue), or Tn2010 (orange) were calculated from total ICE-containing isolates in the PubMLST database (denoted as n = below the pie chart) during: (A) pre-PCV7 era, (B) PCV7 era, and (C) PCV13 era. During the historic era (1916-1994, not shown), there was one US Tn916-related ICE-containing isolate harboring Tn6002.

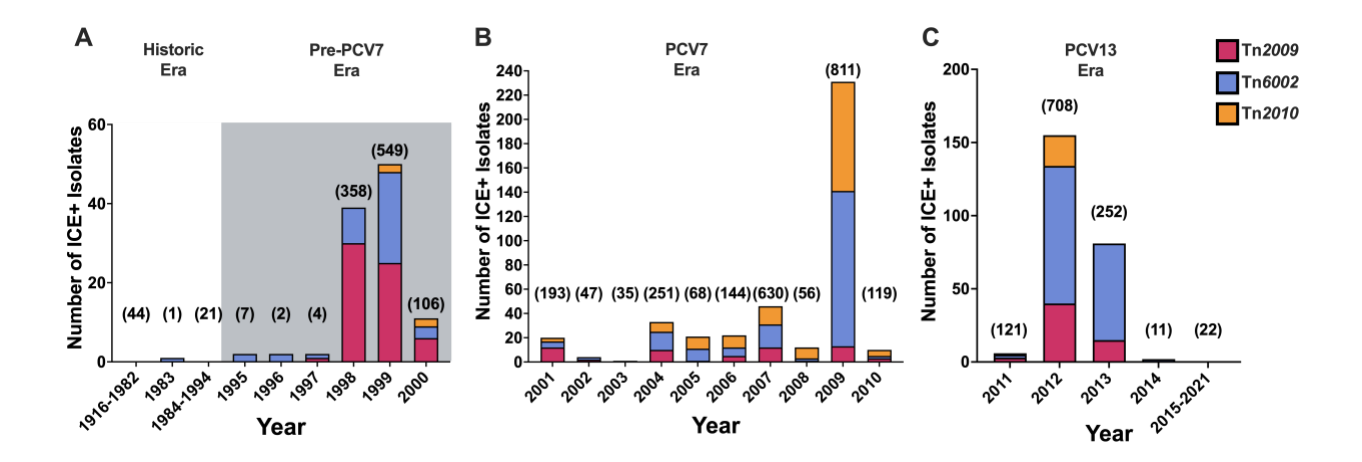
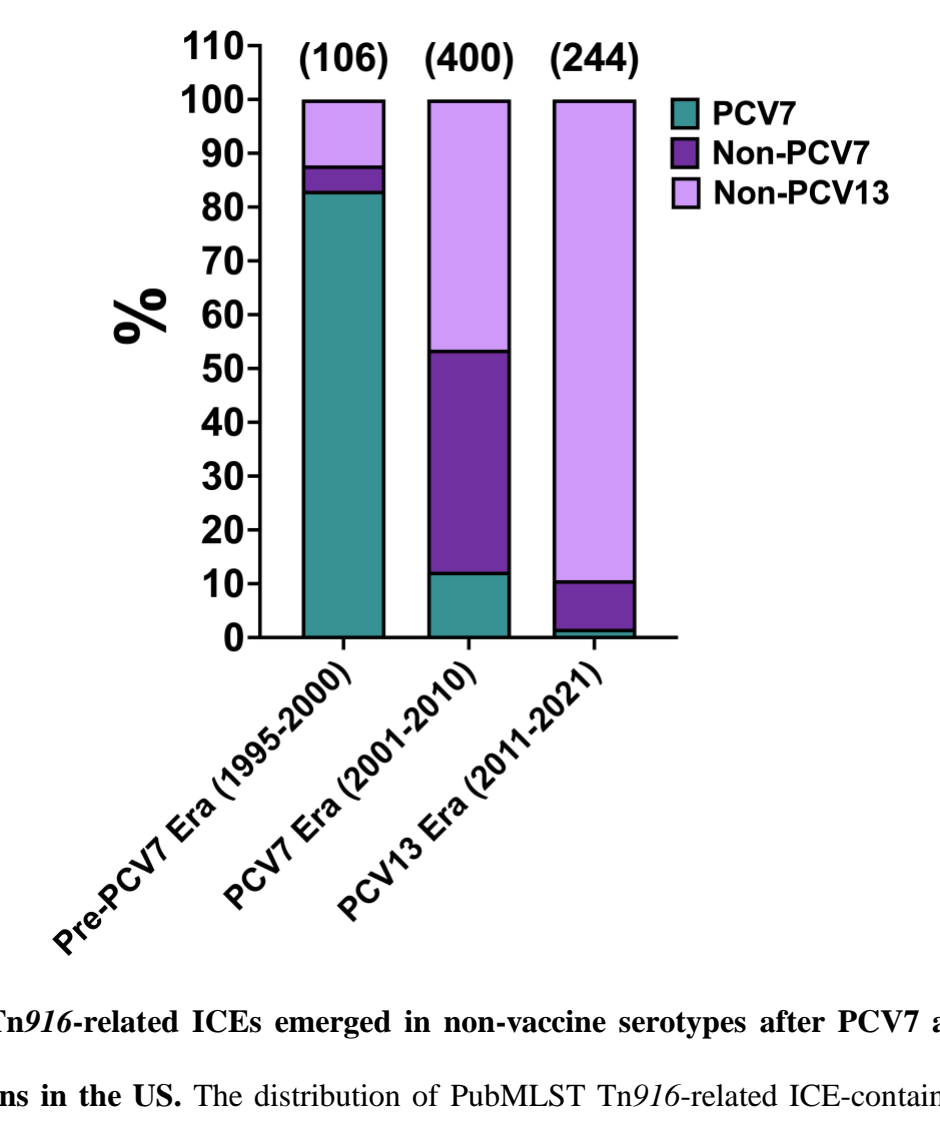


Figure 3. Tn916-related ICE-containing S. pneumoniae isolates from 1916 to 2021 in the US.

Graphs represent the number of ICE-containing isolates for each year of isolation with Tn2009 in magenta, Tn6002 in blue, and Tn2010 in orange. The four eras are represented as: (**A**) the historic era (1916-1994) indicated by the white background and the pre-PCV7 era (1995-2000) indicated by the gray background, (**B**) the PCV7 era (2001-2010), and (**C**) the PCV13 era (2011-2021). The numbers above the bars indicate the total number of US isolates deposited in the PubMLST database during that year.



**Figure 4.** Tn916-related ICEs emerged in non-vaccine serotypes after PCV7 and PCV13 introductions in the US. The distribution of PubMLST Tn916-related ICE-containing isolates from each period categorized into PCV7 serotypes (teal), six serotypes added to PCV13 (non-PCV7, dark purple), and non-PCV13 serotypes (light purple), was analyzed. The numbers above the bars indicate the total number of ICE-containing isolates in the US during that time period. During the historic era (1916-1994, not shown), the single Tn6002-containing US isolate that was isolated in 1983 was of PCV7 vaccine serotype 23F.

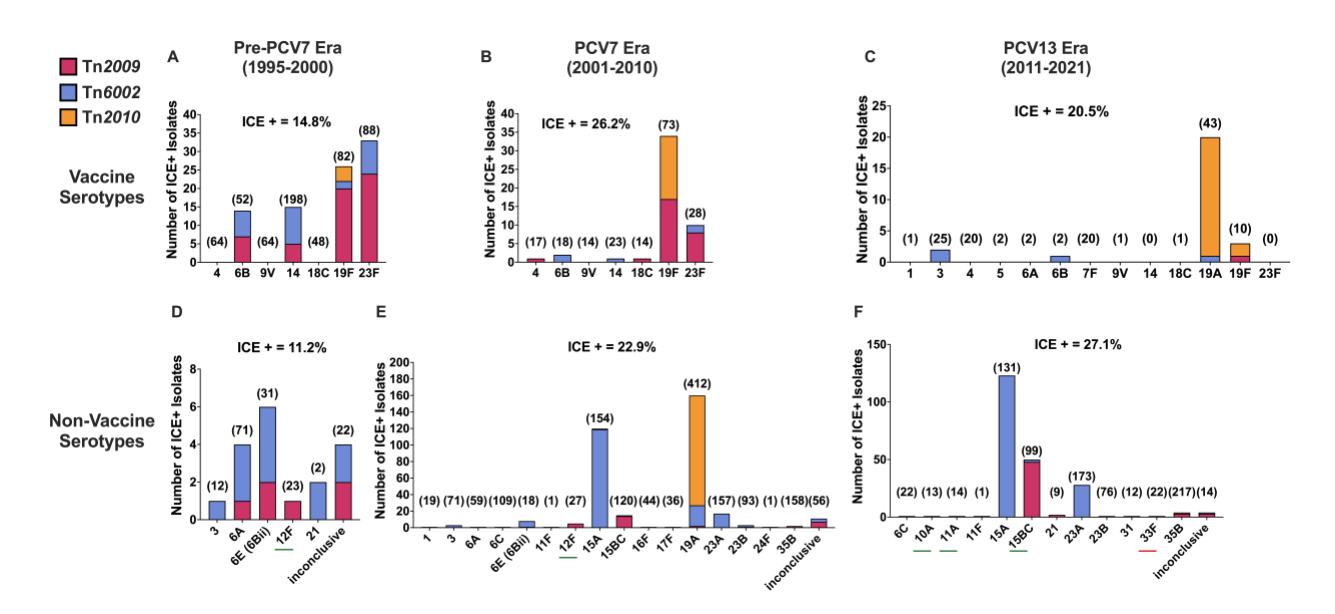
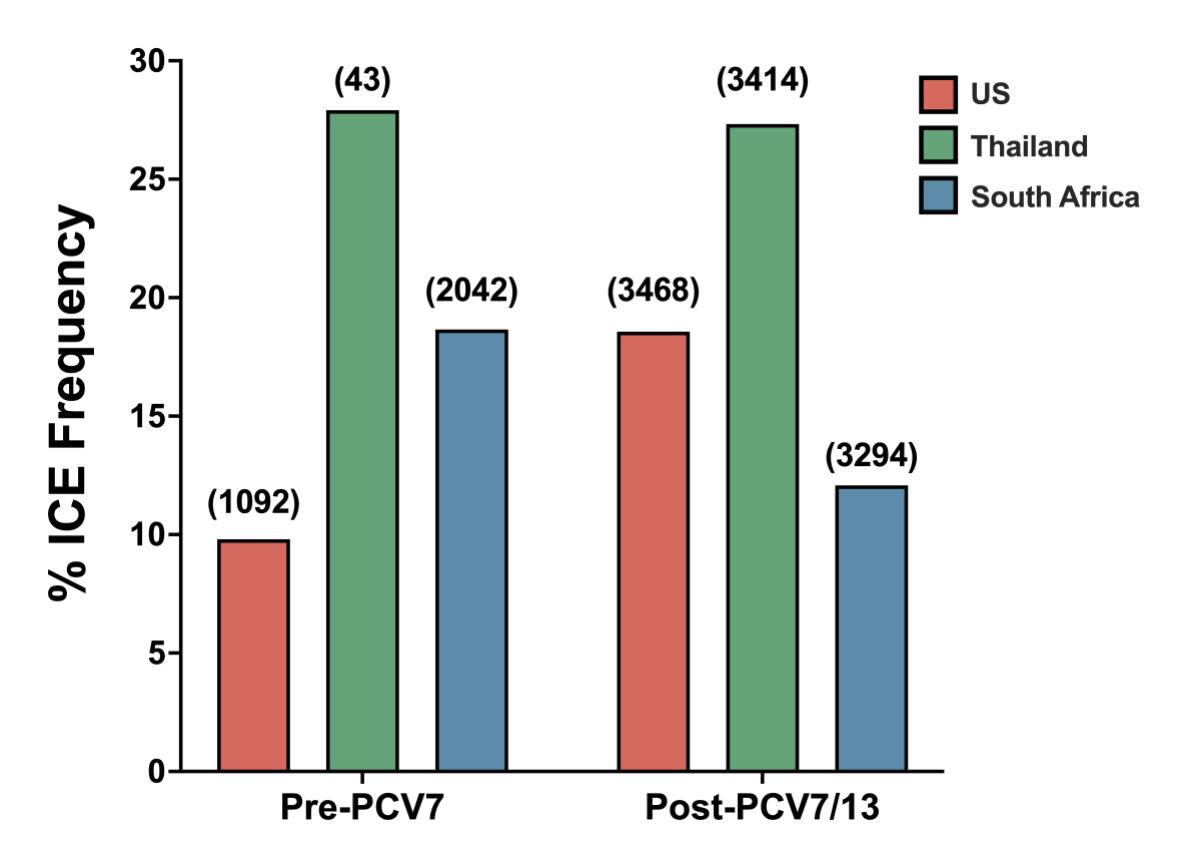


Figure 5. Serotype-specific analysis for Tn916-related ICE-containing isolates in the US, 1995-2021. Top row (panels A-C) represents vaccine serotypes while bottom row (panels D-F) represents non-vaccine serotypes. Three time periods are indicated as columns labeled pre-PCV7 era (panels A and D), PCV7 era (panels B and E), and PCV13 era (panels C and F). For these analyses, vaccine types are defined as serotypes included while non-vaccine types are serotypes not included in the designated vaccines for the corresponding eras. Tn916-related ICE elements are categorized as Tn2009 (magenta), Tn6002 (blue), and Tn2010 (orange). (A) PCV7 vaccine type isolates in pre-PCV7 era (1995-2000), (B) PCV7 vaccine type isolates in PCV7 era (2001-2010), (C) PCV13 vaccine type isolates in PCV13 era (2011-2021), (D) non-vaccine type isolates from PCV7 vaccine in pre-PCV7 era, (E) non-vaccine type isolates from PCV7 vaccine in PCV7 era, and (F) non-vaccine type isolates from PCV13 vaccine in PCV13 era. Red underline (panel F) denotes serotype to be included in PCV15 and green underline (panels D-F) denotes serotypes to be included in PCV20. The numbers above the bars indicate the total number of isolates in the US deposited in the PubMLST database for that specific pneumococcal serotype.

# SUPPLEMENTAL FIGURES



**Figure S1.** *S. pneumoniae* isolates carrying Tn916-related ICEs in US, Thailand, and South Africa during pre-PCV7 and post-PCV7/13 eras. *S. pneumoniae* isolates from the US (coral), Thailand (green), and South Africa (light blue) deposited into the PubMLST database were analyzed for presence of Tn916-related ICEs and categorized into pre-PCV7 and post-PCV7/13 eras. In the US, PCV7 was licensed in 2000 while PCV13 was licensed in 2010. In Thailand, PCV7 was licensed in 2007 while PCV13 was licensed in 2011. In South Africa, PCV7 was licensed in 2009 while PCV13 was licensed in 2011. Data represents the percent ICE frequency of Tn916-related ICEs in isolates. The numbers above the bars indicate the total number of isolates in each country that has been deposited in the PubMLST database during the pre-PCV7 and post-PCV7/13 eras.

#### REFERENCES

- 1. Kyaw MH, Clarke S, Jones IG, Campbell H. Non-invasive pneumococcal disease and antimicrobial resistance: vaccine implications. Epidemiol Infect. 2002;128(1):21-7. Epub 2002/03/16. doi: 10.1017/s0950268801006331. PubMed PMID: 11895087; PMCID: PMC2869791.
- 2. Weiser JN, Ferreira DM, Paton JC. Streptococcus pneumoniae: transmission, colonization and invasion. Nat Rev Microbiol. 2018;16(6):355-67. Epub 2018/03/31. doi: 10.1038/s41579-018-0001-8. PubMed PMID: 29599457; PMCID: PMC5949087.
- 3. Shak JR, Vidal JE, Klugman KP. Influence of bacterial interactions on pneumococcal colonization of the nasopharynx. Trends Microbiol. 2013;21(3):129-35. Epub 2013/01/01. doi: 10.1016/j.tim.2012.11.005. PubMed PMID: 23273566; PMCID: PMC3729046.
- 4. Drijkoningen JJ, Rohde GG. Pneumococcal infection in adults: burden of disease. Clin Microbiol Infect. 2014;20 Suppl 5:45-51. Epub 2013/12/10. doi: 10.1111/1469-0691.12461. PubMed PMID: 24313448.
- 5. Schroeder MR, Stephens DS. Macrolide Resistance in Streptococcus pneumoniae. Front Cell Infect Microbiol. 2016;6:98. Epub 2016/10/07. doi: 10.3389/fcimb.2016.00098. PubMed PMID: 27709102; PMCID: PMC5030221.
- 6. Singer M, Nambiar S, Valappil T, Higgins K, Gitterman S. Historical and regulatory perspectives on the treatment effect of antibacterial drugs for community-acquired pneumonia. Clin Infect Dis. 2008;47 Suppl 3:S216-24. Epub 2008/11/18. doi: 10.1086/591407. PubMed PMID: 18986293.
- 7. Bergman M, Huikko S, Huovinen P, Paakkari P, Seppala H, Finnish Study Group for Antimicrobial R. Macrolide and azithromycin use are linked to increased macrolide resistance in

- Streptococcus pneumoniae. Antimicrob Agents Chemother. 2006;50(11):3646-50. Epub 2006/08/31. doi: 10.1128/AAC.00234-06. PubMed PMID: 16940064; PMCID: PMC1635217.
- 8. Hyde TB, Gay K, Stephens DS, Vugia DJ, Pass M, Johnson S, Barrett NL, Schaffner W, Cieslak PR, Maupin PS, Zell ER, Jorgensen JH, Facklam RR, Whitney CG, Active Bacterial Core Surveillance/Emerging Infections Program N. Macrolide resistance among invasive Streptococcus pneumoniae isolates. JAMA. 2001;286(15):1857-62. Epub 2001/10/26. doi: 10.1001/jama.286.15.1857. PubMed PMID: 11597287.
- 9. Jenkins SG, Farrell DJ. Increase in pneumococcus macrolide resistance, United States. Emerg Infect Dis. 2009;15(8):1260-4. Epub 2009/09/16. doi: 10.3201/eid1508.081187. PubMed PMID: 19751588; PMCID: PMC2815953.
- 10. Nadimpalli M, Delarocque-Astagneau E, Love DC, Price LB, Huynh BT, Collard JM, Lay KS, Borand L, Ndir A, Walsh TR, Guillemot D, Bacterial I, antibiotic-Resistant Diseases among Young children in low-income countries Study G. Combating Global Antibiotic Resistance: Emerging One Health Concerns in Lower- and Middle-Income Countries. Clin Infect Dis. 2018;66(6):963-9. Epub 2018/01/19. doi: 10.1093/cid/cix879. PubMed PMID: 29346620.
- 11. Chancey ST, Agrawal S, Schroeder MR, Farley MM, Tettelin H, Stephens DS. Composite mobile genetic elements disseminating macrolide resistance in Streptococcus pneumoniae. Front Microbiol. 2015;6:26. Epub 2015/02/25. doi: 10.3389/fmicb.2015.00026. PubMed PMID: 25709602; PMCID: PMC4321634.
- 12. Del Grosso M, Scotto d'Abusco A, Iannelli F, Pozzi G, Pantosti A. Tn2009, a Tn916-like element containing mef(E) in Streptococcus pneumoniae. Antimicrob Agents Chemother. 2004;48(6):2037-42. Epub 2004/05/25. doi: 10.1128/AAC.48.6.2037-2042.2004. PubMed PMID: 15155196; PMCID: PMC415626.

- 13. Cochetti I, Tili E, Vecchi M, Manzin A, Mingoia M, Varaldo PE, Montanari MP. New Tn916-related elements causing erm(B)-mediated erythromycin resistance in tetracycline-susceptible pneumococci. J Antimicrob Chemother. 2007;60(1):127-31. Epub 2007/05/08. doi: 10.1093/jac/dkm120. PubMed PMID: 17483548.
- 14. Del Grosso M, Northwood JG, Farrell DJ, Pantosti A. The macrolide resistance genes erm(B) and mef(E) are carried by Tn2010 in dual-gene Streptococcus pneumoniae isolates belonging to clonal complex CC271. Antimicrob Agents Chemother. 2007;51(11):4184-6. Epub 2007/08/22. doi: 10.1128/AAC.00598-07. PubMed PMID: 17709465; PMCID: PMC2151421.
- 15. Antezana BS, Lohsen S, Wu X, Vidal JE, Tzeng YL, Stephens DS. Dissemination of Tn916-Related Integrative and Conjugative Elements in Streptococcus pneumoniae Occurs by Transformation and Homologous Recombination in Nasopharyngeal Biofilms. Microbiol Spectr. 2023:e0375922. Epub 2023/03/14. doi: 10.1128/spectrum.03759-22. PubMed PMID: 36912669.
- 16. Grabenstein JD, Klugman KP. A century of pneumococcal vaccination research in humans. Clin Microbiol Infect. 2012;18 Suppl 5:15-24. Epub 2012/08/14. doi: 10.1111/j.1469-0691.2012.03943.x. PubMed PMID: 22882735.
- 17. Watson DA, Musher DM, Jacobson JW, Verhoef J. A brief history of the pneumococcus in biomedical research: a panoply of scientific discovery. Clin Infect Dis. 1993;17(5):913-24. Epub 1993/11/01. doi: 10.1093/clinids/17.5.913. PubMed PMID: 8286641.
- 18. Daniels CC, Rogers PD, Shelton CM. A Review of Pneumococcal Vaccines: Current Polysaccharide Vaccine Recommendations and Future Protein Antigens. J Pediatr Pharmacol Ther. 2016;21(1):27-35. Epub 2016/03/22. doi: 10.5863/1551-6776-21.1.27. PubMed PMID: 26997927; PMCID: PMC4778694.

- 19. Rodgers GL, Klugman KP. The future of pneumococcal disease prevention. Vaccine. 2011;29 Suppl 3:C43-8. Epub 2011/09/16. doi: 10.1016/j.vaccine.2011.07.047. PubMed PMID: 21896352.
- 20. Pilishvili T, Lexau C, Farley MM, Hadler J, Harrison LH, Bennett NM, Reingold A, Thomas A, Schaffner W, Craig AS, Smith PJ, Beall BW, Whitney CG, Moore MR, Active Bacterial Core Surveillance/Emerging Infections Program N. Sustained reductions in invasive pneumococcal disease in the era of conjugate vaccine. J Infect Dis. 2010;201(1):32-41. Epub 2009/12/02. doi: 10.1086/648593. PubMed PMID: 19947881.
- 21. Schroeder MR, Chancey ST, Thomas S, Kuo WH, Satola SW, Farley MM, Stephens DS. A Population-Based Assessment of the Impact of 7- and 13-Valent Pneumococcal Conjugate Vaccines on Macrolide-Resistant Invasive Pneumococcal Disease: Emergence and Decline of Streptococcus pneumoniae Serotype 19A (CC320) With Dual Macrolide Resistance Mechanisms. Clin Infect Dis. 2017;65(6):990-8. Epub 2017/09/15. doi: 10.1093/cid/cix446. PubMed PMID: 28903506; PMCID: PMC5850556.
- 22. Haber M, Barskey A, Baughman W, Barker L, Whitney CG, Shaw KM, Orenstein W, Stephens DS. Herd immunity and pneumococcal conjugate vaccine: a quantitative model. Vaccine. 2007;25(29):5390-8. Epub 2007/06/23. doi: 10.1016/j.vaccine.2007.04.088. PubMed PMID: 17583392.
- 23. Bar-Zeev N, Swarthout TD, Everett DB, Alaerts M, Msefula J, Brown C, Bilima S, Mallewa J, King C, von Gottberg A, Verani JR, Whitney CG, Mwansambo C, Gordon SB, Cunliffe NA, French N, Heyderman RS, VacSurv C. Impact and effectiveness of 13-valent pneumococcal conjugate vaccine on population incidence of vaccine and non-vaccine serotype invasive pneumococcal disease in Blantyre, Malawi, 2006-18: prospective observational time-series and

case-control studies. Lancet Glob Health. 2021;9(7):e989-e98. Epub 2021/06/19. doi: 10.1016/S2214-109X(21)00165-0. PubMed PMID: 34143997; PMCID: PMC8220129 from GlaxoSmithKline Biologicals, outside of the submitted work. NAC reports receiving investigator-initiated grants and non-financial support from GlaxoSmithKline Biologicals, outside the submitted work. NB-Z reports investigator-initiated research grants from Merck and Serum Institute of India, outside the submitted work. AvG has received research grants from Pfizer and Sanofi, outside the submitted work. All other authors declare no competing interests.

- 25. Desai AP, Sharma D, Crispell EK, Baughman W, Thomas S, Tunali A, Sherwood L, Zmitrovich A, Jerris R, Satola SW, Beall B, Moore MR, Jain S, Farley MM. Decline in Pneumococcal Nasopharyngeal Carriage of Vaccine Serotypes After the Introduction of the 13-Valent Pneumococcal Conjugate Vaccine in Children in Atlanta, Georgia. Pediatr Infect Dis J. 2015;34(11):1168-74. Epub 2015/08/01. doi: 10.1097/INF.00000000000000849. PubMed PMID: 26226445.
- 26. Hawkins PA, Chochua S, Jackson D, Beall B, McGee L. Mobile elements and chromosomal changes associated with MLS resistance phenotypes of invasive pneumococci recovered in the United States. Microb Drug Resist. 2015;21(2):121-9. Epub 2014/08/15. doi: 10.1089/mdr.2014.0086. PubMed PMID: 25115711; PMCID: PMC5735413.
- 27. Stephens DS, Zughaier SM, Whitney CG, Baughman WS, Barker L, Gay K, Jackson D, Orenstein WA, Arnold K, Schuchat A, Farley MM, Georgia Emerging Infections P. Incidence of

- macrolide resistance in Streptococcus pneumoniae after introduction of the pneumococcal conjugate vaccine: population-based assessment. Lancet. 2005;365(9462):855-63. Epub 2005/03/09. doi: 10.1016/S0140-6736(05)71043-6. PubMed PMID: 15752529.
- 28. Pneumococcal Vaccination: What Everyone Should Know. Centers for Disease Control and Prevention.2023. [April 6, 2023]. Available from: <a href="https://www.cdc.gov/vaccines/vpd/pneumo/public/index.html">https://www.cdc.gov/vaccines/vpd/pneumo/public/index.html</a>.
- 29. Kobayashi M, Farrar, J.L., Gierke, R., et al. Use of 15-Valent Pneumococcal Conjugate Vaccine and 20-Valent Pneumococcal Conjugate Vaccine Among U.S. Adults: Updated Recommendations of the Advisory Committee on Immunization Practices United States, 2022. Centers for Disease Control and Prevention.2022. [April 6, 2023]. Available from: <a href="https://www.cdc.gov/mmwr/volumes/71/wr/mm7104a1.htm">https://www.cdc.gov/mmwr/volumes/71/wr/mm7104a1.htm</a>.
- 30. Prevnar 20. Food and Drug Administration. 2023. [April 30, 2023]. Available from: https://www.fda.gov/vaccines-blood-biologics/vaccines/prevnar-20.
- 31. Jolley KA, Bray JE, Maiden MCJ. Open-access bacterial population genomics: BIGSdb software, the PubMLST.org website and their applications. Wellcome Open Res. 2018;3:124. Epub 2018/10/23. doi: 10.12688/wellcomeopenres.14826.1. PubMed PMID: 30345391; PMCID: PMC6192448.
- 32. Gay K, Baughman W, Miller Y, Jackson D, Whitney CG, Schuchat A, Farley MM, Tenover F, Stephens DS. The emergence of Streptococcus pneumoniae resistant to macrolide antimicrobial agents: a 6-year population-based assessment. J Infect Dis. 2000;182(5):1417-24. Epub 2000/10/07. doi: 10.1086/315853. PubMed PMID: 11023465.
- 33. Wierzbowski AK, Boyd D, Mulvey M, Hoban DJ, Zhanel GG. Expression of the mef(E) gene encoding the macrolide efflux pump protein increases in Streptococcus pneumoniae with

increasing resistance to macrolides. Antimicrob Agents Chemother. 2005;49(11):4635-40. Epub 2005/10/28. doi: 10.1128/AAC.49.11.4635-4640.2005. PubMed PMID: 16251306; PMCID: PMC1280166.

- 34. Hanage WP, Finkelstein JA, Huang SS, Pelton SI, Stevenson AE, Kleinman K, Hinrichsen VL, Fraser C. Evidence that pneumococcal serotype replacement in Massachusetts following conjugate vaccination is now complete. Epidemics. 2010;2(2):80-4. Epub 2010/10/30. doi: 10.1016/j.epidem.2010.03.005. PubMed PMID: 21031138; PMCID: PMC2963072.
- 35. Klugman KP. The significance of serotype replacement for pneumococcal disease and antibiotic resistance. Adv Exp Med Biol. 2009;634:121-8. Epub 2009/03/14. doi: 10.1007/978-0-387-79838-7\_11. PubMed PMID: 19280854.
- 36. Kelley MA, Weber DJ, Gilligan P, Cohen MS. Breakthrough pneumococcal bacteremia in patients being treated with azithromycin and clarithromycin. Clin Infect Dis. 2000;31(4):1008-11. Epub 2000/10/26. doi: 10.1086/318157. PubMed PMID: 11049784.
- 37. Suda KJ, Hicks LA, Roberts RM, Hunkler RJ, Taylor TH. Trends and seasonal variation in outpatient antibiotic prescription rates in the United States, 2006 to 2010. Antimicrob Agents Chemother. 2014;58(5):2763-6. Epub 2014/03/05. doi: 10.1128/AAC.02239-13. PubMed PMID: 24590486; PMCID: PMC3993241.
- 38. Azarian T, Grant LR, Arnold BJ, Hammitt LL, Reid R, Santosham M, Weatherholtz R, Goklish N, Thompson CM, Bentley SD, O'Brien KL, Hanage WP, Lipsitch M. The impact of serotype-specific vaccination on phylodynamic parameters of Streptococcus pneumoniae and the pneumococcal pan-genome. PLoS Pathog. 2018;14(4):e1006966. Epub 2018/04/05. doi: 10.1371/journal.ppat.1006966. PubMed PMID: 29617440; PMCID: PMC5902063 not related to

- this paper from Pfizer and PATH Vaccine Solutions. W.P.H. and M.L. have consulted for Antigen Discovery Inc. The authors have declared that no competing interests exist.
- 39. Gladstone RA, Lo SW, Lees JA, Croucher NJ, van Tonder AJ, Corander J, Page AJ, Marttinen P, Bentley LJ, Ochoa TJ, Ho PL, du Plessis M, Cornick JE, Kwambana-Adams B, Benisty R, Nzenze SA, Madhi SA, Hawkins PA, Everett DB, Antonio M, Dagan R, Klugman KP, von Gottberg A, McGee L, Breiman RF, Bentley SD, Global Pneumococcal Sequencing C. International genomic definition of pneumococcal lineages, to contextualise disease, antibiotic resistance and vaccine impact. EBioMedicine. 2019;43:338-46. Epub 2019/04/21. doi: 10.1016/j.ebiom.2019.04.021. PubMed PMID: 31003929; PMCID: PMC6557916.
- 40. van Tonder AJ, Gladstone RA, Lo SW, Nahm MH, du Plessis M, Cornick J, Kwambana-Adams B, Madhi SA, Hawkins PA, Benisty R, Dagan R, Everett D, Antonio M, Klugman KP, von Gottberg A, Breiman RF, McGee L, Bentley SD, The Global Pneumococcal Sequencing C. Putative novel cps loci in a large global collection of pneumococci. Microb Genom. 2019;5(7). Epub 2019/06/12. doi: 10.1099/mgen.0.000274. PubMed PMID: 31184299; PMCID: PMC6700660.
- 41. Bogaardt C, van Tonder AJ, Brueggemann AB. Genomic analyses of pneumococci reveal a wide diversity of bacteriocins including pneumocyclicin, a novel circular bacteriocin. BMC Genomics. 2015;16(1):554. Epub 2015/07/29. doi: 10.1186/s12864-015-1729-4. PubMed PMID: 26215050; PMCID: PMC4517551.
- 42. Croucher NJ, Finkelstein JA, Pelton SI, Mitchell PK, Lee GM, Parkhill J, Bentley SD, Hanage WP, Lipsitch M. Population genomics of post-vaccine changes in pneumococcal epidemiology. Nat Genet. 2013;45(6):656-63. Epub 2013/05/07. doi: 10.1038/ng.2625. PubMed PMID: 23644493; PMCID: PMC3725542.

- 43. Andam CP, Mitchell PK, Callendrello A, Chang Q, Corander J, Chaguza C, McGee L, Beall BW, Hanage WP. Genomic Epidemiology of Penicillin-Nonsusceptible Pneumococci with Nonvaccine Serotypes Causing Invasive Disease in the United States. J Clin Microbiol. 2017;55(4):1104-15. Epub 2017/01/20. doi: 10.1128/JCM.02453-16. PubMed PMID: 28100596; PMCID: PMC5377837.
- 44. Schroeder MR, Lohsen S, Chancey ST, Stephens DS. High-Level Macrolide Resistance Due to the Mega Element [mef(E)/mel] in Streptococcus pneumoniae. Front Microbiol. 2019;10:868. Epub 2019/05/21. doi: 10.3389/fmicb.2019.00868. PubMed PMID: 31105666; PMCID: PMC6491947.
- 45. Bowers JR, Driebe EM, Nibecker JL, Wojack BR, Sarovich DS, Wong AH, Brzoska PM, Hubert N, Knadler A, Watson LM, Wagner DM, Furtado MR, Saubolle M, Engelthaler DM, Keim PS. Dominance of multidrug resistant CC271 clones in macrolide-resistant streptococcus pneumoniae in Arizona. BMC Microbiol. 2012;12:12. Epub 2012/01/19. doi: 10.1186/1471-2180-12-12. PubMed PMID: 22251616; PMCID: PMC3285076.
- 46. Sharma D, Baughman W, Holst A, Thomas S, Jackson D, da Gloria Carvalho M, Beall B, Satola S, Jerris R, Jain S, Farley MM, Nuorti JP. Pneumococcal carriage and invasive disease in children before introduction of the 13-valent conjugate vaccine: comparison with the era before 7-valent conjugate vaccine. Pediatr Infect Dis J. 2013;32(2):e45-53. Epub 2012/10/20. doi: 10.1097/INF.0b013e3182788fdd. PubMed PMID: 23080290.
- 47. Moore MR, Gertz RE, Jr., Woodbury RL, Barkocy-Gallagher GA, Schaffner W, Lexau C, Gershman K, Reingold A, Farley M, Harrison LH, Hadler JL, Bennett NM, Thomas AR, McGee L, Pilishvili T, Brueggemann AB, Whitney CG, Jorgensen JH, Beall B. Population snapshot of

- emergent Streptococcus pneumoniae serotype 19A in the United States, 2005. J Infect Dis. 2008;197(7):1016-27. Epub 2008/04/19. doi: 10.1086/528996. PubMed PMID: 18419539.
- 48. van Selm S, van Cann LM, Kolkman MA, van der Zeijst BA, van Putten JP. Genetic basis for the structural difference between Streptococcus pneumoniae serotype 15B and 15C capsular polysaccharides. Infect Immun. 2003;71(11):6192-8. Epub 2003/10/24. doi: 10.1128/IAI.71.11.6192-6198.2003. PubMed PMID: 14573636; PMCID: PMC219561.
- 49. Venkateswaran PS, Stanton N, Austrian R. Type variation of strains of Streptococcus pneumoniae in capsular serogroup 15. J Infect Dis. 1983;147(6):1041-54. Epub 1983/06/01. doi: 10.1093/infdis/147.6.1041. PubMed PMID: 6854063.
- 50. Hao L, Kuttel MM, Ravenscroft N, Thompson A, Prasad AK, Gangolli S, Tan C, Cooper D, Watson W, Liberator P, Pride MW, Jansen KU, Anderson AS, Scully IL. Streptococcus pneumoniae serotype 15B polysaccharide conjugate elicits a cross-functional immune response against serotype 15C but not 15A. Vaccine. 2022;40(33):4872-80. Epub 2022/07/10. doi: 10.1016/j.vaccine.2022.06.041. PubMed PMID: 35810060.
- 51. Sheppard C, Fry NK, Mushtaq S, Woodford N, Reynolds R, Janes R, Pike R, Hill R, Kimuli M, Staves P, Doumith M, Harrison T, Livermore DM. Rise of multidrug-resistant non-vaccine serotype 15A Streptococcus pneumoniae in the United Kingdom, 2001 to 2014. Euro Surveill. 2016;21(50). Epub 2016/12/23. doi: 10.2807/1560-7917.ES.2016.21.50.30423. PubMed PMID: 28006650; PMCID: PMC5291132.
- 52. van der Linden M, Perniciaro S, Imohl M. Increase of serotypes 15A and 23B in IPD in Germany in the PCV13 vaccination era. BMC Infect Dis. 2015;15:207. Epub 2015/05/06. doi: 10.1186/s12879-015-0941-9. PubMed PMID: 25940580; PMCID: PMC4424534.

- 53. Su LH, Kuo AJ, Chia JH, Li HC, Wu TL, Feng Y, Chiu CH. Evolving pneumococcal serotypes and sequence types in relation to high antibiotic stress and conditional pneumococcal immunization. Sci Rep. 2015;5:15843. Epub 2015/11/03. doi: 10.1038/srep15843. PubMed PMID: 26522920; PMCID: PMC4629140.
- 54. Ono T, Watanabe M, Hashimoto K, Kume Y, Chishiki M, Okabe H, Sato M, Norito S, Chang B, Hosoya M. Serotypes and Antibiotic Resistance of Streptococcus pneumoniae before and after the Introduction of the 13-Valent Pneumococcal Conjugate Vaccine for Adults and Children in a Rural Area in Japan. Pathogens. 2023;12(3). Epub 2023/03/30. doi: 10.3390/pathogens12030493. PubMed PMID: 36986414; PMCID: PMC10056172.
- 55. Fleming-Dutra K, Mbaeyi C, Link-Gelles R, Alexander N, Guh A, Forbes E, Beall B, Winchell JM, Carvalho Mda G, Pimenta F, Kodani M, Vanner C, Stevens H, Brady D, Caulcrick-Grimes M, Bandy U, Moore MR. Streptococcus pneumoniae serotype 15A in psychiatric unit, Rhode Island, USA, 2010-2011. Emerg Infect Dis. 2012;18(11):1889-93. Epub 2012/10/25. doi: 10.3201/eid1811.120454. PubMed PMID: 23092658; PMCID: PMC3559171.
- 56. Liu Z, Nachamkin I, Edelstein PH, Lautenbach E, Metlay JP. Serotype emergence and genotype distribution among macrolide-resistant invasive Streptococcus pneumoniae isolates in the postconjugate vaccine (PCV-7) era. Antimicrob Agents Chemother. 2012;56(2):743-50. Epub 2011/11/30. doi: 10.1128/AAC.05122-11. PubMed PMID: 22123697; PMCID: PMC3264211.
- 57. Kim SH, Chung DR, Song JH, Baek JY, Thamlikitkul V, Wang H, Carlos C, Ahmad N, Arushothy R, Tan SH, Lye D, Kang CI, Ko KS, Peck KR, Asian Network for Surveillance of Resistant P. Changes in serotype distribution and antimicrobial resistance of Streptococcus pneumoniae isolates from adult patients in Asia: Emergence of drug-resistant non-vaccine

- serotypes. Vaccine. 2020;38(38):6065-73. Epub 2019/10/09. doi: 10.1016/j.vaccine.2019.09.065. PubMed PMID: 31590932.
- 58. Wu CJ, Lai JF, Huang IW, Shiau YR, Wang HY, Lauderdale TL. Serotype Distribution and Antimicrobial Susceptibility of Streptococcus pneumoniae in Pre- and Post- PCV7/13 Eras, Taiwan, 2002-2018. Front Microbiol. 2020;11:557404. Epub 2020/11/17. doi: 10.3389/fmicb.2020.557404. PubMed PMID: 33193140; PMCID: PMC7642986.
- 59. Waight PA, Andrews NJ, Ladhani SN, Sheppard CL, Slack MP, Miller E. Effect of the 13-valent pneumococcal conjugate vaccine on invasive pneumococcal disease in England and Wales 4 years after its introduction: an observational cohort study. Lancet Infect Dis. 2015;15(5):535-43. Epub 2015/03/25. doi: 10.1016/S1473-3099(15)70044-7. PubMed PMID: 25801458.
- 60. Mendes RE, Costello AJ, Jacobs MR, Biek D, Critchley IA, Jones RN. Serotype distribution and antimicrobial susceptibility of USA Streptococcus pneumoniae isolates collected prior to and post introduction of 13-valent pneumococcal conjugate vaccine. Diagn Microbiol Infect Dis. 2014;80(1):19-25. Epub 2014/06/30. doi: 10.1016/j.diagmicrobio.2014.05.020. PubMed PMID: 24974272.
- 61. Pai R, Gertz RE, Whitney CG, Beall B. Clonal association between Streptococcus pneumoniae serotype 23A, circulating within the United States, and an internationally dispersed clone of serotype 23F. J Clin Microbiol. 2005;43(11):5440-4. Epub 2005/11/08. doi: 10.1128/JCM.43.11.5440-5444.2005. PubMed PMID: 16272467; PMCID: PMC1287803.
- 62. Farrell DJ, Couturier C, Hryniewicz W. Distribution and antibacterial susceptibility of macrolide resistance genotypes in Streptococcus pneumoniae: PROTEKT Year 5 (2003-2004). Int J Antimicrob Agents. 2008;31(3):245-9. Epub 2008/01/08. doi: 10.1016/j.ijantimicag.2007.10.022. PubMed PMID: 18178388.

- 63. Hu T, Song Y, Done N, Liu Q, Sarpong EM, Lemus-Wirtz E, Signorovitch J, Mohanty S, Weiss T. Incidence of invasive pneumococcal disease in children with commercial insurance or Medicaid coverage in the United States before and after the introduction of 7- and 13-valent pneumococcal conjugate vaccines during 1998-2018. BMC Public Health. 2022;22(1):1677. Epub 2022/09/06. doi: 10.1186/s12889-022-14051-6. PubMed PMID: 36064378; PMCID: PMC9442936.
- 64. Phongsamart W, Srifeungfung S, Chatsuwan T, Nunthapisud P, Treerauthaweeraphong V, Rungnobhakhun P, Sricharoenchai S, Chokephaibulkit K. Changing trends in serotype distribution and antimicrobial susceptibility of Streptococcus pneumoniae causing invasive diseases in Central Thailand, 2009-2012. Hum Vaccin Immunother. 2014;10(7):1866-73. Epub 2014/11/27. doi: 10.4161/hv.28675. PubMed PMID: 25424794; PMCID: PMC4186036.
- of the SA, de Gouveia L, Tempia S, Quan V, Meiring S, von Mollendorf C, Madhi SA, Zell ER, Verani JR, O'Brien KL, Whitney CG, Klugman KP, Cohen C, Investigators G-S. Effects of vaccination on invasive pneumococcal disease in South Africa. N Engl J Med. 2014;371(20):1889-99. Epub 2014/11/12. doi: 10.1056/NEJMoa1401914. PubMed PMID: 25386897.

Chapter 4: Extracellular vesicles and transformation of antimicrobial resistance genetic determinants in Streptococcus pneumoniae Brenda S. Antezana<sup>a</sup>, Yih-Ling Tzeng<sup>b</sup>, David S. Stephens<sup>b</sup> <sup>a</sup> Microbiology and Molecular Genetics Program, Graduate Division of Biological and Biomedical Sciences, Emory University Laney Graduate School, Atlanta, Georgia, USA <sup>b</sup> Department of Medicine, Division of Infectious Diseases, Emory University School of Medicine, Atlanta, Georgia, USA #Address correspondence to David S. Stephens, <u>dstep01@emory.edu</u>.

## Paper in preparation

B. Antezana purified all vesicle preparations, performed all transformation experiments, wrote and edited the chapter.

## **ABSTRACT**

The alarming spread of antimicrobial resistance in *Streptococcus pneumoniae* is driven by horizontal gene transfer via transformation of extracellular DNA (eDNA). S. pneumoniae releases extracellular vesicles (EVs), and EVs have been shown in some bacterial species to be a vehicle for delivery of transforming DNA. EVs isolated from late-log broth cultures of multiple S. pneumoniae strains were found to have ~1 to ~17 ng DNA/µg EV protein. This EV DNA encoded different classes of antimicrobial resistance genes. In vitro transformations of competent planktonic cells with D39<sup>Str</sup>Δ*ply::ermB* EVs and selecting for either point mutation-mediated streptomycin resistance or ermB-mediated erythromycin resistance yielded recombinants at frequencies (rFs) of ~10<sup>-4</sup>. Although rFs were ~10<sup>-3</sup> using similar concentrations of purified genomic DNAs, the differences were not statistically significant. In vitro transformation with GA71819 DNA carrying the 5.4-kb erythromycin resistance Mega element resulted in a rF of ~ 10<sup>-6</sup> but no recombinants were recovered when transformed with GA71819 EVs (rF <10<sup>-9</sup>), which were isolated at a low yield of 0.89 ng DNA/µg EV protein. DNase I-treated EVs completely lost transforming ability indicating that EV-associated DNA was surface-exposed and not protected by the vesicles. S. pneumoniae biofilms on human nasopharyngeal cells enhanced EV-mediated uptake of D39<sup>Str</sup>Δ*ply*::*ermB* resistance (rF ~10<sup>-3</sup>) and uptake of larger DNA fragments (GA71819 Mega, rF of ~10-7). SNP analyses of biofilm EV recombinants revealed homologous recombination of ~9-26 kb DNA fragments. EV-associated eDNA is likely bound to the EV surface and may contribute to pneumococcal transformation and horizontal gene transfer.

### **IMPORTANCE**

Widespread dissemination of antimicrobial resistance in *Streptococcus pneumoniae* has led to limitations of treatment options and to treatment failures. Consequently, the World Health Organization (WHO) recognized *S. pneumoniae* as a priority pathogen for research and development of novel therapeutics. *S. pneumoniae* can form multi-strain biofilms in the human nasopharynx that enhance exchange of antimicrobial resistance determinants primarily via transformation. We investigated the role of extracellular vesicles (EVs) secreted by *S. pneumoniae* in disseminating antibiotic resistance determinants. Isolated pneumococcal EVs associated with surface-exposed extracellular DNA containing antibiotic resistance determinants indeed mediate transformation of planktonic and biofilm-associated *S. pneumoniae*. However, EV-mediated transformation occurred at lower recombination frequencies as compared to free extracellular DNA.

### INTRODUCTION

The burden of antimicrobial resistance is a leading public health concern worldwide. Estimates demonstrate that the increasing trends of antimicrobial resistance will result in 10 million deaths per year by 2050 and lead to a global economic toll of up to \$100 trillion (1). Six different bacterial pathogens caused 4.95 million deaths associated with antimicrobial resistance in 2019, and 1.27 million of these deaths were directly attributed to antimicrobial resistance (2). Of the six pathogens, *Streptococcus pneumoniae* (or pneumococcus) was responsible for ~600,000 deaths associated with resistance of which 150,000 deaths were directly attributed to antimicrobial resistance<sup>(2)</sup>.

S. pneumoniae is a nasopharyngeal colonizer that can cause localized infections, such as otitis media and pneumonia, or invasive disease, such as bacteremia and meningitis  $^{(3, 4)}$ . At-risk individuals for invasive disease include children ( $\leq 2$  years of age), the elderly ( $\geq 65$  years of age), and the immunocompromised  $^{(5, 6)}$ . Beta-lactam treatment for pneumococcal infections first consisted of penicillin as it became available in the  $1940s^{(7)}$ . However, a penicillin-resistant S. pneumoniae strain was isolated in Australia from sputum of a patient in  $1967^{(8, 9)}$  and penicillin resistance has subsequently emerged worldwide. The initial treatment for pneumococcal infections switched to macrolides, which became a first line of therapy for community-acquired pneumonia and suspected pneumococcal upper respiratory infections  $^{(10, 11)}$ . As with penicillin, the widespread use of macrolides resulted in increased macrolide resistance during the  $1990s^{(12-16)}$ . Due to the rise of antimicrobial resistance in the species, in 2017, the World Health Organization named S. pneumoniae a priority pathogen for research and development of novel treatment options  $^{(17)}$ .

The dominant underlying mechanism for spread of antimicrobial resistance in *S. pneumoniae* is horizontal gene transfer via genetic transformation and homologous recombination of extracellular DNA. However, recently extracellular membrane vesicles (EVs) were discovered to

be released by S. pneumoniae. Membrane vesicles, or lipid-membrane bound particles, are secreted by both Gram-negative (known as outer membrane vesicles, OMVs) and Gram-positive (known as EVs) bacteria (18, 19). Though EVs released by Gram-positive organisms were initially considered unlikely due to the thick cell wall, EVs are now well recognized in Staphylococcus aureus<sup>(20)</sup>, Bacillus anthracis<sup>(21)</sup>, Bacillus subtilis<sup>(22)</sup>, Listeria monocytogenes<sup>(23)</sup>, and several streptococcal species, such as Streptococcus mutans<sup>(24)</sup> and S. pneumoniae<sup>(25)</sup> with potential mechanisms of release under study<sup>(26)</sup>. S. pneumoniae secretes significant amounts of EVs that range from 20-80 nm in diameter during the late-log growth phase<sup>(25)</sup>. Purified pneumococcal EVs have also been shown to elicit protective immunogenicity in hosts, and thus are considered as potential vaccine candidates (25, 27, 28). Pneumococcal EVs have been observed to be composed of short-chain fatty acids and contain S. pneumoniae surface proteins, such as PspA and PspC, as well as virulence factors, such as the pneumolysin toxin, Ply<sup>(25)</sup>. In ruminococci, EVs have been shown to be a vehicle for delivering transforming DNA to bacterial cells<sup>(29)</sup>, but the role of S. pneumoniae EVs in the horizontal transfer of pneumococcal DNA, such as antimicrobial resistance determinants, remains unclear.

In this study, pneumococcal secreted EVs were purified from multiple antibiotic resistant *S. pneumoniae* strains and EV-associated DNA content determined. Purified pneumococcal EVs were evaluated in classic *in vitro* transformation reactions as well as transformation assays of biofilms formed on human nasopharyngeal cell monolayers. EV-associated DNA was susceptible to DNase I treatment. EV-associated DNA transformed both planktonic pneumococci and pneumococcal biofilms but at lower frequencies than free extracellular DNA. Whole genome sequencing and SNP variant analyses of recombinant genomes revealed that *S. pneumoniae* EVs could transform larger antimicrobial resistance determinants in human nasopharyngeal cell

biofilms, again highlighting the importance of biofilms for genetic exchange of large DNA fragments.

### **RESULTS**

S. pneumoniae EV-associated DNA transformed planktonic cells and nasopharyngeal biofilms but at lower frequencies compared to extracellular DNA.

Membrane-bound vesicles from several bacterial species have been demonstrated to contain nucleic acids<sup>(27, 30)</sup>. S. pneumoniae EVs were purified from spent media of late-log phase broth cultures by ultracentrifugation<sup>(25)</sup>. The DNA concentrations in EV preparations were determined by quantitative PCR (qPCR) reactions targeting the relevant genome-encoded resistance gene and normalized to EV protein content measured by the bicinchoninic acid (BCA) protein assay (Table 1). First, two EV preparations were isolated from a D39<sup>Str</sup>Δ*ply::ermB* strain with an average yield of 5.24 ng DNA per ug protein targeting ermB. Transmission electron microscopy (TEM) of the purified EVs showed the presence of membrane-bound vesicles (Fig 1A). Classic in vitro transformation reactions of planktonic D39 cells using D39<sup>Str</sup>Δply::ermB EVs as the genetic material and erythromycin (Ery) selection recovered recombinants at a recombination frequency (rF) of 5.51x10<sup>-4</sup>±5.15x10<sup>-4</sup> per µg DNA (Fig 2A). Though not statistically significant (p-value of 0.46), the rF of EV DNA was 2.85-fold lower compared to the rF of 1.57x10<sup>-3</sup>±2.11x10<sup>-3</sup> per µg DNA obtained using equivalent quantities of purified genomic DNA from D39<sup>Str</sup>Δ*ply::ermB* (Fig. 2A). When selecting for streptomycin (Str) resistance conferred by a point mutation K56T in rpsL (31), the rFs for EV DNA and free DNA were  $7.37 \times 10^{-4} \pm 6.20 \times 10^{-4}$  and  $2.13 \times 10^{-3} \pm 2.17 \times 10^{-3}$ , respectively (p-value of 0.54) (Fig 2A), again demonstrating a 2.89-fold reduction for EVmediated transformation compared to free genomic DNA controls.

Biofilm formation enhances pneumococcal transformation<sup>(32)</sup>. To determine if the S. pneumoniae biofilm environment influences EV-mediated transformation, a trimethoprim (Tmp)resistant recipient, D39<sup>Tmp</sup>, was inoculated on human nasopharyngeal cell monolayers. Biofilms were allowed to form over a period of 4 hours in 24-well plates. Following biofilm formation, complete transformation media containing 100 ng/mL competence stimulating peptide (CSP) was added along with 100 ng of D39<sup>Str</sup>Δ*ply::ermB* EVs. Reactions with 100 ng of genomic DNA were conducted in parallel as controls. Biofilm transformations were incubated for an additional 4 hours, and recombinants were selected for dual Ery+Tmp or Str+Tmp resistance. When normalized to µg DNA, purified DNA controls resulted in rFs of 2.98x10<sup>-3</sup>±3.14x10<sup>-4</sup> for Ery+Tmp and 3.45x10<sup>-1</sup> <sup>3</sup>±1.20x10<sup>-3</sup> for Str+Tmp while the biofilm transformation with EVs yielded rFs at 1.53x10<sup>-</sup>  $^{3}\pm8.95\times10^{-4}$  for Ery+Tmp and  $1.55\times10^{-3}\pm7.48\times10^{-4}$  for Str+Tmp (Fig 2A). Comparing the EV versus free DNA transformations resulted in non-significant p-values of 0.16 and 0.20 for Ery+Tmp and Str+Tmp, respectively. The nasopharyngeal biofilm environment (rF of ~10<sup>-3</sup>) resulted in greater frequency for the uptake of EV-associated DNA from the D39<sup>Str</sup>Δ*ply*::*ermB* EVs relative to *in vitro* conditions (rF of ~10<sup>-4</sup>). However, under biofilm conditions, rFs obtained with EV-associated DNA were still ~2-fold lower compared to their genomic DNA controls.

### EV-associated DNA was not protected from DNase I during transformation.

Nucleic acids associated with bacterial vesicles have been reported on the external surface as well as protected within vesicles<sup>(30)</sup>. We examined the potential localization of DNA associated with pneumococcal vesicles utilizing DNase I treatment. In the absence of DNase I, EVs and purified genomic DNA of D39<sup>Str</sup> $\Delta$ *ply::ermB* transformed D39 at rFs of 5.15x10<sup>-4</sup>±4.87x10<sup>-4</sup> and 1.06x10<sup>-3</sup>±2.78x10<sup>-3</sup>, respectively, per  $\mu$ g DNA (Fig 2B). However, the addition of DNase I into transformation reactions eliminated the recovery of recombinants with calculated rFs of <3.45x10<sup>-1</sup>

<sup>7</sup>±3.71x10<sup>-7</sup> and <2.42x10<sup>-7</sup>±2.00x10<sup>-7</sup> for EV and DNA, respectively (Fig 2B), indicating that the DNA associated with pneumococcal EVs was not protected or secluded inside *S. pneumoniae* vesicles.

# S. pneumoniae EVs transformed larger antimicrobial resistance determinants only in nasopharyngeal biofilms.

With the successful EV-mediated transformation of the Str resistance-conferring point mutation and the 738-bp *ermB* gene, we assessed whether larger antimicrobial resistance genetic determinants can be transferred via EVs. EVs were isolated from a *S. pneumoniae* clinical isolate GA71819 carrying a chromosomal 5.4-kb macrolide resistance determinant, Mega-2.II<sup>(33)</sup>. The EV yield was 0.89 ng DNA per μg protein based on qPCR quantification of *mefE* (Table 1) and TEM imaging confirmed the presence of membrane vesicles (Fig 1B). Selecting for Ery resistance, GA71819 EVs did not transform planktonic D39 cells (rF <9.17x10<sup>-9</sup>±6.68x10<sup>-9</sup>), whereas genomic DNA resulted in recombinants at a rF of 2.22x10<sup>-6</sup>±2.67x10<sup>-7</sup> per μg DNA and this difference was significant (p-value of 0.007) (Fig 3).

Given the evidence for enhanced transformation in pneumococcal biofilms relative to the *in vitro* conditions<sup>(32)</sup>, GA71819 EVs were incubated with D39<sup>Tmp</sup> nasopharyngeal biofilms in the presence of 100 ng/mL synthetic CSP. In contrast to classic *in vitro* transformation of planktonic D39 cells (rF <10<sup>-9</sup>), dual-resistant Ery+Tmp recombinants were recovered with GA71819 EVs at a rF of 5.93x10<sup>-7</sup>±7.91x10<sup>-7</sup> per μg DNA (Fig 3) under the biofilm condition (p-value of 0.33). Although not statistically significant, this biofilm EV-mediated rF was ~65-fold greater than that obtained under *in vitro* conditions (rF <10<sup>-9</sup>), consistent with the notion that biofilm conditions enhanced uptake of EV-associated DNA. The GA71819 genomic DNA controls of the nasopharyngeal biofilm transformation resulted in a rF of 3.72x10<sup>-4</sup>±5.41x10<sup>-4</sup> per μg DNA (Fig

3), which was 627-fold higher than the rF achieved with EV-associated DNA. Therefore, EV-mediated transformation was less efficient than free DNA-facilitated transformation in both *in vitro* and nasopharyngeal biofilm conditions, and the difference was more pronounced with the delivery of the larger Mega-2.II resistance element (as compared to the data in Fig 2A), suggesting an interfering effect of EVs on transforming DNA.

# S. pneumoniae EV-mediated transformation of human nasopharyngeal biofilms occurred without exogenously added synthetic competence stimulating peptide (CSP).

Natural competence development of S. pneumoniae strains in a biofilm without exogenously added synthetic CSP has been shown to result in successful transformation<sup>(32)</sup>. Exogenous CSP was added in our initial experiments described above, thus we repeated the static biofilm transformation assays with recipient D39<sup>Tmp</sup> and equal quantities of D39<sup>Str</sup>Δply::ermB EVs or genomic DNA in the presence or absence of exogenous CSP. In the presence of CSP, we obtained a statistically lower Ery+Tmp rF of 4.10x10<sup>-4</sup>±2.67x10<sup>-4</sup> per µg DNA for EV transformation compared to the DNA control (rF of 1.62x10<sup>-3</sup>±4.17x10<sup>-4</sup> per µg DNA) with a calculated p-value of 0.01 (Fig 4). When synthetic CSP was omitted, EVs and purified DNA of D39<sup>Str</sup>Δ*ply::ermB* yielded an Ery+Tmp rF of 2.35x10<sup>-4</sup>±2.82x10<sup>-4</sup> and 4.47x10<sup>-4</sup>±3.73x10<sup>-4</sup>, respectively, per μg DNA (Fig 4). Though in the same order of magnitude, the calculated CSP- rF for Ery+Tmp recombinants transformed with EVs was 1.90-fold lower than the genomic DNA control. Selection for Str+Tmp recombinants was also performed for biofilm transformations in CSP+ and CSPconditions. In the presence of exogenous CSP, D39<sup>Str</sup>Δply::ermB EVs yielded a Str+Tmp rF of 8.30x10<sup>-4</sup>±5.34x10<sup>-4</sup> while the genomic DNA transformed at the 3.17-fold greater rF of 2.63x10<sup>-</sup> <sup>3</sup>±1.34x10<sup>-3</sup> when normalized to μg DNA (Fig 4). Interestingly, for CSP- Str+Tmp recombinants, EVs transformed at a 1.21-fold greater rF of 5.97x10<sup>-4</sup>±8.95x10<sup>-4</sup> per μg DNA compared to the

genomic DNA control (rF of 4.92x10<sup>4</sup>±5.61x10<sup>-4</sup> per µg DNA), but no statistical significance for this increased EV rF was demonstrated (Fig 4). Overall, there was no statistically significant difference between CSP+ and CSP- conditions except for selection of Ery+Tmp recombinants with DNA transformation where the calculated p-value was 0.02. Thus, natural transformation of EV-associated DNA in biofilm conditions was demonstrated to occur at similar frequencies to that of CSP+ conditions, though still at lower frequencies than the parallel free genomic DNA controls for the most part.

Nasopharyngeal biofilms facilitated transformation of >20 kb integrative and conjugative element via pneumococcal EVs.

To further evaluate EV influence on transformation of larger DNA fragments encoding antibiotic resistance, EVs were isolated from a clinical isolate GA16833 that carries the 23.5-kb Tn2009 integrative and conjugative element (ICE), which harbors a tetracycline resistance gene *tetM* as well as macrolide resistance via Mega-1.V. Quantitative PCR determined an average EV yield of 9.84 ng DNA per μg protein based on *tetM* quantification from two EV preparations (Table 1), and TEM once again demonstrated membrane particles (Fig 1C). We have previously reported that genomic DNA of GA16833 failed to transform D39 competent cells with Tet resistance by classic *in vitro* transformation assays<sup>(34)</sup>. Similarly, no Tet-resistant recombinants were recovered with GA16833 EVs using *in vitro* transformation assays (rF <3.15x10<sup>-6</sup>±3.62x10<sup>-6</sup>). However, when examining GA16833 EVs under biofilm transformation conditions (both CSP+ and CSP-), we recovered a single Tet-resistant recombinant in the absence of synthetic CSP, resulting in a rF of 1.52x10<sup>-7</sup> per μg DNA.

Large EV-associated DNA fragments incorporated into recipient genomes by homologous recombination.

Four D39 recombinants from independent biological replicates of the biofilm transformation assays with GA71819 EVs were characterized with whole genome sequencing (WGS) analyses. Since the recombinants were recovered from a single-strain biofilm of D39<sup>Tmp</sup> and the EV preparations were free of bacteria, unsurprisingly all recombinants were of sequence type 595 of the D39<sup>Tmp</sup> recipient determined by multi-locus sequence typing (MLST)<sup>(35)</sup>. There was no capsule switching as the capsule locus of the four recombinants was the serotype 2 of D39<sup>Tmp</sup>. The single Tet+Tmp D39 recombinant that arose from the biofilm transformation with GA16833 EVs under a CSP- condition also had a sequence type of 595 and a serotype 2 capsule.

To probe the junctions of *S. pneumoniae* EV transformation, single nucleotide polymorphism (SNP) variant analyses and sequence alignments were performed for each recombinant to estimate the integrated donor fragment sizes. Recombined fragments were identified by a collection of consecutive donor-specific SNPs flanked by recipient sequence and the outermost 5' and 3' donor SNPs were used to determine the minimum length of the donor fragment. Donor DNA fragments were integrated into the recombinant genomes at the same locus as that of the donor GA71819, which is within a DNA-methyladenine glycosidase gene (SP\_0180, TIGR4 annotation) on fragment sizes of ~11.2, ~13.0, ~15.1, and ~9.14 kb and contained the intact Mega-2.II element (Table 2). The single Tet-resistant D39<sup>Tmp</sup> recombinant recovered from GA16833 EV biofilm transformation contained an intact 23.5-kb Tn2009 ICE on a large donor DNA fragment of ~25.7 kb (Table 2). Thus, pneumococcal EVs transformed biofilms with DNA ranging from ~9 kb to ~26 kb in length. Moreover, the simultaneous co-transformation of distant DNA fragments into the same cell, known as congression, has been described in *S. pneumoniae* (36). SNP variant analyses of all five EV-mediated recombinants also demonstrated other recombination events at

various genomic loci. The different lengths of incorporated donor DNA supported a homologous recombination mechanism for integration of DNA delivered by *S. pneumoniae* EVs.

### **DISCUSSION**

The widespread dissemination of antimicrobial resistance in *S. pneumoniae* remains a global public health concern despite the sequential introductions of highly effective pneumococcal conjugate vaccines. While the horizontal genetic exchange of antimicrobial resistance determinants is accredited to multiple mechanisms<sup>(37, 38)</sup>, transformation of free extracellular DNA, is the major way of shaping genomic evolution in *S. pneumoniae*. EVs have been shown to be released during pneumococcal planktonic and biofilm growth<sup>(39)</sup>. Bacterial vesicles have also been demonstrated to readily associate with extracellular DNA<sup>(40)</sup>. The role of extracellular vesicles as a potential means for DNA delivery for *S. pneumoniae* transformation was investigated in this study.

Various types of nucleic acids are associated with vesicles secreted by both Gram-positive and Gram-negative bacteria, such as chromosomal DNA, plasmid DNA, rRNA, mRNA, and tRNA<sup>(27)</sup>. Domenech et al. showed that detectable concentrations of DNA were associated with planktonic culture-derived and biofilm-derived pneumococcal EVs isolated during late-log phase<sup>(39)</sup>. In our studies, we also demonstrated that EVs isolated from several *S. pneumoniae* strains contained DNA, ranging from ~1 to ~17 ng DNA per μg protein. The DNA associated with pneumococcal EVs was confirmed to harbor the antimicrobial resistance determinants *ermB*, *mefE*, or *tetM*<sup>(10, 41)</sup>. Previously, Kleive et al.<sup>(29)</sup> found that EVs isolated from Gram-positive ruminococci can rescue a mutant phenotype via transformation. The potential and efficiency for pneumococcal EVs in the transformation of antimicrobial resistance determinants were probed in this study.

We performed classic in vitro transformations of planktonic pneumococcal cells using EVs as the transforming genetic material. EVs of D39<sup>Str</sup>Δ*ply::ermB* were capable of transforming D39 to be Ery- (mediated by ermB) or Str- (mediated by rpsL/K56T) resistant at rFs of ~10<sup>-4</sup>, which was lower but not statistically different from control reactions using free genomic DNA at rFs of ~10<sup>-1</sup> <sup>3</sup>. Similar trends were observed when utilizing EVs or genomic DNA of the 5.4-kb Mega-2.IIcontaining GA71819 strain for in vitro transformation. No recovery of Ery recombinants occurred with EVs (rF <10<sup>-9</sup>) whereas genomic DNA readily transformed Mega-mediated Ery resistance at a rF of ~10<sup>-6</sup>. Thus, EV-mediated transformation of planktonic pneumococci results in acquisition of antibiotic resistance determinants conferred by point mutations (Str) or by a 738-bp gene (ermB), but larger determinants (>5 kb) were not transformed. DNA uptake of antimicrobial resistance determinants mediated by EVs occurred at lower frequencies than free genomic DNA, implying a modulation impact of EVs in natural transformation. This interference of pneumococcal EVs to transformation could be due to the DNA-retaining characteristics that have been shown by other bacterial vesicles, such as with *Pseudomonas aeruginosa* (40). The interaction of DNA with vesicles may prevent the type IV pilus of pneumococci from disassociating DNA from vesicles to allow for efficient DNA uptake as compared to free extracellular DNA fragments that can be readily bound by the pilus.

Our data demonstrated that pneumococcal EV-associated DNA was not protected from DNase I digestion, which was also shown by Domenech et al.<sup>(39)</sup>. Given the late-log phase isolation of pneumococcal EVs in our experiments, autolysis that is typically induced in stationary phase, would not have contributed significantly as the source of EV-associated DNA. However, release of extracellular DNA during active growth has been shown in pneumococci <sup>(24)</sup>, even with the absence of three main autolytic enzymes, LytA, LytC, and CbpD<sup>(39)</sup>. Moreover, induction of

competence during log-phase growth can lead to fratricide, the lysis of a sub-population of non-competent pneumococcal cells, and thus DNA release <sup>(42)</sup>. If these independently released DNA fragments are the major source of DNA that associates with the external surface of pneumococcal EVs, it would be consistent with our results with the lack of recombinants upon treating pneumococcal EVs with DNase I.

Marks et al. found that horizontal genetic exchange in S. pneumoniae is more efficient in highly structured dual-strain biofilms formed on fixed epithelial cells over 72 hours. Exchange of genetic material and dual-resistant transformants were recovered at high frequencies (32, 43). The close cellto-cell contact provided by biofilms is proposed to facilitate transformation of larger DNA fragments (34, 36). Using a static D39<sup>Tmp</sup> biofilm formed on fixed human nasopharyngeal cells during a 4-hour incubation at 34°C, we explored EV-mediated biofilm transformation of antibiotic resistance determinants and indeed obtained rFs that were greater than classic in vitro reactions. The size of the determinants appeared to have an influence on the rF difference between the two DNA sources: EVs or purified, genomic DNA. Under biofilm conditions, transfer of the 738-bp ermB via EVs was ~2-fold lower than the equivalent genomic DNA controls while the difference between EV and free DNA was  $\sim$ 1000-fold for the 5.4-kb Mega-2.II element at rFs of  $\sim$ 10<sup>-7</sup> versus ~10<sup>-4</sup>, respectively. Therefore, the interfering effect of EVs on transformation was more evident when transforming larger DNA fragments. Together, these data further support that a biofilm environment indeed facilitates transfer of larger antimicrobial resistance determinants supplied as either EV-associated or free DNA, but that EV-associated DNA remains less optimal compared to free DNA.

While a prerequisite for *in vitro* transformation, the presence or absence of synthetic CSP did not influence the efficiency of EV-mediated transformation under biofilm conditions, consistent

with the report by Marks et al. that used genomic DNA as the transforming material<sup>(32)</sup>. Overall, between CSP+ and CSP- conditions, there was no statistical difference in frequency of EV transformation. Moreover, the single Tn2009-containing recombinant recovered using GA16833 EVs occurred in the biofilm transformation in the absence of exogenous CSP addition. Thus, EV-mediated transformation can also naturally ensue without synthetic CSP addition in biofilms formed in the human nasopharynx.

Whole genome sequencing of four independent recombinants derived from the GA71819 EV biofilm transformation confirmed the insertion of an intact 5.4-kb Mega-2.II element at the expected genomic locus. SNP variant analyses and genome alignments estimated the minimum size of Mega-containing recombined donor fragments to be ~9 to ~15 kb in size. For the single Tn2009 recombinant derived with GA16833 EVs, a donor DNA fragment of ~26 kb containing the entire Tn2009 ICE element was identified. These recombined fragments were much larger than what is typically observed in *S. pneumoniae* transformation via *in vitro* conditions using purified DNA, which is generally ~2-6 kb DNA fragments (44-46). Overall, homologous recombination of large DNA fragments ranging from ~9 kb to ~26 kb was observed with DNA supplied by pneumococcal EVs, confirming that pneumococcal EVs can harbor large (>20 kb) DNA fragments carrying antimicrobial resistance determinants.

In conclusion, extracellular vesicle associated DNA of *S. pneumoniae* transforms but possibly at lower frequencies than free DNA both in *in vitro* planktonic cells and nasopharyngeal biofilms, suggesting modulation by pneumococcal EVs of DNA transformation. The nasopharyngeal biofilm environment was necessary for the EV-mediated transformation of large antimicrobial resistance determinants (>5 kb) and biofilm transformation occurred without the addition of

synthetic CSP. Integration of very large donor DNA fragments (~9 to ~26 kb) supplied by *S. pneumoniae* EVs occurred in biofilms by homologous recombination.

### MATERIALS AND METHODS

**Bacterial strains and antibiotics.** Strains of *S. pneumoniae* used for this study are listed in Table S1. All *S. pneumoniae* strains were grown on blood agar plates or with Todd Hewitt broth with yeast extract (THY broth) and grown at 37°C with 5% CO<sub>2</sub>. The following antibiotics were used for selection where indicated: tetracycline (1 μg/mL), streptomycin (220 μg/mL), erythromycin (0.5 μg/mL), and trimethoprim (14 μg/mL). All antibiotics were bought from Millipore-Sigma (Saint Louis, MO).

**Isolation of extracellular vesicles (EVs).** Primary cultures of 1 L or 2 L of *S. pneumoniae* were grown in THY to late-log phase (OD<sub>600</sub> 0.6-0.8). Broth cultures were spun down in a Beckman Coulter high-speed centrifuge at 17,000 rcf for 30 minutes at 4°C. Supernatants were then passed through 0.45 μm pore filters and concentrated using the Centricon Plus 70 filter with a 100 kDa cut-off per manufacturer's instructions. Concentrated supernatants were ultracentrifuged at 100,000 rcf for 1.5 hours at 4°C to recover EV pellets, which were then resuspended in 200 μL of molecular grade water or 1X DPBS. Pellets were stored at -20°C for future use.

Quantification of EV protein. Protein content was quantified using the Thermo Fisher Scientific Pierce BCA Protein Assay kit (Waltham, MA) per manufacturer's instructions. Briefly, 1, 2, and 5 μL of EV samples were diluted in 24, 23, or 20 μL of 1X DPBS or molecular grade water and mixed with 200 μL of BCA (bicinchoninic acid) working reagent. Tested alongside a bovine serum albumin standard curve, the microplates were incubated at 37°C for 30 minutes in the dark and then read at OD<sub>562</sub>.

Quantification of antibiotic resistance gene DNA concentration. Quantitative PCR was performed for determining the copy number of antibiotic resistance genes that were present in the strain from which EVs were isolated using the Bio-rad iQ SYBR Green Supermix (Hercules, CA). Primers utilized are listed in Table S2. Five-fold dilutions of EV samples were tested alongside a standard curve using genomic DNA from the corresponding *S. pneumoniae* strains, which was composed of the following genome equivalents: 8.58x10<sup>6</sup>, 8.58x10<sup>5</sup>, 8.58x10<sup>4</sup>, 8.58x10<sup>3</sup>, 8.58x10<sup>1</sup>, 4.29x10<sup>1</sup>, 4.29. Utilizing a Bio-Rad CFX96 Touch real-time PCR machine (Hercules, CA), the following cycle conditions were used: 1 cycle at 95°C for 3 minutes as well as 40 cycles at 95°C for 15 seconds, 57 °C or 60°C for 15 seconds, and 72°C for 30 seconds. Considering the size of the *S. pneumoniae* genome (~2.15 Mbp), antibiotic resistance gene copy number, and the mass per single copy of the gene, DNA concentration for each antibiotic resistance gene was determined.

**Transmission electron microscopy** (**TEM**). *S. pneumoniae* EV preparations were submitted to the Emory University Integrated Electron Microscopy Core to be imaged. Briefly, CFlat-400-Cu grids were glow-discharged for 30 seconds on a PELCO EasyGlow prior to applying the samples to the grids. After blotting away excess solution from the grids, 0.75% uranyl formate was added to the grids for imaging via negative staining and then the grids were air-dried for 5 minutes at room temperature. Imaging was conducted on a Thermo Fisher Scientific 120 kV Talos L120C transmission electron microscope. Images were collected using a BM-Ceta camera at a calibrated magnification of 57,000X, yielding a pixel size of 2.52 Å on the object scale.

**DNA extraction.** DNA was extracted from overnight (14- to 16-hour incubation) plate cultures of *S. pneumoniae* strains. Briefly, a lysis buffer containing 100 μL of TE Buffer (10 mM Tris, 1 mM EDTA, pH 8.0), 40 mg/mL of lysozyme, and 75 U/mL of mutanolysin, was added to each of the

samples and incubated for one hour at 37°C. Two hundred microliters of Qiagen Buffer AL and  $20~\mu L$  of Qiagen Proteinase K were added and samples were incubated for another 30 minutes at 56°C. DNA was extracted using the Qiagen QIAamp DNA Mini Kit (Valencia, CA) per manufacturer's instructions. DNA was eluted in  $40~\mu L$  of molecular grade water and frozen in -20°C for future use.

In vitro transformation assay. Competent cells of *S. pneumoniae* strains were generated using standard methods<sup>(47)</sup>. Using an overnight plate culture, primary cultures were inoculated and grown to grown to OD<sub>600</sub> of 0.6-0.7, which were then used to inoculate secondary cultures that were grown to OD<sub>600</sub> of 0.35-0.45 (mid-log phase). Transformation reactions were set up with complete transformation media (CTM)<sup>(47)</sup> containing 100 ng/mL CSP1 (competence stimulating peptide), and 100 ng or 500 ng of transforming genetic material (EVs or DNA) in 300 μL total reaction volumes. CSP1 peptide was synthesized at GenScript (Piscataway, NJ). Where indicated, 10 μg/mL of DNase I was added to the transformation reactions. Reactions were incubated at 37°C with 5% CO<sub>2</sub> for 2-4 hours and recombination frequencies were calculated as number of recombinants divided by total population of *S. pneumoniae* and normalized to μg of transforming DNA.

Cell culture. Detroit 562 human pharyngeal cells (ATCC CCL-138) were cultured using 1X minimum essential medium (1X MEM) augmented with 10% fetal bovine serum, 1% 100X non-essential amino acids, 1% 200 mM L-glutamine, 1% 1 M HEPES buffer, and 1% 10,000 U/mL penicillin-streptomycin. For passaging of cells, 0.25% 1 mM trypsin-EDTA was used to detach the cells. The cells were resuspended in cell culture medium and maintained in a sterile incubator at 37°C with 5% CO<sub>2</sub>. Cell culture media and components were purchased from Life Technologies, Gibco (Gaithersburg, MD).

Nasopharyngeal cell biofilm transformation assay. Confluent monolayers of Detroit 562 pharyngeal cells were grown in each well of a 24-well plate. At the start of each experiment, the cell monolayers were fixed with 4% paraformaldehyde for 10 minutes at room temperature and washed three times with 1X DPBS. The cells were inoculated with an S. pneumoniae recipient strain at a starting OD<sub>600</sub> of 0.1 (10<sup>6</sup> CFU) in 1X MEM supplemented with 5% FBS, 1% nonessential amino acids, 1% L-glutamine, 1% HEPES buffer, and 4.3% NaHCO<sub>3</sub> and then were statically incubated for 4 hours at 34°C to allow biofilm formation. Following biofilm growth, CTM components were added: 20% bovine serum albumin, 1 mM CaCl<sub>2</sub>, 100 ng/mL CSP1 as well as 100 ng of EVs or purified DNA. Where indicated, CSP1 addition was omitted. An additional four hours of static incubation at 34°C allowed for transformation reactions to occur. Following the transformation incubation period, the single-strain biofilms formed on the Detroit 562 cells were sonicated for 20 seconds in a Branson ultrasonic water bath (Danbury, CT). The bacteria were suspended by extensive pipetting and vortexing and serial dilutions in 1X DPBS were performed. Recombinants were selected on dual antibiotic blood agar plates with concentrations noted previously while the total S. pneumoniae population was determined by plating serial dilutions on non-selective blood agar plates. Recombination frequencies were calculated the same as *in vitro* transformation assays.

Whole genome sequencing and variant analysis. Genomic DNA from recombinants was purified utilizing the Qiagen QIAamp DNA Mini Kit. DNA samples were submitted to SeqCenter (Pittsburgh, PA) for whole genome sequencing. Briefly, libraries were prepared with the Illumina DNA Prep kit as well as Integrated DNA Technologies 10 bp UDI indices (unique dual indices) and sequenced with the Illumina NextSeq 2000 platform to produce 2x151 bp reads. The paired end read data was further trimmed using Trim Galore to discard adaptor sequences<sup>(48)</sup>. Assembly

and annotation of the paired end read data was performed on the PATRIC Bacterial and Viral Bioinformatics Resource Center. To determine the sizes of recombined donor fragments, the antimicrobial resistance determinant and its insertion site were first identified in the recombinants and EV donor strain. Flanking sequences to the junctions of the antimicrobial resistance determinant or insertion site were aligned using the DNAStar MegAlign Pro program. A clustering of consecutive donor SNPs flanked by recipient sequence was considered as a recombination block and the outermost 5' and 3' donor SNPs were used to estimate the minimal length of the recombined donor DNA fragment. For single nucleotide polymorphism (SNP) variant analyses, the paired end reads from the D39<sup>Tmp</sup> recipient were first mapped onto the closed genome of the reference S. pneumoniae strain D39 (NC\_008533.2) using the DNAStar NGen program. SNPs present in D39<sup>Tmp</sup> were identified relative to the reference D39 and discounted from the referenceguided assemblies of the EV-mediated biofilm recombinants. The remaining SNPs from the biofilm recombinant assemblies were those introduced by the donor strain. Recombination blocks were identified by calculating the distance from one donor SNP to the next. If the distance between two consecutive SNPs was greater than 1 kb, then it was considered as a separate recombination block.

**Statistical analysis.** Recombination frequencies were analyzed using two-tailed t-tests (with equal or unequal variances) on Microsoft Excel's Data Analysis Toolpak.

**Data Availability.** The research findings of this study are composed of data included within the research article and in the supplemental material.

### **ACKNOWLEDGEMENTS**

We thank the National Institute of Allergy and Infectious Diseases of the National Institutes of Health for supporting this study under award numbers F31 AI154792 and R21 AI144571. We are also grateful for the Georgia Emerging Infections Program for providing *Streptococcus* pneumoniae isolates.

## FIGURES AND TABLES

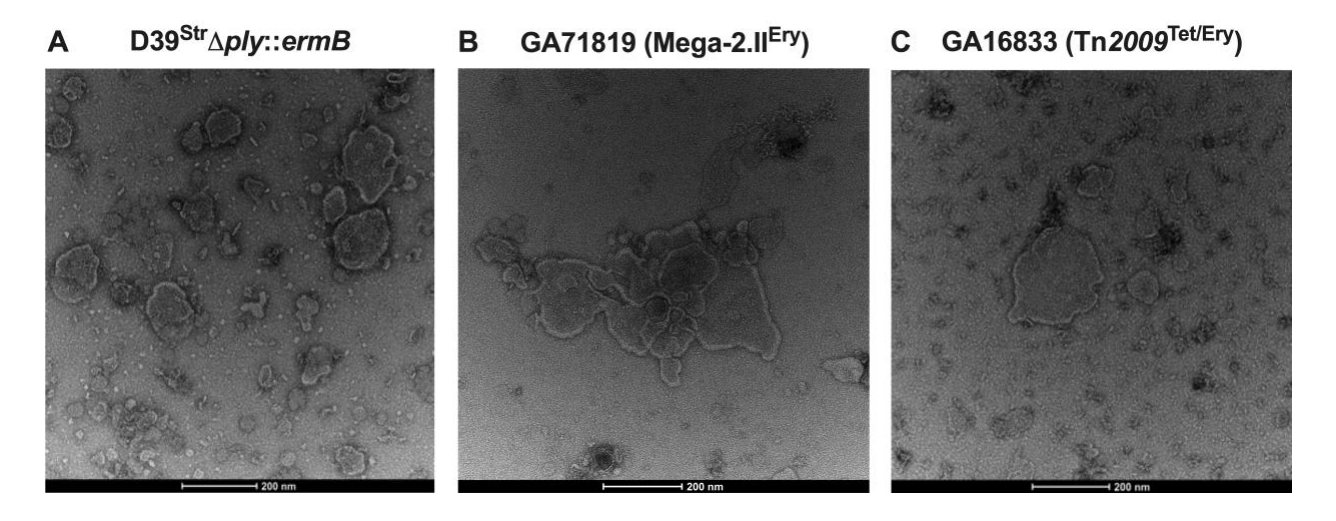


**Figure 1. Transmission electron microscopy (TEM) images of** *S. pneumoniae* **extracellular vesicles.** TEM was performed on EV preparations isolated at late-log phase from *S. pneumoniae* strains: (**A**) D39<sup>Str</sup>Δ*ply*::*ermB*, (**B**) GA71819 (containing Mega-2.II), and (**C**) GA16833 (containing Tn2009).

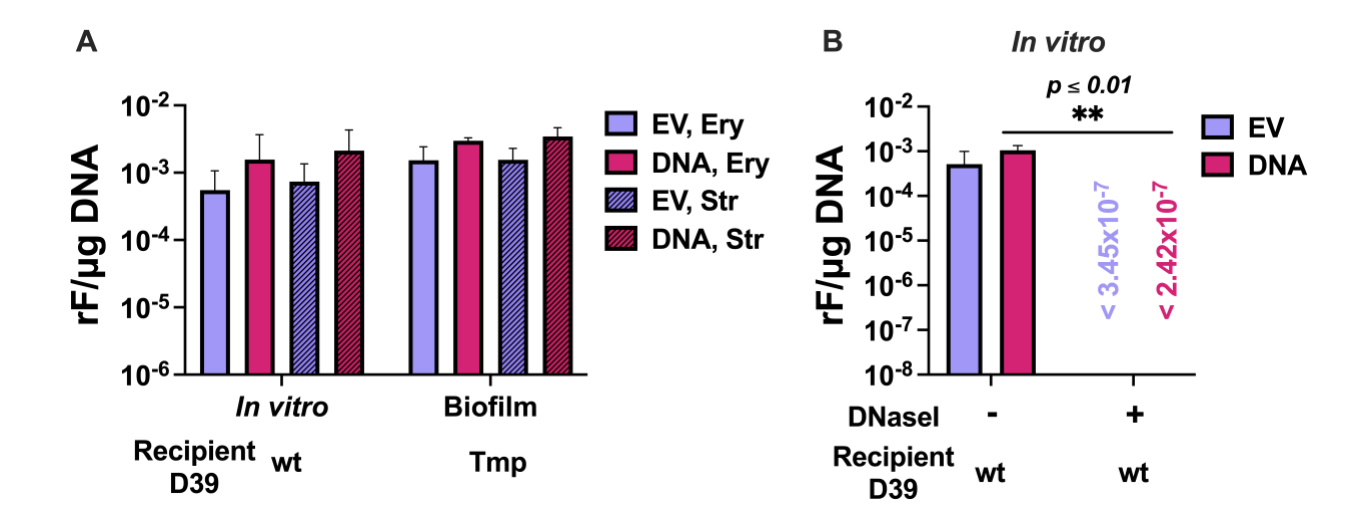


Figure 2. *S. pneumoniae* extracellular vesicles transform externally associated DNA into planktonic cells or pneumococcal biofilms at reduced frequencies compared to genomic DNA transformation. (A) *In vitro* transformations of wildtype planktonic D39 cells (37°C) or nasopharyngeal biofilm transformations of D39<sup>Tmp</sup> (34°C) were performed using 100 ng/mL competence stimulating peptide and equivalent quantities of D39<sup>Str</sup> $\Delta ply::ermB$  extracellular vesicles (light purple) or genomic DNA (magenta). No statistical significance was found between EV (light purple) and DNA (magenta) samples or in *in vitro* versus biofilm conditions as demonstrated by two-tailed t-tests (p-value > 0.05). (B) *In vitro* transformations were carried out as previously described in the presence or absence of 10  $\mu$ g/mL DNase I. Statistical significance for genomic DNA transformations in DNase I – and + conditions was demonstrated with a p-value of 0.003. *In vitro* recombinants were selected on single antibiotics erythromycin [Ery, (solid bars)] or streptomycin [Str, (hatched bars)] while biofilm recombinants were selected on dual antibiotics Ery+Tmp (solid bars) or Str+Tmp (hatched bars) and recombination frequencies (rF) were calculated and normalized to micrograms of DNA used to transform.

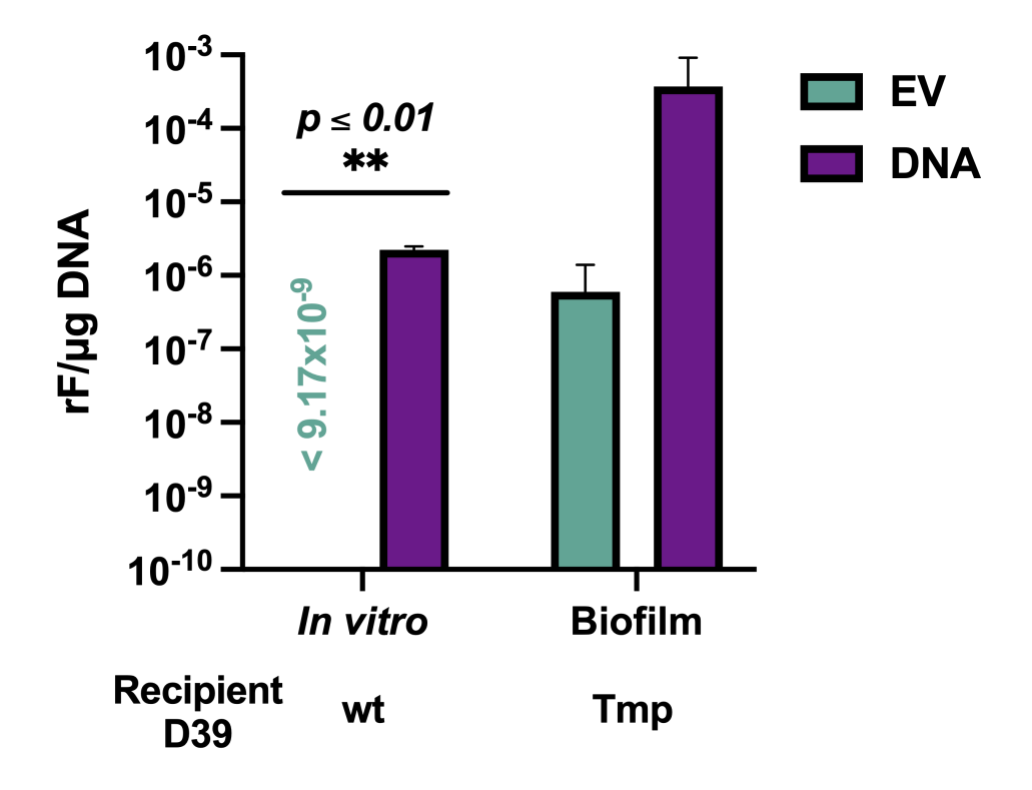
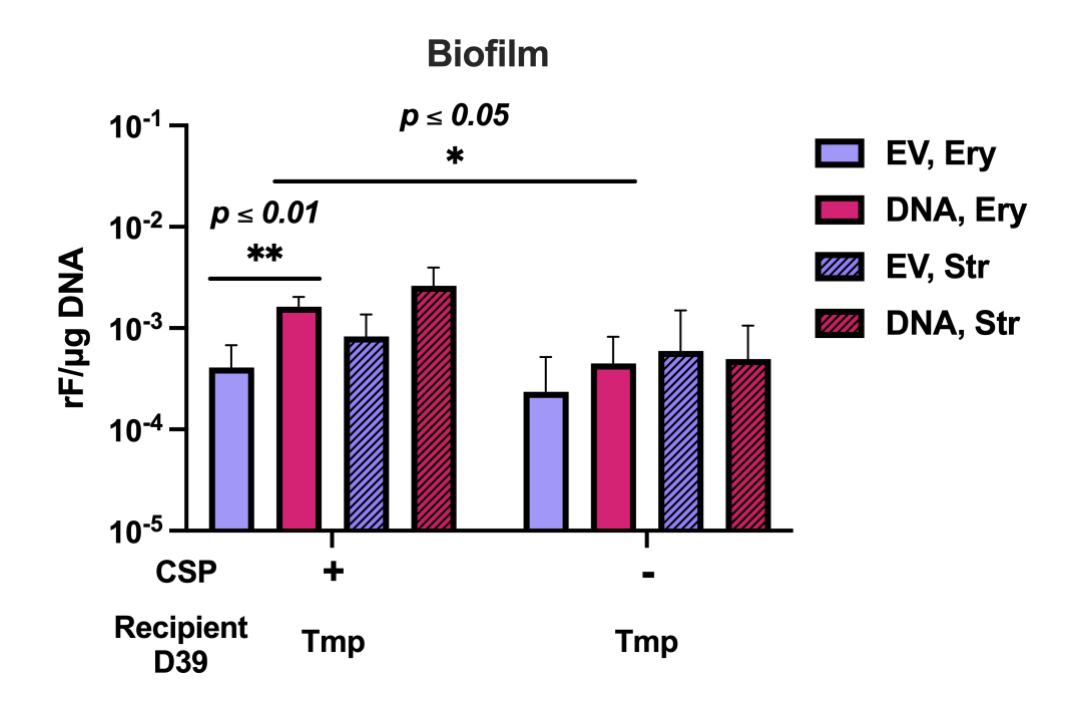


Figure 3. EV-mediated transformation of larger antimicrobial resistance determinant occurs in pneumococcal biofilms as opposed to planktonic cells though at reduced frequencies compared to genomic DNA transformation. *In vitro* transformations of wildtype planktonic D39 cells (37°C) or nasopharyngeal biofilm transformations of D39<sup>Tmp</sup> (34°C) were performed using 100 ng/mL competence stimulating peptide and equivalent quantities of Mega-2.II-containing GA71819 extracellular vesicles (teal) or genomic DNA (dark purple). *In vitro* recombinants were selected on Ery while biofilm recombinants were selected on Ery+Tmp and recombination frequencies (rF) were calculated and normalized to micrograms of DNA used to transform. No statistical significance was found between EV (teal) and DNA (dark purple) samples in the biofilm condition as well as for *in vitro* versus biofilm conditions as demonstrated via two-tailed t-tests (p-value > 0.05). Statistical significance was demonstrated between EV (teal) and DNA (dark purple) samples in *in vitro* transformation conditions with a p-value of 0.007.



**Figure 4. EV-mediated transformation of pneumococcal biofilms occurs in presence or absence of synthetic competence stimulating peptide.** Nasopharyngeal biofilm transformations of D39<sup>Tmp</sup> (34°C) were performed using equivalent quantities of D39<sup>Str</sup>Δ*ply::ermB* extracellular vesicles (light purple) or genomic DNA (magenta) in the presence (CSP +) or absence (CSP -) of cognate competence stimulating peptide. Recombination frequencies were calculated and normalized to micrograms of DNA used to transform for dual-resistant recombinants selected on Ery+Tmp (solid bars) or Str+Tmp (hatched bars). Statistical significance was found between EV (light purple) and DNA (magenta) samples in CSP + conditions for Ery+Tmp recombinants (solid bars) with a calculated p-value of 0.01 (two-tailed t-test). Statistical significance was found between CSP + and CSP – conditions for Ery+Tmp recombinants transformed with genomic DNA (solid magenta bars) with a calculated p-value of 0.02 (two-tailed t-test).

**Table 1.** Quantification of *S. pneumoniae* extracellular vesicle (EV) protein and DNA content.

EVs from S. pneumoniae strain	Resistance gene quantified by qPCR	DNA concentration per μg protein (ng/μg EV protein)
D39 <sup>Str</sup> Δ <i>ply</i> :: <i>ermB</i>	ermB	5.88, 4.60
GA71819 (Mega-2.II)	mefE	0.89
GA16833 (Tn2009)	tetM	2.37, 17.3

**Table 2.** Integration of donor DNA fragments delivered by *S. pneumoniae* extracellular vesicles occurs via homologous recombination.

Donor EVs (MLST)	Recipient (MLST)	Recombinant (MLST)	Size of Integrated Donor DNA Fragment (bp)	
GA71819	D39 Tmp	Ery+Tmp rec 1	11,199	
(ST 338)	(ST 595)	(ST 595)	11,199	
GA71819	D39 Tmp	Ery+Tmp rec 2	13,036	
(ST 338)	(ST 595)	(ST 595)	13,030	
GA71819	D39 Tmp	Ery+Tmp rec 3	15,093	
(ST 338)	(ST 595)	(ST 595)	15,095	
GA71819	D39 Tmp	Ery+Tmp rec 4	9,135	
(ST 338)	(ST 595)	(ST 595)		
GA16833	D39 Tmp	Tet+Tmp	25,698	
(ST 236)	(ST 595)	(ST 595)	23,090	

# SUPPLEMENTAL TABLES

 $\textbf{Table S1.} \ \textbf{Strains used in this study.}$ 

Bacterial Strain	Description, Relevant Genotype and	Reference or	
Dacterial Strain	Phenotype	Source	
WT D39	Avery strain, serotype 2	(49)	
	$D39\Delta ply - ply$ coding sequence deleted and	(50)	
D39Δ <i>ply</i> :: <i>ermB</i> <sup>Str</sup>	replaced with <i>ermB</i> gene (Ery resistant) and also		
	has K56T point mutation in <i>rpsL</i> (Str resistant)		
	Serotype 23A isolate from Georgia Emerging		
GA71819	Infections Program with Mega-2.II, which	(33)	
	harbors <i>mefE/mel</i> (macrolide resistance)		
	Serotype 19F isolate from Georgia Emerging	(41)	
GA16833	Infections Program with Tn2009, which harbors		
	tetM (tetracycline resistance) and mefE/mel on		
	Mega-1.V (macrolide resistance)		
	WT D39 transformed with genomic DNA		
WT D39 <sup>Tmp</sup>	containing I100L point mutation in folA, making	This study	
	it Tmp resistant		

Table S2. Primers used in this study.

Primer Name	Primer Sequence 5' → 3'	Reference or Source			
Quantitative PCR					
ermB_qF1	TTTTGAAAGCCGTGCGTCTG	(34)			
ermB_qR1	CATCTGTGGTATGGCGGGTA	(34)			
qmef_F3	GTATTCCCGAAACGGCTAAACTG	(33)			
qmef_R3	TGGAACGCCTGTGCATATTTC	(33)			
tetM_qF1	AGGAAGCGTGGACAAAGGTA	(34)			
tetM_qR1	GAGTTTGTGCTTGTACGCCA	(34)			

### REFERENCES

- 1. O'Neill J. Antimicrobial Resistance: Tackling a crisis for the health and wealth of nations 2014 [March 8, 2023]. Available from: <a href="https://amrreview.org/sites/default/files/AMR%20Review%20Paper%20-%20Tackling%20a%20crisis%20for%20the%20health%20and%20wealth%20of%20nations\_1.p">https://amrreview.org/sites/default/files/AMR%20Review%20Paper%20-%20Tackling%20a%20crisis%20for%20the%20health%20and%20wealth%20of%20nations\_1.p</a>
- 2. Antimicrobial Resistance C. Global burden of bacterial antimicrobial resistance in 2019: a systematic analysis. Lancet. 2022;399(10325):629-55. Epub 2022/01/24. doi: 10.1016/S0140-6736(21)02724-0. PubMed PMID: 35065702; PMCID: PMC8841637.
- 3. Shak JR, Vidal JE, Klugman KP. Influence of bacterial interactions on pneumococcal colonization of the nasopharynx. Trends Microbiol. 2013;21(3):129-35. Epub 2013/01/01. doi: 10.1016/j.tim.2012.11.005. PubMed PMID: 23273566; PMCID: PMC3729046.
- 4. Weiser JN, Ferreira DM, Paton JC. Streptococcus pneumoniae: transmission, colonization and invasion. Nat Rev Microbiol. 2018;16(6):355-67. Epub 2018/03/31. doi: 10.1038/s41579-018-0001-8. PubMed PMID: 29599457; PMCID: PMC5949087.
- 5. Backhaus E, Berg S, Andersson R, Ockborn G, Malmstrom P, Dahl M, Nasic S, Trollfors B. Epidemiology of invasive pneumococcal infections: manifestations, incidence and case fatality rate correlated to age, gender and risk factors. BMC Infect Dis. 2016;16:367. Epub 2016/08/05. doi: 10.1186/s12879-016-1648-2. PubMed PMID: 27487784; PMCID: PMC4972955.
- 6. Fletcher MA, Laufer DS, McIntosh ED, Cimino C, Malinoski FJ. Controlling invasive pneumococcal disease: is vaccination of at-risk groups sufficient? Int J Clin Pract. 2006;60(4):450-6. Epub 2006/04/20. doi: 10.1111/j.1368-5031.2006.00858.x. PubMed PMID: 16620359; PMCID: PMC1448695.

- 7. Singer M, Nambiar S, Valappil T, Higgins K, Gitterman S. Historical and regulatory perspectives on the treatment effect of antibacterial drugs for community-acquired pneumonia. Clin Infect Dis. 2008;47 Suppl 3:S216-24. Epub 2008/11/18. doi: 10.1086/591407. PubMed PMID: 18986293.
- 8. Hansman D, Glasgow H, Sturt J, Devitt L, Douglas R. Increased resistance to penicillin of pneumococci isolated from man. N Engl J Med. 1971;284(4):175-7. Epub 1971/01/28. doi: 10.1056/NEJM197101282840403. PubMed PMID: 4395334.
- 9. Appelbaum PC. Antimicrobial resistance in Streptococcus pneumoniae: an overview. Clin Infect Dis. 1992;15(1):77-83. Epub 1992/07/01. doi: 10.1093/clinids/15.1.77. PubMed PMID: 1617076.
- 10. Schroeder MR, Stephens DS. Macrolide Resistance in Streptococcus pneumoniae. Front Cell Infect Microbiol. 2016;6:98. Epub 2016/10/07. doi: 10.3389/fcimb.2016.00098. PubMed PMID: 27709102; PMCID: PMC5030221.
- 11. von Specht M, Garcia Gabarrot G, Mollerach M, Bonofiglio L, Gagetti P, Kaufman S, Vigliarolo L, Toresani I, Lopardo HA. Resistance to beta-lactams in Streptococcus pneumoniae. Rev Argent Microbiol. 2021;53(3):266-71. Epub 2021/04/21. doi: 10.1016/j.ram.2021.02.007. PubMed PMID: 33875295.
- 12. Bergman M, Huikko S, Huovinen P, Paakkari P, Seppala H, Finnish Study Group for Antimicrobial R. Macrolide and azithromycin use are linked to increased macrolide resistance in Streptococcus pneumoniae. Antimicrob Agents Chemother. 2006;50(11):3646-50. Epub 2006/08/31. doi: 10.1128/AAC.00234-06. PubMed PMID: 16940064; PMCID: PMC1635217.
- 13. Corso A, Severina EP, Petruk VF, Mauriz YR, Tomasz A. Molecular characterization of penicillin-resistant Streptococcus pneumoniae isolates causing respiratory disease in the United

- States. Microb Drug Resist. 1998;4(4):325-37. Epub 1999/02/13. doi: 10.1089/mdr.1998.4.325. PubMed PMID: 9988052.
- 14. Gay K, Baughman W, Miller Y, Jackson D, Whitney CG, Schuchat A, Farley MM, Tenover F, Stephens DS. The emergence of Streptococcus pneumoniae resistant to macrolide antimicrobial agents: a 6-year population-based assessment. J Infect Dis. 2000;182(5):1417-24. Epub 2000/10/07. doi: 10.1086/315853. PubMed PMID: 11023465.
- 15. Malhotra-Kumar S, Lammens C, Coenen S, Van Herck K, Goossens H. Effect of azithromycin and clarithromycin therapy on pharyngeal carriage of macrolide-resistant streptococci in healthy volunteers: a randomised, double-blind, placebo-controlled study. Lancet. 2007;369(9560):482-90. Epub 2007/02/13. doi: 10.1016/S0140-6736(07)60235-9. PubMed PMID: 17292768.
- 16. Nishijima T, Saito Y, Aoki A, Toriya M, Toyonaga Y, Fujii R. Distribution of mefE and ermB genes in macrolide-resistant strains of Streptococcus pneumoniae and their variable susceptibility to various antibiotics. J Antimicrob Chemother. 1999;43(5):637-43. Epub 1999/06/26. doi: 10.1093/jac/43.5.637. PubMed PMID: 10382884.
- 17. Nadimpalli M, Delarocque-Astagneau E, Love DC, Price LB, Huynh BT, Collard JM, Lay KS, Borand L, Ndir A, Walsh TR, Guillemot D, Bacterial I, antibiotic-Resistant Diseases among Young children in low-income countries Study G. Combating Global Antibiotic Resistance: Emerging One Health Concerns in Lower- and Middle-Income Countries. Clin Infect Dis. 2018;66(6):963-9. Epub 2018/01/19. doi: 10.1093/cid/cix879. PubMed PMID: 29346620.
- 18. Dell'Annunziata F, Folliero V, Giugliano R, De Filippis A, Santarcangelo C, Izzo V, Daglia M, Galdiero M, Arciola CR, Franci G. Gene Transfer Potential of Outer Membrane Vesicles of

- Gram-Negative Bacteria. Int J Mol Sci. 2021;22(11). Epub 2021/07/03. doi: 10.3390/ijms22115985. PubMed PMID: 34205995; PMCID: PMC8198371.
- 19. Domingues S, Nielsen KM. Membrane vesicles and horizontal gene transfer in prokaryotes. Curr Opin Microbiol. 2017;38:16-21. Epub 2017/04/26. doi: 10.1016/j.mib.2017.03.012. PubMed PMID: 28441577.
- 20. Lee EY, Choi DY, Kim DK, Kim JW, Park JO, Kim S, Kim SH, Desiderio DM, Kim YK, Kim KP, Gho YS. Gram-positive bacteria produce membrane vesicles: proteomics-based characterization of Staphylococcus aureus-derived membrane vesicles. Proteomics. 2009;9(24):5425-36. Epub 2009/10/17. doi: 10.1002/pmic.200900338. PubMed PMID: 19834908.
- 21. Rivera J, Cordero RJ, Nakouzi AS, Frases S, Nicola A, Casadevall A. Bacillus anthracis produces membrane-derived vesicles containing biologically active toxins. Proc Natl Acad Sci U S A. 2010;107(44):19002-7. Epub 2010/10/20. doi: 10.1073/pnas.1008843107. PubMed PMID: 20956325; PMCID: PMC2973860.
- 22. Brown L, Kessler A, Cabezas-Sanchez P, Luque-Garcia JL, Casadevall A. Extracellular vesicles produced by the Gram-positive bacterium Bacillus subtilis are disrupted by the lipopeptide surfactin. Mol Microbiol. 2014;93(1):183-98. Epub 2014/05/16. doi: 10.1111/mmi.12650. PubMed PMID: 24826903; PMCID: PMC4079059.
- 23. Lee JH, Choi CW, Lee T, Kim SI, Lee JC, Shin JH. Transcription factor sigmaB plays an important role in the production of extracellular membrane-derived vesicles in Listeria monocytogenes. PLoS One. 2013;8(8):e73196. Epub 2013/08/27. doi: 10.1371/journal.pone.0073196. PubMed PMID: 23977379; PMCID: PMC3748028.

- 24. Liao S, Klein MI, Heim KP, Fan Y, Bitoun JP, Ahn SJ, Burne RA, Koo H, Brady LJ, Wen ZT. Streptococcus mutans extracellular DNA is upregulated during growth in biofilms, actively released via membrane vesicles, and influenced by components of the protein secretion machinery. J Bacteriol. 2014;196(13):2355-66. Epub 2014/04/22. doi: 10.1128/JB.01493-14. PubMed PMID: 24748612; PMCID: PMC4054167.
- 25. Olaya-Abril A, Prados-Rosales R, McConnell MJ, Martin-Pena R, Gonzalez-Reyes JA, Jimenez-Munguia I, Gomez-Gascon L, Fernandez J, Luque-Garcia JL, Garcia-Lidon C, Estevez H, Pachon J, Obando I, Casadevall A, Pirofski LA, Rodriguez-Ortega MJ. Characterization of protective extracellular membrane-derived vesicles produced by Streptococcus pneumoniae. J Proteomics. 2014;106:46-60. Epub 2014/04/29. doi: 10.1016/j.jprot.2014.04.023. PubMed PMID: 24769240.
- 26. Brown L, Wolf JM, Prados-Rosales R, Casadevall A. Through the wall: extracellular vesicles in Gram-positive bacteria, mycobacteria and fungi. Nat Rev Microbiol. 2015;13(10):620-30. Epub 2015/09/02. doi: 10.1038/nrmicro3480. PubMed PMID: 26324094; PMCID: PMC4860279.
- 27. Briaud P, Carroll RK. Extracellular Vesicle Biogenesis and Functions in Gram-Positive Bacteria. Infect Immun. 2020;88(12). Epub 2020/09/30. doi: 10.1128/IAI.00433-20. PubMed PMID: 32989035; PMCID: PMC7671900.
- 28. Choi CW, Park EC, Yun SH, Lee SY, Kim SI, Kim GH. Potential Usefulness of Streptococcus pneumoniae Extracellular Membrane Vesicles as Antibacterial Vaccines. J Immunol Res. 2017;2017:7931982. Epub 2017/02/18. doi: 10.1155/2017/7931982. PubMed PMID: 28210633; PMCID: PMC5292160.

- 29. Klieve AV, Yokoyama MT, Forster RJ, Ouwerkerk D, Bain PA, Mawhinney EL. Naturally occurring DNA transfer system associated with membrane vesicles in cellulolytic Ruminococcus spp. of ruminal origin. Appl Environ Microbiol. 2005;71(8):4248-53. Epub 2005/08/09. doi: 10.1128/AEM.71.8.4248-4253.2005. PubMed PMID: 16085810; PMCID: PMC1183309.
- 30. Bitto NJ, Chapman R, Pidot S, Costin A, Lo C, Choi J, D'Cruze T, Reynolds EC, Dashper SG, Turnbull L, Whitchurch CB, Stinear TP, Stacey KJ, Ferrero RL. Bacterial membrane vesicles transport their DNA cargo into host cells. Sci Rep. 2017;7(1):7072. Epub 2017/08/03. doi: 10.1038/s41598-017-07288-4. PubMed PMID: 28765539; PMCID: PMC5539193.
- 31. Salles C, Creancier L, Claverys JP, Mejean V. The high level streptomycin resistance gene from Streptococcus pneumoniae is a homologue of the ribosomal protein S12 gene from Escherichia coli. Nucleic Acids Res. 1992;20(22):6103. Epub 1992/11/25. doi: 10.1093/nar/20.22.6103. PubMed PMID: 1461744; PMCID: PMC334482.
- 32. Marks LR, Reddinger RM, Hakansson AP. High levels of genetic recombination during nasopharyngeal carriage and biofilm formation in Streptococcus pneumoniae. mBio. 2012;3(5). Epub 2012/09/28. doi: 10.1128/mBio.00200-12. PubMed PMID: 23015736; PMCID: PMC3448161.
- 33. Schroeder MR, Lohsen S, Chancey ST, Stephens DS. High-Level Macrolide Resistance Due to the Mega Element [mef(E)/mel] in Streptococcus pneumoniae. Front Microbiol. 2019;10:868. Epub 2019/05/21. doi: 10.3389/fmicb.2019.00868. PubMed PMID: 31105666; PMCID: PMC6491947.
- 34. Antezana BS, Lohsen S, Wu X, Vidal JE, Tzeng YL, Stephens DS. Dissemination of Tn916-Related Integrative and Conjugative Elements in Streptococcus pneumoniae Occurs by

- Transformation and Homologous Recombination in Nasopharyngeal Biofilms. Microbiol Spectr. 2023:e0375922. Epub 2023/03/14. doi: 10.1128/spectrum.03759-22. PubMed PMID: 36912669.
- 35. Jolley KA, Bray JE, Maiden MCJ. Open-access bacterial population genomics: BIGSdb software, the PubMLST.org website and their applications. Wellcome Open Res. 2018;3:124. Epub 2018/10/23. doi: 10.12688/wellcomeopenres.14826.1. PubMed PMID: 30345391; PMCID: PMC6192448.
- 36. Cowley LA, Petersen FC, Junges R, Jimson DJM, Morrison DA, Hanage WP. Evolution via recombination: Cell-to-cell contact facilitates larger recombination events in Streptococcus pneumoniae. PLoS Genet. 2018;14(6):e1007410. Epub 2018/06/14. doi: 10.1371/journal.pgen.1007410. PubMed PMID: 29897968; PMCID: PMC6016952.
- 37. Burmeister AR. Horizontal Gene Transfer. Evol Med Public Health. 2015;2015(1):193-4. Epub 2015/08/01. doi: 10.1093/emph/eov018. PubMed PMID: 26224621; PMCID: PMC4536854.
- 38. Thomas CM, Nielsen KM. Mechanisms of, and barriers to, horizontal gene transfer between bacteria. Nat Rev Microbiol. 2005;3(9):711-21. Epub 2005/09/03. doi: 10.1038/nrmicro1234. PubMed PMID: 16138099.
- 39. Domenech M, Garcia, E. Autolysin-Independent DNA Release in Streptococcus pneumoniae Invitro Biofilms. Clinical Infectious Diseases: Open Access. 2018;2(3):114.
- 40. Schooling SR, Hubley A, Beveridge TJ. Interactions of DNA with biofilm-derived membrane vesicles. J Bacteriol. 2009;191(13):4097-102. Epub 2009/05/12. doi: 10.1128/JB.00717-08. PubMed PMID: 19429627; PMCID: PMC2698485.
- 41. Chancey ST, Agrawal S, Schroeder MR, Farley MM, Tettelin H, Stephens DS. Composite mobile genetic elements disseminating macrolide resistance in Streptococcus pneumoniae. Front

- Microbiol. 2015;6:26. Epub 2015/02/25. doi: 10.3389/fmicb.2015.00026. PubMed PMID: 25709602; PMCID: PMC4321634.
- 42. Steinmoen H, Knutsen E, Havarstein LS. Induction of natural competence in Streptococcus pneumoniae triggers lysis and DNA release from a subfraction of the cell population. Proc Natl Acad Sci U S A. 2002;99(11):7681-6. Epub 2002/05/29. doi: 10.1073/pnas.112464599. PubMed PMID: 12032343; PMCID: PMC124321.
- 43. Marks LR, Parameswaran GI, Hakansson AP. Pneumococcal interactions with epithelial cells are crucial for optimal biofilm formation and colonization in vitro and in vivo. Infect Immun. 2012;80(8):2744-60. Epub 2012/05/31. doi: 10.1128/IAI.00488-12. PubMed PMID: 22645283; PMCID: PMC3434590.
- 44. Croucher NJ, Harris SR, Barquist L, Parkhill J, Bentley SD. A high-resolution view of genome-wide pneumococcal transformation. PLoS Pathog. 2012;8(6):e1002745. Epub 2012/06/22. doi: 10.1371/journal.ppat.1002745. PubMed PMID: 22719250; PMCID: PMC3375284.
- 45. Gurney T, Jr., Fox MS. Physical and genetic hybrids formed in bacterial transformation. J Mol Biol. 1968;32(1):83-100. Epub 1968/02/28. doi: 10.1016/0022-2836(68)90147-2. PubMed PMID: 4384454.
- 46. Lacks S. Integration efficiency and genetic recombination in pneumococcal transformation. Genetics. 1966;53(1):207-35. Epub 1966/01/01. doi: 10.1093/genetics/53.1.207. PubMed PMID: 4379022; PMCID: PMC1211003.
- 47. Havarstein LS, Coomaraswamy G, Morrison DA. An unmodified heptadecapeptide pheromone induces competence for genetic transformation in Streptococcus pneumoniae. Proc

Natl Acad Sci U S A. 1995;92(24):11140-4. Epub 1995/11/21. doi: 10.1073/pnas.92.24.11140. PubMed PMID: 7479953; PMCID: PMC40587.

- 48. Krueger F. Trim Galore. [April 2, 2023]. Available from: https://www.bioinformatics.babraham.ac.uk/projects/trim\_galore/.
- 49. Avery OT, Macleod CM, McCarty M. Studies on the Chemical Nature of the Substance Inducing Transformation of Pneumococcal Types: Induction of Transformation by a Desoxyribonucleic Acid Fraction Isolated from Pneumococcus Type Iii. J Exp Med. 1944;79(2):137-58. Epub 1944/02/01. doi: 10.1084/jem.79.2.137. PubMed PMID: 19871359; PMCID: PMC2135445.
- 50. Shak JR, Ludewick HP, Howery KE, Sakai F, Yi H, Harvey RM, Paton JC, Klugman KP, Vidal JE. Novel role for the Streptococcus pneumoniae toxin pneumolysin in the assembly of biofilms. mBio. 2013;4(5):e00655-13. Epub 2013/09/12. doi: 10.1128/mBio.00655-13. PubMed PMID: 24023386; PMCID: PMC3774193.

## **Chapter 5: Conclusions and future directions**

# I. Antibiotic resistance in S. pneumoniae

Streptococcus pneumoniae (or pneumococcus) colonizes the human nasopharynx generally as a commensal where exchange of genetic determinants can occur<sup>(1, 2)</sup>. However, *S. pneumoniae* can become an opportunistic pathogen and spread to other local sites, causing non-invasive infections, such as acute otitis media and non-bacteremic pneumonia<sup>(3, 4)</sup>, or invade the bloodstream and access other sterile sites leading to life-threatening diseases, such as bacteremia or meningitis<sup>(4)</sup>. In 2015, there were approximately 9.2 million cases of pneumococcal disease<sup>(5)</sup> while, in 2019, there were 600,000 deaths due to pneumococcal infections of which 150,000 were directly attributed to antimicrobial resistance<sup>(6)</sup>. The primary antibiotic treatment for *S. pneumoniae* upper respiratory infections include macrolides<sup>(7)</sup> and with the increased prescription and use of these drugs, macrolide-resistant pneumococci emerged worldwide during the 1990s <sup>(8-10)</sup>. Increased antibiotic resistance in *S. pneumoniae* continues to be a global public health concern due to the lack of alternative treatment options for pneumococcal infections.

# II. Efficient horizontal exchange of S. pneumoniae Tn916-related ICEs

In *S. pneumoniae*, Tn916-related integrative and conjugative elements (ICEs), which confer both tetracycline and macrolide resistance, contribute to the widespread presence of macrolide resistance<sup>(11)</sup>. As the term "integrative and conjugative element" implies, these are mobile genetic elements integrated in a donor chromosome that normally transfer to a recipient via conjugation<sup>(12)</sup>. The prototype of this family of ICEs is Tn916, which has been extensively shown to move by a conjugation apparatus that is upregulated by tetracycline<sup>(13, 14)</sup>. In *S. pneumoniae*, Tn916-related ICEs include: Tn2009 with the macrolide efflux genetic assembly (Mega) element inserted in *orf*6

of Tn916<sup>(15)</sup>, Tn6002 with the *ermB* gene integrated in orf20 of Tn916<sup>(16)</sup>, and Tn2010 with both orf6::Mega and orf20::ermB in Tn916<sup>(17)</sup>.

As shown in Chapter 2, the conjugative genes found on pneumococcal Tn2009, Tn6002, and Tn2010 contain >99% sequence identity to those of prototype Tn916. However, we demonstrated that conjugation was not the major mechanism responsible for transfer of these Tn916-related ICEs in *S. pneumoniae*. Under planktonic and nasopharyngeal biofilm conditions, we found limited ICE conjugative gene expression, absence of prerequisite circular intermediates, and no effect on ICE transfer frequency with deletion of a critical conjugative gene in the donor strain. However, another major mechanism of horizontal dissemination of genetic determinants is transformation via uptake of extracellular DNA. We provided evidence that highly efficient ICE transfer in dual-strain pneumococcal nasopharyngeal biofilms occurred via transformation and confirmed that these ICE elements integrated through homologous recombination of large donor DNA fragments.

Genomic analyses had demonstrated the widespread presence of Tn916-related ICEs in *S. pneumoniae*. Wyres et al. analyzed 38 *S. pneumoniae* genomes for the presence of *tetM*, *ermB*, *mefE*, and *int* and found that two strains from 1967 and 1968 contain Tn916-related ICE elements<sup>(18)</sup>. Another genomic analysis of 240 pneumococcal isolates of the PMEN1 lineage collected between 1984-2008 showed the presence of several Tn916-related ICEs harboring the *ermB*-containing Omega element, *ermB*-containing Tn917 element, and Mega element, all integrated in Tn916<sup>(19)</sup>. Seventy-five recent serotype 12F *S. pneumoniae* isolates in Japan were also analyzed using the reference Tn916 sequence from *Enterococcus faecalis*<sup>(20)</sup>. These studies solely analyzed pneumococcal genomes for the presence of Tn916-related ICEs but did not examine how these ICEs were disseminating. Our studies provided insight on the molecular

mechanism for the efficient horizontal transfer of Tn916-related ICEs among *S. pneumoniae* in *in vitro* nasopharyngeal biofilms<sup>(21)</sup>.

We utilized a continuous flow bioreactor system where a donor-recipient, dual-strain pneumococcal biofilm formed on a confluent monolayer of nasopharyngeal Detroit 562 cells<sup>(22)</sup> and compared it to classic *in vitro* transformation reactions that comprised of planktonic recipient *S. pneumoniae*, synthetic competence stimulating peptide (CSP), and exogenous DNA<sup>(23)</sup>. While the bioreactor system is an environment that better mimics pneumococcal colonization of the human nasopharynx compared to the classic transformation reaction, this experimental setup is still considered to be *in vitro*. Future research would optimize the experimental conditions in even more relevant settings.

Instead of immortalized cell lines, primary human cells isolated directly from human tissue could be utilized in the bioreactor, which would preserve many of the properties seen *in vivo*. Marks et al. imaged multi-layer pneumococcal biofilms formed on live primary human tracheobronchial epithelial cells over a 24-hour period where an extracellular matrix and bacterial interconnections were also observed<sup>(24)</sup>. Compared to mucoepidermoid bronchial carcinoma cells, the primary tracheobronchial epithelial cells that maintain a host immune response, served as a better model to image mature biofilms as the carcinoma cells were quickly killed with pneumococcal inoculation<sup>(24)</sup>. While tracheobronchial epithelial cells form a part of the lower respiratory tract, primary human nasal epithelial cells found in the upper respiratory tract are also commercially available and could be utilized for future biofilm studies. Although Chun et al. did not explicitly state that they investigated *S. pneumoniae* biofilms, they studied the binding affinity of pneumococcal capsular polysaccharides to primary human nasal epithelial cells<sup>(25)</sup>. They found that pneumococcal colonization was tolerated by these human nasal primary cells for up to 24

hours and even up to 168 hours with daily medium changes as well as that *S. pneumoniae* remained viable for at least 48 hours after inoculation of these primary cells<sup>(25)</sup>. Thus, *ex vivo* primary respiratory epithelial cells are a future option to determine frequencies for exchange of antibiotic resistance determinants in dual-strain pneumococcal biofilms.

Animal colonization models could simulate infection and biofilm formation in the presence of an intact mammalian immune system. For instance, Marks et al. utilized six-week-old BALB/cByJ mice for co-colonization and sequential co-colonization of the nasopharynges with two S. pneumoniae strains harboring penicillin-binding protein-mediated penicillin resistance and ermBconferring erythromycin resistance and found that exchange of resistance markers occurred at frequencies of ~10<sup>-2</sup> (26). Although this murine nasopharyngeal colonization model showed robust exchange of antibiotic resistance determinants between pneumococcal strains, S. pneumoniae is strictly a human colonizer and thus, the applicability of the observations in mice to humans remains a concern. Other concerns to using murine animal models include the forced inoculation of lab mice via syringe compared to natural inhalation of S. pneumoniae for human colonization<sup>(27)</sup>, the increased bacterial density required to establish colonization in mice versus humans<sup>(27, 28)</sup>, potentially distinct immune responses to pneumococcal colonization in mice compared to humans<sup>(27)</sup>, and the artificial environments of laboratory mice versus day-to-day environments that humans engage in with microbe contact. Nonetheless, in vivo animal models could provide additional insights to validate the *in vitro* bioreactor observations.

The bioreactor biofilm model demonstrated nearly an ~1,000-fold improvement in the transfer of >20 kb Tn916-related ICEs from donor to recipient *S. pneumoniae* with frequencies (rF) of ~10<sup>-4</sup> relative to the *in vitro* transformation conditions (rF <10<sup>-7</sup>). The molecular mechanism for this enhanced frequency of large DNA fragment transfer in the nasopharyngeal bioreactor biofilm

remains undefined and warrants future investigation. Biofilms are enclosed bacterial communities that are shielded by an extracellular matrix<sup>(29)</sup>, allowing for close contact between donors and naïve recipients as well as for the accumulation of DNA in local concentrations for enhanced uptake. To probe the importance for an enclosed bacterial community for enhanced transfer of large DNA fragments, imaging experiments of the dual-strain bioreactor biofilms with the donor and recipient tagged with specific fluorescent proteins and a fluorescently labeled ICE element could be utilized to better understand spatial and temporal patterns for localization, movement, and uptake of DNA fragments.

## III. US distribution of S. pneumoniae Tn916-related ICEs pre- and post-PCV introductions

The efficient dissemination (rFs of ~10<sup>-4</sup>) of Tn916-related ICEs between *S. pneumoniae* strains in nasopharyngeal biofilms prompted us to investigate the evolution of ICEs conferring macrolide resistance among the US *S. pneumoniae* population. With the upsurge of beta-lactam resistance in the late 1980s, primary treatment transitioned to macrolide antibiotics for upper respiratory infections and community-acquired pneumonia<sup>(7)</sup>. The rise in prescription and use of macrolides, such as the semi-synthetic azithromycin and clarithromycin, led to the emergence of macrolide-resistant *S. pneumoniae* in the 1990s<sup>(8, 9, 30, 31)</sup>. Introductions of the pneumococcal conjugate vaccines PCV7 and PCV13 in 2000 and 2010, respectively, in the US were effective in reducing serotype-specific carriage and invasive pneumococcal disease but were also associated with increases in non-vaccine serotypes <sup>(32-34)</sup>.

In Chapter 3, we investigated the contribution of Tn916-related ICEs to the increase in macrolide resistance observed in the US as well as the influence of PCV introductions on the spread of these ICE elements in the US pneumococcal population. A collection of 4,560 US isolates from 1916 to 2021 in the PubMLST *Streptococcus pneumoniae* database<sup>(35)</sup> was

categorized into distinct time periods: historic (1916-1994), pre-PCV7 (1995-2000), PCV7 (2001-2010) and PCV13 (2011-2021). Out of the total 4,560 US isolates, 751 contained one of three ICEs, Tn2009, Tn6002, or Tn2010. We observed an increase in frequency of Tn916-related ICEs in US isolates over time from 1.52% to 21.9%. The major mechanism for macrolide resistance in North America during the 1990s and early 2000s was efflux mediated by the mefE/mel genes encoded on Mega<sup>(9, 36, 37)</sup>. While this was confirmed in our analysis for macrolide resistance conferred by Tn916-related ICEs, we also found that the predominant mechanism for Tn916related ICE macrolide resistance switched to ermB-conferring ribosomal methylation by the late 2000s and 2010s. In addition, the study found that while PCV introductions markedly decreased Tn916-related ICE-containing vaccine serotype isolates, an increase in ICE frequency associated with non-vaccine serotypes was detected. Non-vaccine serotypes 15A and 23A with Tn916-related ICEs were increasingly found by the 2010s (PCV13 era) but they are not included in the current PCV15 nor PCV20 vaccines licensed in the US for use in children in 2022 and 2023, respectively, as well as in adults in 2021. Our studies contribute to the understanding of macrolide resistance conferred by Tn916-related ICEs in the US and can potentially be considered in future PCV formulations.

The use of the PubMLST *Streptococcus pneumoniae* database for analyzing epidemiological changes has limitations due to the potential bias associated with deposits of isolates that are not of population-based surveillance. As described in Chapter 3, some years had more isolates deposited than others and these data came from several large studies conducted by Azarian et al.<sup>(38)</sup>, Gladstone et al.<sup>(39)</sup>, van Tonder et al.<sup>(40)</sup>, Bogaardt et al.<sup>(41)</sup>, Croucher et al.<sup>(42)</sup>, and Andam et al.<sup>(43)</sup>. Therefore, while our results that examine over 4,500 isolates correlate with other studies, our analysis relied heavily on isolates added to the PubMLST database by investigators. This limitation

can be addressed by genome analysis and surveillance data from the CDC's Active Bacterial Core surveillance (ABCs) database<sup>(44)</sup>. The CDC's ABCs oversees the collection of invasive *S. pneumoniae* from California, Colorado, Connecticut, Georgia, Maryland, Minnesota, New Mexico, New York, Oregon, and Tennessee. This population-based database will allow for more accurate estimates of incidence rates for invasive pneumococcal disease caused by Tn916-related ICE-containing isolates. Additional metagenomic details in this database, such as sites of isolation and description of isolates as carriage or disease, as well as comprehensive carriage studies can provide further insights into Tn916-related ICE circulation in the pneumococcal population.

How applicable are our findings to other global regions? Erythromycin resistance is geographically variable ranging from <10% to >50% of isolates<sup>(45)</sup>. We performed preliminary analyses of Tn916-related ICE frequency in Thailand and South Africa using the PubMLST database and categorized isolates into pre-PCV7 and post-PCV7/13 eras. The frequency for Tn916-related ICEs remained relatively constant at ~27% in Thailand during both eras and decreased from 18.7% to 12.1% in South Africa. A detailed analysis of serotypes must be conducted with the Thailand and South Africa data to understand the trends compared to the US. Moreover, analogous analyses can be conducted using data from the UK Health Security Agency (UKHSA)<sup>(46)</sup>, which conducts surveillance of invasive pneumococcal disease in the United Kingdom and has all isolates characterized.

# IV. S. pneumoniae extracellular vesicle-associated DNA transformation

The upwards trend of antimicrobial resistance has been predicted to result in 10 million deaths per year and \$100 trillion economic burden by 2050<sup>(47)</sup>. Despite the success of two PCV introductions in reducing carriage and invasive disease caused by vaccine serotypes<sup>(32, 34)</sup>, *S. pneumoniae* continues to cause severe infections where ~600,000 deaths were associated with

antimicrobial resistance and of those, 150,000 deaths were directly attributed to this resistance<sup>(6)</sup>. Although the primary method by which *S. pneumoniae* horizontally exchanges antimicrobial resistance determinants is transformation of extracellular DNA obtained through a type IV pilus <sup>(48-50)</sup>, extracellular membrane vesicles secreted by pneumococci during late-log phase that range from 20-80 nm in diameter and carry genomic content<sup>(51, 52)</sup> may also play a role in DNA delivery and transformation<sup>(53, 54)</sup>. Such an example of EV-mediated transformation was shown in Grampositive ruminococci in which a mutant's phenotype was rescued with transforming EVs <sup>(55)</sup>.

In the studies demonstrated in Chapter 4, we examined the role of secreted *S. pneumoniae* EVs in transformation of antimicrobial resistance determinants. Late-log EVs were isolated from liquid cultures of three different *S. pneumoniae* strains with variably sized resistance determinants: 1) D39<sup>Str</sup>Δ*ply::ermB* with a **738 bp** *ermB* gene and a *rpsL*/K56T point mutation conferring streptomycin (Str) resistance, 2) GA71819 carrying a **5.4 kb** Mega element with *mefE/mel* efflux genes, and 3) GA16833 with a **23.5 kb** Tn2009 ICE encoding *tetM* and Mega. The ability of these EVs for transforming these different sized resistance determinants was compared to transformation using genomic DNA from the same strains in classic *in vitro* transformation and in static nasopharyngeal biofilms. Our findings demonstrated that EV transformation in static nasopharyngeal biofilms resulted in homologous recombination of larger DNA fragments (~9-26 kb) independent of the presence or absence of exogenously added synthetic CSP. However, EV-associated DNA transformation occurred at reduced frequencies compared to free DNA in planktonic cells and biofilms, suggesting that pneumococcal EVs modulated transformation of associated DNA.

To date, the role of Gram-positive membrane vesicles in DNA transformation is not well understood. *S. pneumoniae* EVs have been extensively studied for their protein cargo<sup>(51, 56)</sup>, lipid

content<sup>(51)</sup>, and ability to modulate host immune responses<sup>(57)</sup>, thus viewed as potential vaccine candidates<sup>(58, 59)</sup>. However, EV-mediated transformation was not investigated previously in detail in *S. pneumoniae* even though the pneumococcus is naturally competent for extracellular DNA uptake and pneumococcal vesicles carry DNA content<sup>(50, 52)</sup>. Our Chapter 4 studies elucidated pneumococcal transformation of EV-associated DNA, providing frequencies of EV transformation in planktonic cells and biofilms and estimating the minimum DNA lengths that EVs can deliver.

The source of *S. pneumoniae* DNA found associated with pneumococcal EVs remains unclear and should be further elucidated in future studies. DNase I treatment prevented recombinant recovery, suggesting that EV-associated DNA was not protected by the vesicles and was localized to the external surface of the EVs. In *S. pneumoniae*, two major mechanisms, autolysis and fratricide, contribute to the release of extracellular DNA. Autolysis is typically induced during stationary phase<sup>(60, 61)</sup> and since we isolated pneumococcal EVs during late-log phase, autolysis is not likely the primary source of extracellular DNA that associates with EVs. In contrast, fratricide is induced in mid-log phase during competence development<sup>(62-64)</sup>, prior to the time point for pneumococcal EV isolation in our studies. Competence-induced fratricide in *S. pneumoniae* is the mechanism where non-competent cells are killed by their competent neighbors using lytic enzymes LytA, LytC, and CbpD <sup>(62, 63, 65, 66)</sup>. The role of fratricide can be investigated with single or triple mutants of these fratricide-involved lytic enzymes. These future efforts could further provide insight into the origin of EV-associated DNA and shed further light on the role of EV-mediated transformation in *S. pneumoniae*.

### V. Final thoughts

DNA transformation was first demonstrated in 1928 in the seminal paper by Frederick Griffith<sup>(67)</sup> and validated by subsequent investigations by Avery et al. (1944) and Hershey et al.

(1952)<sup>(68, 69)</sup>. Since then, multiple studies demonstrated that DNA uptake via transformation is the major mechanism for genetic exchange in S. pneumoniae facilitating genomic evolution<sup>(50)</sup>. Molecular mechanisms for recombination of ~2-6 kb DNAs were confirmed with classic in vitro transformation of planktonic cells or in murine animal models<sup>(26, 70, 71)</sup>. However, evidence for larger recombination events (>20 kb) in pneumococcal genomes from human carriage or disease isolates were identified without confirming the transfer mechanism<sup>(18, 19)</sup>. Our new studies of antibiotic resistance determinant dissemination by Tn916-related ICEs suggest that the frequency and prevalence of transformation is a complex and dynamic process in S. pneumoniae. We show that S. pneumoniae biofilms formed on human nasopharyngeal cells facilitate the exchange of large DNA fragments (>20 kb and up to 101 kb) compared to planktonic recipient cells. The horizontal dissemination of large S. pneumoniae resistance determinants via transformation was clearly augmented in this biologically relevant bacterial environment. Transformation frequency and efficiency was likely enhanced by biofilm characteristics, such as close donor-recipient contact and accumulation of DNA in local concentrations for enhanced uptake. Additionally, we found in US S. pneumoniae isolates that the spread of resistance determinants carried by large, complex Tn916-related ICEs continues to occur and increases despite successful PCV introductions and dramatic reductions of specific serotypes. Continuing to understand the horizontal spread of S. pneumoniae antimicrobial resistance determinants in human populations is critical for making decisions on vaccine design and/or treatment strategies. Antibiotic resistance obtained through transformation can provide selective benefits for the survival of S. pneumoniae but at the cost of limiting treatment options for pneumococcal infections in the human host.

#### REFERENCES

- 1. Henriques-Normark B, Tuomanen EI. The pneumococcus: epidemiology, microbiology, and pathogenesis. Cold Spring Harb Perspect Med. 2013;3(7). Epub 2013/07/03. doi: 10.1101/cshperspect.a010215. PubMed PMID: 23818515; PMCID: PMC3685878.
- 2. Shak JR, Vidal JE, Klugman KP. Influence of bacterial interactions on pneumococcal colonization of the nasopharynx. Trends Microbiol. 2013;21(3):129-35. Epub 2013/01/01. doi: 10.1016/j.tim.2012.11.005. PubMed PMID: 23273566; PMCID: PMC3729046.
- 3. Scelfo C, Menzella F, Fontana M, Ghidoni G, Galeone C, Facciolongo NC. Pneumonia and Invasive Pneumococcal Diseases: The Role of Pneumococcal Conjugate Vaccine in the Era of Multi-Drug Resistance. Vaccines (Basel). 2021;9(5). Epub 2021/05/01. doi: 10.3390/vaccines9050420. PubMed PMID: 33922273; PMCID: PMC8145843.
- 4. Weiser JN, Ferreira DM, Paton JC. Streptococcus pneumoniae: transmission, colonization and invasion. Nat Rev Microbiol. 2018;16(6):355-67. Epub 2018/03/31. doi: 10.1038/s41579-018-0001-8. PubMed PMID: 29599457; PMCID: PMC5949087.
- 5. Wahl B, O'Brien KL, Greenbaum A, Majumder A, Liu L, Chu Y, Luksic I, Nair H, McAllister DA, Campbell H, Rudan I, Black R, Knoll MD. Burden of Streptococcus pneumoniae and Haemophilus influenzae type b disease in children in the era of conjugate vaccines: global, regional, and national estimates for 2000-15. Lancet Glob Health. 2018;6(7):e744-e57. Epub 2018/06/16. doi: 10.1016/S2214-109X(18)30247-X. PubMed PMID: 29903376; PMCID: PMC6005122.
- 6. Antimicrobial Resistance C. Global burden of bacterial antimicrobial resistance in 2019: a systematic analysis. Lancet. 2022;399(10325):629-55. Epub 2022/01/24. doi: 10.1016/S0140-6736(21)02724-0. PubMed PMID: 35065702; PMCID: PMC8841637.

- 7. Schroeder MR, Stephens DS. Macrolide Resistance in Streptococcus pneumoniae. Front Cell Infect Microbiol. 2016;6:98. Epub 2016/10/07. doi: 10.3389/fcimb.2016.00098. PubMed PMID: 27709102; PMCID: PMC5030221.
- 8. Bergman M, Huikko S, Huovinen P, Paakkari P, Seppala H, Finnish Study Group for Antimicrobial R. Macrolide and azithromycin use are linked to increased macrolide resistance in Streptococcus pneumoniae. Antimicrob Agents Chemother. 2006;50(11):3646-50. Epub 2006/08/31. doi: 10.1128/AAC.00234-06. PubMed PMID: 16940064; PMCID: PMC1635217.
- 9. Hyde TB, Gay K, Stephens DS, Vugia DJ, Pass M, Johnson S, Barrett NL, Schaffner W, Cieslak PR, Maupin PS, Zell ER, Jorgensen JH, Facklam RR, Whitney CG, Active Bacterial Core Surveillance/Emerging Infections Program N. Macrolide resistance among invasive Streptococcus pneumoniae isolates. JAMA. 2001;286(15):1857-62. Epub 2001/10/26. doi: 10.1001/jama.286.15.1857. PubMed PMID: 11597287.
- 10. Jenkins SG, Farrell DJ. Increase in pneumococcus macrolide resistance, United States. Emerg Infect Dis. 2009;15(8):1260-4. Epub 2009/09/16. doi: 10.3201/eid1508.081187. PubMed PMID: 19751588; PMCID: PMC2815953.
- 11. Chancey ST, Agrawal S, Schroeder MR, Farley MM, Tettelin H, Stephens DS. Composite mobile genetic elements disseminating macrolide resistance in Streptococcus pneumoniae. Front Microbiol. 2015;6:26. Epub 2015/02/25. doi: 10.3389/fmicb.2015.00026. PubMed PMID: 25709602; PMCID: PMC4321634.
- 12. Johnson CM, Grossman AD. Integrative and Conjugative Elements (ICEs): What They Do and How They Work. Annu Rev Genet. 2015;49:577-601. Epub 2015/10/17. doi: 10.1146/annurev-genet-112414-055018. PubMed PMID: 26473380; PMCID: PMC5180612.

- 13. Delavat F, Miyazaki R, Carraro N, Pradervand N, van der Meer JR. The hidden life of integrative and conjugative elements. FEMS Microbiol Rev. 2017;41(4):512-37. Epub 2017/04/04. doi: 10.1093/femsre/fux008. PubMed PMID: 28369623; PMCID: PMC5812530.
- 14. Su YA, He P, Clewell DB. Characterization of the tet(M) determinant of Tn916: evidence for regulation by transcription attenuation. Antimicrob Agents Chemother. 1992;36(4):769-78. Epub 1992/04/01. doi: 10.1128/AAC.36.4.769. PubMed PMID: 1323953; PMCID: PMC189400.
- 15. Del Grosso M, Scotto d'Abusco A, Iannelli F, Pozzi G, Pantosti A. Tn2009, a Tn916-like element containing mef(E) in Streptococcus pneumoniae. Antimicrob Agents Chemother. 2004;48(6):2037-42. Epub 2004/05/25. doi: 10.1128/AAC.48.6.2037-2042.2004. PubMed PMID: 15155196; PMCID: PMC415626.
- 16. Cochetti I, Tili E, Vecchi M, Manzin A, Mingoia M, Varaldo PE, Montanari MP. New Tn916-related elements causing erm(B)-mediated erythromycin resistance in tetracycline-susceptible pneumococci. J Antimicrob Chemother. 2007;60(1):127-31. Epub 2007/05/08. doi: 10.1093/jac/dkm120. PubMed PMID: 17483548.
- 17. Del Grosso M, Northwood JG, Farrell DJ, Pantosti A. The macrolide resistance genes erm(B) and mef(E) are carried by Tn2010 in dual-gene Streptococcus pneumoniae isolates belonging to clonal complex CC271. Antimicrob Agents Chemother. 2007;51(11):4184-6. Epub 2007/08/22. doi: 10.1128/AAC.00598-07. PubMed PMID: 17709465; PMCID: PMC2151421.
- 18. Wyres KL, van Tonder A, Lambertsen LM, Hakenbeck R, Parkhill J, Bentley SD, Brueggemann AB. Evidence of antimicrobial resistance-conferring genetic elements among pneumococci isolated prior to 1974. BMC Genomics. 2013;14:500. Epub 2013/07/25. doi: 10.1186/1471-2164-14-500. PubMed PMID: 23879707; PMCID: PMC3726389.

- 19. Croucher NJ, Harris SR, Fraser C, Quail MA, Burton J, van der Linden M, McGee L, von Gottberg A, Song JH, Ko KS, Pichon B, Baker S, Parry CM, Lambertsen LM, Shahinas D, Pillai DR, Mitchell TJ, Dougan G, Tomasz A, Klugman KP, Parkhill J, Hanage WP, Bentley SD. Rapid pneumococcal evolution in response to clinical interventions. Science. 2011;331(6016):430-4. Epub 2011/01/29. doi: 10.1126/science.1198545. PubMed PMID: 21273480; PMCID: PMC3648787.
- 20. Nakano S, Fujisawa T, Ito Y, Chang B, Matsumura Y, Yamamoto M, Suga S, Ohnishi M, Nagao M. Streptococcus pneumoniae Serotype 12F-CC4846 and Invasive Pneumococcal Disease after Introduction of 13-Valent Pneumococcal Conjugate Vaccine, Japan, 2015-2017. Emerg Infect Dis. 2020;26(11):2660-8. Epub 2020/10/21. doi: 10.3201/eid2611.200087. PubMed PMID: 33079039; PMCID: PMC7588537.
- 21. Antezana BS, Lohsen S, Wu X, Vidal JE, Tzeng YL, Stephens DS. Dissemination of Tn916-Related Integrative and Conjugative Elements in Streptococcus pneumoniae Occurs by Transformation and Homologous Recombination in Nasopharyngeal Biofilms. Microbiol Spectr. 2023;11(2):e0375922. Epub 2023/03/14. doi: 10.1128/spectrum.03759-22. PubMed PMID: 36912669; PMCID: PMC10101023.
- 22. Lattar SM, Wu X, Brophy J, Sakai F, Klugman KP, Vidal JE. A Mechanism of Unidirectional Transformation, Leading to Antibiotic Resistance, Occurs within Nasopharyngeal Pneumococcal Biofilm Consortia. mBio. 2018;9(3). Epub 2018/05/17. doi: 10.1128/mBio.00561-18. PubMed PMID: 29764945; PMCID: PMC5954218.
- 23. Havarstein LS, Coomaraswamy G, Morrison DA. An unmodified heptadecapeptide pheromone induces competence for genetic transformation in Streptococcus pneumoniae. Proc

- Natl Acad Sci U S A. 1995;92(24):11140-4. Epub 1995/11/21. doi: 10.1073/pnas.92.24.11140. PubMed PMID: 7479953; PMCID: PMC40587.
- 24. Marks LR, Parameswaran GI, Hakansson AP. Pneumococcal interactions with epithelial cells are crucial for optimal biofilm formation and colonization in vitro and in vivo. Infect Immun. 2012;80(8):2744-60. Epub 2012/05/31. doi: 10.1128/IAI.00488-12. PubMed PMID: 22645283; PMCID: PMC3434590.
- 25. Chun YY, Tan KS, Yu L, Pang M, Wong MHM, Nakamoto R, Chua WZ, Huee-Ping Wong A, Lew ZZR, Ong HH, Chow VT, Tran T, Yun Wang D, Sham LT. Influence of glycan structure on the colonization of Streptococcus pneumoniae on human respiratory epithelial cells. Proc Natl Acad Sci U S A. 2023;120(13):e2213584120. Epub 2023/03/22. doi: 10.1073/pnas.2213584120. PubMed PMID: 36943879; PMCID: PMC10068763.
- 26. Marks LR, Reddinger RM, Hakansson AP. High levels of genetic recombination during nasopharyngeal carriage and biofilm formation in Streptococcus pneumoniae. mBio. 2012;3(5). Epub 2012/09/28. doi: 10.1128/mBio.00200-12. PubMed PMID: 23015736; PMCID: PMC3448161.
- 27. Metersky M, Waterer G. Can animal models really teach us anything about pneumonia? Con. Eur Respir J. 2020;55(1). Epub 2020/01/04. doi: 10.1183/13993003.01525-2019. PubMed PMID: 31896677.
- 28. Orihuela CJ, Maus UA, Brown JS. Can animal models really teach us anything about pneumonia? Pro. Eur Respir J. 2020;55(1). Epub 2020/01/04. doi: 10.1183/13993003.01539-2019. PubMed PMID: 31896678.
- 29. Moscoso M, Garcia E, Lopez R. Biofilm formation by Streptococcus pneumoniae: role of choline, extracellular DNA, and capsular polysaccharide in microbial accretion. J Bacteriol.

- 2006;188(22):7785-95. Epub 2006/08/29. doi: 10.1128/JB.00673-06. PubMed PMID: 16936041; PMCID: PMC1636320.
- 30. Kelley MA, Weber DJ, Gilligan P, Cohen MS. Breakthrough pneumococcal bacteremia in patients being treated with azithromycin and clarithromycin. Clin Infect Dis. 2000;31(4):1008-11. Epub 2000/10/26. doi: 10.1086/318157. PubMed PMID: 11049784.
- 31. Malhotra-Kumar S, Lammens C, Coenen S, Van Herck K, Goossens H. Effect of azithromycin and clarithromycin therapy on pharyngeal carriage of macrolide-resistant streptococci in healthy volunteers: a randomised, double-blind, placebo-controlled study. Lancet. 2007;369(9560):482-90. Epub 2007/02/13. doi: 10.1016/S0140-6736(07)60235-9. PubMed PMID: 17292768.
- Desai AP, Sharma D, Crispell EK, Baughman W, Thomas S, Tunali A, Sherwood L, Zmitrovich A, Jerris R, Satola SW, Beall B, Moore MR, Jain S, Farley MM. Decline in Pneumococcal Nasopharyngeal Carriage of Vaccine Serotypes After the Introduction of the 13-Valent Pneumococcal Conjugate Vaccine in Children in Atlanta, Georgia. Pediatr Infect Dis J. 2015;34(11):1168-74. Epub 2015/08/01. doi: 10.1097/INF.000000000000000849. PubMed PMID: 26226445.
- 33. Hawkins PA, Chochua S, Jackson D, Beall B, McGee L. Mobile elements and chromosomal changes associated with MLS resistance phenotypes of invasive pneumococci recovered in the United States. Microb Drug Resist. 2015;21(2):121-9. Epub 2014/08/15. doi: 10.1089/mdr.2014.0086. PubMed PMID: 25115711; PMCID: PMC5735413.
- 34. Stephens DS, Zughaier SM, Whitney CG, Baughman WS, Barker L, Gay K, Jackson D, Orenstein WA, Arnold K, Schuchat A, Farley MM, Georgia Emerging Infections P. Incidence of macrolide resistance in Streptococcus pneumoniae after introduction of the pneumococcal

- conjugate vaccine: population-based assessment. Lancet. 2005;365(9462):855-63. Epub 2005/03/09. doi: 10.1016/S0140-6736(05)71043-6. PubMed PMID: 15752529.
- 35. Jolley KA, Bray JE, Maiden MCJ. Open-access bacterial population genomics: BIGSdb software, the PubMLST.org website and their applications. Wellcome Open Res. 2018;3:124. Epub 2018/10/23. doi: 10.12688/wellcomeopenres.14826.1. PubMed PMID: 30345391; PMCID: PMC6192448.
- 36. Gay K, Baughman W, Miller Y, Jackson D, Whitney CG, Schuchat A, Farley MM, Tenover F, Stephens DS. The emergence of Streptococcus pneumoniae resistant to macrolide antimicrobial agents: a 6-year population-based assessment. J Infect Dis. 2000;182(5):1417-24. Epub 2000/10/07. doi: 10.1086/315853. PubMed PMID: 11023465.
- 37. Wierzbowski AK, Boyd D, Mulvey M, Hoban DJ, Zhanel GG. Expression of the mef(E) gene encoding the macrolide efflux pump protein increases in Streptococcus pneumoniae with increasing resistance to macrolides. Antimicrob Agents Chemother. 2005;49(11):4635-40. Epub 2005/10/28. doi: 10.1128/AAC.49.11.4635-4640.2005. PubMed PMID: 16251306; PMCID: PMC1280166.
- 38. Azarian T, Grant LR, Arnold BJ, Hammitt LL, Reid R, Santosham M, Weatherholtz R, Goklish N, Thompson CM, Bentley SD, O'Brien KL, Hanage WP, Lipsitch M. The impact of serotype-specific vaccination on phylodynamic parameters of Streptococcus pneumoniae and the pneumococcal pan-genome. PLoS Pathog. 2018;14(4):e1006966. Epub 2018/04/05. doi: 10.1371/journal.ppat.1006966. PubMed PMID: 29617440; PMCID: PMC5902063 not related to this paper from Pfizer and PATH Vaccine Solutions. W.P.H. and M.L. have consulted for Antigen Discovery Inc. The authors have declared that no competing interests exist.

- 39. Gladstone RA, Lo SW, Lees JA, Croucher NJ, van Tonder AJ, Corander J, Page AJ, Marttinen P, Bentley LJ, Ochoa TJ, Ho PL, du Plessis M, Cornick JE, Kwambana-Adams B, Benisty R, Nzenze SA, Madhi SA, Hawkins PA, Everett DB, Antonio M, Dagan R, Klugman KP, von Gottberg A, McGee L, Breiman RF, Bentley SD, Global Pneumococcal Sequencing C. International genomic definition of pneumococcal lineages, to contextualise disease, antibiotic resistance and vaccine impact. EBioMedicine. 2019;43:338-46. Epub 2019/04/21. doi: 10.1016/j.ebiom.2019.04.021. PubMed PMID: 31003929; PMCID: PMC6557916.
- 40. van Tonder AJ, Gladstone RA, Lo SW, Nahm MH, du Plessis M, Cornick J, Kwambana-Adams B, Madhi SA, Hawkins PA, Benisty R, Dagan R, Everett D, Antonio M, Klugman KP, von Gottberg A, Breiman RF, McGee L, Bentley SD, The Global Pneumococcal Sequencing C. Putative novel cps loci in a large global collection of pneumococci. Microb Genom. 2019;5(7). Epub 2019/06/12. doi: 10.1099/mgen.0.000274. PubMed PMID: 31184299; PMCID: PMC6700660.
- 41. Bogaardt C, van Tonder AJ, Brueggemann AB. Genomic analyses of pneumococci reveal a wide diversity of bacteriocins including pneumocyclicin, a novel circular bacteriocin. BMC Genomics. 2015;16(1):554. Epub 2015/07/29. doi: 10.1186/s12864-015-1729-4. PubMed PMID: 26215050; PMCID: PMC4517551.
- 42. Croucher NJ, Finkelstein JA, Pelton SI, Mitchell PK, Lee GM, Parkhill J, Bentley SD, Hanage WP, Lipsitch M. Population genomics of post-vaccine changes in pneumococcal epidemiology. Nat Genet. 2013;45(6):656-63. Epub 2013/05/07. doi: 10.1038/ng.2625. PubMed PMID: 23644493; PMCID: PMC3725542.
- 43. Andam CP, Mitchell PK, Callendrello A, Chang Q, Corander J, Chaguza C, McGee L, Beall BW, Hanage WP. Genomic Epidemiology of Penicillin-Nonsusceptible Pneumococci with

Nonvaccine Serotypes Causing Invasive Disease in the United States. J Clin Microbiol. 2017;55(4):1104-15. Epub 2017/01/20. doi: 10.1128/JCM.02453-16. PubMed PMID: 28100596; PMCID: PMC5377837.

- 44. Active Bacterial Core Surveillance (ABCs). Centers for Disease Control and Prevention. 2021 [April 20, 2023]. Available from: <a href="https://www.cdc.gov/abcs/index.html">https://www.cdc.gov/abcs/index.html</a>.
- 45. Farrell DJ, Couturier C, Hryniewicz W. Distribution and antibacterial susceptibility of macrolide resistance genotypes in Streptococcus pneumoniae: PROTEKT Year 5 (2003-2004). Int J Antimicrob Agents. 2008;31(3):245-9. Epub 2008/01/08. doi: 10.1016/j.ijantimicag.2007.10.022. PubMed PMID: 18178388.
- 46. Pneumococcal disease: guidance, data, and analysis. UK Health Security Agency. 2021 [April 20, 2023]. Available from: <a href="https://www.gov.uk/government/collections/pneumococcal-disease-guidance-data-and-analysis">https://www.gov.uk/government/collections/pneumococcal-disease-guidance-data-and-analysis</a>.
- 47. O'Neill J. Antimicrobial Resistance: Tackling a crisis for the health and wealth of nations.

  2014. [April 20, 2023]. Available from: <a href="https://amr-review.org/sites/default/files/AMR%20Review%20Paper%20-">https://amr-review.org/sites/default/files/AMR%20Review%20Paper%20-</a>

  %20Tackling%20a%20crisis%20for%20the%20health%20and%20wealth%20of%20nations\_1.p

  df.
- 48. Andam CP, Hanage WP. Mechanisms of genome evolution of Streptococcus. Infect Genet Evol. 2015;33:334-42. Epub 2014/12/03. doi: 10.1016/j.meegid.2014.11.007. PubMed PMID: 25461843; PMCID: PMC4430445.
- 49. Laurenceau R, Pehau-Arnaudet G, Baconnais S, Gault J, Malosse C, Dujeancourt A, Campo N, Chamot-Rooke J, Le Cam E, Claverys JP, Fronzes R. A type IV pilus mediates DNA binding during natural transformation in Streptococcus pneumoniae. PLoS Pathog.

- 2013;9(6):e1003473. Epub 2013/07/05. doi: 10.1371/journal.ppat.1003473. PubMed PMID: 23825953; PMCID: PMC3694846.
- 50. Straume D, Stamsas GA, Havarstein LS. Natural transformation and genome evolution in Streptococcus pneumoniae. Infect Genet Evol. 2015;33:371-80. Epub 2014/12/03. doi: 10.1016/j.meegid.2014.10.020. PubMed PMID: 25445643.
- 51. Olaya-Abril A, Prados-Rosales R, McConnell MJ, Martin-Pena R, Gonzalez-Reyes JA, Jimenez-Munguia I, Gomez-Gascon L, Fernandez J, Luque-Garcia JL, Garcia-Lidon C, Estevez H, Pachon J, Obando I, Casadevall A, Pirofski LA, Rodriguez-Ortega MJ. Characterization of protective extracellular membrane-derived vesicles produced by Streptococcus pneumoniae. J Proteomics. 2014;106:46-60. Epub 2014/04/29. doi: 10.1016/j.jprot.2014.04.023. PubMed PMID: 24769240.
- 52. Domenech M, Garcia, E. Autolysin-Independent DNA Release in Streptococcus pneumoniae Invitro Biofilms. Clinical infectious Diseases: Open Access. 2018;2(3):114.
- 53. Bitto NJ, Chapman R, Pidot S, Costin A, Lo C, Choi J, D'Cruze T, Reynolds EC, Dashper SG, Turnbull L, Whitchurch CB, Stinear TP, Stacey KJ, Ferrero RL. Bacterial membrane vesicles transport their DNA cargo into host cells. Sci Rep. 2017;7(1):7072. Epub 2017/08/03. doi: 10.1038/s41598-017-07288-4. PubMed PMID: 28765539; PMCID: PMC5539193.
- 54. Briaud P, Carroll RK. Extracellular Vesicle Biogenesis and Functions in Gram-Positive Bacteria. Infect Immun. 2020;88(12). Epub 2020/09/30. doi: 10.1128/IAI.00433-20. PubMed PMID: 32989035; PMCID: PMC7671900.
- 55. Klieve AV, Yokoyama MT, Forster RJ, Ouwerkerk D, Bain PA, Mawhinney EL. Naturally occurring DNA transfer system associated with membrane vesicles in cellulolytic Ruminococcus

- spp. of ruminal origin. Appl Environ Microbiol. 2005;71(8):4248-53. Epub 2005/08/09. doi: 10.1128/AEM.71.8.4248-4253.2005. PubMed PMID: 16085810; PMCID: PMC1183309.
- 56. Jhelum H, Sori H, Sehgal D. A novel extracellular vesicle-associated endodeoxyribonuclease helps Streptococcus pneumoniae evade neutrophil extracellular traps and is required for full virulence. Sci Rep. 2018;8(1):7985. Epub 2018/05/24. doi: 10.1038/s41598-018-25865-z. PubMed PMID: 29789571; PMCID: PMC5964101.
- 57. Yerneni SS, Werner S, Azambuja JH, Ludwig N, Eutsey R, Aggarwal SD, Lucas PC, Bailey N, Whiteside TL, Campbell PG, Hiller NL. Pneumococcal Extracellular Vesicles Modulate Host Immunity. mBio. 2021;12(4):e0165721. Epub 2021/07/14. doi: 10.1128/mBio.01657-21. PubMed PMID: 34253061; PMCID: PMC8406339.
- 58. Parveen S, Subramanian K. Emerging Roles of Extracellular Vesicles in Pneumococcal Infections: Immunomodulators to Potential Novel Vaccine Candidates. Front Cell Infect Microbiol. 2022;12:836070. Epub 2022/03/04. doi: 10.3389/fcimb.2022.836070. PubMed PMID: 35237534; PMCID: PMC8882830.
- 59. Choi CW, Park EC, Yun SH, Lee SY, Kim SI, Kim GH. Potential Usefulness of Streptococcus pneumoniae Extracellular Membrane Vesicles as Antibacterial Vaccines. J Immunol Res. 2017;2017:7931982. Epub 2017/02/18. doi: 10.1155/2017/7931982. PubMed PMID: 28210633; PMCID: PMC5292160.
- 60. Tomasz A, Albino A, Zanati E. Multiple antibiotic resistance in a bacterium with suppressed autolytic system. Nature. 1970;227(5254):138-40. Epub 1970/07/11. doi: 10.1038/227138a0. PubMed PMID: 4393335.
- 61. Mellroth P, Daniels R, Eberhardt A, Ronnlund D, Blom H, Widengren J, Normark S, Henriques-Normark B. LytA, major autolysin of Streptococcus pneumoniae, requires access to

- nascent peptidoglycan. J Biol Chem. 2012;287(14):11018-29. Epub 2012/02/16. doi: 10.1074/jbc.M111.318584. PubMed PMID: 22334685; PMCID: PMC3322828.
- 62. Steinmoen H, Knutsen E, Havarstein LS. Induction of natural competence in Streptococcus pneumoniae triggers lysis and DNA release from a subfraction of the cell population. Proc Natl Acad Sci U S A. 2002;99(11):7681-6. Epub 2002/05/29. doi: 10.1073/pnas.112464599. PubMed PMID: 12032343; PMCID: PMC124321.
- 63. Guiral S, Mitchell TJ, Martin B, Claverys JP. Competence-programmed predation of noncompetent cells in the human pathogen Streptococcus pneumoniae: genetic requirements. Proc Natl Acad Sci U S A. 2005;102(24):8710-5. Epub 2005/06/02. doi: 10.1073/pnas.0500879102. PubMed PMID: 15928084; PMCID: PMC1150823.
- 64. Claverys JP, Martin B, Havarstein LS. Competence-induced fratricide in streptococci. Mol Microbiol. 2007;64(6):1423-33. Epub 2007/06/09. doi: 10.1111/j.1365-2958.2007.05757.x. PubMed PMID: 17555432.
- 65. Moscoso M, Claverys JP. Release of DNA into the medium by competent Streptococcus pneumoniae: kinetics, mechanism and stability of the liberated DNA. Mol Microbiol. 2004;54(3):783-94. Epub 2004/10/20. doi: 10.1111/j.1365-2958.2004.04305.x. PubMed PMID: 15491367.
- 66. Kausmally L, Johnsborg O, Lunde M, Knutsen E, Havarstein LS. Choline-binding protein D (CbpD) in Streptococcus pneumoniae is essential for competence-induced cell lysis. J Bacteriol. 2005;187(13):4338-45. Epub 2005/06/22. doi: 10.1128/JB.187.13.4338-4345.2005. PubMed PMID: 15968042; PMCID: PMC1151764.

- 67. Griffith F. The Significance of Pneumococcal Types. J Hyg (Lond). 1928;27(2):113-59. Epub 1928/01/01. doi: 10.1017/s0022172400031879. PubMed PMID: 20474956; PMCID: PMC2167760.
- 68. McCarty M. Discovering genes are made of DNA. Nature2003 [March 21, 2023]. Available from: <a href="https://www.nature.com/scitable/content/Discovering-genes-are-made-of-DNA-14028/">https://www.nature.com/scitable/content/Discovering-genes-are-made-of-DNA-14028/</a>.
- 69. O'Connor C. Isolating Hereditary Material: Frederick Griffith, Oswald Avery, Alfred Hershey, and Martha Chase. Nature Education2008 [January 17, 2023]. Available from: <a href="https://www.nature.com/scitable/topicpage/isolating-hereditary-material-frederick-griffith-oswald-avery-336/">https://www.nature.com/scitable/topicpage/isolating-hereditary-material-frederick-griffith-oswald-avery-336/</a>.
- 70. Gurney T, Jr., Fox MS. Physical and genetic hybrids formed in bacterial transformation. J Mol Biol. 1968;32(1):83-100. Epub 1968/02/28. doi: 10.1016/0022-2836(68)90147-2. PubMed PMID: 4384454.
- 71. Lacks S. Integration efficiency and genetic recombination in pneumococcal transformation. Genetics. 1966;53(1):207-35. Epub 1966/01/01. doi: 10.1093/genetics/53.1.207. PubMed PMID: 4379022; PMCID: PMC1211003.

**Appendix A:** Interaction between *Streptococcus pneumoniae* and *Staphylococcus aureus*Generates \*OH Radicals That Rapidly Kill *Staphylococcus aureus* Strains

Xueqing Wu<sup>#, a, b</sup>, Oren Gordon<sup>#, c</sup>, Wenxin Jiang<sup>#, a</sup>, **Brenda S. Antezana**<sup>d</sup>, Uriel A. Angulo-Zamudio<sup>e</sup>, Carlos Del Rio<sup>a</sup>, Abraham Moller<sup>d</sup>, Terry Brissac<sup>f</sup>, Aimee R.P. Tierney<sup>d</sup>, Kurt Warncke<sup>g</sup>, Carlos J. Orihuela<sup>f</sup>, Timothy D. Read<sup>d, h, i</sup>, Jorge E. Vidal<sup>d, h, j</sup>

<sup>a</sup> Hubert Department of Global Health, Rollins School of Public Health, Emory University, Atlanta, Georgia, USA.

<sup>b</sup> Department of Infectious Disease, Sir Run Run Shaw Hospital, College of Medicine, Zhejiang University, Hangzhou, China.

<sup>c</sup> Department of Pediatrics, Hadassah-Hebrew University Medical Center, Jerusalem, Israel.

<sup>d</sup> Graduate Program in Microbiology and Molecular Genetics, Emory University, Atlanta, Georgia, USA.

<sup>e</sup> Regional Program for the Doctorate in Biotechnology, Faculty of Chemical Sciences Biological, Autonomous University of Sinaloa, Sinaloa, Mexico.

<sup>f</sup> Department of Microbiology, University of Alabama at Birmingham, Birmingham, Alabama, USA.

<sup>g</sup> Department of Physics, Emory University, Atlanta, Georgia, USA.

<sup>h</sup> Antibiotic Research Center, Emory University, Atlanta, Georgia, USA.

<sup>i</sup> School of Medicine, Emory University, Atlanta, Georgia, USA.

<sup>j</sup> Hubert Department of Global Health, Rollins School of Public Health, Emory University, Atlanta, Georgia, USA jvidal@umc.edu.

\*Contributed equally.

# Published in

# Journal of Bacteriology

# October 2019, Volume 201, Number 21

# **Citation:**

Wu X, Gordon O, Jiang W, Antezana BS, Angulo-Zamudio UA, Del Rio C, Moller A, Brissac T, Tierney ARP, Warncke K, Orihuela CJ, Read TD, Vidal JE. Interaction between Streptococcus pneumoniae and Staphylococcus aureus Generates (.)OH Radicals That Rapidly Kill Staphylococcus aureus Strains. J Bacteriol. 2019;201(21). Epub 2019/08/14. doi: 10.1128/JB.00474-19. PubMed PMID: 31405914; PMCID: PMC6779455.

B. Antezana created deletion mutant of spxB, quantified hydrogen peroxide production, and assisted with data interpretation and editing of manuscript.



# Interaction between *Streptococcus pneumoniae* and *Staphylococcus aureus* Generates 'OH Radicals That Rapidly Kill *Staphylococcus aureus* Strains

Xueqing Wu,<sup>a,f</sup> Oren Gordon,<sup>9</sup> Wenxin Jiang,<sup>a</sup> Brenda S. Antezana,<sup>b</sup> Uriel A. Angulo-Zamudio,<sup>h</sup> Carlos del Rio,<sup>a</sup> Abraham Moller,<sup>b</sup> Terry Brissac,<sup>i</sup> Aimee R. P. Tierney,<sup>b</sup> Kurt Warncke,<sup>e</sup> © Carlos J. Orihuela,<sup>i</sup> Timothy D. Read,<sup>b,c,d</sup> Jorge E. Vidal<sup>a,b,c\*</sup>

<sup>a</sup>Hubert Department of Global Health, Rollins School of Public Health, Emory University, Atlanta, Georgia, USA

ABSTRACT Streptococcus pneumoniae rapidly kills Staphylococcus aureus by producing membrane-permeable hydrogen peroxide (H2O2). The mechanism by which S. pneumoniae-produced H<sub>2</sub>O<sub>2</sub> mediates S. aureus killing was investigated. An in vitro model that mimicked S. pneumoniae-S. aureus contact during colonization of the nasopharynx demonstrated that S. aureus killing required outcompeting densities of S. pneumoniae. Compared to the wild-type strain, isogenic S. pneumoniae  $\Delta lctO$  and S. pneumoniae ΔspxB, both deficient in production of H<sub>2</sub>O<sub>2</sub>, required increased density to kill S. aureus. While residual H2O2 activity produced by single mutants was sufficient to eradicate S. aureus, an S. pneumoniae ΔspxB ΔlctO double mutant was unable to kill S. aureus. A collection of 20 diverse methicillin-resistant S. aureus (MRSA) and methicillin-susceptible S. aureus (MSSA) strains showed linear sensitivity (R2 = 0.95) for S. pneumoniae killing, but the same strains had different susceptibilities when challenged with pure H<sub>2</sub>O<sub>2</sub> (5 mM). There was no association between the S. aureus clonal complex and sensitivity to either S. pneumoniae or H2O2. To kill S. aureus, S. pneumoniae produced  $\sim$ 180  $\mu$ M H<sub>2</sub>O<sub>2</sub> within 4 h of incubation, while the killing-defective S. pneumoniae ΔspxB and S. pneumoniae ΔspxB ΔlctO mutants produced undetectable levels. Remarkably, a sublethal dose (1 mM) of pure H<sub>2</sub>O<sub>2</sub> incubated with S. pneumoniae ΔspxB eradicated diverse S. aureus strains, suggesting that S. pneumoniae bacteria may facilitate conversion of H<sub>2</sub>O<sub>2</sub> to a hydroxyl radical (OH). Accordingly, S. aureus killing was completely blocked by incubation with scavengers of OH radicals, dimethyl sulfoxide (Me<sub>2</sub>SO), thiourea, or sodium salicylate. The OH was detected in S. pneumoniae cells by spin trapping and electron paramagnetic resonance. Therefore, S. pneumoniae produces H<sub>2</sub>O<sub>2</sub>, which is rapidly converted to a more potent oxidant, hydroxyl radicals, to rapidly intoxicate S. aureus strains.

**IMPORTANCE** *Streptococcus pneumoniae* strains produce hydrogen peroxide  $(H_2O_2)$  to kill bacteria in the upper airways, including pathogenic *Staphylococcus aureus* strains. The targets of *S. pneumoniae*-produced  $H_2O_2$  have not been discovered, in part because of a lack of knowledge about the underlying molecular mechanism. We demonstrated that an increased density of *S. pneumoniae* kills *S. aureus* by means of  $H_2O_2$  produced by two enzymes, SpxB and LctO. We discovered that SpxB/

Citation Wu X, Gordon O, Jiang W, Antezana BS, Angulo-Zamudio UA, del Rio C, Moller A, Brissac T, Tierney ARP, Warncke K, Orihuela CJ, Read TD, Vidal JE. 2019. Interaction between Streptococcus pneumoniae and Staphylococcus aureus generates OH radicals that rapidly kill Staphylococcus aureus strains. J Bacteriol 201:e00474-19. https://doi.org/10.1128/JB

**Editor** Michael J. Federle, University of Illinois at Chicago

**Copyright** © 2019 American Society for Microbiology. All Rights Reserved.

Address correspondence to Jorge E. Vidal, jvidal@umc.edu.

\* Present address: Jorge E. Vidal, Department of Microbiology and Immunology, University of Mississippi Medical Center, Jackson, Mississippi, USA.

X.W., O.G., and W.J. contributed equally to this work

Received 17 July 2019 Accepted 8 August 2019

Accepted manuscript posted online 12
August 2019

August 2019

Published 4 October 2019

<sup>&</sup>lt;sup>b</sup>Graduate Program in Microbiology and Molecular Genetics, Emory University, Atlanta, Georgia, USA

<sup>&</sup>lt;sup>c</sup>Antibiotic Research Center, Emory University, Atlanta, Georgia, USA

dSchool of Medicine, Emory University, Atlanta, Georgia, USA

eDepartment of Physics, Emory University, Atlanta, Georgia, USA

Department of Infectious Disease, Sir Run Run Shaw Hospital, College of Medicine, Zhejiang University, Hangzhou, China

<sup>&</sup>lt;sup>9</sup>Department of Pediatrics, Hadassah-Hebrew University Medical Center, Jerusalem, Israel

hRegional Program for the Doctorate in Biotechnology, Faculty of Chemical Sciences Biological, Autonomous University of Sinaloa, Sinaloa, Mexico

<sup>&</sup>lt;sup>i</sup>Department of Microbiology, University of Alabama at Birmingham, Birmingham, Alabama, USA

LctO-produced  $H_2O_2$  is converted into a hydroxyl radical (OH) that rapidly intoxicates and kills *S. aureus*. We successfully inhibited the toxicity of OH with three different scavengers and detected OH in the supernatant. The target(s) of the hydroxyl radicals represents a new alternative for the development of antimicrobials against *S. aureus* infections.

**KEYWORDS** *Staphylococcus aureus, Streptococcus pneumoniae*, eradication, hydrogen peroxide, hydroxyl radicals

Streptococcus pneumoniae and Staphylococcus aureus colonize the upper airways of humans, forming persistent biofilms (1–9). Once in the nasopharynx, *S. pneumoniae* forms a biofilm that increases resistance to desiccation and antibiotic resistance and also provides a source of planktonic bacteria that migrate to the ears, lower respiratory tract, circulation, heart, and meninges, causing pneumococcal disease, the burden of which is extremely high in the human population (5, 6, 10–13). *S. aureus* strains colonize the skin of >30% of the human population but also reside in the nasopharynx, causing severe pathologies, including bacteremia and pneumonia (1, 3, 7, 11, 14, 15).

Over the last few years, our laboratories and others have conducted carriage studies of important human pathogens in the nasopharynxes of children of different ethnicities. These studies demonstrated a negative association for the concurrent carriage of *S. pneumoniae* and *S. aureus* (3, 7, 16). Soon after pneumococcal conjugate vaccines (PCV) became available, a potential mechanistic competition between *S. pneumoniae* and *S. aureus* for the colonization of the upper airways was observed. Some of the first studies showed that nasopharyngeal carriage of *S. aureus* increased in children who had received PCV. The increased *S. aureus* colonization was attributed to the decreased carriage of pneumococcal serotypes targeted by PCV (1, 7, 8). It is therefore clear that *S. pneumoniae in vivo* interferes with colonization by *S. aureus*.

Although evidence that S. pneumoniae was capable of killing S. aureus was published over 100 years ago (17, 18), studies of the molecular mechanism(s) behind these epidemiological observations were reinitiated when the pneumococcal vaccine was licensed in early 2000 in developed countries. Pericone et al. (19), and then other investigators, demonstrated that pneumococcal strains isolated from disease or carriage interfered with the growth of S. aureus in broth cultures. The proposed mechanism involved the production of hydrogen peroxide (H<sub>2</sub>O<sub>2</sub>) that was released by S. pneumoniae into the supernatant (20). This H<sub>2</sub>O<sub>2</sub>-mediated killing of S. aureus occurred within 6 h post-inoculation of S. pneumoniae, but it was inhibited in cocultures with catalase added; by incubating these cocultures in an anaerobic chamber; or by a mutation within the spxB gene, encoding the enzyme streptococcal pyruvate oxidase, which endogenously produces H<sub>2</sub>O<sub>2</sub> during conversion of acetylphosphate from pyruvate (19–23). Notably, SpxB accounts for  $\sim$ 85% of the membrane-permeable  $H_2O_2$  that is released by the bacteria into the supernatant (24, 25). A second contributor to the pool of H<sub>2</sub>O<sub>2</sub> released by bacteria is the enzyme lactate dehydrogenase (LctO), which converts lactate to pyruvate (24, 26). While the mechanism by which S. pneumoniae kills S. aureus strains has been related to production of  $H_2O_2$ , only spxB mutants have been assessed (20, 27).

SpxB-produced  $H_2O_2$  has also been involved in inducing cytotoxicity to lung cells, apoptosis, and the toxic events observed when *S. pneumoniae* invades the central nervous system and heart, albeit the specific mechanism(s) mediating this damage is still to be clarified (12, 13). Moreover, *S. pneumoniae* mutants in the *spxB* gene produced less capsule, due to the lack of acetylated capsule precursors, and were attenuated for virulence in mouse models of pneumococcal disease (25, 28). The attenuated virulence phenotype can be explained in part by a recent publication showing that endogenously produced  $H_2O_2$  was required to release the toxin pneumolysin (29).

In contrast to the *in vitro* evidence presented above, studies conducted using an animal model of colonization demonstrated that *S. aureus* colonized the nasal cavity of neonatal rats even when it was inoculated concurrently with *S. pneumoniae* strain

TIGR4 or with an  $H_2O_2$ -deficient TIGR4  $\Delta spxB$  mutant (30). When the TIGR4 wild type (wt) or an isogenic TIGR4  $\Delta spxB$  mutant was inoculated along with *S. aureus* in animals, *S. aureus* colonization densities were similar whether *S. pneumoniae* produced hydrogen peroxide or not (30, 31). Therefore, the role of *S. pneumoniae*-produced  $H_2O_2$  in interfering with *S. aureus* growth has been debated (32). Killing of *S. aureus* by incubation with pure  $H_2O_2$ , however, has already been documented (33, 34). A dose of ~10 mM  $H_2O_2$  was required to kill *S. aureus* bacteria (19), whereas preloading *S. aureus* with iron reduced the bactericidal dose to ~1 mM (33, 34). The presence of intracellular iron was required to generate, by the Fenton reaction, the hydroxyl radical (OH) (34), which is a stronger oxidant than  $H_2O_2$  itself (35). Other bacterial species are also susceptible to  $H_2O_2$  at a concentration similar to that killing *S. aureus*, with ~2.5 mM  $H_2O_2$  showing the maximal killing rate for *Escherichia coli* (35–37).

We recently demonstrated that the *S. pneumoniae*-induced killing of *S. aureus* biofilms, including those formed by methicillin-resistant *S. aureus* (MRSA) strains, was enhanced by physical contact (23). Complete eradication of  $\sim 10^9$  *S. aureus* bacteria within *S. pneumoniae-S. aureus* biofilms occurred within 4 h of incubation. Furthermore, washed *S. pneumoniae* bacteria were more lethal to *S. aureus* strains than their  $\rm H_2O_2$ -containing supernatants, suggesting pneumococcal cells may be required to convert  $\rm H_2O_2$  into a more potent intoxicant (23). Moreover, our studies and those of others (19, 38) demonstrated that, when *S. aureus* has been completely killed, *S. pneumoniae* produced significantly less  $\rm H_2O_2$  (e.g., TIGR4,  $< 200~\mu$ M) than the demonstrated minimal bactericidal concentration (MBC) of pure  $\rm H_2O_2$  (10 mM) for *S. aureus* strains (19, 38).

In this study, we used *in vitro* models mimicking *S. pneumoniae-S. aureus* cocolonization of the upper airways and demonstrated that an outcompeting density of *S. pneumoniae* was necessary to kill *S. aureus*. We also demonstrated that the interaction between *S. pneumoniae* and *S. aureus* stimulates the conversion of hydrogen peroxide into the strongest oxidative radical, hydroxyl (OH), which reacts at nearly diffusion rates with most substrates, inducing DNA degradation and leading to the intoxication and death of *S. aureus* bacteria. The target(s) of the OH radicals represents an exciting new alternative for the development of therapeutics against *S. aureus* infections.

#### **RESULTS**

Contact-mediated killing of S. aureus by S. pneumoniae requires a threshold **pneumococcal density.** We previously demonstrated that killing of *S. aureus* strains by S. pneumoniae in liquid cultures required physical contact (23). We therefore reasoned that killing was likely to occur on solid media and designed a contact-mediated killing assay on blood agar plates. In this assay, we inoculated increasing densities of earlylog-phase cultures of S. pneumoniae with different densities of S. aureus (i.e., 106 CFU/ml of S. aureus versus 106, 107, 108, or 109 CFU/ml of S. pneumoniae), and the plates were incubated overnight. In most mixtures where the density of S. pneumoniae outcompeted that of S. aureus by at least 2 log units (i.e., S. pneumoniae, 108 CFU/ml, and S. aureus, 106 CFU/ml), S. pneumoniae completely eradicated S. aureus (Fig. 1A). S. pneumoniae inoculated at 109 CFU/ml eradicated all S. aureus inocula. Similar results were obtained when two other S. aureus strains, NRS170 and NRS408, were assessed (not shown). To confirm the killing of S. aureus and the observed loss of chromosomal DNA observed by confocal microscopy (explained below), we isolated DNA from each mixture presented in Fig. 1A or single cultures (control). The DNA was used as a template in quantitative PCRs (qPCRs) targeting either S. pneumoniae or S. aureus. As expected, the number of genome equivalents (GenEqu) of S. aureus per milliliter did not change when the density outcompeted that of S. pneumoniae (not shown). When DNA was isolated from experiments where the S. pneumoniae density was greater than that of S. aureus, a density-dependent decrease of S. aureus GenEqu per milliliter was observed to a point where DNA from S. aureus was no longer detected (Fig. 1B to D; see Fig. S1 in the supplemental material). The number of GenEqu per milliliter of S. pneumoniae DNA (median,  $1.4 \times 10^9$  GenEqu/ml) was not affected by incubation with

Wu et al. Journal of Bacteriology

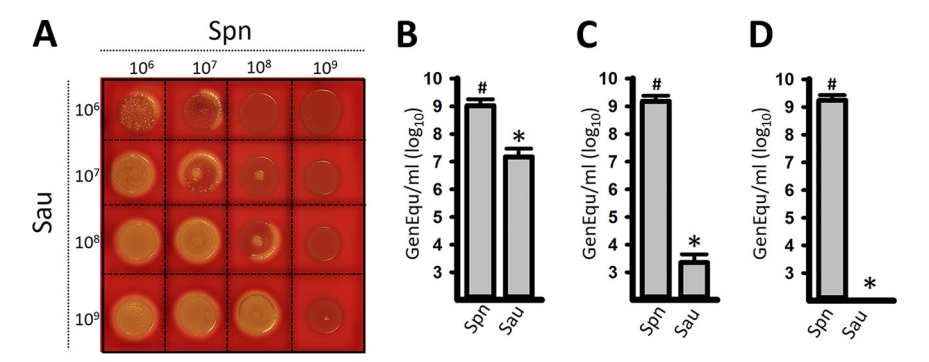


FIG 1 Contact-, and density-dependent killing of S. aureus (Sau) by S. pneumoniae (Spn). (A) S. pneumoniae strain TIGR4 and S. aureus strain Newman were inoculated concurrently at the indicated densities (CFU per milliliter). Once inoculated, the plates were incubated for 24 h at 37°C. (B to D) To quantify genome equivalents per milliliter of S. pneumoniae or S. aureus, bacteria growing on spots inoculated with 108 CFU/ml of S. pneumoniae and 108 (B), 107 (C), or 106 (D) CFU/ml of S. aureus were collected; DNA was extracted; and the DNA was used as a template in species-specific qPCRs. The error bars represent the standard errors of the means calculated using data from at least three independent experiments. \*, P < 0.05 compared to S. aureus control incubated alone; #, P > 0.67 compared to S. pneumoniae control inoculated alone.

any density of S. aureus. Density-dependent killing of S. aureus was also confirmed by culture (see Fig. S2 in the supplemental material).

Confocal micrographs using antibodies against their capsules showed that, when inoculated at similar densities (i.e., ~106 CFU/ml), S. pneumoniae and S. aureus were observed intact and with areas of strong colocalization (Fig. 2, bottom row, arrowheads). DAPI (4',6-diamidino-2-phenylindole) staining showed DNA from both species. In micrographs where S. pneumoniae outcompeted S. aureus (e.g., S. pneumoniae,  $\sim 10^7$ 

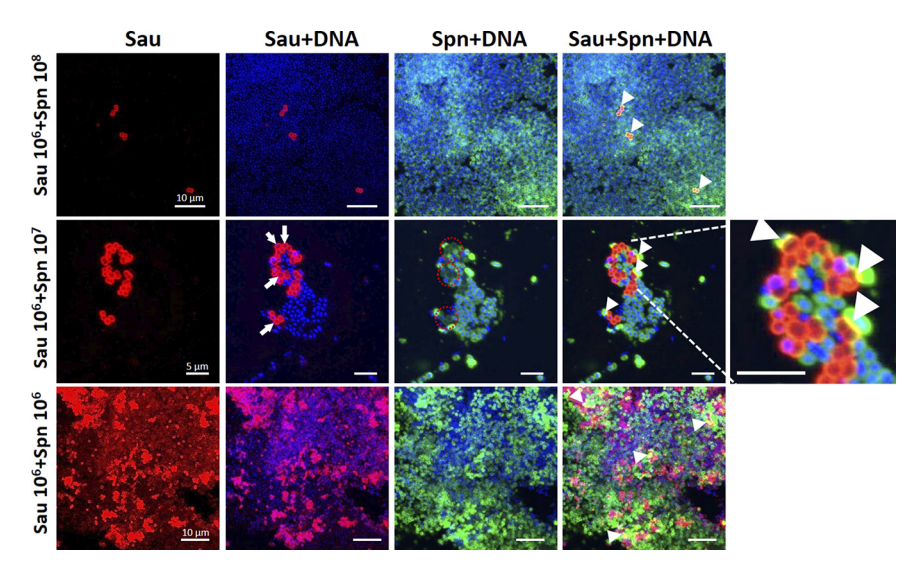


FIG 2 S. pneumoniae (Spn) contact-dependent killing of S. aureus (Sau) induces loss of DNA signal. Bacteria growing on blood agar plates from the experiments presented in Fig. 1, inoculated with the specific density of each species shown on the left, were imprinted onto glass slides. The preparations were fixed with paraformaldehyde, and S. aureus bacteria were stained with an anti-S. aureus antibody followed by an anti-rabbit Alexa Fluor 555-labeled antibody. S. pneumoniae was stained with an Alexa Fluor 488-labeled anti-S. pneumoniae antibody, while the DNA was stained with DAPI. The preparations were analyzed with a confocal microscope. Shown are 3D reconstructions of z stacks obtained from xv optical sections. The specific channel of each panel is shown at the top. The arrows point to S. aureus bacteria stained red with a loss of DNA signal, while the red dashed circles indicate areas where DNA signal is missing, corresponding to the arrows. The arrowheads show physical colocalization (yellow) of S. aureus and S. pneumoniae. The dimensions of the scale bars shown in the left column apply to all the images in the same row. The image on the far right was digitally enlarged to show details of the area indicated by the dashed lines.

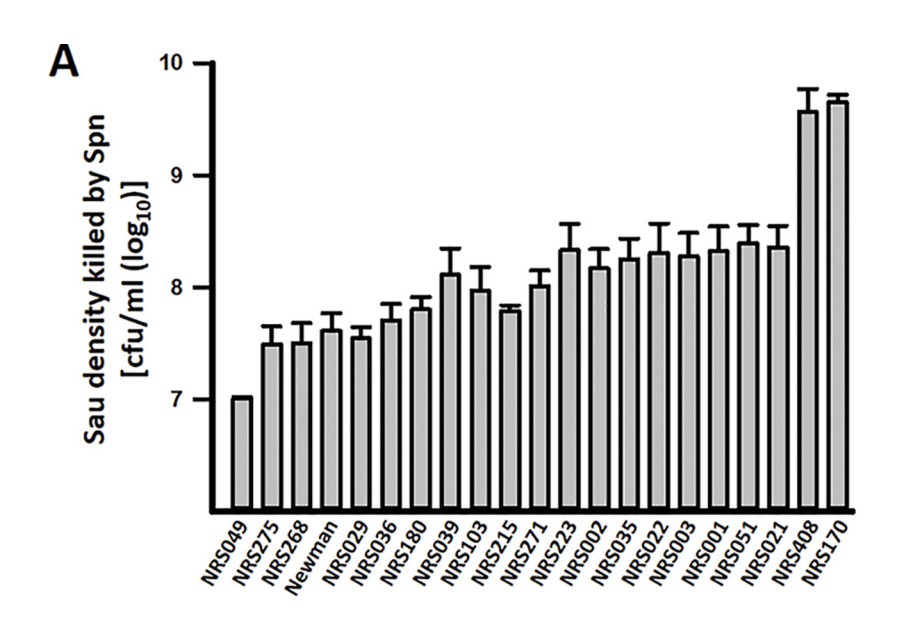
CFU/ml versus *S. aureus*,  $\sim 10^6$  CFU/ml), only a few *S. aureus* cells were observed in comparison to the abundant pneumococci (Fig. 2, middle and top rows). Moreover, three-dimensional (3D) reconstruction of z stacks revealed that, in the majority of *S. aureus* cells in mixtures with outcompeting *S. pneumoniae*, the DAPI signal was absent, suggesting that the DNA had been degraded (Fig. 2, arrows). Absence of DNA in *S. aureus* particularly coincided with the bacteria colocalizing with *S. pneumoniae* (Fig. 2, enlarged image). Together, these results identified dose- and contact-dependent killing of *S. aureus* by *S. pneumoniae* that included DNA degradation.

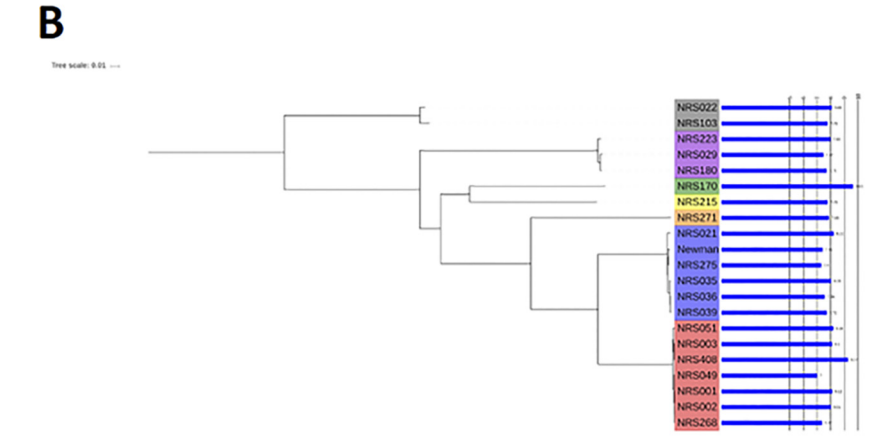
Differential sensitivities of S. aureus strains to killing by S. pneumoniae. Different S. aureus strains have distinct sensitivities to H<sub>2</sub>O<sub>2</sub> killing; thus, it was possible that the results described above were not representative. We therefore tested a collection of 20 MRSA (including vancomycin-intermediate S. aureus [VISA]) and methicillinsusceptible S. aureus (MSSA) strains from seven clonal complexes (see Table S1 in the supplemental material) for their sensitivities to killing when incubated along with S. pneumoniae. To quantify the maximum density of S. aureus killed by S. pneumoniae, we utilized a microplate model with 4 h of coculture incubation at 37°C. All the S. aureus strains were killed by S. pneumoniae, but we noted statistically significant differences across strains (P = 0.002) (Fig. 3A). The most sensitive strain, NRS170, had a 426-fold difference (P = 0.008) in sensitivity to S. pneumoniae compared to the most resistant strain, NRS049 (Fig. 3A; see Table S1). Increased sensitivity of NRS170 to S. pneumoniae killing was also observed using the plate-killing model (not shown). The rest of the strains, including S. aureus strain Newman, showed linear distributions in their sensitivities to S. pneumoniae ( $R^2 = 0.95$ ) that spanned an  $\sim 30$ -fold range. The variability among this group (excluding NRS170 and NRS408) was also statistically significant (P = 0.05). Surprisingly, there was no association between the clonal complex and sensitivity to S. pneumoniae (Fig. 3B).

Hydrogen peroxide has been implicated as the main factor produced by *S. pneumoniae* to kill *S. aureus* strains (14, 20). We hypothesized that the level of sensitivity of an *S. aureus* strain to  $H_2O_2$  correlated with sensitivity to *S. pneumoniae* killing. Differential sensitivity to  $H_2O_2$  was observed in our experiments, with the growth of some strains (i.e., NRS3 and NRS21) completely inhibited by  $H_2O_2$  whereas a subset of strains were not susceptible at all to challenge with even 5 mM  $H_2O_2$  (not shown). However, contrary to our hypothesis, the level of *S. pneumoniae* killing did not correlate with retardation of growth by  $H_2O_2$  (Fig. 3C). These results showed that there was a complex genetic relationship between the ability to grow in the presence of hydrogen peroxide and the degree of sensitivity to *S. pneumoniae* killing. The finding that the genetic background (clonal complex) was not strongly associated with the level of killing suggests that recently acquired mutations may play a major role in determining the level of susceptibility of each individual *S. aureus* strain.

Resistant S. aureus strains can protect sensitive strains from killing by S. pneumoniae. To study the effect of S. pneumoniae sensitivity on S. aureus strain selection, we utilized one of the most sensitive strains (NRS408) and one of the most resistant strains (NRS049). Strain NRS049 was resistant to tetracycline, and we isolated an NRS408-derived rifampin-resistant mutant (NRS408J) to track the growth of the strain. There was a significant difference between strains NRS049 and NRS408J (P < 0.05) in *S. pneumoniae* sensitivity (Fig. 4A). There was no significant difference in NRS049 S. pneumoniae sensitivity measurements or NRS408 relative to NRS408J measurements between results presented in Fig. 3A and 4A. We then competed the resistant NRS049 strain and the sensitive NRS408J strain (5 imes 10 $^6$  CFU/ml of each strain, the minimum concentration at which NRS049 was predicted to survive) in the presence of TIGR4 (1.5  $\times$  10 $^7$  CFU/ml). While this dose of *S. pneumoniae* killed NRS408J but not the NRS049 strain, coincubation of the two S. aureus strains led to survival of both under S. pneumoniae challenge (Fig. 4B). Given that killing of S. aureus is density dependent, to determine whether this competition outcome was affected by the S. aureus strain density, we performed several endpoint S. aureus growth assays over a

Wu et al. Journal of Bacteriology





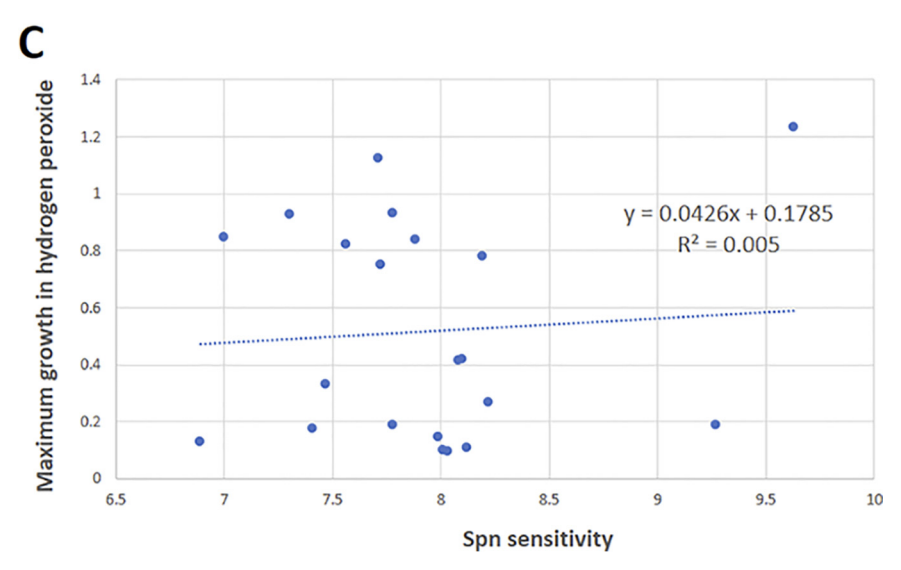
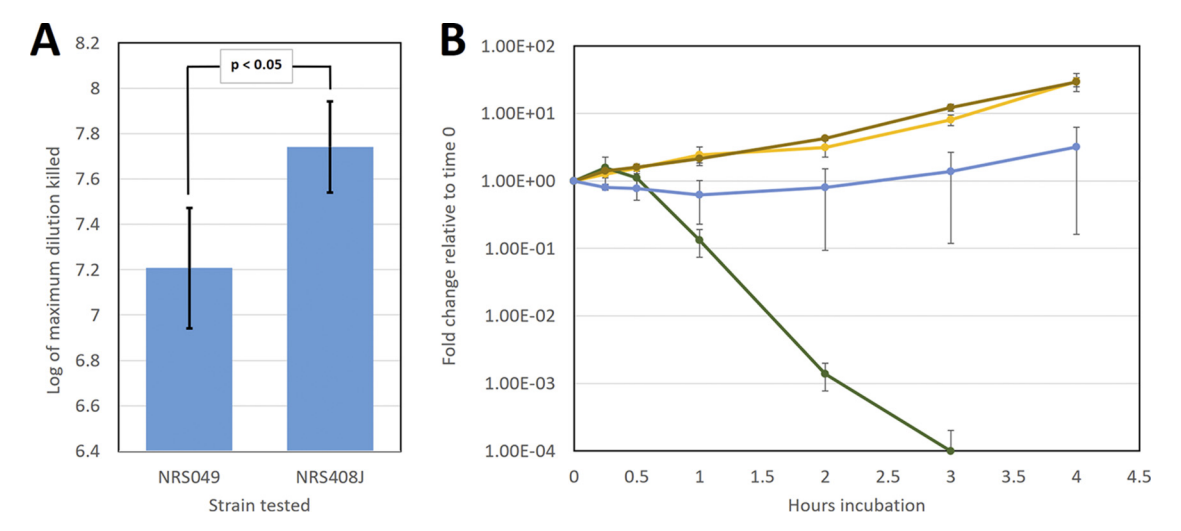


FIG 3 Variability in S. aureus (Sau) strain sensitivity to S. pneumoniae (Spn). (A) Decreasing densities of the indicated S. aureus strains spanning  $\sim 1 \times 10^{10}$  and  $\sim 1 \times 10^6$  CFU/ml were cocultured with  $1.5 \times 10^7$ CFU/ml of S. pneumoniae in THY and incubated for 4 h at 37°C. Cultures were serially diluted and plated on TSA supplemented with optochin. The maximum S. aureus inoculum completely killed by  $1.5 \times 10^7$ CFU/ml of S. pneumoniae was then determined from the maximum concentration killed. The standard errors of the mean of three independent experiments are shown. (B) Maximum-likelihood phylogeny of (Continued on next page)



**FIG 4** Competition between *S. pneumoniae*-sensitive and *S. pneumoniae*-resistant *S. aureus* strains in the presence of *S. pneumoniae*. (A) Sensitivities of *S. aureus* strains NRS049 and NRS408J to *S. pneumoniae* (TIGR4) killing. Sensitivity was measured as described in the legend to Fig. 3A. The results represent three biological replicates and two independent experiments. The results are presented with two standard errors above and below the mean. (B) Competition experiments between resistant (NRS049) and sensitive (NRS408J) *S. aureus* strains (5e6 CFU/ml) in the presence of *S. pneumoniae* (TIGR4; 1.5e7 CFU/ml). Strains NRS049, NRS408J, and TIGR4 at the previously stated doses were cocultured in THY for 4 h at 37°C without agitation. Coculture samples were collected at 0 min, 15 min, 1 min, 1 h, 2 h, 3 h, and 4 h. Coculture sample dilutions were then spotted on TSA supplemented with  $16 \mu g/ml$  tetracycline or  $4 \mu g/ml$  rifampin and grown overnight at 37°C to determine the concentrations of NRS049 and the NRS408 rifampin-resistant mutant (NRS408J) at corresponding time points. The fold change of the rifampin-resistant mutant NRS408J relative to time zero is shown with TIGR4 alone (green), TIGR4 and NRS049 (blue), NRS049 (brown), and the mutant itself alone (yellow). The results represent three biological replicates and are presented with one standard error above and one below the mean.

range of NRS049 and NRS408J densities (see Table S2 in the supplemental material). The sensitive NRS408J survived under all conditions under which the resistant NRS049 strain survived, regardless of whether the total *S. aureus* dose was  $5 \times 10^6$  CFU/ml or more (see Table S2).

Mutations in spxB and IctO are required to inhibit S. pneumoniae killing of S. aureus. The experiments shown in Fig. 3 suggested that killing of S. aureus strains was not the sole consequence of exposure to  $H_2O_2$ . In S. pneumoniae, most  $H_2O_2$  (~85%) is produced during the oxidation of pyruvate to acetyl-phosphate (acetyl∼P) by SpxB (Fig. 5A). Although to a lesser extent, hydrogen peroxide is also produced during the oxidation of lactate to pyruvate by the enzyme LctO (Fig. 5A) (26). To gain insight into this contact-dependent, molecular-mechanism-mediated killing of S. aureus, we generated single ΔspxB and ΔlctO mutants and a ΔspxB ΔlctO double mutant in TIGR4. We then assessed killing of S. aureus by these mutants using our density-controlled experimental models. When incubated along with  $\sim 10^7$  CFU/ml S. aureus in the contact-dependent plate model, the TIGR4  $\Delta lctO$  mutant killed S. aureus to the same extent as the TIGR4 wild-type strain at all tested S. pneumoniae densities (Fig. 5B). At a density of ~10° CFU/ml, TIGR4 ΔspxB did not kill S. aureus. Surprisingly, TIGR4 ΔspxB killed S. aureus when we increased the challenge density to >108 CFU/ml (Fig. 5B). S. pneumoniae strain Pn20, isolated from the nasopharynx of a child (20), and its ΔspxB mutant derivative were also tested with essentially similar results (i.e., an increased density killed S. aureus [data not shown]). Furthermore, a similar 100-fold-increased density of TIGR4 ΔspxB killing S. aureus, in comparison to the TIGR4 wild type, was observed when another S. aureus strain, NRS049, was challenged (Fig. 5C). These results

#### FIG 3 Legend (Continued)

strains tested with  $\log_{10}$  bactericidal efficiency of *S. pneumoniae* plotted as a bar chart. The clonal complex designation of each strain is shown by the color range. (C) Maximum growth (OD<sub>600</sub> measured after 12 h of incubation at 37°C) in hydrogen peroxide (2.5 mM)-supplemented TSB plotted against *S. pneumoniae* sensitivity of the corresponding strain. The values represent averages from at least three replicates for each strain.

Wu et al. Journal of Bacteriology

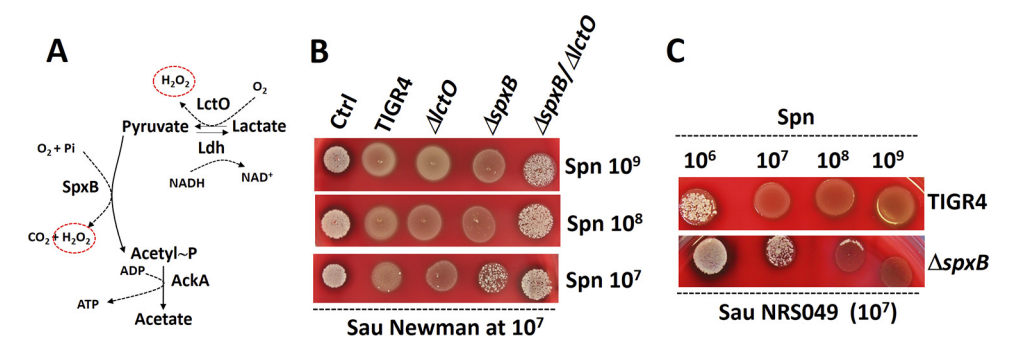
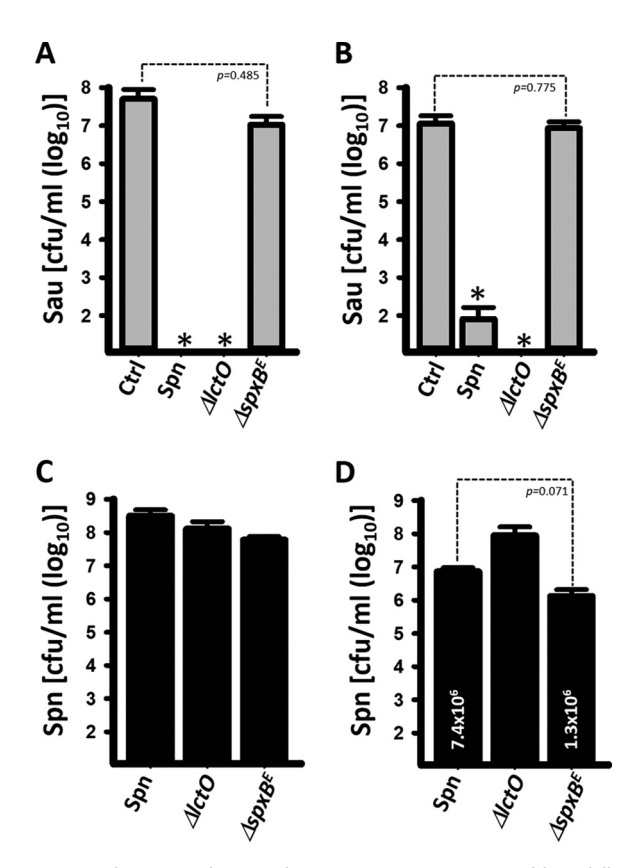


FIG 5 S. pneumoniae (Spn) contact-mediated killing of S. aureus (Sau) requires enzymes SpxB and LctO. (A) Oxidation of pyruvate to acetyl~P by the enzyme pyruvate oxidase (SpxB). The reaction uses molecular O<sub>2</sub> and inorganic phosphate  $(P_i)$ , producing  $CO_2$  and  $H_2O_2$  (circled). Acetyl $\sim P$  is then converted to acetyl coenzyme A by acetate kinase (AckA) in a reaction that produces ATP. The enzyme lactate oxidase (LctO) catalyzes the formation of pyruvate from lactate, producing H<sub>2</sub>O<sub>2</sub>. (B) S. pneumoniae strains TIGR4, TIGR4 ΔIctO, TIGR4 ΔspxB, and TIGR4 ΔspxB ΔlctO were inoculated on blood agar plates at the densities indicated on the right (CFU per milliliter) concurrently with S. aureus strain Newman, which was inoculated at a density of  $\sim 10^7$  CFU/ml. (C) S. pneumoniae strains were inoculated at the densities shown at the top concurrently with S. aureus strain NRS049, inoculated at  $\sim 10^7$  CFU/ml. The agar plates were incubated overnight at 37°C.

suggested that H<sub>2</sub>O<sub>2</sub> generated by LctO was sufficient to induce killing of S. aureus. Confirming this, the TIGR4 \( \Delta spx B \( \Delta lctO \) mutant was unable to kill \( S. \) aureus even at a high density of  $\sim 10^9$  CFU/ml (Fig. 5B).

We then used the microplate model to quantitatively assess S. aureus killing by these mutant strains. Experiments revealed that neither planktonic S. aureus nor biofilm S. aureus cells were killed by TIGR4 ΔspxB in comparison with the wild-type strain (Fig. 6A and B). The same phenotype was observed when two other independent TIGR4-derived ΔspxB mutants were tested (see Fig. S3 in the supplemental material). Similar to what we observed using the plate model, the TIGR4 Δ/ctO mutant killed S. aureus strains at rates similar to that of wild-type TIGR4 (Fig. 6A and B). As expected, as a mutation in spxB was enough to block S. aureus killing in this model, the  $\Delta$ spxB  $\Delta$ lctO double mutant was unable to kill S. aureus strain Newman (not shown). Under the culture conditions utilized (i.e., incubation in Todd-Hewitt broth containing 0.5% [wt/vol] yeast extract [THY], with environmental oxygen and 5% CO<sub>2</sub>), S. pneumoniae strains TIGR4 and TIGR4  $\Delta lctO$  produced, after 4 h of incubation, ~180  $\mu$ M and ~140  $\mu$ M H<sub>2</sub>O<sub>2</sub>, respectively (Table 1). Cultures of three different spxB mutants, however, yielded undetectable levels of hydrogen peroxide (Table 1). Overall, our experiments demonstrated that both H<sub>2</sub>O<sub>2</sub>-producing enzymes, SpxB and LctO, contribute to the contact-dependent killing of S. aureus strains.

A hydroxyl radical (OH) is generated during the interaction between S. pneumoniae and S. aureus to rapidly kill S. aureus. Given that our experiments demonstrated that even  $\sim$ 5 mM pure  $H_2O_2$  did not affect the viability of some *S. aureus* strains (Fig. 3) but that cultures of the same strains were killed by S. pneumoniae producing  $\sim$ 36-fold less H<sub>2</sub>O<sub>2</sub> (i.e.,  $\sim$ 140  $\mu$ M), the possibility was raised that SpxB/LctO-produced H<sub>2</sub>O<sub>2</sub> was converted into the OH radical. To test this hypothesis, we first conducted a dose-response study to identify three sublethal doses of H<sub>2</sub>O<sub>2</sub> for S. aureus, 1.0, 1.2, and 1.4 mM (Fig. 7). For example, 1 mM  $H_2O_2$  allowed the survival of  $>1 \times 10^6$  CFU/ml S. aureus when challenged against three different S. aureus strains (Fig. 7). We reasoned that if H<sub>2</sub>O<sub>2</sub> is converted to a hydroxyl radical, then incubating S. aureus, TIGR4 ΔspxB (which does not produce significant amounts of H<sub>2</sub>O<sub>2</sub>), and a sublethal dose of H<sub>2</sub>O<sub>2</sub> would allow killing. As shown in Fig. 7, the density of any of the three S. aureus strains incubated with TIGR4 ΔspxB was similar to the density in control wells containing S. aureus alone (Fig. 7A to C). Incubation of S. aureus; TIGR4 ΔspxB; and 1.0, 1.2, or 1.4 mM H<sub>2</sub>O<sub>2</sub> was sufficient to completely eradicate cultures of S. aureus strain Newman, NRS408, and NRS049, respectively. Experiments with S. aureus strain Newman incubated with TIGR4  $\Delta spxB$   $\Delta lctO$  and 1 mM  $H_2O_2$  showed essentially the same result



**FIG 6** A mutation in spxB, but not in IctO, renders S. pneumoniae (Spn) unable to kill S. aureus (Sau) in a microplate model. S. aureus strain Newman ( $\sim 1 \times 10^6$  CFU/ml) was inoculated alone (Ctrl) or along with the indicated S. pneumoniae strains ( $\sim 1 \times 10^6$  CFU/ml) in microplates containing THY and incubated for 4 h at 37°C. Bacteria were harvested and then diluted and plated onto SMA (A and B) or BAP with gentamicin (C and D) to obtain counts of S. aureus planktonic cells (A), S. aureus biofilms (B), S. pneumoniae planktonic cells (C), or S. pneumoniae biofilms (D). The error bars represent the standard errors of the means calculated using data from at least three independent experiments. (A and B) \*, P < 0.05 compared to S. aureus control incubated alone. (D) For comparison, the median (CFU per milliliter) is shown inside two of the bars.

(Fig. 7D). These experiments strengthened our hypothesis that  $\rm H_2O_2$  was converted into a hydroxyl radical (OH).

Thiourea (15 mM), sodium salicylate, and dimethyl sulfoxide (Me<sub>2</sub>SO [300 mM]), are specific OH scavengers (34); thiourea and Me<sub>2</sub>SO reduced H<sub>2</sub>O<sub>2</sub> killing of *S. aureus* by 98% and 38%, respectively (34). As shown in Fig. 8A, incubating *S. aureus* strain Newman, *S. pneumoniae*, and 10 mM thiourea was enough to significantly inhibit killing of *S. aureus*, whereas 20 mM and 40 mM completely inhibited H<sub>2</sub>O<sub>2</sub>-mediated killing. The density of *S. pneumoniae* was not affected by incubation with any amount of thiourea (Fig. 8B). Similar protection from challenge with *S. pneumoniae* was conferred on *S. aureus* by incubating the two species, along with a scavenger of hydroxyl radicals, Me<sub>2</sub>SO (Fig. 8C and D) or sodium salicylate (see Fig. S4 in the supplemental material).

**TABLE 1** Production of H<sub>2</sub>O<sub>2</sub> by TIGR4 and isogenic derivative mutants

	Production of H <sub>2</sub> O <sub>2</sub> at (h):			
Strain	0	1	2	4
TIGR4	5.7 μM	35.6 μM	50.3 μM	179.6 μΜ
TIGR4 ∆ <i>lctO</i>	<50 nM <sup>a</sup>	$9.9 \mu\text{M}$	$45.1 \mu M$	136.3 $\mu$ M
TIGR4 ΔspxB <sup>U</sup>	<50 nM	<50 nM	<50 nM	<50 nM
TIGR4 $\Delta spxB^{E}$	<50 nM	<50 nM	<50 nM	<50 nM
TIGR4 $\Delta spxB^{E}$ $\Delta lctO$	<50 nM	<50 nM	<50 nM	<50 nM

<sup>&</sup>lt;sup>a</sup>Limit of detection.

Wu et al. Journal of Bacteriology

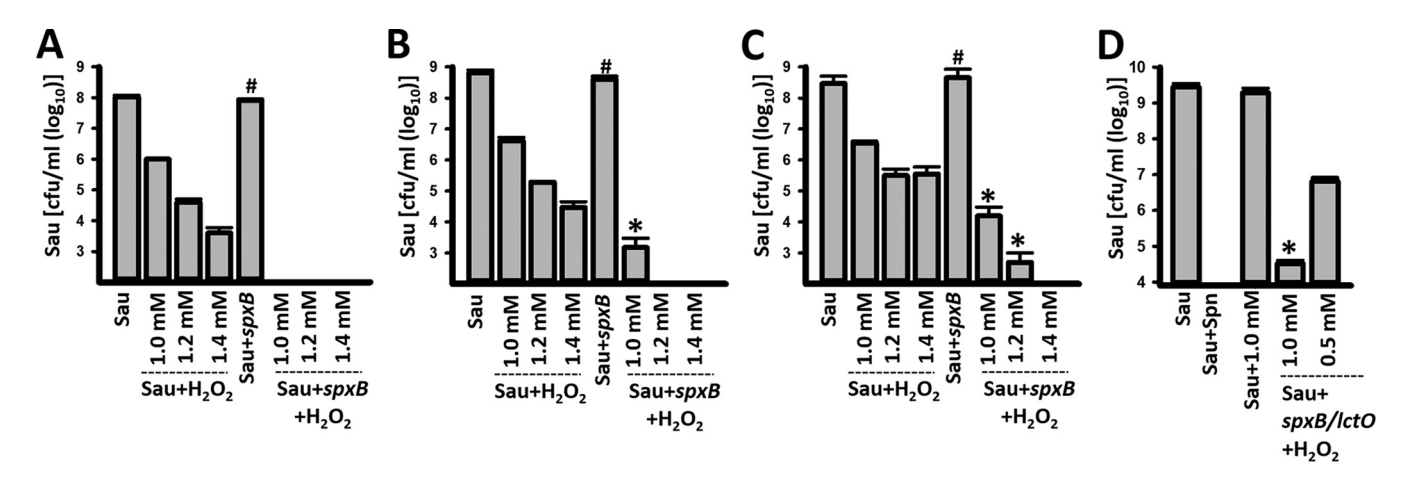


**FIG 7** *S. pneumoniae* (Spn) produces a stronger oxidant from  $H_2O_2$  to kill *S. aureus* (Sau) strains. *S. aureus* strain Newman (A and D), NRS408 (B), or NRS049 (C) was incubated alone at a density of  $\sim$ 1 × 10° CFU/ml, with the indicated molarity of  $H_2O_2$ , TIGR4  $\Delta spxB$  ( $\sim$ 1 × 10° CFU/ml), TIGR4  $\Delta spxB$  ( $\sim$ 1 × 10° CFU/ml) and  $H_2O_2$  or with TIGR4  $\Delta spxB$  *lctO* ( $\sim$ 1 × 10° CFU/ml). Bacteria were incubated for 4 h at 37°C and then harvested, diluted, and plated on SMA to obtain counts of *S. aureus*. The error bars represent the standard errors of the means calculated using data from at least three independent experiments. \*, P < 0.05 compared to the corresponding concentration of  $H_2O_2$ ; #, P > 0.30 compared to *S. aureus* control incubated alone.

To identify the *in vivo* formation of hydroxyl radicals, we utilized the  $\alpha$ -(4-pyridyl-1-oxide)-*N-tert*-butyl nitrone (4-POBN)– ethanol spin-trapping system. Figure 9 shows a marked increase in the hydroxyethyl radical spin adduct in bacterial cells of the TIGR4 wt in comparison to signals from a reaction mixture containing TIGR4 wt cells and a

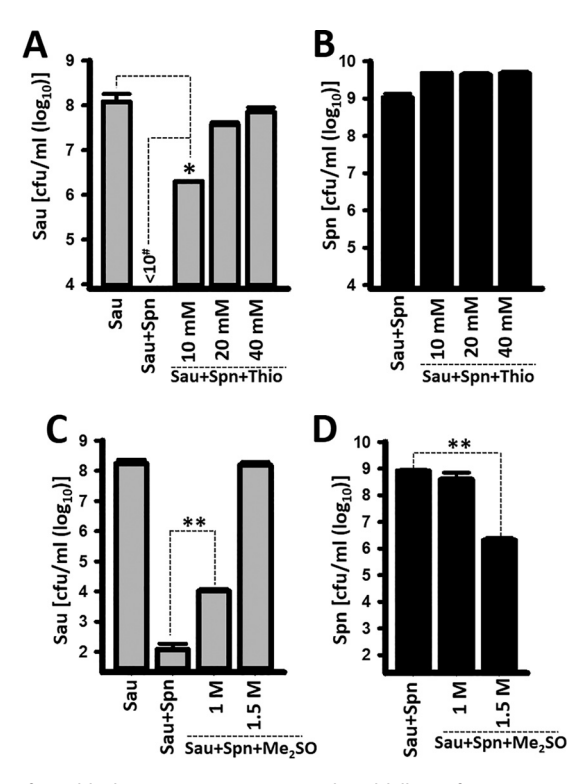


**FIG 8** Scavengers of OH block *S. pneumoniae* (Spn)-induced killing of *S. aureus* (Sau). *S. aureus* strain Newman was inoculated ( $\sim$ 1  $\times$  10° CFU/ml) alone, with *S. pneumoniae* TIGR4 ( $\sim$ 1  $\times$  10° CFU/ml), with *S. pneumoniae* and thiourea (Thio), or with *S. pneumoniae* and Me<sub>2</sub>SO. After 4 h of incubation at 37°C, bacteria were harvested, diluted, and plated to obtain counts of *S. aureus* (A and C) or *S. pneumoniae* (B and D). The error bars represent the standard errors of the mean calculated using data from at least three independent experiments. \*, P < 0.05 compared with *S. aureus* control; \*\*, P < 0.005 compared to the density of *S. aureus* incubated with *S. pneumoniae*; #, limit of detection.

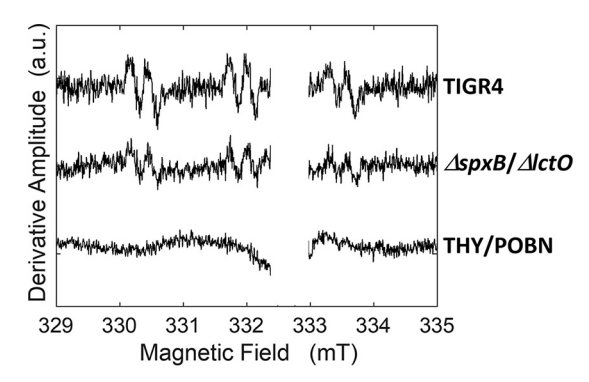


**FIG 9** Detection of OH radicals in pneumococci by 4-POBN and DETAPAC-ethanol spin trapping. Shown are the EPR spectra of 4-POBN spin trapping in wild-type and double-mutant samples and, for comparison, a medium-only sample. The unassigned signal near the free-electron g value of 2.0023 (333.0 mT) was deleted. The EPR conditions were as follows: microwave frequency, 9.346 GHz; microwave power, 10 mW; modulation amplitude, 0.2 mT; modulation frequency, 100 kHz; temperature, 295 K. The spectra of wild-type and double-mutant samples represent an average of 96 scans minus the bacterial-medium spectrum. The bacterial-medium spectrum represents an average of 224 scans, with polynomial baseline correction. The spectra were baseline corrected using a polynomial function.

reaction mixture with bacterial cells harvested from cultures of the TIGR4  $\Delta spxB$   $\Delta lctO$  double mutant.

#### **DISCUSSION**

We have demonstrated in this study that the interaction between *S. pneumoniae* and *S. aureus* stimulates the conversion of  $H_2O_2$  into a stronger oxidant, the hydroxyl radical, OH, to rapidly kill *S. aureus* bacteria. The toxic effects of several pneumococcal strains against *S. aureus* have been documented (14, 19, 20, 23, 27, 38). Hydrogen peroxide had long been believed to be the killing factor, but contrasting data suggesting that  $H_2O_2$  was not required for killing have been published in the last few years (23, 30–32). Compelling evidence within this study has now identified highly reactive OH radicals generated from  $H_2O_2$ , because of interaction between the species, as the effector of such a mechanism. Given that  $H_2O_2$  is permeable but a sublethal dose of  $H_2O_2$  killed *S. aureus* strains when incubated along with  $H_2O_2$ -deficient *S. pneumoniae* strains, the conversion to OH radicals may be facilitated by pneumococcal cells. Certainly, other possibilities exist, including increased free Fe<sup>2+</sup> in *S. aureus* due to the interaction with *S. pneumoniae*, which could be the result of stimulated iron uptake. The OH generated reacts at nearly diffusion-limited rates near the site of its generation (22, 39).

Although S. aureus can also produce H<sub>2</sub>O<sub>2</sub>, its potent catalase fully scavenges the H<sub>2</sub>O<sub>2</sub> before it can cross the cytoplasmic membrane, and therefore, levels of hydrogen peroxide in the supernatant are undetectable (19). Intracellular levels of H<sub>2</sub>O<sub>2</sub> in S. aureus have not been investigated, but in E. coli, these levels are maintained at 0.1 to  $0.2~\mu M$  during aerobic growth (40). Therefore, the experiments in this study, along with data from other laboratories (14, 19, 20, 31, 41), support a model where S. pneumoniae secretes large amounts of H<sub>2</sub>O<sub>2</sub> near S. aureus bacteria—but beyond a concentration that catalase would successfully scavenge—and then, due to a still unknown mechanism, it is rapidly converted into 'OH radicals that intoxicate S. aureus cells. We hypothesize that the target(s) of 'OH radicals on S. aureus cells is absent in pneumococci, and therefore, S. pneumoniae is less susceptible to these radicals (see below for more details). S. aureus intoxication with 'OH radicals may be accompanied by degradation of DNA, as confocal micrographs and quantitative PCRs demonstrated absence of DNA in S. aureus bacteria incubated with H<sub>2</sub>O<sub>2</sub>-producing S. pneumoniae. Hydroxyl radicals attack at the sugar or the base of the DNA, leading to sugar fragmentation, base loss, and a strand break with a terminal fragmented sugar residue (42). The resistance of S. pneumoniae to DNA damage has been speculated to occur by sequestration of Fe<sup>2+</sup>, required to produce OH through the Fenton reaction, away from its DNA (22).

Animal studies demonstrated that S. pneumoniae (TIGR4) and S. aureus (Newman) cohabited in the nasal cavities of rats when the strains were inoculated at the same density (30, 31). One would expect that in this animal cocolonization model, only S. pneumoniae would be able to colonize, but this outcome did not occur. Instead, coinoculation of wild-type S. pneumoniae did not affect colonization by S. aureus, and neither a mutation in the pneumococcal spxB gene nor a mutation in the S. aureus katG gene (encoding catalase) had a positive or negative effect, respectively, on S. aureus density. If S. pneumoniae kills S. aureus, why did they cocolonize? Experiments in this study offer an explanation. When TIGR4 and S. aureus strain Newman were inoculated at similar densities, S. aureus in fact survived the challenge with S. pneumoniae (Fig. 1). However, with an outcompeting density of S. pneumoniae, staphylococci succumbed to the challenge. The killing was negated when S. aureus was incubated with the hydrogen peroxide production-defective S. pneumoniae ΔspxB ΔlctO mutant. We speculate that, in the surface-bound environment of the nasal cavity of rats or in the plate model, the close proximity of S. pneumoniae to S. aureus allows inactivation of H<sub>2</sub>O<sub>2</sub> by the S. aureus-produced catalase but that increased production of H<sub>2</sub>O<sub>2</sub> (i.e., by outcompeting pneumococci) overcomes the catalase-mediated inactivation, and thus, H<sub>2</sub>O<sub>2</sub> is converted into OH radicals. We hypothesize that the conflicting results obtained in population studies where a negative association, or no association, has been demonstrated between concurrent carriage (i.e., colonization) of S. pneumoniae and S. aureus would have been resolved if the density of the strains had been taken into consideration.

The finding that the level of sensitivity is variable across S. aureus strains (Fig. 3A) and the surprising result that S. pneumoniae and  $H_2O_2$  sensitivity in S. aureus are not correlated (Fig. 3B) suggest that other, undiscovered factors modulate S. aureus killing. We found that S. aureus strains can apparently cross-protect in mixtures, suggesting that a diffusible molecule is possibly involved. This result needs to be followed up in future work. Since the phenotype is variable across S. aureus strains without being closely linked to a particular clade, it may be possible to identify the genetic loci responsible by using a hypothesis-free genome-wide association study (GWAS) approach.

Studies conducted with *E. coli* demonstrated that  $H_2O_2$ -mediated killing occurred only in actively metabolizing cells (35, 42). Exogenously added  $H_2O_2$  also kills *S. aureus* strains with a calculated 90% lethal dose (LD<sub>90</sub>) and MBC of  $\sim$ 10 mM (19, 34). A 10-fold decrease in the sublethal concentration was determined and utilized in our studies (presented in Fig. 7) against strain Newman and two MRSA strains. The membrane-permeable  $H_2O_2$  enters bacterial cells, reacting with the intracellular Fe<sup>2+</sup> by Fenton reactions to produce OH radicals (34). The concentration of  $H_2O_2$  quantified in the supernatant of *S. pneumoniae* to reach the LD<sub>90</sub>, however, was  $\sim$ 7-fold lower ( $\sim$ 140  $\mu$ M) than a sublethal dose of exogenous  $H_2O_2$  and  $\sim$ 70-fold lower than the LD<sub>90</sub> of exogenously added  $H_2O_2$  ( $\sim$ 10 mM). This decreased amount of  $H_2O_2$  in the *S. pneumoniae* supernatant, the fact that an  $H_2O_2$  production-defective strain, when incubated with a sublethal dose of  $H_2O_2$  ( $\sim$ 1 mM), killed *S. aureus* strains, our experiments showing that *S. aureus* killing was blocked by hydroxyl scavengers, and spintrapping experiments supported the hypothesis that production of OH radicals was stimulated by the interaction between pneumococcal cells and *S. aureus*.

Given that  $H_2O_2$  targets metabolically active (i.e., respiring) *E. coli* cells (35) and that *S. aureus* undergoes cellular respiration whereas *S. pneumoniae* does not encode proteins of the respiratory chain (43), we speculate that hydroxyl radicals either target a component(s) of the respiratory chain or require a reducing equivalent from the respiratory chain to generate toxic hydroxyl radicals. In fact, the pneumococcus could be intoxicated by incubating it with increasing amounts of  $H_2O_2$ , but it required at least 10 mM  $H_2O_2$  to completely eradicate *S. pneumoniae* bacteria. A challenge with such a large amount of  $H_2O_2$  was partially inhibited by incubation with the OH scavenger thiourea (see Fig. S4 in the supplemental material).

An investigation by Selva et al. suggested that  $\rm H_2O_2$ -mediated interference was triggered by lysogenic *S. aureus* phages, although in their study they obtained a 3- to

TABLE 2 Pneumococcal and staphylococcal strains used in this study

Strain	Description <sup>a</sup>	Reference(s) or source
TIGR4	Invasive clinical isolate; phenotype CSP2; capsular serotype 4	43
TIGR4 ΔspxB <sup>H</sup>	TIGR4 with an insertion within the spxB gene; spxB::kan-rpsL+	20, 27
TIGR4 ΔspxB <sup>U</sup>	TIGR4 with a deletion of the spxB gene by transformation of erm(B); Eryr cassette	13
SPJV29 (TIGR4 ΔspxBE)	TIGR4 with a deletion of the spxB gene by transformation of erm(B); Eryr cassette	This study
TIGR4 Δ <i>lctO</i>	TIGR4 with a deletion of the <i>lctO</i> gene by transformation of a spectinomycin cassette	This study
TIGR4 ΔspxB ΔlctO	TIGR4 Δspxβ <sup>U</sup> with a deletion of the <i>lctO</i> gene by transformation of a spectinomycin cassette	This study
Pn20	Serotype 35B; nasopharyngeal human isolate	20
Pn20∆ <i>spxB</i>	Pn20 ΔspxB::kan-rpsL <sup>+</sup> by transformation with PCR product of TIGR4 ΔspxB <sup>H</sup>	20
S. aureus Newman	NCTC 8178, ATCC 13420	56
NRS408J	S. aureus NRS408 spontaneous rifampin-resistant mutant	This study
RN4220	S. aureus Hla- nonlysogenic strain	57

<sup>&</sup>lt;sup>α</sup>Ery<sup>r</sup>, erythromycin resistance; H, *spxB* mutant strain obtained from M. Lipsitch at Harvard; U, *spxB* mutant strain prepared by C. J. Orihuela's group at UAB; E, *spxB* mutant prepared at Emory University (SPJV29).

4-log-unit reduction in *S. aureus* density, but not eradication, under similar culture conditions (41). Whereas some *S. aureus* strains utilized in the current study may be lysogenic, we tested a nonlysogenic *S. aureus* strain (RN4220) and obtained density-dependent, SpxB/LctO-dependent killing (data not shown). The detailed mechanism(s) and its target(s) are under active investigation in our laboratories. The target(s) of the OH radicals represents an exciting new alternative for the development of therapeutics against *S. aureus* infections.

#### **MATERIALS AND METHODS**

**Bacterial strains and culture media.** The *S. pneumoniae* and *S. aureus* wild-type strains and mutant derivatives utilized in this study are listed in Table 2. *S. pneumoniae* strains were cultured on blood agar plates (BAP) or BAP with 25  $\mu$ g/ml gentamicin, whereas *S. aureus* strains were grown on salt mannitol agar (SMA) plates or tryptic soy agar (TSA) plates with or without 5  $\mu$ g/ml optochin or on Luria-Bertani agar (LBA) (1% tryptone [Becton-Dickinson], 0.5% yeast extract, 1% NaCl, and 1.5% agar [Becton-Dickinson]). THY was utilized in all the experiments.

**Preparation of inoculum for experiments.** The inoculum was prepared essentially as previously described (44, 45). Briefly, an overnight BAP (for *S. pneumoniae*) or LBA (for *S. aureus*) culture was used to prepare a cell suspension in THY broth to an optical density at 600 nm (OD $_{600}$ ) of  $\sim$ 0.08. This suspension was incubated at 37°C in a 5% CO $_{2}$  atmosphere until the culture reached an OD $_{600}$  of  $\sim$ 0.2 (early log phase). Then, glycerol was added to give a final 10% (vol/vol) concentration, and the suspension was stored at -80°C until it was used. An aliquot of these stocks was further diluted and plated to obtain bacterial counts (CFU per milliliter).

**Mixed-culture killing assay on plates.** Blood agar plates were coinoculated with both *S. pneumoniae* and *S. aureus* strains at different densities ranging from  $\sim 10^6$  through  $\sim 10^9$  CFU/ml. The inoculated plates were then incubated at  $37^{\circ}$ C in a 5% CO $_2$  atmosphere overnight. A creamy-yellow color on the BAP culture and the presence of a beta-hemolytic halo around each culture indicated growth of *S. aureus*. To quantify the densities of strains, cultures were harvested and an aliquot was diluted and plated to obtain bacterial counts, whereas DNA was extracted from another aliquot using a QlAamp DNA minikit (Qiagen) according to the manufacturer's instructions. DNA preparations were eluted with  $100~\mu l$  of elution buffer, quantified using a Nanodrop spectrophotometer, and stored at  $-80^{\circ}$ C until they were used.

**Quantitative PCRs.** Strain-specific qPCRs were performed to measure the densities of strains. Primers, probes, and the concentrations utilized are listed in Table 3. The total *S. pneumoniae* density was quantified using the panpneumococcus *lytA* assay (46), and detection of the *nuc* gene was used to quantify *S. aureus* density (47). Reactions were run along with serially diluted DNA standards corresponding to  $4.29 \times 10^5$ ,  $4.29 \times 10^4$ ,  $4.29 \times 10^3$ ,  $4.29 \times 10^1$ , and  $2.14 \times 10^1$  genome equivalents of *S. pneumoniae* or  $3.29 \times 10^5$ ,  $3.29 \times 10^4$ ,  $3.29 \times 10^3$ ,  $3.29 \times 10^2$ ,  $3.29 \times 10^1$ , and  $3.14 \times 10^1$  genome equivalents of *S. aureus*. Reactions were carried out using a Bio-Rad CFX96 Touch real-time PCR detection system (Bio-Rad, Hercules, CA) and the following cycling parameters:  $50^\circ$ C for 2 min,  $95^\circ$ C for 2 min, and 40 cycles of  $95^\circ$ C for 15 s and  $60^\circ$ C for 1 min. The final numbers of genome equivalents per milliliter were calculated using the CFX software (Bio-Rad, Hercules, CA).

**Determination of S. aureus strain sensitivity to S. pneumoniae.** Inocula of S. aureus strains prepared as stated above, with known densities, were serially diluted in THY to generate inocula. Decreasing densities of S. aureus strains were inoculated along with  $1.5 \times 10^7$  CFU/ml of S. pneumoniae and incubated for 4 h in 96-well microplates. The cultures were diluted and plated on TSA supplemented with optochin (5  $\mu$ g/ml). The highest density of each S. aureus strain killed by  $1.5 \times 10^7$  CFU/ml of S. pneumoniae within 4 h was then determined.

Competition between resistant and sensitive *S. aureus* strains under *S. pneumoniae* selection. For the competition experiments, we prepared an NRS408-derived rifampin-resistant mutant (NRS408J) by plating an overnight tryptic soy broth (TSB) culture concentrated 10-fold on a TSA plate supplemented with  $4 \mu g/ml$  rifampin. *S. pneumoniae* strain TIGR4 (1.5  $\times$  10<sup>7</sup> CFU/ml) was then cocultured in

Journal of Bacteriology

Wu et al.

TABLE 3 Primers and probes used in this study

Target	Primer or probe sequence (5'-3')a	Reference
S. pneumoniae lytA	F, ACGCAATCTAGCAGATGAAGCA	46
	R, TCGTGCGTTTTAATTCCAGCT	
	Probe, FAM-TGCCGAAAACGCTTGATACAGGGAG	
S. aureus nuc	F, GTTGCTTAGTGTTAACTTTAGTTGTA	47
	R, AATGTCGCAGGTTCTTTATGTAATTT	
	Probe, HEX-AAGTCTAAGTAGCTCAGCAAATGCA	
UP_spxB_DN	F, TATCAATCACGCTCCTGC	13
	R, CTCGTTATGGACAATGCT	
Xbal-erm(B)-Xhol	F, CAGTCTAGAAAAAATTTGTAATTAAGAAGGAGT	This study
	R, CAGCTCGAGCCAAATTTACAAAAGCGACTCA	·
lctO_UP-FW	TGGAAAGTAGGCATCAGC	This study
IctO_UP (Spl_KnSpc)-RV	TCCTCCTCACTATTTTGATAAACTGTCCTCCTCG	This study
IctO_DN (Spl_KnSpc)-FW	TGGAAACACTTCGTGAAGACTTAAAATTGTATTG	This study
IctO_DN-RV	CGTAATTCCACTTGATCC	This study
SpcK7-FW	CAAAATAGTGAGGAGGA	This study
SpcK7-RV	TTCACGAAGTGTTTCCA	This study

<sup>°</sup>F, forward; R, reverse; FAM, 6-carboxyfluorescein; HEX, 6-carboxy-2,4,4,5,7,7-hexachlorofluorescein. Sequences overlapping the spectinomycin resistance cassette are in boldface.

THY with three different mixtures of *S. aureus* strains (5  $\times$  106 CFU/ml of each *S. aureus* strain). A mixture contained NRS049, NRS408J, or both strains NRS049 and NRS408J. Experiments with negative controls without *S. pneumoniae* were performed for each of the *S. aureus* strain mixtures. All the cultures (3 ml each) were incubated without shaking at 37°C in a 5% CO $_2$  atmosphere. Cocultures were sampled at 0-, 15-, and 30-min and 1-, 2-, 3-, and 4-h time points. Sample dilutions were then spotted on TSA plates supplemented with 16  $\mu$ g/ml tetracycline or 4  $\mu$ g/ml rifampin to detect NRS049 and the NRS408 rifampin-resistant mutant (NRS408J), respectively. The following day, spot colonies were enumerated to calculate the number of residual CFU per milliliter at each time point.

**Growth curves and hydrogen peroxide sensitivity.** Strains were grown at 37°C in TSB or TSB supplemented with 0.1, 2.5, or 5.0 mM  $\rm H_2O_2$ . The initial ODs were normalized to between 0.1 and 0.2 (roughly a 1/100 dilution of the overnight culture) readings from a microplate reader (Eon; BioTek, Inc.) before the growth curves were performed. Growth curves (OD<sub>600</sub>) were determined in a plate reader collecting data every 10 minutes for up to 12 h.

**Confocal-microscopy studies.** Bacteria grown in experiments performed using the plate model (Fig. 1A) were imprinted onto rounded glass slides and immediately fixed with 2% paraformaldehyde (PFA) for 15 min at room temperature. The fixed bacteria were then blocked with 1% bovine serum albumin (BSA) for 30 min at 37°C and incubated first with a rabbit polyclonal anti-5. *aureus* antibody (4  $\mu$ g/ml; Santa Cruz Biotechnology, Inc.) for 1 h at room temperature, followed by phosphate-buffered saline (PBS) washes and 1 h of incubation with a secondary Alexa Fluor 555-labeled goat anti-rabbit antibody (20  $\mu$ g/ml; Molecular Probes). The preparation was then washed with sterile PBS and incubated for 30 min with anti-5. *pneumoniae* antibodies raised in rabbit (Statens Serum Institute) that had been previously labeled with Alexa Fluor 488 (50  $\mu$ g/ml; Molecular Probes). The stained preparations were finally washed twice with PBS, mounted with ProLong Diamond antifade mountant with DAPI (Molecular Probes), and analyzed with an Olympus FV1000 confocal microscope. The confocal images were analyzed with Image J version 1.49k (National Institutes of Health).

**Preparation of TIGR4-derived**  $\Delta spxB$ ,  $\Delta lctO$ , and  $\Delta spxB$   $\Delta lctO$  mutants. Isogenic spxB mutant derivatives of S. pneumoniae strain TIGR4 (43) were prepared as described in our recent publication (13). A deletion within the lctO gene in the wild-type TIGR4, or TIGR4  $\Delta spxB$ , was generated using a cassette containing lctO upstream (lctO\_UP-FW and lctO\_UP-RV) and downstream (lctO\_DN-FW and lctO\_DN-RV) sequences and the spectinomycin resistance gene (SpcK7-FW and SpcK7-RV). This cassette was prepared by splicing overlap extension PCR with primers (in parentheses above and listed in Table 3) (48, 49) and transformed into pneumococci using standard procedures (50). BAP with spectinomycin (100  $\mu$ g/ml) or erythromycin (0.5  $\mu$ g/ml) was used to select lctO or spxB mutants, respectively. All deletions were confirmed by PCR and sequencing.

Microplate model to investigate killing of *S. aureus* by *S. pneumoniae* strains. An *S. pneumoniae* strain was inoculated along with *S. aureus* strain Newman at a density of  $\sim$ 1  $\times$  10<sup>6</sup> CFU/ml in a 6-well microplate containing THY and incubated for 4 h at 37°C in a 5% CO<sub>2</sub> atmosphere. Control wells were inoculated with only *S. pneumoniae* or only *S. aureus*. In another set of experiments, *S. aureus* was inoculated, along with increasing amounts of hydrogen peroxide (Sigma), with the TIGR4  $\Delta spxB^E$  (SPJV29) mutant alone or with TIGR4  $\Delta spxB^E$  and hydrogen peroxide. Technical duplicates were included throughout these experiments. At the end of the incubation, planktonic cells were removed, diluted, and plated onto BAP with gentamicin to obtain the number of CFU of *S. pneumoniae* per milliliter or onto LBA plates with optochin to obtain the number of CFU of *S. aureus* per milliliter. The biofilms were washed once with PBS, resuspended

in 1 ml of sterile PBS, and sonicated for 15 s using a Bransonic ultrasonic water bath (Branson, Danbury, CT), followed by extensive pipetting to remove the remaining attached biofilm bacteria. The biofilms were then diluted and plated as described above. Experiments were repeated three times.

**Quantifying production of hydrogen peroxide.** *S. pneumoniae* strains were inoculated at a density of  $\sim 1 \times 10^6$  CFU/ml in a 6-well plate containing THY and incubated at 37°C in a 5% CO $_2$  atmosphere. The supernatant containing planktonic bacteria was collected 0, 1, 2, or 4 h postinoculation and then centrifuged at 8,000 rpm for 10 min to separate the planktonic cells; the supernatant was further filtered through a 0.45- $\mu$ m syringe filter. The concentration of H $_2$ O $_2$  present in each cell-free supernatant was assessed using an Amplex Red hydrogen peroxide/peroxidase assay kit (Invitrogen) following the manufacturer's instructions.

**Detection of hydroxyl radicals by spin trapping.** A spin-trapping system was utilized to detect the formation of hydroxyl radicals essentially as described previously (38, 51). Briefly, pneumococci were grown in 100 ml of THY broth to an  $OD_{600}$  of 0.4 to 0.5. The pellets were harvested and washed twice with Hanks balanced salt solution lacking calcium and magnesium (HBSS) and finally resuspended in 500  $\mu$ l of HBSS. The reaction mixtures included 200  $\mu$ l of cell suspension,  $100~\mu$ M diethylenetriamine-pentaacetic acid (DETAPAC), 10 mM 4-POBN, 170 mM ethanol, and HBSS for a final volume of 1 ml. The reaction mixture was incubated for 10 min at room temperature and immediately transferred to a quartz capillary tube (2-mm outer diameter), and X-band electron paramagnetic resonance (EPR) spectra were acquired under the following conditions: microwave frequency, 9.346 GHz; microwave power, 10 mW; modulation amplitude, 0.2 mT; modulation frequency, 100 kHz; temperature, 295 K; the spectra represent an average of 92 scans minus a medium baseline (224 scans).

**S. aureus strain sequence and phylogeny.** In brief, Nextera random shotgun libraries were prepared, and 300-bp paired-end reads were sequenced to >20 to 100× coverage. Sequence types were ascribed based on BLASTN against the BIGSdb database (52, 53). The phylogeny was created using Parsnp (54) based on mapping to the Newman reference. The tree was midpoint rooted and visualized using iTOL (55).

**Statistical analysis.** Differences between *S. aureus* strain sensitivities to *S. pneumoniae* were calculated by a Kruskal-Wallis test for overall variability in the collection. The test was performed for all strains with or without the two most sensitive strains (NRS408 and NRS170). All other statistical analysis was performed using a two-tailed Student *t* test and the software SigmaPlot version 14.0.

**Accession number(s).** The data were deposited in NCBI BioProject under accession no. PRJNA289526 as part of a larger study that will be described in more detail elsewhere.

### **SUPPLEMENTAL MATERIAL**

Supplemental material for this article may be found at https://doi.org/10.1128/JB

SUPPLEMENTAL FILE 1, PDF file, 0.3 MB.

### **ACKNOWLEDGMENTS**

This study was supported by a grant from the National Institutes of Health (NIH) (R21AI112768-01A1 and 1R21AI144571-01 to J.E.V.). The confocal studies were in part supported by funds from the Integrated Cellular Imaging (ICI) pediatric core and the Emory+Children's Pediatric Research Center to J.E.V. Funds from the Raymond F. Schinazi International Exchange Program (SIEP), a faculty exchange program between the Read laboratory at Emory University and the Hadassah Medical Organization to promote collaborative research and education, supported O.G. EPR spectroscopy was supported by NIH grants R01DK054514 and NIH RR17767 (to K.W.). U.A.A.-Z. thanks CONACyT for mobility scholarship 291250.

The content is solely our responsibility and does not necessarily represent the official views of the National Institutes of Health.

We thank Faidad Khan (Emory University) for his assistance in some experiments and Marc Lipsitch (Harvard T. H. Chan School of Public Health) for providing us with TIGR4 and Pn20 hydrogen peroxide-deficient mutants.

### **REFERENCES**

- Regev-Yochay G, Dagan R, Raz M, Carmeli Y, Shainberg B, Derazne E, Rahav G, Rubinstein E. 2004. Association between carriage of Streptococcus pneumoniae, and Staphylococcus aureus in children. JAMA 292: 716–720. https://doi.org/10.1001/jama.292.6.716.
- Bakaletz LO. 2007. Bacterial biofilms in otitis media: evidence and relevance. Pediatr Infect Dis J 26:S17–S19. https://doi.org/10.1097/ INF.0b013e318154b273.
- 3. Dunne EM, Smith-Vaughan HC, Robins-Browne RM, Mulholland EK, Satzke C. 2013. Nasopharyngeal microbial interactions in the era of
- pneumococcal conjugate vaccination. Vaccine 31:2333–2342. https://doi.org/10.1016/j.vaccine.2013.03.024.
- Shak JR, Cremers AJ, Gritzfeld JF, de Jonge MI, Hermans PW, Vidal JE, Klugman KP, Gordon SB. 2014. Impact of experimental human pneumococcal carriage on nasopharyngeal bacterial densities in healthy adults. PLoS One 9:e98829. https://doi.org/10.1371/journal.pone.0098829.
- Shak JR, Vidal JE, Klugman KP. 2013. Influence of bacterial interactions on pneumococcal colonization of the nasopharynx. Trends Microbiol 21:129–135. https://doi.org/10.1016/j.tim.2012.11.005.

Wu et al. Journal of Bacteriology

- Vidal JE, Howery KE, Ludewick HP, Nava P, Klugman KP. 2013. Quorumsensing systems LuxS/Autoinducer 2 and Com regulate Streptococcus pneumoniae biofilms in a bioreactor with living cultures of human respiratory cells. Infect Immun 81:1341–1353. https://doi.org/10.1128/IAI .01096-12.
- Chien YW, Vidal JE, Grijalva CG, Bozio C, Edwards KM, Williams JV, Griffin MR, Verastegui H, Hartinger SM, Gil Al, Lanata CF, Klugman KP. 2013. Density interactions among Streptococcus pneumoniae, Haemophilus influenzae and Staphylococcus aureus in the nasopharynx of young Peruvian children. Pediatr Infect Dis J 32:72–77. https://doi.org/10.1097/ INF.0b013e318270d850.
- Bogaert D, van Belkum A, Sluijter M, Luijendijk A, de Groot R, Rumke HC, Verbrugh HA, Hermans PW. 2004. Colonisation by Streptococcus pneumoniae and Staphylococcus aureus in healthy children. Lancet 363: 1871–1872. https://doi.org/10.1016/S0140-6736(04)16357-5.
- Chao Y, Marks LR, Pettigrew MM, Hakansson AP. 2014. Streptococcus pneumoniae biofilm formation and dispersion during colonization and disease. Front Cell Infect Microbiol 4:194. https://doi.org/10.3389/fcimb .2014.00194.
- Gritzfeld JF, Cremers AJ, Ferwerda G, Ferreira DM, Kadioglu A, Hermans PW, Gordon SB. 2014. Density and duration of experimental human pneumococcal carriage. Clin Microbiol Infect 20:O1145–1151. https://doi.org/10.1111/1469-0691.12752.
- 11. Yarwood JM, Bartels DJ, Volper EM, Greenberg EP. 2004. Quorum sensing in Staphylococcus aureus biofilms. J Bacteriol 186:1838–1850. https://doi.org/10.1128/jb.186.6.1838-1850.2004.
- Shenoy AT, Brissac T, Gilley RP, Kumar N, Wang Y, Gonzalez-Juarbe N, Hinkle WS, Daugherty SC, Shetty AC, Ott S, Tallon LJ, Deshane J, Tettelin H, Orihuela CJ. 2017. Streptococcus pneumoniae in the heart subvert the host response through biofilm-mediated resident macrophage killing. PLoS Pathog 13:e1006582. https://doi.org/10.1371/ journal.ppat.1006582.
- Brissac T, Shenoy AT, Patterson LA, Orihuela CJ. 2018. Cell invasion and pyruvate oxidase derived H2O2 are critical for Streptococcus pneumoniae mediated cardiomyocyte killing. Infect Immun 86:e00569-17. https://doi.org/10.1128/IAI.00569-17.
- Regev-Yochay G, Malley R, Rubinstein E, Raz M, Dagan R, Lipsitch M. 2008. In vitro bactericidal activity of Streptococcus pneumoniae and bactericidal susceptibility of Staphylococcus aureus strains isolated from cocolonized versus noncocolonized children. J Clin Microbiol 46: 747–749. https://doi.org/10.1128/JCM.01781-07.
- Bhattacharya M, Wozniak DJ, Stoodley P, Hall-Stoodley L. 2015. Prevention and treatment of Staphylococcus aureus biofilms. Expert Rev Anti-Infect Ther 13:1499–1516. https://doi.org/10.1586/14787210.2015.1100533.
- Chochua S, D'Acremont V, Hanke C, Alfa D, Shak J, Kilowoko M, Kyungu E, Kaiser L, Genton B, Klugman KP, Vidal JE. 2016. Increased nasopharyngeal density and concurrent carriage of Streptococcus pneumoniae, Haemophilus influenzae, and Moraxella catarrhalis are associated with pneumonia in febrile children. PLoS One 11:e0167725. https://doi.org/10.1371/journal.pone.0167725.
- Morgan HJ, Avery OT. 1924. Growth-inhibitory substances in pneumococcus cultures. J Exp Med 39:335–346. https://doi.org/10.1084/jem.39 3 335
- Avery OT, Morgan HJ. 1924. The occurrence of peroxide in cultures of Pneumococcus. J Exp Med 39:275–287. https://doi.org/10.1084/jem.39.2
- Pericone CD, Overweg K, Hermans PW, Weiser JN. 2000. Inhibitory and bactericidal effects of hydrogen peroxide production by Streptococcus pneumoniae on other inhabitants of the upper respiratory tract. Infect Immun 68:3990–3997. https://doi.org/10.1128/IAI.68.7.3990-3997.2000.
- Regev-Yochay G, Trzcinski K, Thompson CM, Malley R, Lipsitch M. 2006. Interference between Streptococcus pneumoniae and Staphylococcus aureus: in vitro hydrogen peroxide-mediated killing by Streptococcus pneumoniae. J Bacteriol 188:4996–5001. https://doi.org/10.1128/JB.00317-06.
- Pericone CD, Bae D, Shchepetov M, McCool T, Weiser JN. 2002. Short-sequence tandem and nontandem DNA repeats and endogenous hydrogen peroxide production contribute to genetic instability of Streptococcus pneumoniae. J Bacteriol 184:4392–4399. https://doi.org/10.1128/jb.184.16.4392-4399.2002.
- Yesilkaya H, Andisi VF, Andrew PW, Bijlsma JJ. 2013. Streptococcus pneumoniae and reactive oxygen species: an unusual approach to living

- with radicals. Trends Microbiol 21:187–195. https://doi.org/10.1016/j.tim.2013.01.004.
- Khan F, Wu X, Matzkin GL, Khan MA, Sakai F, Vidal JE. 2016. Streptococcus pneumoniae eradicates preformed Staphylococcus aureus biofilms through a mechanism requiring physical contact. Front Cell Infect Microbiol 6:104. https://doi.org/10.3389/fcimb.2016.00104.
- Lisher JP, Tsui HT, Ramos-Montanez S, Hentchel KL, Martin JE, Trinidad JC, Winkler ME, Giedroc DP. 2017. Biological and chemical adaptation to endogenous hydrogen peroxide production in Streptococcus pneumoniae D39. mSphere 2:e00291-16. https://doi.org/10.1128/mSphere .00291-16.
- Ramos-Montanez S, Tsui HC, Wayne KJ, Morris JL, Peters LE, Zhang F, Kazmierczak KM, Sham LT, Winkler ME. 2008. Polymorphism and regulation of the spxB (pyruvate oxidase) virulence factor gene by a CBS-HotDog domain protein (SpxR) in serotype 2 Streptococcus pneumoniae. Mol Microbiol 67:729 –746. https://doi.org/10.1111/j.1365-2958.2007.06082.x.
- Taniai H, Iida K, Seki M, Saito M, Shiota S, Nakayama H, Yoshida S. 2008. Concerted action of lactate oxidase and pyruvate oxidase in aerobic growth of Streptococcus pneumoniae: role of lactate as an energy source. J Bacteriol 190:3572–3579. https://doi.org/10.1128/JB.01882-07.
- Park B, Nizet V, Liu GY. 2008. Role of Staphylococcus aureus catalase in niche competition against Streptococcus pneumoniae. J Bacteriol 190: 2275–2278. https://doi.org/10.1128/JB.00006-08.
- Echlin H, Frank MW, Iverson A, Chang TC, Johnson MD, Rock CO, Rosch JW. 2016. Pyruvate oxidase as a critical link between metabolism and capsule biosynthesis in Streptococcus pneumoniae. PLoS Pathog 12: e1005951. https://doi.org/10.1371/journal.ppat.1005951.
- Bryant JC, Dabbs RC, Oswalt KL, Brown LR, Rosch JW, Seo KS, Donaldson JR, McDaniel LS, Thornton JA. 2016. Pyruvate oxidase of Streptococcus pneumoniae contributes to pneumolysin release. BMC Microbiol 16:271. https://doi.org/10.1186/s12866-016-0881-6.
- Margolis E. 2009. Hydrogen peroxide-mediated interference competition by Streptococcus pneumoniae has no significant effect on Staphylococcus aureus nasal colonization of neonatal rats. J Bacteriol 191:571–575. https://doi.org/10.1128/JB.00950-08.
- Margolis E, Yates A, Levin BR. 2010. The ecology of nasal colonization of Streptococcus pneumoniae, Haemophilus influenzae and Staphylococcus aureus: the role of competition and interactions with host's immune response. BMC Microbiol 10:59. https://doi.org/10.1186/ 1471-2180-10-59.
- Reiss-Mandel A, Regev-Yochay G. 2016. Staphylococcus aureus and Streptococcus pneumoniae interaction and response to pneumococcal vaccination: myth or reality? Hum Vaccin Immunother 12:351–357. https://doi.org/10.1080/21645515.2015.1081321.
- Hoepelman IM, Bezemer WA, Vandenbroucke-Grauls CM, Marx JJ, Verhoef J. 1990. Bacterial iron enhances oxygen radical-mediated killing of Staphylococcus aureus by phagocytes. Infect Immun 58:26–31.
- Repine JE, Fox RB, Berger EM. 1981. Hydrogen peroxide kills Staphylococcus aureus by reacting with staphylococcal iron to form hydroxyl radical. J Biol Chem 256:7094–7096.
- 35. Imlay JA, Chin SM, Linn S. 1988. Toxic DNA damage by hydrogen peroxide through the Fenton reaction in vivo and in vitro. Science 240:640–642. https://doi.org/10.1126/science.2834821.
- Quillin SJ, Hockenberry AJ, Jewett MC, Seifert HS. 2018. Neisseria gonorrhoeae exposed to sublethal levels of hydrogen peroxide mounts a complex transcriptional response. mSystems 3:e00156-18. https://doi .org/10.1128/mSystems.00156-18.
- Wong SM, Alugupalli KR, Ram S, Akerley BJ. 2007. The ArcA regulon and oxidative stress resistance in Haemophilus influenzae. Mol Microbiol 64:1375–1390. https://doi.org/10.1111/j.1365-2958.2007.05747.x.
- Pericone CD, Park S, Imlay JA, Weiser JN. 2003. Factors contributing to hydrogen peroxide resistance in Streptococcus pneumoniae include pyruvate oxidase (SpxB) and avoidance of the toxic effects of the Fenton reaction. J Bacteriol 185:6815–6825. https://doi.org/10.1128/jb.185.23 .6815-6825.2003.
- Imlay JA. 2008. Cellular defenses against superoxide and hydrogen peroxide. Annu Rev Biochem 77:755–776. https://doi.org/10.1146/ annurev.biochem.77.061606.161055.
- Gonzalez-Flecha B, Demple B. 1995. Metabolic sources of hydrogen peroxide in aerobically growing Escherichia coli. J Biol Chem 270: 13681–13687. https://doi.org/10.1074/jbc.270.23.13681.
- 41. Selva L, Viana D, Regev-Yochay G, Trzcinski K, Corpa JM, Lasa I, Novick RP, Penadés JR. 2009. Killing niche competitors by remote-control bac-

- teriophage induction. Proc Natl Acad Sci U S A 106:1234–1238. https://doi.org/10.1073/pnas.0809600106.
- 42. Imlay JA, Linn S. 1988. DNA damage and oxygen radical toxicity. Science 240:1302–1309. https://doi.org/10.1126/science.3287616.
- 43. Tettelin H, Nelson KE, Paulsen IT, Eisen JA, Read TD, Peterson S, Heidelberg J, DeBoy RT, Haft DH, Dodson RJ, Durkin AS, Gwinn M, Kolonay JF, Nelson WC, Peterson JD, Umayam LA, White O, Salzberg SL, Lewis MR, Radune D, Holtzapple E, Khouri H, Wolf AM, Utterback TR, Hansen CL, McDonald LA, Feldblyum TV, Angiuoli S, Dickinson T, Hickey EK, Holt IE, Loftus BJ, Yang F, Smith HO, Venter JC, Dougherty BA, Morrison DA, Hollingshead SK, Fraser CM. 2001. Complete genome sequence of a virulent isolate of *Streptococcus pneumoniae*. Science 293:498–506. https://doi.org/10.1126/science.1061217.
- Vidal JE, Ludewick HP, Kunkel RM, Zahner D, Klugman KP. 2011. The LuxS-dependent quorum-sensing system regulates early biofilm formation by Streptococcus pneumoniae strain D39. Infect Immun 79: 4050–4060. https://doi.org/10.1128/IAI.05186-11.
- Wu X, Jacobs NT, Bozio C, Palm P, Lattar SM, Hanke CR, Watson DM, Sakai F, Levin BR, Klugman KP, Vidal JE. 2017. Competitive dominance within biofilm consortia regulates the relative distribution of pneumococcal nasopharyngeal density. Appl Environ Microbiol 83:e00953-17. https:// doi.org/10.1128/AEM.00953-17.
- Carvalho MDGS, Tondella ML, McCaustland K, Weidlich L, McGee L, Mayer LW, Steigerwalt A, Whaley M, Facklam RR, Fields B, Carlone G, Ades EW, Dagan R, Sampson JS. 2007. Evaluation and improvement of real-time PCR assays targeting *lytA*, *ply*, and *psaA* genes for detection of pneumococcal DNA. J Clin Microbiol 45:2460–2466. https://doi.org/10 .1128/JCM.02498-06.
- Kilic A, Muldrew KL, Tang YW, Basustaoglu AC. 2010. Triplex real-time polymerase chain reaction assay for simultaneous detection of Staphylococcus aureus and coagulase-negative staphylococci and determination of methicillin resistance directly from positive blood culture bottles. Diagn Microbiol Infect Dis 66:349–355. https://doi.org/10 .1016/j.diagmicrobio.2009.11.010.
- 48. Higuchi R, Krummel B, Saiki RK. 1988. A general method of in vitro preparation and specific mutagenesis of DNA fragments: study of pro-

- tein and DNA interactions. Nucleic Acids Res 16:7351–7367. https://doi.org/10.1093/nar/16.15.7351.
- Horton RM, Hunt HD, Ho SN, Pullen JK, Pease LR. 1989. Engineering hybrid genes without the use of restriction enzymes: gene splicing by overlap extension. Gene 77:61–68. https://doi.org/10.1016/0378 -1119(89)90359-4.
- Havarstein LS, Coomaraswamy G, Morrison DA. 1995. An unmodified heptadecapeptide pheromone induces competence for genetic transformation in *Streptococcus pneumoniae*. Proc Natl Acad Sci U S A 92: 11140–11144. https://doi.org/10.1073/pnas.92.24.11140.
- Park S, You X, Imlay JA. 2005. Substantial DNA damage from submicromolar intracellular hydrogen peroxide detected in Hpx- mutants of Escherichia coli. Proc Natl Acad Sci U S A 102:9317–9322. https://doi.org/ 10.1073/pnas.0502051102.
- Jolley KA, Maiden MC. 2010. BIGSdb: scalable analysis of bacterial genome variation at the population level. BMC Bioinformatics 11:595–510. https://doi.org/10.1186/1471-2105-11-595.
- 53. Petit RA III, Read TD. 2018. Staphylococcus aureus viewed from the perspective of 40,000+ genomes. Peer J 6:e5261. https://doi.org/10.7717/peerj.5261.
- 54. Treangen TJ, Ondov BD, Koren S, Phillippy AM. 2014. The Harvest suite for rapid core-genome alignment and visualization of thousands of intraspecific microbial genomes. Genome Biol 15:524–510. https://doi.org/10.1186/s13059-014-0524-x.
- Letunic I, Bork P. 2016. Interactive tree of life (iTOL) v3: an online tool for the display and annotation of phylogenetic and other trees. Nucleic Acids Res 44:W242–W245. https://doi.org/10.1093/nar/gkw290.
- Boake WC. 1956. Antistaphylocoagulase in experimental staphylococcal infections. J Immunol 76:89–96.
- Nair D, Memmi G, Hernandez D, Bard J, Beaume M, Gill S, Francois P, Cheung AL. 2011. Whole-genome sequencing of Staphylococcus aureus strain RN4220, a key laboratory strain used in virulence research, identifies mutations that affect not only virulence factors but also the fitness of the strain. J Bacteriol 193:2332–2335. https://doi.org/10 .1128/JB.00027-11.

**Appendix B:** Lactoferrin Disaggregates Pneumococcal Biofilms and Inhibits Acquisition of Resistance Through Its DNase Activity

Uriel A. Angulo-Zamudio<sup>e</sup>, Jorge E. Vidal<sup>d</sup>, Kamran Nazmi, Jan G.M. Bolscher, Claudia Leon-Sicairos, **Brenda S. Antezana**<sup>d</sup>, Adrián Canizalez-Roman, Nidia León-Sicairos

- <sup>a</sup> CIASaP, Facultad de Medicina, Universidad Autónoma de Sinaloa, Culiacán, Mexico
- b Programa Regional del Noroeste para el Doctorado en Biotecnología, Facultad de Ciencias
   Químico-Biológicas, Universidad Autónoma de Sinaloa, Culiacán, Mexico
- <sup>c</sup> Hubert Department of Global Health, Rollins School of Public Health, Emory University, Atlanta, GA, United States
- <sup>d</sup> Department of Microbiology and Immunology, The University of Mississippi Medical Center, Jackson, MS, United States
- <sup>e</sup> Department of Oral Biochemistry, Academic Centre for Dentistry Amsterdam, University of Amsterdam, Amsterdam, Netherlands
- <sup>f</sup> Microbiology and Molecular Genetics Program, Graduate Division of Biological and Biomedical Sciences, Emory University, Atlanta, GA, United States
- g Unidad de Investigación, Hospital de la Mujer, Servicios de Salud de Sinaloa, Culiacán, Mexico

  h Departamento de Investigación del Hospital Pediátrico de Sinaloa, Servicios de Salud de Sinaloa,

  Culiacán, Mexico

### Published in

### Frontiers in Microbiology

October 2019, Volume 10

### Citation:

Angulo-Zamudio UA, Vidal JE, Nazmi K, Bolscher JGM, Leon-Sicairos C, Antezana BS, Canizalez-Roman A, Leon-Sicairos N. Lactoferrin Disaggregates Pneumococcal Biofilms and Inhibits Acquisition of Resistance Through Its DNase Activity. Front Microbiol. 2019;10:2386. Epub 2019/11/05. doi: 10.3389/fmicb.2019.02386. PubMed PMID: 31681240; PMCID: PMC6813537.

B. Antezana assisted with bioreactor biofilm experiments and data interpretation.





# Lactoferrin Disaggregates Pneumococcal Biofilms and Inhibits Acquisition of Resistance Through Its DNase Activity

Uriel A. Angulo-Zamudio<sup>1,2</sup>, Jorge E. Vidal<sup>3,4</sup>, Kamran Nazmi<sup>5</sup>, Jan G. M. Bolscher<sup>5</sup>, Claudia Leon-Sicairos<sup>2</sup>, Brenda S. Antezana<sup>6</sup>, Adrián Canizalez-Roman<sup>1,7</sup> and Nidia León-Sicairos<sup>1,8</sup>\*

<sup>1</sup> CIASaP, Facultad de Medicina, Universidad Autónoma de Sinaloa, Culiacán, Mexico, <sup>2</sup> Programa Regional del Noroeste para el Doctorado en Biotecnología, Facultad de Ciencias Químico-Biológicas, Universidad Autónoma de Sinaloa, Culiacán, Mexico, <sup>3</sup> Hubert Department of Global Health, Rollins School of Public Health, Emory University, Atlanta, GA, United States, <sup>4</sup> Department of Microbiology and Immunology, The University of Mississippi Medical Center, Jackson, MS, United States, <sup>5</sup> Department of Oral Biochemistry, Academic Centre for Dentistry Amsterdam, University of Amsterdam, Amsterdam, Netherlands, <sup>6</sup> Microbiology and Molecular Genetics Program, Graduate Division of Biological and Biomedical Sciences, Emory University, Atlanta, GA, United States, <sup>7</sup> Unidad de Investigación, Hospital de la Mujer, Servicios de Salud de Sinaloa, Culiacán, Mexico, <sup>8</sup> Departamento de Investigación del Hospital Pediátrico de Sinaloa, Servicios de Salud de Sinaloa, Culiacán, Mexico

### **OPEN ACCESS**

### Edited by:

Mattias Collin, Lund University, Sweden

### Reviewed by:

Mukesh Kumar Yadav, Korea University, South Korea Rosalia Cavaliere, University of Technology Sydney, Australia

### \*Correspondence:

Nidia León-Sicairos nidialeon@uas.edu.mx

### Specialty section:

This article was submitted to Antimicrobials, Resistance and Chemotherapy, a section of the journal Frontiers in Microbiology

Received: 23 August 2019 Accepted: 01 October 2019 Published: 18 October 2019

### Citation:

Angulo-Zamudio UA, Vidal JE,
Nazmi K, Bolscher JGM,
Leon-Sicairos C, Antezana BS,
Canizalez-Roman A and
León-Sicairos N (2019) Lactoferrin
Disaggregates Pneumococcal
Biofilms and Inhibits Acquisition
of Resistance Through Its DNase
Activity. Front. Microbiol. 10:2386.
doi: 10.3389/fmicb.2019.02386

Streptococcus pneumoniae colonizes the upper airways of children and the elderly. Colonization progresses to persistent carriage when S. pneumoniae forms biofilms, a feature required for the development of pneumococcal disease. Nasopharyngeal biofilms are structured with a matrix that includes extracellular DNA (eDNA), which is sourced from the same pneumococci and other bacteria. This eDNA also allows pneumococci to acquire new traits, including antibiotic resistance genes. In this study, we investigated the efficacy of lactoferrin (LF), at physiological concentrations found in secretions with bactericidal activity [i.e., colostrum (100 µM), tears (25 µM)], in eradicating pneumococcal biofilms from human respiratory cells. The efficacy of synthetic LF-derived peptides was also assessed. We first demonstrated that LF inhibited colonization of S. pneumoniae on human respiratory cells without affecting the viability of planktonic bacteria. LF-derived peptides were, however, bactericidal for planktonic pneumococci but they did not affect viability of pre-formed biofilms. In contrast, LF (40 and 80 µM) eradicated pneumococcal biofilms that had been pre-formed on abiotic surfaces (i.e., polystyrene) and on human pharyngeal cells, as investigated by viable counts and confocal microscopy. LF also eradicated biofilms formed by S. pneumoniae strains with resistance to multiple antibiotics. We investigated whether treatment with LF would affect the biofilm structure by analyzing eDNA. Surprisingly, in pneumococcal biofilms treated with LF, the eDNA was absent in comparison to the untreated control (~10 µg/ml) or those treated with LF-derived peptides. EMSA assays showed that LF binds S. pneumoniae DNA and a timecourse study of DNA decay demonstrated that the DNA is degraded when bound

1

by LF. This LF-associated DNase activity inhibited acquisition of antibiotic resistance genes in both *in vitro* transformation assays and in a life-like bioreactor system. In conclusion, we demonstrated that LF eradicates pneumococcal-colonizing biofilms at a concentration safe for humans and identified a LF-associated DNAse activity that inhibited the acquisition of resistance.

Keywords: lactoferrin, disaggregates, pneumococcal biofilms, DNAse activity, resistance acquisition

### INTRODUCTION

Streptococcus pneumoniae is a Gram positive bacterium that resides in the children nasopharynx principally. These bacteria reside asymptomatically in the host, but may become invasive, resulting in pneumococcal disease (Shak et al., 2013). S. pneumoniae is the most common cause of communityacquired pneumonia, primarily affecting children (<5 years old) and the elderly (>65 years old). However, it can lead to a variety of other pathologies, such as otitis media, meningitis, or septicemia (Klein, 1994; Schuchat et al., 1997; Musher et al., 2000; Syrogiannopoulos et al., 2002; Regev-Yochay et al., 2004; Nunes et al., 2005). S. pneumoniae is a major cause of morbidity and mortality, where about 15 million individuals suffer from a pneumococcal disease and nearly 500,000 people die each year (O'brien et al., 2009). This burden of morbidity and mortality is greatly attributed to S. pneumoniae's virulence factors including the ability to colonize the human host forming biofilms.

Biofilms are a community of bacteria that attach to inert or living surfaces. Once attached, the bacteria produce an exopolysaccharide matrix to encase the biofilm and protect it against the host immune response and antibiotics (Dunne, 2002). Biofilm formation initiates as the bacteria sense their own cell density via a process known as quorum sensing (QS), in which *S. pneumoniae*'s competence-stimulating peptide (CSP) plays a critical role via *comC* and the *luxS* system (Oggioni et al., 2004, 2006; Vidal et al., 2011; Yadav et al., 2018). Another major constituent of biofilms is extracellular DNA (eDNA), which can stimulate adherence, transfer genetic information, provide structural stability, and act as an energy source (Das et al., 2013).

Biofilm formation and acquisition of new traits by genetic transformation appear to be linked in S. pneumoniae and perhaps other naturally transformable bacteria. As such, a variety of proteins and peptides from the immune system, including lactoferrin, are natural candidates to disaggregate biofilms and/or inhibit acquisition of resistance. Lactoferrin is a cationic monomeric glycoprotein that is a part of the transferrin family because it binds iron. This protein is produced by acinary cells and glands present in different mucosal sites, at different concentrations. For example, the colostrum contains 100 µM of LF, and tears have 25 µM of LF whereas saliva, cerebrospinal fluid, and serum only contains <0.11 µM. In addition, LF is released by the secondary granules of neutrophils present in inflamed sites; its function at these sites is to sequester the iron, a crucial element for the growth and proliferation of pathogens (Vogel, 2012). LF is a multifunctional protein whose function is determined by the location in which it is found, thus being termed as a moonlighting protein (Baker and Baker, 2009).

Once ingested, LF, as other proteins, is digested in the gastrointestinal tract and this leads to the release of different peptides that also exhibit bioactive properties. Because of this evidence, peptides derived from LF have been synthetically produced. Among them, LFcin17–30 and LFampin265–284 have shown important microbicidal activities. These peptides were synthetically bound using a lysine, creating the peptide LFchimera, which is more active, compared to its peptides of origin (Van Der Kraan et al., 2004; Bolscher et al., 2009).

Due to its structure and ability to bind iron, LF presents two important effects against bacteria. LF is a bacteriostatic antimicrobial because it sequesters iron from the environment, acting as an iron chelator, inhibiting the bacterial metabolism and growth (Oram and Reiter, 1968). LF has also a demonstrated bactericidal effect mainly related to its cationic charge, which was also preserved in those LF-derivative peptides. The cationic charge allows LF to interact with negatively charged cell membrane, specifically lipopolysaccharides (LPS) in Gram negative bacteria or lipotechoic acids (LTA) in Gram positive bacteria, leading to membrane destabilization and loss of selective permeability, inducing bacterial lysis (Van Der Kraan et al., 2004, 2005; Haney et al., 2007; Leon-Sicairos et al., 2009; Lopez-Soto et al., 2009; Flores-Villasenor et al., 2010).

Bactericidal activity of LF and its peptides have been demonstrated in different bacteria such as Escherichia coli, Staphylococcus aureus, and Vibrio parahaemolyticus (Leon-Sicairos et al., 2009; Flores-Villasenor et al., 2010). LF has a high isoelectric point and can bind or interact with several molecules such as LPS, DNA, RNA, and several cell receptors. In fact, LF's strong concentration of positive charge in residues 1-5 and in the C-terminal end of helix 1 (residues 27-30), forms the proposed binding site for DNA. In a report with S. aureus and LF, it was demonstrated that LF and LF peptides presented high affinity for bacterial DNA (Huo et al., 2011). Whether binding of LF to DNA leads to changes in the DNA structure, or degradation, have not been investigated. The ability of LF to bind DNA could change expression of some genes. In our previous study, we demonstrated that treatment of cultures of pneumococcus with LF decreased the transcription of the luxS gene, a gene whose product is involved in the regulation of early steps of biofilm formation in S. pneumoniae strains. Furthermore, it was also demonstrated that bLF and LF peptides decreased >90% of S. pneumoniae viability, perhaps through stable complexes formed among LF and LTA that were potentially liberated from the membrane, causing cell permeabilization (Leon-Sicairos et al., 2014).

The overall goal of this work was to evaluate the antimicrobial effect of LF used at concentrations spanning those found in

human colostrum (100  $\mu$ M) and tears (25  $\mu$ M) and LF-derivative peptides against pneumococcal biofilms. The current study demonstrated a remarkable antimicrobial activity of bLF against pneumococci colonizing human respiratory cells, including antimicrobial activity against antibiotic resistant strains at a concentration safe for humans of <80  $\mu$ M. We also described a non-previously recognized DNAse activity of bLF.

### **MATERIALS AND METHODS**

### Strains and Bacterial Culture Media

Streptococcus pneumoniae strains utilized in this study are shown in **Table 1**. Strains were cultured on blood agar plates (BAP), brain heart infusion broth (BHI), or in Todd Hewitt broth containing 0.5% (w/v) yeast extract (THY). Where indicated, streptomycin (Str), trimethoprim (Tmp), or tetracycline (Tet) was added.

### **Lactoferrin and Peptides**

Bovine LF (bLF), approximately 20% iron saturated, was purchased from Abial Biotech (Spain). LPS contamination and iron concentration were previously evaluated (Cutone et al., 2014). Synthetic peptides LFcin17–30, LFampin265–284, and LFchimera were produced by solid phase peptide synthesis using Fmoc chemistry, as described previously (Bolscher et al., 2009, 2012).

### HEp-2, A549, and Detroit Cells

HEp-2 (ATCC CCL-23) human laryngeal cells, A549 (ATCC CC-L185) human lung cells, and Detroit 562 (ATCC CCL-138) human nasopharyngeal cells were used in this study, the cells were thawed and resuspended in aseptic conditions in a T-25 culture flask (Corning, NY, United States) in EMEM (Detroit and HEp-2) and F-12K (A-549) media supplemented with 10% fetal bovine serum, antibiotics 1% (Streptomycin 10 mg/ml + Penicillin 10,000 IU/ml). They were incubated at  $37^{\circ}\mathrm{C}$  in a 5% CO<sub>2</sub> atmosphere until about 85–100% confluency for future use in experiments.

TABLE 1 | Streptococcus pneumoniae strains used in this study.

S. pneumoniae strain	Characteristics	References
D39	Serotype 2 strain	Avery et al. (1944)
TIGR4	Serotype 4, isolated from a case of bacteremia	Tettelin et al. (2001)
SPJV22	D39 <sup>str</sup>	Lattar et al. (2018)
SPJV17	D39 <sup>tet</sup>	Vidal et al. (2011)
SPJV27	TIGR4 <sup>Tmp</sup>	Lattar et al. (2018)
SPJV23	TIGR4 <sup>str</sup>	Lattar et al. (2018)
GA47281	19F <sup>Tet,Ery,Cm</sup>	Chancey et al. (2011b)
GA44194	19A <sup>Tet,Ery,Cm</sup>	Chancey et al. (2011a)

Str, streptomycin; Tet, tetracycline; Tmp, trimethoprim; Ery, erythromycin; Cm, chloramphenicol.

### Preparation of the Inoculum for Biofilm Assays

Inoculums were prepared as previously described (Vidal et al., 2011). An overnight culture of *S. pneumoniae* grown on blood agar plates (BAP) was used to prepare a bacterial suspension in THY broth. This suspension was incubated at 37°C, 5% CO<sub>2</sub> until the culture reached an OD<sub>600</sub> of  $\sim$ 0.2 (early log phase). Glycerol was then added to give a final 10% (v/v) and stored at  $-80^{\circ}$ C until used.

### Inhibition of Initial Colonization Events by bLF and bLF Peptides

 $7.5 \times 10^4$  CFU/ml of *S. pneumoniae* strain D39 was inoculated in 24-well plates containing A549 cells ( $1 \times 10^4$  confluence) and treated with the following: 40  $\mu$ M bLF, 10  $\mu$ M LFcin17-30, LFampin265-284, or LFchimera, and 20  $\mu$ M erythromycin for 4 or 6 h in F-12K medium without antibiotics and fetal bovine serum, then it was incubated at 37°C in 5% CO<sub>2</sub>. Supernatants were taken to determinate viability of planktonic bacteria by serial dilution and CFU/ml and the density of pneumococcal biofilm was quantified as described earlier (Vidal et al., 2013). Briefly, biofilms were washed three times with sterile 1X PBS and plates were sonicated for 15 s in a Bransonic ultrasonic water bath (Branson, Dunburry, CT, United States). This was followed by extensive pipetting to remove all attached bacteria. Detached biofilms were serially diluted and platted onto BAP, density of biofilms was expressed in CFU/ml.

# Antibacterial Activity of bLF and LF-Derivative Peptides Against Pneumococcal Biofilms

 ${\sim}7\times10^4$  CFU/ml of *S. pneumoniae* (strains with or without antibiotic resistance) were inoculated (1) onto tissue culture-treated, polystyrene, 24-well plates (Corning) and (2) HEp-2 cells (ATCC CCL-23) with a confluency of  $1\times10^4$  of cells per well that were subsequently fixed with 2% paraformaldehyde (Sigma) during 15 min. To form biofilms, samples were incubated during 4 or 8 h, respectively at 37°C in a 5% CO2 atmosphere. After that, planktonic cells were removed and fresh THY or cell culture medium was added. Except in the biofilm control wells, 20, 40, or 80  $\mu$ M bLF, 10  $\mu$ M LFamp265-285, LFcin17-30 or LFchimera were added and incubated for 6 or 12 h at 37°C with 5% CO2. Finally, biofilms were washed and prepared for quantification as was previously mentioned.

### Confocal Microscopy

To visualize the effect of bLF on biofilms of *S. pneumoniae*, biofilms destruction assays were done. *S. pneumoniae* TIGR4 ( $\sim$ 7 × 10<sup>4</sup> CFU/ml) were inoculated onto Detroit 562 cells (ATCC CCL-138) grown to 85–100% confluency. To form biofilms, bacterial suspensions were incubated for 4 h at 37°C in a 5% CO<sub>2</sub> atmosphere. After that, planktonic cells were removed and DMEM medium was added. Once the 4 h-biofilm was grown, 40 and 80  $\mu$ M bLF was added and was incubated for 6 h at 37°C with 5% CO<sub>2</sub>. Following incubation, supernatants were discarded and biofilms were washed and fixed with 2% paraformaldehyde

for 15 min at room temperature (RT). Biofilms were then washed two times with 1X PBS and cells were blocked with 2% BSA for 1 h at RT. For identification of the mammalian cells, sialic acid was stained with 2.5  $\mu$ g/ml Wheat Germ agglutinin (WGA) conjugated with Alexa flour (Molecular probes, Invitrogen) for 15 min at RT (Wright, 1984). After that biofilms were washed once and a serotype-specific polyclonal antibody (labeled with Alexa 488, Molecular Probes, Thermo Fisher Scientific, Grand Island, NY, United States) was used to stain *S. pneumoniae* (40  $\mu$ g/ml) for 1 h at RT (Wu et al., 2017). Then biofilms were washed once and mounted with ProLong Diamond antifade mountant with DAPI (Molecular Probes, Thermo Fisher Scientific, Grand Island, NY, United States). Confocal images were obtained using an Olympus FV1000 confocal microscope and were analyzed with the software ImageJ version 1.49k.

### Purification and Quantification of Extracellular DNA

Streptococcus pneumoniae ( $\sim 7 \times 10^4$  CFU/ml) was inoculated onto (1) tissue culture-treated polystyrene 24-well plates (Corning, NY, United States) or (2) onto  $1 \times 10^4$  HEp-2 cells (ATCC CCL-23) that had been fixed with 2% paraformaldehyde (Sigma Aldrich, St. Luis, MO, United States) and extensively washed to remove the PFA. Inoculated plates, or infected cells, were incubated during 4 h or 8 h, at 37°C with 5% CO<sub>2</sub> to form biofilms. Treatment with bLF (40 and 80  $\mu M$ ) or bLFpeptides (10 µM) was subsequently added as was indicated before. The supernatants were then collected and centrifuged for 10 min at 12,000 × g in a refrigerated centrifuge (Eppendorf, Hamburg, Germany) and filtered by using a 0.2 μM syringe filter. They were subsequently mixed with a 0.5 volume of ethanol and vortexed for 10 s. The DNA from the supernatants was then purified by using the QIAamp DNA minikit (QIAGEN, Hilden, Germany) following the manufacturer's instructions. To quantify amounts of extracellular DNA, quantitative PCR (qPCR) assay, targeting the lytA gene was utilized (Carvalho et al., 2007). Reactions were performed with IQTM SYBR green super mix (BioRad, Hercules, CA, United States), 300 nM of each primer and 4 ng/µl of DNA template. Reactions were run in duplicate using a CFX96 Real-Time PCR Detection System (Bio-Rad, Hercules, CA, United States) with the following conditions: 1 cycle at 55°C for 3 min, 1 cycle at 95°C for 2 min, 40 cycles of 95°C for 15 s, 55°C for 1 min, and 72°C for 1 min. Melting curves were generated utilizing a cycle of 95°C for 1 min, 65°C for 1 min, and 80 cycles starting at 65°C with 0.5°C increments. For quantification purposes, standards containing  $1 \times 10^3$ ,  $1 \times 10^2$ ,  $1 \times 10^{1}$ ,  $1 \times 10^{0}$ ,  $1 \times 10^{-1}$ ,  $5 \times 10^{-2}$ , or  $1 \times 10^{-3}$  pg of S. pneumoniae DNA were run in parallel to generate a standard curve and amounts of eDNA were calculated by using the software Bio-Rad CFX manager (Hercules, CA, United States).

### **EMSA Assay**

Streptococcus pneumoniae D39 ( $\sim$ 7 × 10<sup>4</sup> CFU/ml) was inoculated into THY medium and incubated for 2.5 h at 37°C with 5% CO<sub>2</sub>. The suspension was centrifuged for 10 min at 12,000 × g in a refrigerated centrifuged. DNA was purified by using the Wizard Genomic DNA Purification

Kit (PROMEGA, Madison, WI, United States) following the manufacturer's instructions. To analyze the interactions between bLF and DNA, both bLF and albumin proteins were used and evaluated with the Electrophoretic Mobility-Shift Assay (EMSA) kit (Thermo Fisher Sicientific, Waltham, MA, United States) following the manufacturer's instructions. To visualize the DNA-protein interaction, the samples were separated in a 2% agarose gel and dyed with gel red (Invitrogen, CA, United States). Gels were imaged using the Kodak model E1 logia 100 imaging system.

### **DNA Decay Rate**

DNA purified as above was incubated with 40  $\mu$ M bLF or 40  $\mu$ M albumin for 80 min at 37°C. To measure DNA decay, DNA concentrations were monitored every 10 min using the Nanodrop 2000 spectrophotometer (Thermo Scientific, Waltham, MA, United States).

### **Transformation Frequency Assay**

To evaluate the effect of bLF on genetic transformation of S. pneumoniae, we performed the classic transformation assay. The experiment was carried out in S. pneumoniae D39 competent cells using standard procedures. To induce transformation and test the effect of bLF on S. pneumoniae's ability to transform, a positive control consisting of competent cells, 100 ng of competence-stimulating peptide 1 (CSP1 [EMRLSKFFRDFILQRKK]), 100 ng/mL of DNA purified from strain SPJV22 encoding resistance to Str (200 µg/ml), in complete transformation media was mixed. To test bLF activity against the transformation process, 40 and 80 µM bLF were added to the same reaction as that of the positive control. The negative control lacked CSP1 to prevent transformation. Every sample had a final volume of 200 µl (Havarstein et al., 1995). Samples were incubated for 2 h at 37°C and subsequently plated in the presence or absence of streptomycin. The plates were incubated at 37°C with 5% CO<sub>2</sub> overnight and counted the next day. Transformation frequency was calculated by dividing the number of streptomycin-resistant transformants by the total population obtained on blood agar plates without streptomycin.

# Effect of bLF on Recombination Frequency Between Two Strains of S. pneumoniae in a Bioreactor Model

To evaluate the effect of bLF on recombination frequency (rF), we followed the methodology established by Lattar et al. (2018) with a small modification. Detroit 562 cells (ATCC CCL-138) were grown on snapwell filters (Corning, Corning, NY, United States) for about 4–5 days (until polarized). Snapwells with cells were transferred to the bioreactor chambers and the cells were washed with EMEM media without antibiotics supplemented with 5% fetal serum bovine at a flow rate of 0.20 ml/min using a Master Flex L/S precision pump system (Cole-Parmer, Vernon Hills, IL, United States). Bioreactor chambers were then inoculated with  $\sim \! 1 \times 10^6$  CFU/ml of S. pneumoniae D39<sup>tet</sup> and TIGR4<sup>str</sup>. One chamber was treated with 40  $\mu$ M bLF, a second with 80  $\mu$ M bLF, and a third served as a negative control with no treatment. Each chamber

was incubated at ~35°C. After 8 h of incubation in the bioreactor, biofilms were harvested by sonication for 15 s in a Bransonic ultrasonic water bath. This was followed by extensive pipetting to remove all attached bacteria. To obtain the bacterial density, serial dilutions were done and samples were plated on Tet  $(1 \ \mu g/ml) + Str (200 \ \mu g/ml)$  BAP. These plates were incubated at 37°C with 5% CO<sub>2</sub> overnight. To calculate rF, bacteria growth in obtained from BAP with str and tet was divided between bacteria growth in Tet. Recombination frequency was calculated by dividing the number of Tet + Strresistant recombinants by the total population obtained on blood agar plates without antibiotics.

### **Statistical Analyses**

All experiments were performed in triplicate and analyzed by ANOVA test and student *t*-test using the SigmaPlot software version 12.0 (CA, United States).

### **RESULTS**

# Lactoferrin and LF-Derivative Peptides Inhibit S. pneumoniae Colonization of Human Respiratory Cells

We first sought to evaluate if bLF and LF-derived peptides would inhibit pneumococcal colonization on human respiratory cells, the first step of pneumococcal biofilm formation. To assess this, confluent cultures of human A549 cells were inoculated with *S. pneumoniae* strain D39 and treated with bLF, or LF-derived peptides. As a control, some A549-infected cells were treated with erythromycin. Infected and treated human lung cells were incubated for 4 or 6 h after which the viability of planktonic cells or colonizing biofilms was evaluated by dilution and platting. Experiments demonstrated that the density on planktonic pneumococci was not affected by the treatment with bLF while LF-derivative peptides, and erythromycin, eradicated planktonic bacteria (**Figure 1A**).

Despite bLF did not affect planktonic pneumococci, the viability of pneumococci colonizing human A549 cells and that had been treated with bLF, decreased >90% (Figure 1B). As expected because of the bactericidal activity against planktonic bacteria, LFcin17–30 and LFampin265–284 decreased ~70 and ~80%, respectively, the viability of pneumococci colonizing lung cells while LFchimera eradicated colonizing pneumococci at the same extent as the antibiotic erythromycin did (Figure 1B). A similar antibiotic effect was observed when infected human lung cells were treated with bF, and LF-derivative peptides, and incubated for 6 h (Figures 1C,D).

### Lactoferrin Eradicate *S. pneumoniae* Biofilms

Having demonstrated activity against planktonic and colonizing pneumococci, we then assessed anti-biofilm activity of bLF and LF-derived peptides against pneumococcal biofilms. To assess this, biofilms made by *S. pneumoniae* strain D39 for 4 or 6 h, were challenged with 40  $\mu$ M bLF, or with 10  $\mu$ M of peptides LFcin17–30, LFamp264–285, and LFchimera. Biofilms

were treated for 6 or 12 h. Unexpectedly, treatment of 4 h preformed biofilms with LF-derivative peptides did not induce a significant reduction of pneumococcal biofilms (**Figure 2A**). In contrast, eradication of biofilms was observed in those pneumococcal biofilms treated with bLF, whether biofilms had been preformed during 4 or 6 h, and at both treatment times, 6 or 12 h (**Figures 2B,C**).

We additionally tested the antibacterial effect of bLF against pneumococcal biofilms of antibiotic resistant strains. Biofilms of strain TIGR4<sup>Tmp</sup> that we engineered to bear trimethoprim resistance or two naturally multidrug resistant strains, GA47281<sup>Tet+Ery+Cm</sup> and GA44194<sup>Tet+Ery+Cm</sup> were challenged during 6 h with bLF. **Figure 3** results demonstrated a dose-dependent decrease of the viability of bLF-treated biofilms, in comparison with untreated bacteria.

To further investigate a potential therapeutic and/or prophylactic use, we next determined the effect of bLF on pneumococcal biofilms that had been preformed on human pharyngeal cells. Similarly to the above experiments, bLF induced a statistically significant reduction of viability of pneumococcal biofilms that had been preformed on human pharyngeal cells (Figure 4). Treatment for 6 and 8 h induced a ~80% reduction of viable pneumococci (Figures 4A,B), while 12 h post-treatment a decreased viability of only  $\sim$ 60% was observed indicating that bLF was losing its activity and therefore pneumococci that remained viable after 8 h of incubation started to growth (Figure 4C). Pharyngeal cells colonized by pneumococci, and those colonized and then treated with bLF, were visualized by confocal microscopy. In line with experiments where viable counts were the readout, a number of pneumococci colonizing pharyngeal cells, and with the hallmark pneumococcal infection forming bacterial chains, were observed in the micrographs of the untreated control (Figure 5). These chains were absent in pharyngeal cells infected with pneumococci and treated with bLF at both concentration used, 40 and 80 µM. Moreover, a reduction in the number of pneumococcal cells was observed in cells treated with 40 µM while in those treated with 80 μM pneumococci were scarce (Figure 5, bottom panels). Altogether, our experiments demonstrated a strong anti-bacterial activity of bLF against pneumococci already colonizing human pharyngeal cells.

### Lactoferrin Degrades eDNA Release During Biofilm Formation

To begin evaluating the molecular mechanism utilized by bLF to eradicate pneumococcal biofilms, we assessed the effect of bLF on a main component of the biofilm matrix, the extracellular eDNA. Fascinatingly, eDNA in pneumococcal biofilms formed for 4 h was completely absent in biofilms treated with bLF compared to the untreated control that contained 10  $\mu$ g/ml of eDNA, or compared to those treated with LF-derivate peptides in which eDNA was intact (**Figure 6A**). eDNA was also significantly reduced in biofilms that had been preformed for 8 h and then treated with bLF for 6 h (**Figure 6B**).

Degradation of eDNA was also evaluated in biofilms formed by antibiotic resistance strains (TIGR4<sup>Tmp</sup>, GA47281<sup>Tet+Ery+Cm</sup>,

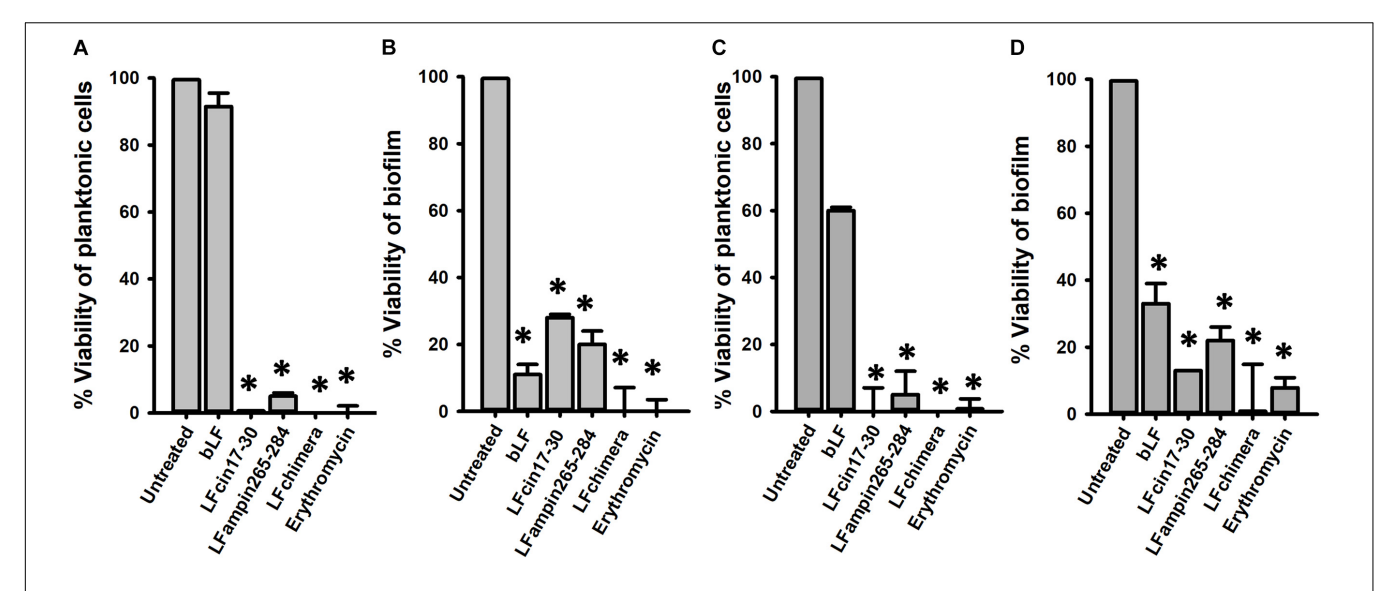


**FIGURE 1** | Bovine Lactoferrin and LF-derived peptides inhibit the viability and attachment of pneumococci present in lung cells and supernatants. Human lung cells A549 were inoculated with  $7.5 \times 10^4$  CFU/ml *Streptococcus pneumoniae* strain D39 and simultaneously treated with 40  $\mu$ M bLF, 10  $\mu$ M LFcin17-30, 10  $\mu$ M LFampinn265-284, 10  $\mu$ M LFchimera, and 20  $\mu$ M Erythromycin. Infected cells were incubated for 4 h **(A,B)** or 6 h **(C,D)** at 37°C with 5% CO<sub>2</sub>. Counts of planktonic pneumococci were obtained in **(A,C)** while biofilm pneumococci were harvested and counted **(B,D)**. Asterisks indicate statistical significance calculated using the ANOVA t test (p < 0.05). Viable counts of pneumococci in the untreated control were adjusted to 100% and viability on those treated was calculated.

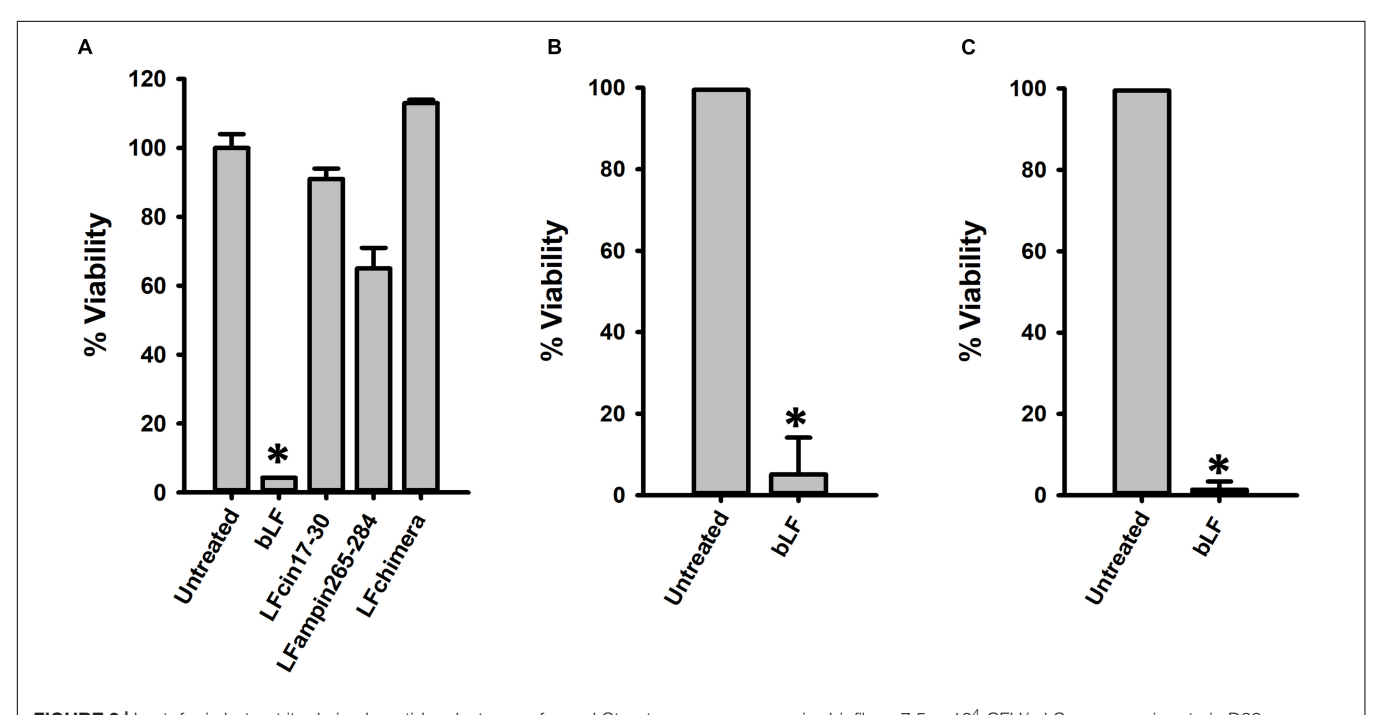


FIGURE 2 | Lactoferrin but not its derived peptides destroy preformed  $Streptococcus\ pneumoniae\ biofilms.\ 7.5 \times 10^4\ CFU/ml\ S.\ pneumoniae\ strain\ D39\ were inoculated in a 24-well plate containing THY and then plates were incubated for 4 h (A,B) or 8 h (C) at 37°C with 5% CO2. After that, planktonic cells were removed, biofilms were washed and then treated with 40 <math>\mu$ M bLF, 10  $\mu$ M LFcin17-30, 10  $\mu$ M LFampinn265-284, and 10  $\mu$ M LFchimera for 6 h (A,C) or 12 h (B). Treated biofilms were harvested, diluted, and platted on blood agar plates to obtain viable counts. Experiments were repeated at least three times. Standard deviation of the mean is shown. Asterisks indicate statistical significance calculated using the ANOVA test ( $\rho$  < 0.05). Viable counts of pneumococci in the untreated control were adjusted to 100% and viability on those treated was calculated.

and GA44194  $^{Tet+Ery+Cm})$  challenged with 20, 40, and 80  $\mu M$  bLF. In all experiments, a statistically significant reduction of eDNA was observed in biofilms treated with bLF (**Figure 7**).

Whereas eDNA from reference strains D39 and TIGR4 was completely absent (i.e., 1  $\times$  10³-fold reduced) after the treatment with 40  $\mu M$  of bLF, eDNA of naturally

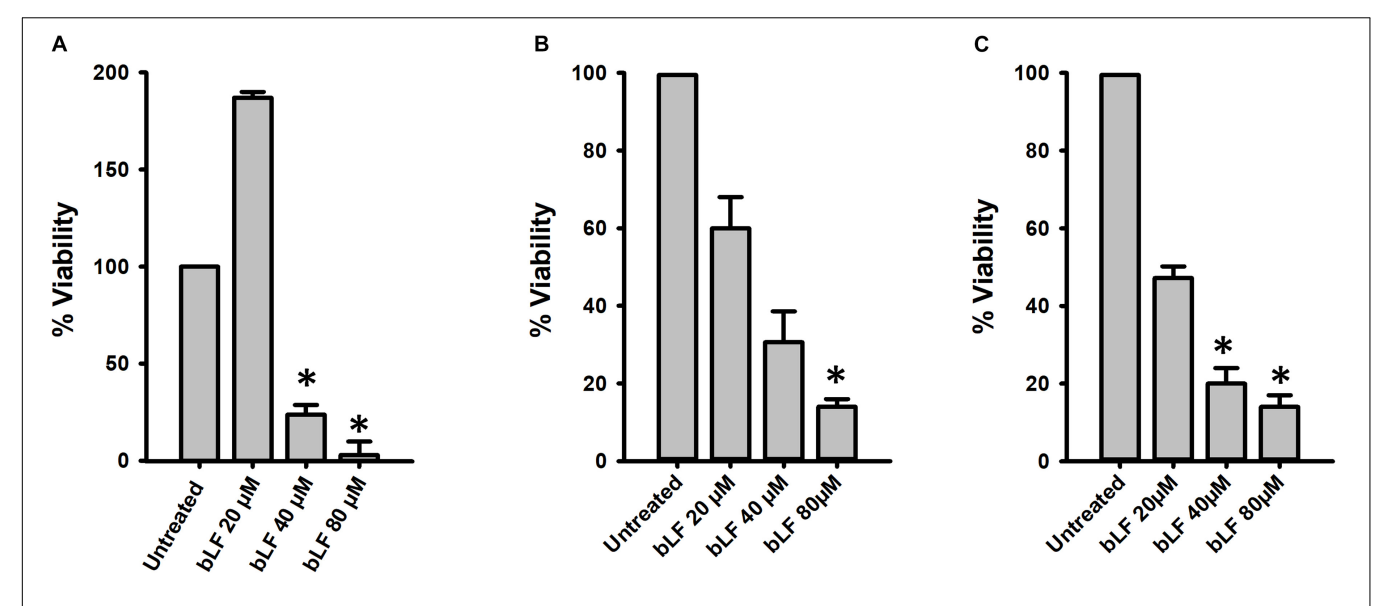
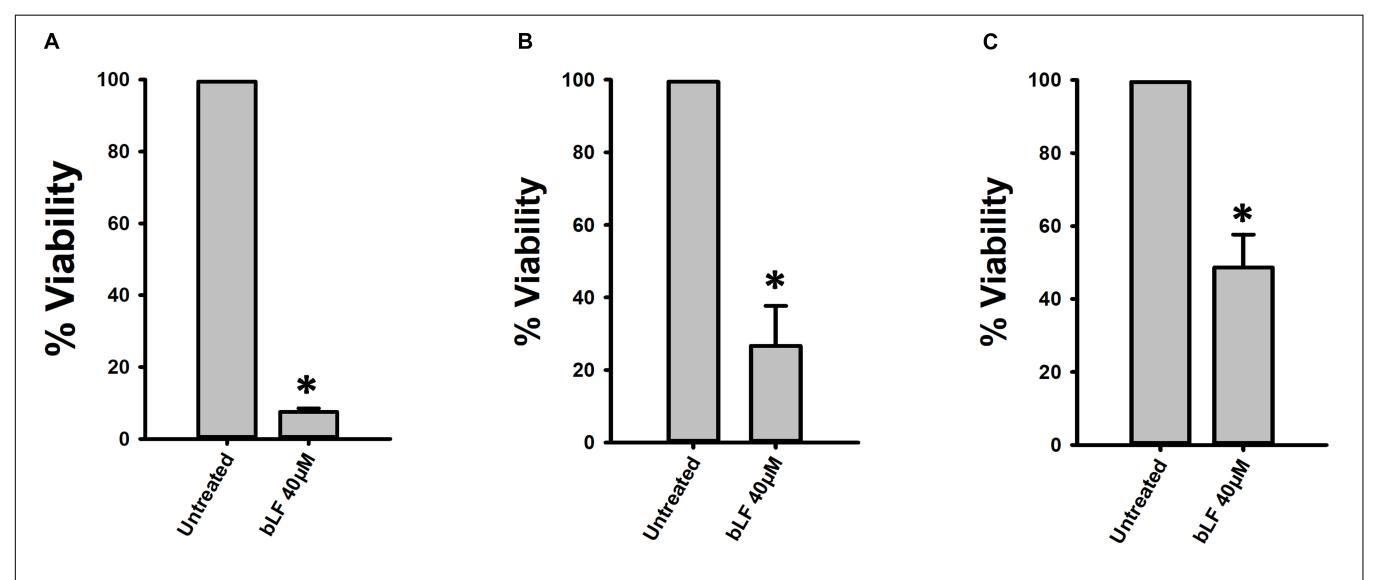


FIGURE 3 | Bovine Lactoferrin eradicates antibiotic-resistance strains of *Streptococcus pneumoniae* biofilms. *S. pneumoniae* strains TIGR4<sup>Tmp</sup> (A), GA47281<sup>Tet+Ery+Cm</sup> (B), and GA44194<sup>Tet+Ery+Cm</sup> (C), were inoculated in a 24-well plate containing THY. The plate was incubated for 4 h at 37°C with a 5% CO<sub>2</sub> atmosphere. Planktonic cells were removed and the remaining biofilms were washed once and bovine Lactoferrin (bLF) was added at the indicated concentration and incubated for 6 h. Treated biofilms were harvested, diluted, and platted on blood agar plates to obtain biofilm viable counts. Experiments were repeated at least three times. Standard deviation of the mean is shown. Asterisks indicate statistical significance calculated using the ANOVA test (p < 0.05). The viability (%) refers to number of live cells present in samples relative to untreated cells.



**FIGURE 4** | Lactoferrin eradicates pneumococcal colonization on human HEp-2 cells. *Streptococcus pneumoniae* strain D39 (7.5 × 10<sup>4</sup> CFU/ml) was inoculated in cultures of human HEp-2 cells and incubated for 4 h **(A,B)** or 8 h **(C)** at 37°C with 5% CO<sub>2</sub>. Planktonic cells were removed and biofilms were washed and treated with bovine Lactoferrin (bLF) for 6 h **(A,C)** or 12 h **(B)**. Treated pneumococci were harvested, diluted, and platted on blood agar plates to obtain viable cells. Experiments were repeated at least three times. Standard deviation of the mean is shown. Asterisks indicate statistical significance calculated using the ANOVA test ( $\rho < 0.05$ ). Viable counts of pneumococci in the untreated control were adjusted to 100% and viability on those treated was calculated.

resistant pneumococcal strains was 10-fold reduced, but not completely degraded, indicating that those strains might have evolved a mechanism to partially inactivate the DNAse activity of bLF.

We finally evaluated whether degradation of eDNA by bLF would be observed in the context of colonization of human

pharyngeal cells. Accordingly, eDNA from strain D39 colonizing human cells was  $\sim 10,000$ -fold reduced in the supernatants of cells infected with pneumococci and treated with bLF for 6 or 12 h in comparison to those infected cells that were left untreated (**Figure 8**). Overall our data indicate that bLF bears DNAse activity.

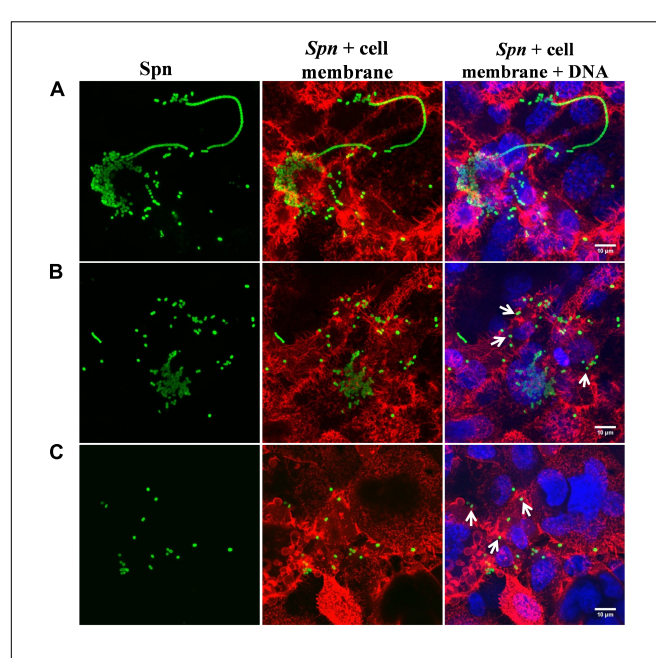


**FIGURE 5** | Lactoferrin eradicates preformed *Streptococcus pneumoniae* biofilms in nasopharynx cells. *S. pneumoniae* (spn) strain TIGR4 (7.5 × 10<sup>4</sup> CFU/ml) was inoculated in a 24-well plate containing Detroit cells and plates were incubated for 4 h at 37°C with 5% CO<sub>2</sub>. Planktonic cells were removed and biofilms were washed and then untreated (**A**) or treated with bovine Lactoferrin bLF, 40 and 80 μM (**B,C**, respectively) for 6 h. Treated biofilms were slowly washed once with PBS, fixed with 2% *P*-formaldehyde, and stained with Wheat gern agglutinin (WGA) for the cell membrane, antibody serotype-specific polyclonal for *S. pneumoniae* and DAPI for DNA. Confocal images with close up of 10 μM were obtained using an Olympus FV1000 confocal microscope and were analyzed with ImageJ version 1.49k. Arrows indicate the decrement of pneumococcal cells in biofilms.

# Lactoferrin Binds and Degrades DNA Inhibiting Acquisition of Resistance by Pneumococcal Strains

If bLF degrades DNA then it should first bind it; we therefore performed an EMSA assay to investigate this possibility with DNA purified from cultures of strain D39. Figure 9A demonstrated that bLF bound genomic DNA, trapping the DNA into the well whereas untreated pneumococcal DNA, or pneumococcal DNA that had been incubated with another serum protein albumin, migrated into the gel. To further investigate degradation of genomic DNA by bLF, we conducted a time-course study of DNA decoy. Genomic DNA (~140 ng/ml) was left untreated, or treated with bLF, or albumin for up to 60 min. Statistically significant degradation of genomic DNA was observed soon after 20 min of incubation with bLF and continued decreasing through the incubation time (Figure 9B). In contrast, DNA signal remained intact in untreated DNAs or in those DNA samples treated with albumin (Figure 9B). Together these experiments demonstrate that bLF binds DNA to induce its degradation.

We then hypothesize that if bLF degrades DNA, it should inhibit acquisition of resistance. We first tested whether

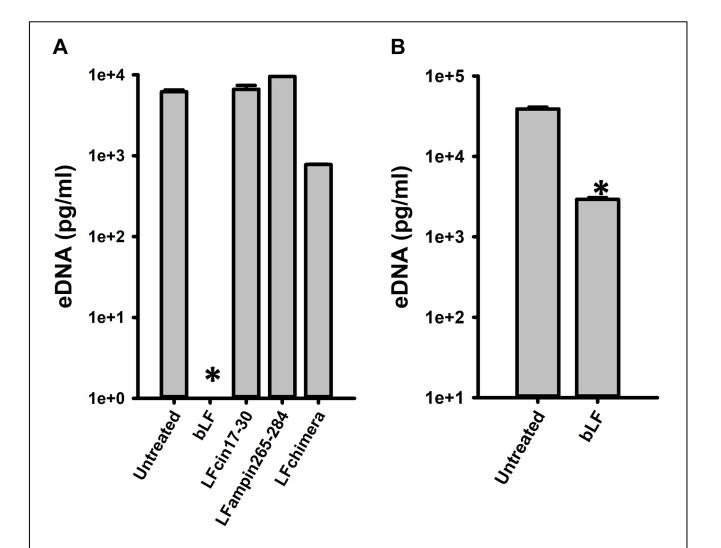


**FIGURE 6** Bovine lactoferrin digest eDNA in preformed *Streptococcus pneumoniae* biofilms. *S. pneumoniae* strain D39 (7.5  $\times$  10 $^4$  CFU/ml) was inoculated in a 24-well plate containing THY and incubated for 4 h (A) or 8 h (B) at 37 $^{\circ}$ C with a 5% CO $_2$  atmosphere. Planktonic cells were removed; biofilms washed once and then treated with 40  $\mu$ M bLF, 10  $\mu$ M, LFcin17-30, 10  $\mu$ M LFampinn265-284, and 10  $\mu$ M LFchimera for 6 h (A) or 12 h (B). After that, the supernatants were removed and DNA extracted. eDNA quantification was performed by using qPCR. Experiments were repeated at least three times. Standard deviation of the mean is shown. Asterisks indicate statistical significance calculated using the ANOVA test ( $\rho <$  0.05).

acquisition of resistance in classic transformation reactions would be inhibited by bLF. As shown in **Figure 9C**, in transformation reactions containing competent D39 pneumococci, DNA encoding resistance to streptomycin, and bLF, the transformation frequency (tF) was significantly decreased in comparison to the tF obtained in the untreated control.

Given that acquisition of resistance by pneumococcal strains is stimulated when strains D39 and TIGR4 are inoculated in pharyngeal cells and incubated under the dynamic system of a bioreactor, we assessed whether treatment with bLF would inhibit acquisition of resistance by evaluating the recombination frequency (rF) in this life-like environment. In bioreactor chambers containing human pharyngeal cells and inoculated with strains D39<sup>Tet</sup> and TIGR4<sup>Str</sup>, a rF of  $\sim \! \! 1 \times 10^{-2}$  of pneumococci bearing tetracycline and streptomycin resistance was obtained (**Figure 9D**). Bioreactors chambers incubated also with 40  $\mu M$  of bLF yielded a similar rF to that in untreated bioreactor chambers, whereas in chambers incubated with 80 mM of bLF the rF was 100-fold reduced confirming that bLF inhibit the acquisition of resistance by degrading eDNA.

### **DISCUSSION**

In the present report, we utilized *in vitro* models to mimic two important biological events leading to persistence of pneumococcus in the human airways (i.e., initial colonization events and persistent pneumococcal biofilms), to evaluate the

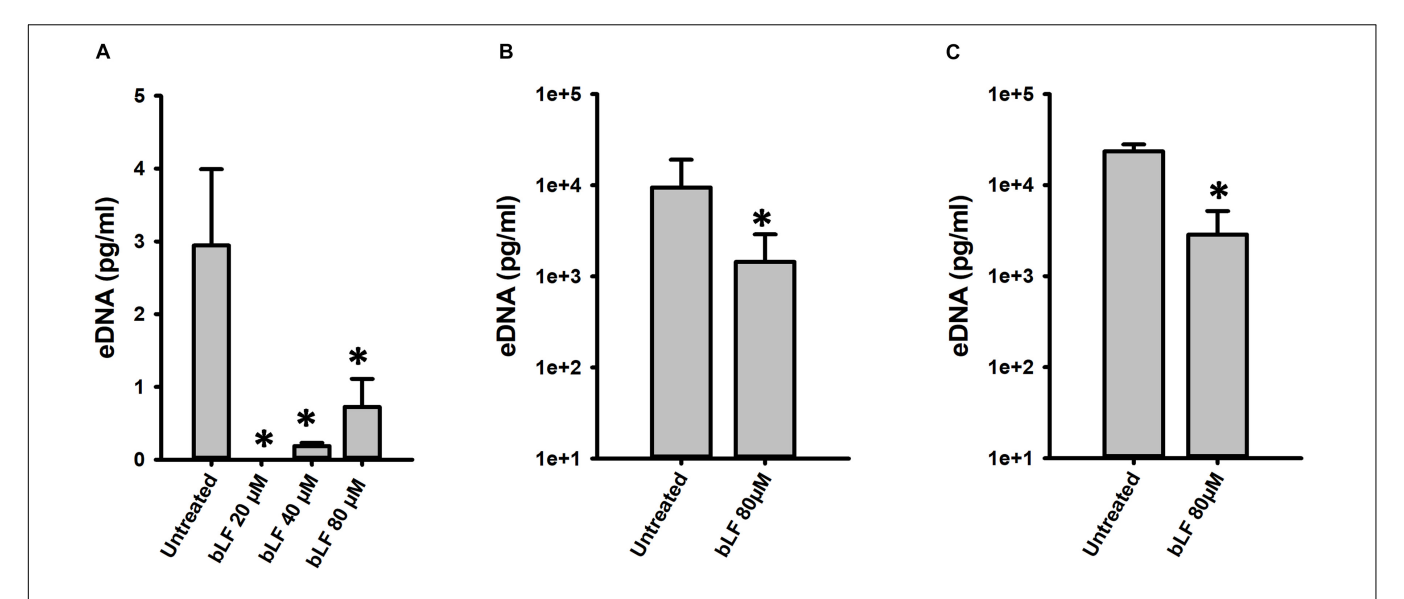
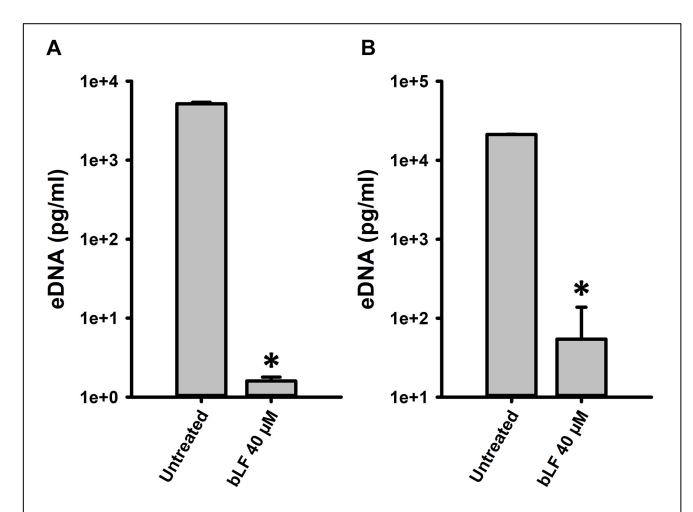


FIGURE 7 | Bovine lactoferrin degrades eDNA from antibiotic-resistance strains of *Streptococcus pneumoniae*. *S. pneumoniae* strains TIGR4<sup>Tmp</sup> (A), GA47281<sup>Tet+Ery+Cm</sup> (B), and GA44194<sup>Tet+Ery+Cm</sup> (C) were inoculated in a 24-well plate containing THY. Then, the plate was incubated for 4 h at 37°C with a 5% CO<sub>2</sub> atmosphere. Planktonic cells were removed, biofilms washed once, and bovine Lactoferrin (bLF) was added at the indicated concentrations and incubated for 6 h. The supernatants were removed, filter-sterilized to eliminate bacteria in supernatant and DNA was extracted. eDNA quantification was performed by using qPCR. Experiments were repeated at least three times. Standard deviation of the mean is shown. Asterisks indicate statistical significance calculated using the ANOVA test (p < 0.05).



**FIGURE 8** | Bovine lactoferrin degrades eDNA in preformed *Streptococcus pneumoniae* biofilms in Hep-2 cells. *S. pneumoniae* strain D39 (7.5  $\times$  10<sup>4</sup> CFU/ml) was inoculated in a 24-well plate containing Hep-2 cells and incubated for 4 h (**A,B**) at 37°C with a 5% CO<sub>2</sub> atmosphere. Then, planktonic cells were removed, biofilms washed once, then treated with bovine Lactoferrin (bLF) for 6 h (**A**) or 12 h (**B**). After that, the supernatants were removed and DNA extracted. eDNA quantification was performed by using qPCR. Experiments were repeated at least three times. Standard deviation of the mean is shown. Asterisks indicate statistical significance calculated using the ANOVA test ( $\rho$  < 0.05).

effect of physiologically relevant concentrations of LF and LF-derivative peptides on biofilm persistence. We first demonstrated that bLF, and LF-derivative peptides, inhibited initial colonization events on human respiratory cells. The mechanism(s) that

blocked colonization was different for bLF compared to that of LF-derivative peptides. For the latter, inhibition of colonization was caused by the antibacterial activity of LF-derivative peptides against planktonic pneumococci. The mechanism utilized by bLF to inhibit pneumococcal colonization was different since bLF presented low antibacterial activity against planktonic bacteria. In line with our experiments, an effect for LF against colonization by other organisms such as Pseudomonas aeruginosa, Streptococcus mutans, and Candida albicans has been demonstrated (Berlutti et al., 2004; O'may et al., 2009; Morici et al., 2016). The iron-chelating activity of LF was demonstrated as the main factor (Singh et al., 2002). The current study, and a previous publication by our laboratories (Leon-Sicairos et al., 2014), allow us to speculate that bLF inhibits biofilm formation through two different mechanisms: (1) a decreased of luxS gene expression, a gene that regulates biofilm formation (Vidal et al., 2011), and the binding of LF to pneumococcal surface protein A (PspA) thus inhibiting adherence of the pneumococcus to human epithelial cells. Blocking adherence through PspA binding has been linked to an increased number of non-adherent pneumococci bacteria (Shaper et al., 2004), such as it was demonstrated in experiments presented in Figures 1B,D.

Despite having a strong bactericidal effect against planktonic bacteria inoculated onto human respiratory cells, to our surprise, LF-derivative peptides did not have an effect against pneumococci already forming a biofilm. Given that LF-derivative peptides were very efficient for eradicating planktonic pneumococci, these peptides likely target metabolically active bacteria and not pneumococci in quiescent state forming a biofilm. The possibility exist that an increased density of pneumococci in the biofilms state, versus planktonic bacteria

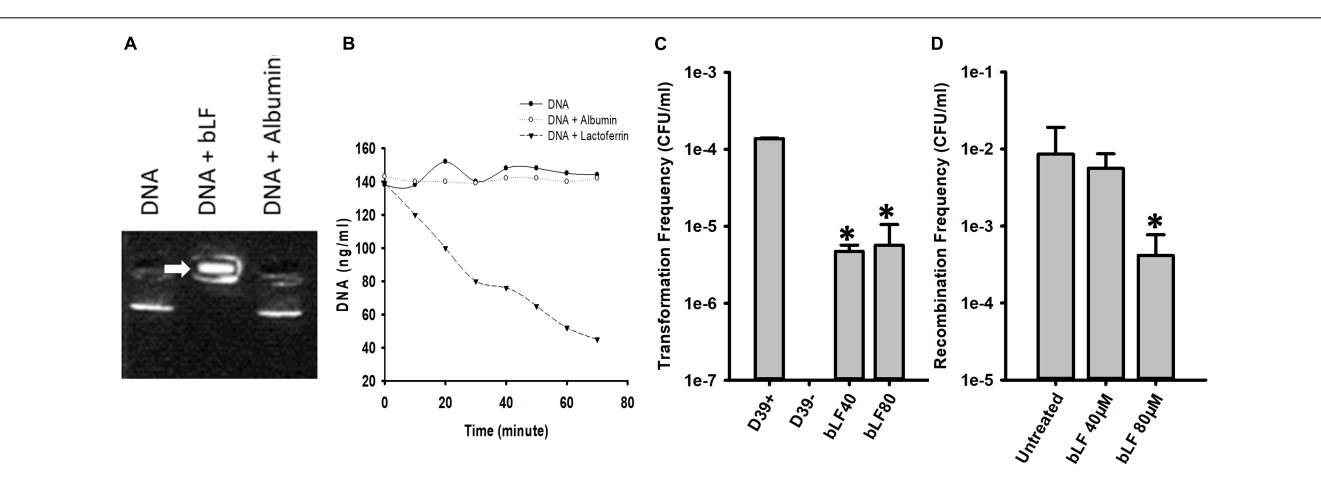


**FIGURE 9** | Bovine lactoferrin binds and degrades DNA, decreasing transformation and recombination frequencies of *Streptococcus pneumoniae*. *S. pneumoniae* D39 DNA was mixed with bovine Lactoferrin or albumin (40  $\mu$ M) for 15 min. An electrophoretic mobility shift assay was done and was separated with 2% agarose gel **(A)**. The mix of DNA-LF or DNA-albumin were also measured every 10 min using nanodrop **(B)**. Competent *S. pneumoniae* D39 was mixed with DNA and CSP 1 in the presence or absence of bLF and incubated at 37°C for 2 h. Transformation frequencies were calculated **(C)**. Bioreactor chambers with D39<sup>tet</sup> and TIGR4<sup>str</sup> were co-incubated for 8 h in the presence of bLF (40 and 80  $\mu$ M) or were left untreated. Bacteria were then counted and the recombination frequencies were calculated **(D)**. Standard deviation of the mean is shown. Asterisks indicate statistical significance calculated using the ANOVA test ( $\rho$  < 0.05).

challenged with LF-peptides, was a factor to the inability of LF-derivative peptides to affect pneumococcal biofilms.

The current study, however, demonstrated that bLF eradicates pneumococci forming biofilms at two different density of biofilm bacteria, those already formed after 4 h of incubation and 8 h post-inoculation. Moreover, the density of these pneumococcal biofilms decreased whether biofilms were formed on abiotic substrates or on human pharyngeal cells, which bears both prophylactic and therapeutic potential to combat nasopharyngeal colonization or pneumococcal disease such as otitis media or sinusitis. The concentration of LF that eradicated pneumococcal biofilms (20, 40, and 80  $\mu M)$  was similar to the concentrator of LF found in colostrum (100  $\mu M)$  and tears (25  $\mu M)$  and therefore it is safe for humans. Both colostrum and tears protect the human host from bacterial infections, in part because of the antimicrobial activity of LF.

It has been reported that LF has anti-biofilm properties when mixed with other molecules. For example, Ammons and colleagues (2009) demonstrated that LF penetrates P. aeruginosa biofilms and reduced 1 log reduction in viability, but in their experiments a combination LF and xylitol reduced ~3 unit/logarithmic (Ammons et al., 2009). Sheffield et al. (2012) tested LF to disrupt E. coli biofilms; LF reduced more than 90% of E. coli biofilms and 100% of Klebsiella pneumoniae biofilms (Sheffield et al., 2012) whereas an anti-biofilm effect against the Gram positive S. mutans decreasing the density of biofilms has also been demonstrated (Allison et al., 2015). These studies, however, were conducted using abiotic substrates to produce biofilms of Gram negative bacteria. Our current studies with the Gram positive S. pneumoniae are in line with these mentioned above but we additionally demonstrated that bLF eradicates biofilms made on biologically relevant substrates (i.e., human respiratory cells) and therefore supports a potential therapeutic and/or prophylactic application for LF.

How bLF induced the decrease of the density of *S. pneumoniae* biofilms? There are a number of possibilities. For example, given that LF chelates iron and although the metabolism in biofilms decreases these quiescent bacteria still may require iron to maintain its structure and/or vital activities. Another possibility is its capacity to interact with negative components of bacteria such as LPS (Ellison et al., 1988; Leon-Sicairos et al., 2014). Besides these two possibilities, we experimentally provided with a mechanism when an important component of the pneumococcal biofilm matrix was evaluated, eDNA and found a significantly decrease of eDNA in the supernatant. Since eDNA is an anionic molecule, our mechanistic experiments demonstrated that in fact bLF binds DNA and that this biding precedes DNA degradation. As expected, degradation was observed in different pneumococcal strains, including multi-drug resistant pneumococci, although at different extents indicating that other individual, strain specific, components of the biofilm matrix interfered with bLF-induced degradation of eDNA. All evidence together led us to formulate the following hypothesis that bLF decreased the density of pneumococcal biofilms by chelating iron necessary to maintain biofilm viability, and binding to negatively charged components of the biofilm matrix such as eDNA, thus degrading this important component of the matrix. Significant more efforts will be required to fully dissect the mechanism of biofilm eradication.

It very interesting that concentration that bLF that we used to demonstrate the antimicrobial activity against pneumococcal biofilms is inside of range or lower of some physiological fluids of human. The higher concentration that we used was 80  $\mu M$ , lower that in colostrum 100  $\mu M$  (Sánchez et al., 1992). It means that concentration used in this work couldn't present adverse effect in human, in fact 40  $\mu M$  of LF was sufficient to alter the biofilms

structure, concentration that is inside of milk range (20–60  $\mu M)$  (Ford et al., 1977; Zavaleta et al., 1995; Hamosh, 1998). The low concentration of LF in upper airways of human (6.25–12.5  $\mu M)$  could to influence to allow the colonization of pneumococcus (Dubin et al., 2004).

Our studies identified an activity of bLF that had not previously been recognized, DNAse activity (Bennett et al., 1986). The aminoacid threonine play a central role in DNA hydrolysis in active site of DNAse 1, this aromatic residue induces distortion of DNA (Parsiegla et al., 2012), in comparison with the active zone of LF to bind DNA located in C-terminal in end of helix in the aminoacids residues 27-30, which contains threonine, fact that could help in DNAse activity of bLF (Baker and Baker, 2009). DNase has been successful used to disaggregates pneumococcal biofilms (Hall-Stoodley et al., 2008), and, of course, DNase has a profound effect on pneumococcal acquisition of new traits (i.e., capsule genes, antibiotic resistance genes) by recombination via transformation. Treatment with DNase completely blocked recombination via transformation in a life-like system such as that utilized in the current study (Lattar et al., 2018). Accordingly, our studies demonstrated that treatment with bLF rendered the pneumococcus unable to uptake DNA whether the transformation reaction was performed in vitro or using our model of recombination in a life-like bioreactor system. Therefore, bLF not only has the capacity to eradicate colonizing pneumococcal biofilms, but also it appears to prevent recombination by its DNase activity. Because human lactoferrin (hLF) has ~72% aminoacids homology with bLF (calculated by BLAST analysis), it is likely that hLF is also able to degrade DNA. We in the field have speculated for a number of years now that the future of therapeutics would include targeting important components of the pneumococcal transformation machinery including the competence stimulating peptide (CSP) and eDNA (Hakenbeck, 2000; Moreno-Gamez et al., 2017; Salvadori et al., 2019). Whereas this was an interesting recommendation, it has

### **REFERENCES**

- Allison, L. M., Walker, L. A., Sanders, B. J., Yang, Z., Eckert, G., and Gregory, R. L. (2015). Effect of human milk and its components on *Streptococcus Mutans* biofilm formation. *J. Clin. Pediatr. Dent.* 39, 255–261. doi: 10.17796/1053-4628-39.3.255
- Ammons, M. C., Ward, L. S., Fisher, S. T., Wolcott, R. D., and James, G. A. (2009). In vitro susceptibility of established biofilms composed of a clinical wound isolate of *Pseudomonas aeruginosa* treated with lactoferrin and xylitol. *Int. J. Antimicrob. Agents* 33, 230–236. doi: 10.1016/j.ijantimicag.2008.08.013
- Avery, O. T., Macleod, C. M., and Mccarty, M. (1944). Studies on the chemical nature of the substance inducing transformation of pneumococcal types. Induction of transformation by a desoxyribonucleic acid fraction isolated from pneumococcus type III. J. Exp. Med. 79, 137–158.
- Baker, E. N., and Baker, H. M. (2009). A structural framework for understanding the multifunctional character of lactoferrin. *Biochimie* 91, 3–10. doi: 10.1016/j. biochi.2008.05.006
- Bennett, R. M., Merritt, M. M., and Gabor, G. (1986). Lactoferrin binds to neutrophilic membrane DNA. Br. J. Haematol. 63, 105–117. doi: 10.1111/j. 1365-2141.1986.tb07500.x
- Berlutti, F., Ajello, M., Bosso, P., Morea, C., Petrucca, A., Antonini, G., et al. (2004). Both lactoferrin and iron influence aggregation and biofilm formation in

not been successfully implemented as of yet, perhaps due to the lack of specific molecules that are safe for humans such as lactoferrin.

### DATA AVAILABILITY STATEMENT

All datasets generated for this study are included in the manuscript/supplementary files.

### **AUTHOR CONTRIBUTIONS**

UA-Z, JV, and NL-S conceived and designed the study. UA-Z, KN, JB, CL-S, and BA collected the data. UA-Z, AC-R, JV, and NL-S analyzed and interpreted the data. UA-Z and BA drafted the manuscript. AC-R, JV, and NL-S critically revised the manuscript. UA-Z, AC-R, KN, JB, CL-S, BA, JV, and NL-S approved the final version of the manuscript.

### **FUNDING**

We wish to thank CONACyT, Mexico and PROFAPI, UAS for support through grants CB-2014-236546 and 2014/105, 2015/140. UA-Z was the recipient of a Ph.D. scholarship from CONACyT, Mexico (291250). Work in JV lab was generously supported by grants from the National Institutes of Health (NIH; R21AI112768-01A1 and 1R21AI144571-01).

### **ACKNOWLEDGMENTS**

The authors thank Dr. David Stephens and Dr. Yih-Ling Tzeng from School of Medicine, Emory University, for providing antibiotic resistant strains.

- Streptococcus mutans. Biometals 17, 271–278. doi: 10.1023/b:biom.0000027704. 53859 d3
- Bolscher, J., Nazmi, K., Van Marle, J., van 't Hof, W., and Veerman, E. (2012). Chimerization of lactoferricin and lactoferrampin peptides strongly potentiates the killing activity against *Candida albicans*. *Biochem. Cell Biol.* 90, 378–388. doi: 10.1139/o11-085
- Bolscher, J. G., Adao, R., Nazmi, K., Van Den Keybus, P. A., van 't Hof, W., Nieuw Amerongen, A. V., et al. (2009). Bactericidal activity of LFchimera is stronger and less sensitive to ionic strength than its constituent lactoferricin and lactoferrampin peptides. *Biochimie* 91, 123–132. doi: 10.1016/j.biochi.2008. 05.019
- Carvalho, M. D. G. S., Tondella, M. L., Mccaustland, K., Weidlich, L., Mcgee, L., Mayer, L. W., et al. (2007). Evaluation and improvement of realtime PCR assays targeting lytA, ply, and psaA genes for detection of pneumococcal DNA. J. Clin. Microbiol. 45, 2460–2466. doi: 10.1128/jcm. 02498-06
- Chancey, S., Kumar, N., Sengamalay, N., Matthews, C., Hine, E., Pallavajjal, A., et al. (2011a). Genomic Sequence of Streptococcus pneumoniae GA44194. Heidelberg: EMBL.
- Chancey, S., Kumar, N., Sengamalay, N., Matthews, C., Hine, E., Pallavajjal, A., et al. (2011b). Genomic Sequence of Streptococcus pneumoniae GA47281. Heidelberg: EMBL.

- Cutone, A., Frioni, A., Berlutti, F., Valenti, P., Musci, G., and Bonaccorsi Di Patti, M. C. (2014). Lactoferrin prevents LPS-induced decrease of the iron exporter ferroportin in human monocytes/macrophages. *Biometals* 27, 807–813. doi: 10.1007/s10534-014-9742-7
- Das, T., Sehar, S., and Manefield, M. (2013). The roles of extracellular DNA in the structural integrity of extracellular polymeric substance and bacterial biofilm development. *Environ. Microbiol. Rep.* 5, 778–786. doi: 10.1111/1758-2229. 12085
- Dubin, R. F., Robinson, S. K., and Widdicombe, J. H. (2004). Secretion of lactoferrin and lysozyme by cultures of human airway epithelium. Am. J. Physiol. Lung Cell Mol. Physiol. 286, L750–L755.
- Dunne, W. M. Jr. (2002). Bacterial adhesion: seen any good biofilms lately? Clin. Microbiol. Rev. 15, 155–166. doi: 10.1128/cmr.15.2.155-166.2002
- Ellison, R. T. III, Giehl, T. J., and Laforce, F. M. (1988). Damage of the outer membrane of enteric gram-negative bacteria by lactoferrin and transferrin. *Infect. Immun.* 56, 2774–2781.
- Flores-Villasenor, H., Canizalez-Roman, A., Reyes-Lopez, M., Nazmi, K., De La Garza, M., Zazueta-Beltran, J., et al. (2010). Bactericidal effect of bovine lactoferrin, LFcin, LFampin and LFchimera on antibiotic-resistant Staphylococcus aureus and Escherichia coli. Biometals 23, 569–578. doi: 10.1007/ s10534-010-9306-4
- Ford, J. E., Law, B. A., Marshall, V. M., and Reiter, B. (1977). Influence of the heat treatment of human milk on some of its protective constituents. *J. Pediatr.* 90, 29–35. doi: 10.1016/s0022-3476(77)80759-2
- Hakenbeck, R. (2000). Transformation in Streptococcus pneumoniae: mosaic genes and the regulation of competence. Res. Microbiol. 151, 453–456. doi: 10.1016/ s0923-2508(00)00170-4
- Hall-Stoodley, L., Nistico, L., Sambanthamoorthy, K., Dice, B., Nguyen, D., Mershon, W. J., et al. (2008). Characterization of biofilm matrix, degradation by DNase treatment and evidence of capsule downregulation in *Streptococcus pneumoniae* clinical isolates. *BMC Microbiol*. 8:173. doi: 10.1186/1471-2180-8-173
- Hamosh, M. (1998). Protective function of proteins and lipids in human milk. Biol. Neonate 74, 163–176. doi: 10.1159/000014021
- Haney, E. F., Lau, F., and Vogel, H. J. (2007). Solution structures and model membrane interactions of lactoferrampin, an antimicrobial peptide derived from bovine lactoferrin. *Biochim. Biophys. Acta* 1768, 2355–2364. doi: 10.1016/j.bbamem.2007.04.018
- Havarstein, L. S., Coomaraswamy, G., and Morrison, D. A. (1995). An unmodified heptadecapeptide pheromone induces competence for genetic transformation in *Streptococcus pneumoniae*. Proc. Natl. Acad. Sci. U.S.A. 92, 11140–11144. doi: 10.1073/pnas.92.24.11140
- Huo, L., Zhang, K., Ling, J., Peng, Z., Huang, X., Liu, H., et al. (2011). Antimicrobial and DNA-binding activities of the peptide fragments of human lactoferrin and histatin 5 against Streptococcus mutans. Arch. Oral Biol. 56, 869–876. doi: 10.1016/j.archoralbio.2011.02.004
- Klein, J. O. (1994). Otitis media. Clin. Infect. Dis. 19, 823-833.
- Lattar, S. M., Wu, X., Brophy, J., Sakai, F., Klugman, K. P., and Vidal, J. E. (2018).
  A mechanism of unidirectional transformation, leading to antibiotic resistance, occurs within nasopharyngeal pneumococcal biofilm consortia. mBio 9:e561-18. doi: 10.1128/mBio.00561-18
- Leon-Sicairos, N., Angulo-Zamudio, U. A., Vidal, J. E., Lopez-Torres, C. A., Bolscher, J. G., Nazmi, K., et al. (2014). Bactericidal effect of bovine lactoferrin and synthetic peptide lactoferrin chimera in *Streptococcus pneumoniae* and the decrease in luxS gene expression by lactoferrin. *Biometals* 27, 969–980. doi: 10.1007/s10534-014-9775-y
- Leon-Sicairos, N., Canizalez-Roman, A., De La Garza, M., Reyes-Lopez, M., Zazueta-Beltran, J., Nazmi, K., et al. (2009). Bactericidal effect of lactoferrin and lactoferrin chimera against halophilic Vibrio parahaemolyticus. Biochimie 91, 133–140. doi: 10.1016/j.biochi.2008.06.009
- Lopez-Soto, F., Gonzalez-Robles, A., Salazar-Villatoro, L., Leon-Sicairos, N., Pina-Vazquez, C., Salazar, E. P., et al. (2009). *Entamoeba histolytica* uses ferritin as an iron source and internalises this protein by means of clathrin-coated vesicles. *Int. J. Parasitol.* 39, 417–426. doi: 10.1016/j.ijpara.2008.08.010
- Moreno-Gamez, S., Sorg, R. A., Domenech, A., Kjos, M., Weissing, F. J., Van Doorn, G. S., et al. (2017). Quorum sensing integrates environmental cues, cell density and cell history to control bacterial competence. *Nat. Commun.* 8:854. doi: 10.1038/s41467-017-00903-y

- Morici, P., Fais, R., Rizzato, C., Tavanti, A., and Lupetti, A. (2016). Inhibition of *Candida albicans* biofilm formation by the synthetic lactoferricin derived peptide hLF1-11. *PLoS One* 11:e0167470. doi: 10.1371/journal.pone.0167470
- Musher, D. M., Alexandraki, I., Graviss, E. A., Yanbeiy, N., Eid, A., Inderias, L. A., et al. (2000). Bacteremic and nonbacteremic pneumococcal pneumonia. *Prospect. Study Med.* 79, 210–221. doi: 10.1097/00005792-200007000-00002
- Nunes, S., Sá-Leão, R., Carriço, J., Alves, C. R., Mato, R., Avô, A. B., et al. (2005). Trends in drug resistance, serotypes, and molecular types of *Streptococcus pneumoniae* colonizing preschool-age children attending day care centers in Lisbon, portugal: a summary of 4 years of annual surveillance. *J. Clin. Microbiol.* 43, 1285–1293. doi: 10.1128/jcm.43.3.1285-1293.2005
- O'brien, K. L., Wolfson, L. J., Watt, J. P., Henkle, E., Deloria-Knoll, M., Mccall, N., et al. (2009). Burden of disease caused by *Streptococcus pneumoniae* in children younger than 5 years: global estimates. *Lancet* 374, 893–902. doi: 10.1016/s0140-6736(09)61204-6
- Oggioni, M. R., Iannelli, F., Ricci, S., Chiavolini, D., Parigi, R., Trappetti, C., et al. (2004). Antibacterial activity of a competence-stimulating peptide in experimental sepsis caused by *Streptococcus pneumoniae*. *Antimicrob. Agents Chemother*. 48, 4725–4732. doi: 10.1128/aac.48.12.4725-4732.2004
- Oggioni, M. R., Trappetti, C., Kadioglu, A., Cassone, M., Iannelli, F., Ricci, S., et al. (2006). Switch from planktonic to sessile life: a major event in pneumococcal pathogenesis. *Mol. Microbiol.* 61, 1196–1210. doi: 10.1111/j.1365-2958.2006. 05310.x
- O'may, C. Y., Sanderson, K., Roddam, L. F., Kirov, S. M., and Reid, D. W. (2009). Iron-binding compounds impair *Pseudomonas aeruginosa* biofilm formation, especially under anaerobic conditions. *J. Med. Microbiol.* 58, 765–773. doi: 10.1099/jmm.0.004416-0
- Oram, J. D., and Reiter, B. (1968). Inhibition of bacteria by lactoferrin and other iron-chelating agents. *Biochim. Biophys. Acta* 170, 351–365. doi: 10.1016/0304-4165(68)90015-9
- Parsiegla, G., Noguere, C., Santell, L., Lazarus, R. A., and Bourne, Y. (2012). The structure of human DNase I bound to magnesium and phosphate ions points to a catalytic mechanism common to members of the DNase I-like superfamily. *Biochemistry* 51, 10250–10258. doi: 10.1021/bi300873f
- Regev-Yochay, G., Raz, M., Dagan, R., Porat, N., Shainberg, B., Pinco, E., et al. (2004). Nasopharyngeal carriage of *Streptococcus pneumoniae* by adults and children in community and family settings. *Clin. Infect. Dis.* 38, 632–639.
- Salvadori, G., Junges, R., Morrison, D. A., and Petersen, F. C. (2019). Competence in *Streptococcus pneumoniae* and close commensal relatives: mechanisms and implications. *Front. Cell Infect. Microbiol.* 9:94. doi: 10.3389/fcimb.2019.00094
- Sánchez, L., Calvo, M., and Brock, J. H. (1992). Biological role of lactoferrin. Arch. Dis. Child. 67, 657–661. doi: 10.1136/adc.67.5.657
- Schuchat, A., Robinson, K., Wenger, J. D., Harrison, L. H., Farley, M., Reingold, A. L., et al. (1997). Bacterial meningitis in the United States in 1995. Active surveillance team. N. Engl. J. Med. 337, 970–976.
- Shak, J. R., Vidal, J. E., and Klugman, K. P. (2013). Influence of bacterial interactions on pneumococcal colonization of the nasopharynx. *Trends Microbiol.* 21, 129–135. doi: 10.1016/j.tim.2012.11.005
- Shaper, M., Hollingshead, S. K., Benjamin, W. H. Jr., and Briles, D. E. (2004).
  PspA protects Streptococcus pneumoniae from killing by apolactoferrin, and antibody to PspA enhances killing of pneumococci by apolactoferrin [corrected]. *Infect. Immun.* 72, 5031–5040. doi: 10.1128/iai.72.9.5031-5040.
- Sheffield, C. L., Crippen, T. L., Poole, T. L., and Beier, R. C. (2012). Destruction of single-species biofilms of *Escherichia coli* or *Klebsiella pneumoniae* subsp. pneumoniae by dextranase, lactoferrin, and lysozyme. *Int. Microbiol.* 15, 185–180
- Singh, P. K., Parsek, M. R., Greenberg, E. P., and Welsh, M. J. (2002). A component of innate immunity prevents bacterial biofilm development. *Nature* 417, 552–555. doi: 10.1038/417552a
- Syrogiannopoulos, G. A., Katopodis, G. D., Grivea, I. N., and Beratis, N. G. (2002). Antimicrobial use and serotype distribution of nasopharyngeal *Streptococcus pneumoniae* isolates recovered from Greek children younger than 2 years old. Clin. Infect. Dis. 35, 1174–1182. doi: 10.1086/343824
- Tettelin, H., Nelson, K. E., Paulsen, I. T., Eisen, J. A., Read, T. D., Peterson, S., et al. (2001). Complete genome sequence of a virulent isolate of *Streptococcus pneumoniae*. *Science* 293, 498–506. doi: 10.1126/science.106

- Van Der Kraan, M. I., Groenink, J., Nazmi, K., Veerman, E. C., Bolscher, J. G., and Nieuw Amerongen, A. V. (2004). Lactoferrampin: a novel antimicrobial peptide in the N1-domain of bovine lactoferrin. *Peptides* 25, 177–183. doi: 10.1016/j.peptides.2003.12.006
- Van Der Kraan, M. I., van Marle, J., Nazmi, K., Groenink, J., Van 't Hof, W., Veerman, E. C., et al. (2005). Ultrastructural effects of antimicrobial peptides from bovine lactoferrin on the membranes of *Candida albicans* and *Escherichia coli. Peptides* 26, 1537–1542. doi: 10.1016/j.peptides.2005.02.011
- Vidal, J. E., Howery, K. E., Ludewick, H. P., Nava, P., and Klugman, K. P. (2013).
  Quorum-sensing systems LuxS/autoinducer 2 and Com regulate Streptococcus pneumoniae biofilms in a bioreactor with living cultures of human respiratory cells. Infect. Immun. 81, 1341–1353. doi: 10.1128/IAI.01096-12
- Vidal, J. E., Ludewick, H. P., Kunkel, R. M., Zahner, D., and Klugman, K. P. (2011). The LuxS-dependent quorum-sensing system regulates early biofilm formation by *Streptococcus pneumoniae* strain D39. *Infect. Immun.* 79, 4050–4060. doi: 10.1128/IAI.05186-11
- Vogel, H. J. (2012). Lactoferrin, a bird's eye view. Biochem. Cell Biol. 90, 233–244. doi: 10.1139/o2012-016
- Wright, C. S. (1984). Structural comparison of the two distinct sugar binding sites in wheat germ agglutinin isolectin II. J. Mol. Biol. 178, 91–104. doi: 10.1016/ 0022-2836(84)90232-8
- Wu, X., Jacobs, N. T., Bozio, C., Palm, P., Lattar, S. M., Hanke, C. R., et al. (2017). Competitive Dominance within Biofilm Consortia Regulates the

- Relative Distribution of Pneumococcal Nasopharyngeal Density. *Appl. Environ. Microbiol.* 83:e953-17. doi: 10.1128/AEM.00953-17
- Yadav, M. K., Vidal, J. E., Go, Y. Y., Kim, S. H., Chae, S. W., and Song, J. J. (2018). The LuxS/AI-2 quorum-sensing system of *Streptococcus pneumoniae* is required to cause disease, and to regulate virulence- and metabolism-related genes in a rat model of middle ear infection. *Front. Cell Infect. Microbiol.* 8:138. doi: 10.3389/fcimb.2018.00138
- Zavaleta, N., Nombera, J., Rojas, R., Hambraeus, L., Gislason, J., and Lönnerdal, B. (1995). Iron and lactoferrin in milk of anemic mothers given iron supplements. *Nutr. Res.* 15, 681–690. doi: 10.1016/0271-5317(95) 00035-h

**Conflict of Interest:** The authors declare that the research was conducted in the absence of any commercial or financial relationships that could be construed as a potential conflict of interest.

Copyright © 2019 Angulo-Zamudio, Vidal, Nazmi, Bolscher, Leon-Sicairos, Antezana, Canizalez-Roman and León-Sicairos. This is an open-access article distributed under the terms of the Creative Commons Attribution License (CC BY). The use, distribution or reproduction in other forums is permitted, provided the original author(s) and the copyright owner(s) are credited and that the original publication in this journal is cited, in accordance with accepted academic practice. No use, distribution or reproduction is permitted which does not comply with these terms.